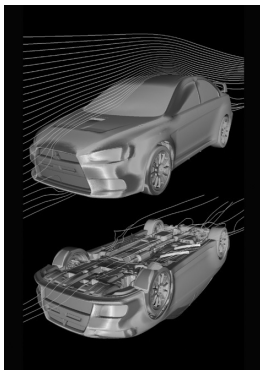


TECHNICAL REVIEW

2008 NO. 20




MITSUBISHI MOTORS



- **Cover Photograph**

The photograph shows the CFD (Computational Fluid Dynamics) analysis results of the LANCER EVOLUTION X. Its massive body design incorporated aerodynamics, in combination with the newly-developed rear air spoiler and floor air guides, delivers superior aerodynamic performance far surpassing that of the previous EVOLUTION models, in terms of not only air resistance but also lift, which is extremely important for steering stability. The floor air guides direct the under floor airflow to the outside of the vehicle to increase the flow velocity at the center area under the floor, and also reduce the pressure under the floor by vortices generated downstream of the air guides, thus effectively reducing the lift.

 **iMiEV**, Mitsubishi's next-generation electric vehicle starring in various events



i MiEV being test-driven on the Tateyama Kurobe Alpine Route, which is normally closed to private cars



i MiEV being used as the chief judge's support car in the 2008 Lake Biwa Mainichi Marathon



i MiEV demonstration drive in a motorsport event at Odaiba



i MiEV pacing the field in a minicar endurance race

MITSUBISHI MOTORS TECHNICAL REVIEW

2008 NO.20

Contents

Foreword	4
-----------------------	---

Technical Perspective

“Vehicle Dynamics Technologies to Provide Driving Pleasure” Round-Table Discussion	6
---	---

Special Feature Driving Pleasure

Technical Papers

Improvement of Vehicle Dynamics by Right-and-Left Torque Vectoring System in Various Drivetrains	14
---	----

New Technologies

Development of Integrated Vehicle Dynamics Control System ‘S-AWC’	21
New 4B11 Turbocharged Engine	26
Newly Developed Twin Clutch SST (Sport Shift Transmission)	30
LANCER EVOLUTION X Chassis Technologies	34
Aerodynamics for LANCER EVOLUTION X	38
Electrical-System Design for LANCER EVOLUTION X	42
Design Concept for LANCER EVOLUTION X	46

Technical Papers

Development of i MiEV Next-Generation Electric Vehicle (Second Report)	52
Development of Technology for Detection of Approaching Objects Using Noseview Cameras	60
Study of Fuel Economy and Exhaust Emission Reduction by Intake Flow Control	68

Photo on first page

The i MiEV (Mitsubishi innovative Electric Vehicle) is a next-generation electric car that’s based on the Mitsubishi “i” and incorporates high-capacity lithium-ion batteries, compact, high-performance motors, and other innovative technologies from Mitsubishi Motors Corporation.

This zero-emission vehicle recently proved its superior running performance and environmental performance on hilly roads at high elevations in a specially permitted test on Japan’s Tateyama Kurobe Alpine Route, which is normally closed to private cars to protect the environment.

Thanks to its clean, quiet operation, the i MiEV is popular as a support car for marathons. It’s also used as a pace car for motor races and is featured at a wide range of other events.

Development of Vibration Calculation Code for Engine Valve-Train	74
Inexperienced Drivers' Behavior, and Control Technology that Adapts Powertrain Behavior to Drivers	83

New Technologies

Development of Plant-Based Plastics Technology, 'Green Plastic'	91
Development of EPS+ (Electric Power Steering Plus)	97
Development of a Rain-Light Sensor	99
Newly Evolved Electronic Time and Alarm Control System (ETACS) of 2008 eK WAGON	103
Development of MITSUBISHI POWER SOUND SYSTEM	109
Usability Evaluation in Product Development	113
Influence of Work Hardening during Metal Forming on Crashworthiness Simulation	117
Design Concept for GALANT FORTIS	121

Awards

EPA Climate Protection Award for High-Efficiency Mobile Air Conditioning System Development of Power-saving Mobile Air Conditioning System	126
---	-----

New Products

GALANT FORTIS	127
LANCER EVOLUTION X	130

A 20-Year History of New Models and Major Technologies at Mitsubishi Motors Corporation

133



Customer Satisfaction is Our Satisfaction

Osamu MASUKO

President

I'm always delighted when customers get in touch to say how pleased and satisfied they are with Mitsubishi vehicles. Here's a selection of comments we've recently received at our customer affairs center:

"The i is a really good car! Driving it felt great. It actually relieves stress."

(from a male i purchaser in his sixties)

"It's easy to drive, and I can cover long distances in it without getting tired. I love it!"

(from a male OUTLANDER purchaser in his forties)

"I never get tired of the design. I suspect I'll keep this vehicle for 10 years or even longer."

(from a male DELICA D:5 purchaser in his forties)

Complimentary comments like these give me tremendous pleasure. They show that everyone at Mitsubishi Motors is working harder than ever to deliver customer satisfaction and to be genuinely useful to society, in line with the company motto:

"We are committed to providing the utmost driving pleasure and safety for our valued customers and our community. On these commitments we will never compromise. This is the Mitsubishi Motors way."

This motto, which we adopted in January 2005, represents a pledge to make customer satisfaction our highest priority. And in addition to the promise to deliver driving pleasure (the fundamental attraction of our vehicles) and long-term user confidence, it reflects our determination to offer new forms of value in the vehicles we make.

This thinking shows in the OUTLANDER, which we launched in October 2005, and in all subsequent new models such as the i, the new eK WAGON, the new PAJERO, the DELICA D:5, the GALANT FORTIS, and the LANCER EVOLUTION X.

It's embodied (among many innovations) by the rear-midship layout of the i, with which we swept away conventional thinking about minicars, and by the S-AWC (Super All Wheel Control) vehicle dynamics control system, which puts intuitive control of the vehicle in the driver's hands. Innovations like these add to customer satisfaction in ways that are unique

to Mitsubishi Motors.

A particularly outstanding example of our dedication to customer satisfaction is the LANCER EVOLUTION X, which we launched in October 2007. Incorporating our very latest technologies, this new model shows our passion to provide a confident, high performance driving experience to customers of all skill levels. Since we launched the LANCER EVOLUTION series in 1992, we've continually enhanced its technologies, feeding know-how gained through motorsport participation into each successive competition model and its marketplace iteration in line with a consistent policy of pushing the limits of performance. In the LANCER EVOLUTION X – the 10th model in the series – we adopted the newly developed TC-SST (Twin Clutch Sport Shift Transmission) and S-AWC to realize a new form of driving pleasure: confidence and comfort in addition to speed.

The enjoyment that the LANCER EVOLUTION X has delivered to many drivers prompted the Japan Car of the Year judges to give the car a special "Most Fun" award.

This 20th edition of the **MITSUBISHI MOTORS TECHNICAL REVIEW** describes the LANCER EVOLUTION X's new technologies in a feature about driving pleasure.

In April this year, Mitsubishi Motors launched a new mid-term business plan called Step Up 2010, which is aimed at realizing sustainable growth as we strive to deliver satisfaction to even more people.

We're keenly aware that automobiles, while convenient and valuable on one hand, play a role with respect to traffic accidents and environmental problems such as global warming on the other. So, the Step Up 2010 plan includes stepped-up production of vehicles with fuel-sipping engines and high-efficiency transmissions, plus accelerated efforts to bring clean diesel engines and our MiEV next-generation electric vehicle to market.

At Mitsubishi Motors, we are determined to continue developing products and technologies that boost customer satisfaction and help to build a sustainable society that harmonizes vehicles with the needs of people and the environment.

“Vehicle Dynamics Technologies to Provide Driving Pleasure” Round-Table Discussion

Abstract

Mitsubishi Motors’ corporate philosophy is encapsulated in the following motto:

“We are committed to providing the utmost driving pleasure and safety for our valued customers and our community. On these commitments we will never compromise. This is the Mitsubishi Motors Way.”

In this issue focusing on driving pleasure, we hear from the engineers in charge of developing the technologies for enhanced vehicle dynamics and 4WD systems, which provide the core support for driving pleasure.

Key words: *Driving Pleasure, Vehicle Dynamics, 4WD System*



From left to right
Advanced Chassis Engineering, Advanced Vehicle Engineering Dept.,
Development Engineering Office
Hiroyuki SUNOUCHI
Drivetrain Design, Drivetrain Engineering Dept.,
Development Engineering Office
Kaoru SAWASE
Master Evaluation, Testing Control Dept.,
Development Engineering Office
Hiroshi FUNO

Vehicle Dynamics Testing Dept., Development Engineering Office
Tsuneaki NISHIDA (Chairman)
Vehicle Control Engineering, Advanced Vehicle Engineering Dept.,
Development Engineering Office
Sumio MOTOYAMA
Ride & Handling Testing, Vehicle Dynamics Testing Dept.,
Development Engineering Office
Hiroshi SUGIMOTO
Advanced Vehicle Engineering Dept., Development Engineering Office
Yusuke KONDO

1. Introduction

Nishida: In recent years, we have seen remarkable progress in vehicle dynamics control technologies. These technologies have the possibilities of allowing drivers to operate a vehicle more safely and comfortably, even in difficult conditions or even if they are unskilled. As you know, Mitsubishi Motors Corporation (MMC) has adopted “utmost driving pleasure” as a key phrase expressing the driveability and roadability that is the fundamental attraction of our vehicles, aimed at producing exciting vehicles. These dynamic control technologies are incorporated in the LANCER EVOLUTION and other MMC vehicles and now support driving pleasure as well as “toughness and safety”, which is another of our key phrases. On the other hand, vehicle systems that work on these control technologies do not necessarily meet the driver’s expectation, sometimes

leading to the driver feeling that this spoils the fun of driving the vehicle. This suggests that electronic control is not always welcome and there are areas where intrinsic performance of the vehicle reigns. I think that achieving an optimum combination of the two is an ultimate goal as we strive to offer driving pleasure to our customers. Needless to say, the application of latest testing and analysis technologies, extensive field trials, and stringent and accurate evaluation are all indispensable to achieving the goal.

With this in mind, it is worth reviewing to what point our vehicle manufacturing has advanced in the field of vehicle dynamics technology. Today, we have attending engineers who are involved in vehicle dynamics technology development, from the control technology, basic technology and testing and evaluation sections. Please share your thoughts with everyone freely, including any difficulties you experienced.

2. Chassis control technology

Nishida: In the 1980s, vehicles incorporating dynamics control technologies were launched at MMC. These included the antilock brake system (ABS), traction control system (TCL), four-wheel steering system (4WS), variable-characteristic shock absorbers, height control system on air suspended vehicles, roll angle reduction control, and stabilizer-bar on-off control. And also the electronic control of the steering reaction force was applied to the power steering system. Today, some of these are installed as standard, while others do not appear to be as popular as they once were.

Motoyama: The categories that went through the most fluctuations were the 4WS and so-called variable characteristics suspension technologies, including damping-force-switching shock absorbers, air suspension and hydraulic suspensions. They boomed in the late 1980s, but did not gain long-term popularity. In the 1990s, there were no significant developments in their application. Recently, variable characteristics suspension technologies have regained popularity, mostly in Europe, especially with shock absorbers that have the capability of continuously varying rather than switching damping force characteristics. The temporary decline they experienced earlier was due to the immaturity of the systems, in both the hardware and software. Another reason appears to be the immaturity of the envisioned goals of these systems.

Funo: As a specific case, the 4WS was a system that was developed to focus on a single area of a vehicle's functions. In fact, it displayed remarkable performance in this area, but the driver sometimes had difficulty in using it.

Motoyama: Back then, the Japanese automakers were ahead of competitors in other countries in developing these technologies. Both the manufacturers and the market here found value in something new that these systems offered. However, the market did not fully appreciate the functions that the new technologies offered, partly because most of them remained immature, even after being developed as products, due to a lack of refinement. For example, the market appreciated the 4WS for its ability to help in tight turns but not for its other abilities. Customers generally did not fully realize what benefits the 4WS could provide in what scenarios. Enhanced controllability and stability of a vehicle is difficult to feel as it is present or absent, depending on the driving environment, unlike significantly-improved ride comfort, which customers can easily perceive.

Sunouchi: A changing economic background has also influenced the popularity of these technologies. During the bubble years in Japan, people avidly looked for something technologically advanced and novel. After the bubble burst, people focused on value for money. Additional vehicle functions only work fully when the vehicle's performance itself is sound. European manufacturers continued refining the vehicle's basic performance over the years, and today, with a strong economic background, they have advanced to

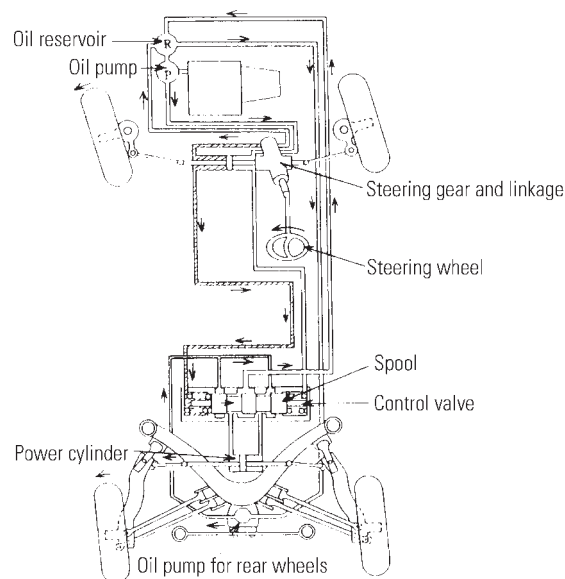


Fig. 1 4WS system (1987 GALANT VR4)

the point of adding value to the equipment. Japanese vehicle manufacturers, on the other hand, are now focusing on enhancing basic vehicle performance from the step they reached during the bubble years.

Sugimoto: The 4WS was not optimized for all speed ranges. Actually, the systems on the models for the European market were tuned to specifications different from Japanese market models.

Motoyama: Unpleasant feel, by its nature, is an unavoidable problem with the 4WS. A steering system completely devoid from such unpleasant feel is only the conventional front wheel steering system. It is also true that, no matter how well you familiarize yourself with the system, unpleasant feel will never become familiar and comfortable. To enjoy the full benefit of 4WS, maybe you must think, "the 4WS steers my car better than I can" just before driving the vehicle.

Funo: For a vehicle to be stable and controllable, the rear wheels must remain firmly in position. This is a basic rule. Therefore, there is inevitably argument regarding the 4WS as to whether a system that involves positional movement of the rear wheels can be said to be beneficial. Finding an optimal method of controlling its positional movement will pave the way to progress of the 4WS.

Motoyama: The 4WS has the potential to substantially expand the degree of freedom in toe control. Today's technology is still not that advanced. Perhaps, chassis control developments, assuming a 4WS-based platform, would drastically increase the possibilities.

Nishida: That is the active steering control working on the four wheels, including the front wheels. Front steering systems with variable gear ratio control have been introduced and some of them are combined with rear wheel steering control. MMC has also made its own technology relating with this control public. As with the steering system, development of the suspension system to enhance its variable characteristics by

such means as controlling the damping force has become increasingly active today. Do you have any thoughts on this?

Motoyama: Technologies for selecting suspension characteristics were predominant in development in this field, but the trend has now shifted toward technologies for varying them continuously. The former technologies aimed at selecting the best characteristics, but actually selected characteristics might be neither better nor worse, while the latter aims at continually adjusting the system to optimum characteristics. Today, variable characteristics suspension systems are mostly employed on high-end luxury cars, but they will become popular with lower-priced vehicles. The key factor that decides whether the systems on high-end cars will evolve further will be the energy they consume. The weight of the additional control system for the drivetrain or steering system is greater than that of the braking system. The additional system for the suspension system is heavier than that of the drivetrain or steering system. As the weight increases, more power is consumed. An active steering system, for example, requires a maximum current of 10 A, approximately the same current as that of brake lamps, but an extra control system added to the suspension system weighs more and therefore consumes more current.

Sunouchi: Currently, air suspension systems are employed in some high-end sedans and sport utility vehicles (SUV). Hydraulically operated fully active suspensions were used in the past, but what we have today is classified as a semi-active type of suspension.

Motoyama: Hydraulic systems consume sufficient power to change the result of emissions test cycle driving. In this sense, electric active suspensions will be more feasible than hydraulic systems. Electric systems allow energy to be regenerated. Another merit is a much larger range of control.

Nishida: The conversion of various chassis systems into electrically operated systems is now advancing. The most important of these is electric power steering (EPS).

Sunouchi: EPS has had a issue in its steering feel. However, it can now give almost the same level of feeling as a hydraulic system. Nevertheless, friction and motor inertia remain an EPS challenge to be addressed. Besides the hardware, the approach may include enhancing the software.

Funo: EPS control technology may have the potential to give the driver a sporty feel.

Motoyama: The increased worm gear friction with the EPS is caused by road surface inputs. It is possible to solve this problem by developing the control technology, but this requires tremendous skill. Even with the best EPS today, the steering feel it provides is not as good as that with the best hydraulic power steering system in particular aspects.

Nishida: The EPS reduces fuel consumption. How about its contribution to the vehicle's dynamic performance?

Motoyama: We are going to expand the application of the stability control and brake-related control sys-

tems under the key theme of safety. The systems that follow these will be steering-related control systems because they have the potential to offer a high degree of freedom. Of course, one option is a system that combines these. The largest benefit of the EPS is a high degree of freedom of control. Its control is so free that we can even generate steering torque in the opposite direction to that of the driver's input.

Sunouchi: The EPS contributes less to the reduction of fuel consumption on larger vehicles. For these vehicles, the EPS will find its application in added functions, such as lane keeping and parking-assist systems, to assist the driver rather than to reduce the fuel consumption. The EPS will offer more potential in this area where the capabilities offered by hydraulic means have reached a limit.

Motoyama: I think another key point for success in the EPS is the embodiment of steering feel that is available only with an electric system control. The target is not something on a par with, but rather that exceeds hydraulic systems. Steering feel adds "flavor" to the vehicle.

Nishida: On a different topic, electric systems remind me of MMC's MiEV electric vehicle.

Funo: The MiEV has a low center of gravity, which means good stability in vehicle control. It sways little and only has a small load transfer in cornering, so you feel like the center of gravity is near the wheel axis. The location of the battery has been optimized, so the distribution of the vehicle mass is well controlled. Because the electric motor responds much better to accelerator operation than a mechanical engine, I think it is reasonable to design the response rather conservatively to prevent the driver from perceiving a surprising difference from gasoline engine vehicles when using the accelerator, although suppressing a good response is wasteful. What is important is a good-feeling response, low electricity consumption and problem-free running distances. The i MiEV runs really well. It is definitely a next-generation electric car.

3. Drivetrain control technology

Nishida: How about drivetrain control? Electronics have been applied to 4WD and other drivetrain controls to enhance the vehicle's dynamic performance.

Sawase: Electronic traction control technologies intended to enhance cornering performance, in addition to traction, are becoming the mainstream. Early electronic control applied to the 4WD system was an on-demand system that allowed high-speed on-road driving and distributed more torque to the rear wheels as lateral acceleration increased. At MMC, the first drivetrain control introduced as a means of enhancing the vehicle's dynamic performance was the system employed in the 1992 GALANT. This is the first fully-fledged system that controls the distribution of traction between the front and rear wheels by using the center differential full-time 4WD as a base system. Few people will know about this system because it was only produced in small volumes (laughter). Today, electronic

control prevails in the on-demand 4WD system. Electronically controlled systems make up 60 to 70 % of all on-demand 4WD systems. Electronically controlled systems have become popular because not only do they add to vehicle dynamic performance, but they are also beneficial to weight reduction and fuel economy. The MMC's system employed on the OUTLANDER has very simple control logic and is well refined. It has been well received in the market, with critics saying, "The system is pretty well matched to the vehicle. This must be the result of extensive test driving". The OUTLANDER has good basic characteristics, and this gives the system positive effects.

Motoyama: What inspired us to start developing technology for lateral traction distribution was an idea that came from a simple question: "Our past traction control development was concerned with longitudinal traction distribution. What would happen if lateral torque distribution is controlled?" Only a short while after joining MMC, I started conducting simulations on this theme. I learned through simulation that changing the lateral traction could cause an enormous yaw moment to be generated and its generation could be completely stopped. I also learned that lateral traction control was very useful if it was combined with vehicle behavior feedback technology. I saw that this was also effective in enhancing traction. What mattered was not distribution but rather the shifting of traction. Zero traction remains zero traction even after distribution. We found that even under zero traction conditions, a vehicle's dynamic performance could be drastically enhanced by turning one wheel faster than the other. That was in my third year with MMC, when I discussed that subject with Mr. Sawase. One week later, he appeared with a conceptual drawing of an active yaw control (AYC) differential.

Sawase: No! I came up with it in just three days (laughter).

Motoyama: The initial design was an independent four-wheel drive system that used clutches. What was horrible about the system was that it would not allow you to turn normally. It also allowed the driver to drift the vehicle and experience an exceptional thrill. When I asked my boss to try the vehicle with the system, he said, "It is really difficult to drive but you have something sufficiently worthwhile to develop a way of controlling it". The conclusion was that we should work on not traction distribution but torque transfer.

Sawase: Yes, I remember that. During the first discussions with Mr. Motoyama, the theme presented was: "development of a lateral traction distribution system". Then, I initially considered some distribution mechanisms. As the discussion advanced, however, I realized that what needed to be controlled was not the lateral traction distribution ratio but the right-left traction difference that produced the yawing moment. I soon came up with the idea of using the slipping clutch theory, which means that a slipping clutch transmits torque only in one direction. I also thought that an actual system would need a differential gear to allow the vehicle to run normally when the control was inactive. I

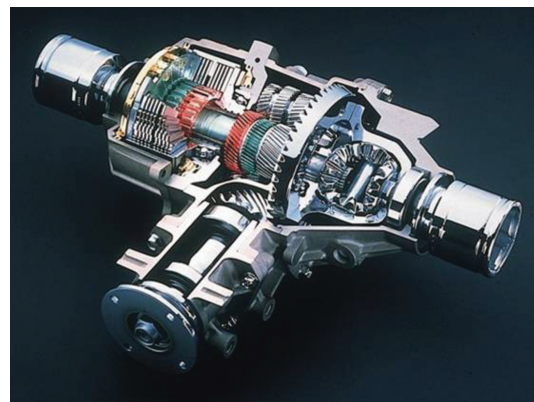


Fig. 2 AYC differential gear (1996 LANCER EVOLUTION IV)

thought of the Automatic Yaw Control (AYC) differential while taking a bath, but the real challenge then began. The first prototype system took the testing staff one full day to assemble and mount on the test vehicle. But, the system broke only five seconds after the test started. At the end of the third of similar breakage, our manager was quite naturally not happy.

Putting these hardships behind us, the AYC system made its debut on the 1996 GALANT/LEGNUM and LANCER EVOLUTION IV. The latest system employed on the EVOLUTION X comes with yaw rate feedback control, the concept that Mr. Motoyama conceived of 10 years ago.

Sawase: Like any first-of-a-kind product, the AYC system initially received a number of negative evaluations. The reason, as you may suppose, was the unpleasant feel the system gave the driver. But, if you completely remove the odd feel, you would not be able to enjoy the benefits of the system, and vice versa. We tirelessly tried to refine the system until it was eventually granted "citizenship". The LANCER EVOLUTION was the best platform on which to demonstrate the benefits of the system. However, even here, the system received negative comments initially.

Funo: Negative comments?

Sawase: Yes, that the system was "unusual". In particular, critics said that the system caused the vehicle to turn when the accelerator was pressed and to move outwards when the accelerator was released. The feedforward, tack-in restraining control that prevented the rear inner wheel from tracking too tight a curve in corners was responsible for this, which was excessively effective. This gave the driver an odd feel.

Nishida: It is difficult to stop here, but time is limited today. Someday, perhaps we shall schedule a running discussion of this kind in the Technical Review. By the way, is "torque vectoring" a common expression for the effect being discussed here?

Sawase: Yes, it is the English counterpart of "lateral torque shift", a direct translation from the Japanese term that we use to indicate the same effect. We can use it as a definite English expression for the effect. Ricardo of England first used it. This expression provided the opportunity for MMC's AYC system to be

identified as an embodiment of the concept in question in Europe. In Japan, the concept is called "Direct Yaw Moment Control" or "DYC".

Nishida: MMC has now introduced the concept in the All Wheel Control (AWC) and Super All Wheel Control (S-AWC).

Sawase: AWC is a set of 4WD-based technologies to optimally control and use the performance available from the four tires fully. Its most advanced form is the S-AWC system. The system mounted on the LANCER EVOLUTION series is the result of steady enhancement over the years, and its high degree of perfection and speed performance having been verified in a number of races. Application of the technology should not be limited to the LANCER EVOLUTION.

4. S-AWC on the LANCER EVOLUTION X

Nishida: What was the initial market reaction to the S-AWC at the launch of the LANCER EVOLUTION X?

Funo: I attended press events; the S-AWC was given a very high mark. The system enables truly stable driving without the need for the driver to use any special form of control.

Nishida: Were there any "unpleasant feel" comments?

Funo: There were almost no comments of this kind. Compared with the previous model (the LANCER EVOLUTION IX), the new system operates in many more scenarios and with greater control. Nonetheless, the system enables the vehicle to respond faithfully to the driver's control. The previous system sometimes required the driver to use special maneuvers so that it could fully demonstrate its performance. Such driver considerations are not necessary with the new system. It indeed gives a natural feel. To make this possible, the workload is increased on the part of the vehicle's system.

Sawase: The driver can control the LANCER EVOLUTION X even in situations where he or she would not be able to handle an ordinary vehicle, during high lateral acceleration cornering for example, without the need for special maneuvers.

Motoyama: I often heard comments like, "It feels as if my driving skills have improved". Racing drivers made comments like, "It makes driving easier".

Sawase: It generally has a reputation for being just amazing. The vehicle behaves quite stably. Our development goal for the system was stable running and the market appreciates that goal.

Nishida: How did you determine the target quality of each control factor while building up the overall performance of the system?

Sawase: When we started handling so-called vehicle dynamics control systems, we placed more importance on numerical values than on other factors, but what we now respect more than numerical values is the solid performance of the system during driving tests. We adjust the control factors according to comments and suggestions from test drivers. In development now, we recognize that a goal cannot be determined on

numerical values alone, so we do not consider only the data. Indeed, there are good and bad images of a vehicle's dynamic characteristics, but the image can be expressed in words rather than in numerical values.

Funo: During the development of the S-AWC, we evaluated performance by using a sensory method and the results were expressed in a point rating system. However, the rating alone could not represent the full picture, so we tried to convey our views on the sensation, flavor and feel of the vehicle in close communication with the system developers, using descriptive comments.

Motoyama: I can tell you that data were used only for the presentation at the completion meeting of the system development, ... data that we collected a long time ago (laughter).

Nishida: Were there any negative comments by the participants?

Funo: There were a few. If the system is not in sync with the driver, he or she may initially feel that the system restricts the driver's control of the vehicle. Some drivers fear that, after trying a vehicle with S-AWC, their driving skill could suffer when they return to their own cars.

Sawase: Even if you are not a highly skilled driver, the system lets you drive with fewer mistakes and, should you make a mistake, the system helps you to quickly recover from it. Paradoxically, this causes concern, but the EVOLUTION X still makes driving fun and helps the driver hone their skills in "toughness and safety" before "upgrading" to cars without S-AWC.

Funo: The excellent performance of the S-AWC can be fully demonstrated provided the vehicle itself has good characteristics. No matter how sophisticated the system, it cannot demonstrate its full capability and the driver cannot enjoy it unless the vehicle itself has solid characteristics. For example, the system cannot perform properly unless the vehicle can reflect the lateral acceleration it receives exactly. The basic performance of the vehicle is very important.

The tires are also key for a successful demonstration of the system's performance. The tires selected for the LANCER EVOLUTION X were low rolling resistance tires, which now offer good grip due to recent technical developments. As a person who works with system evaluation, I certainly feel that tire performance is generally enhancing. In the LANCER EVOLUTION X, you will find that its tires wear in an even pattern. This shows that the S-AWC acts positively on the tires. The front tires carry a lower load.

We also sought optimum control of road contact loads of the four wheels in developing the AWC system. To obtain better traction and braking control efficiency from tires, you must keep proper control of the tires' road contact loads. Our success in this area depends significantly on optimizing the vehicle dimensions (a wider track width and lower center of gravity) to prevent excessive variation in the tires' vertical loads, which would result from load transfer. It is also important to control vertical loads for traction control. Lower vertical loads result in less transmission of traction, which

makes it more difficult to control the vehicle's attitude. Maintaining proper vertical loads for all four wheels provides the basis for effective vehicle attitude control. This has great merit.

Nishida: We also have our own philosophy on body design.

Kondo: The LANCER EVOLUTION X uses aluminum materials for the roof, hood, fenders and bumper beam. By using aluminum in these areas that are far from the center of gravity, we lowered the center of gravity and reduced the moment of inertia. The aluminum hood has another purpose: pedestrian protection. Because a light hood can absorb less energy, it provides less protection for the driver's head. We specifically designed the shapes of the inner structural components to overcome this problem. Furthermore, structural members are spot-welded at more locations to increase stiffness.

Nishida: I heard that the aluminum roof presented various challenges.

Kondo: Yes, there were a number of obstacles to clear, although I only became involved in the project just before the start of volume production of the LANCER EVOLUTION X. As mentioned before, aluminum roofs lower the center of gravity, but had never been used for mass-produced vehicles in Japan. One of the biggest challenges was the technology needed to join aluminum and steel materials. Generally, spot welding is used for steel-to-steel joints, but this method is not suitable for joining different metals. After trying various alternatives, we chose self-piercing rivets and succeeded in the trial production. We found that in addition to lowering the center of gravity, the aluminum roof substantially reduces rolling moment of inertia, thus enhancing the LANCER EVOLUTION X's dynamic performance, so we decided to use it.

To cope with electric corrosion, which was another issue, we used an adhesive between the aluminum and steel parts to prevent direct contact, in addition to sealant to prevent water ingress. We also had to address heat distortion. During the body coating process, the roof is heated to as high as 180 °C, but at this temperature the body panels tend to distort because aluminum and steel have different coefficients of thermal expansion. So, after extensive study, including CAE analysis, we decided to provide beads on the sides of the roof panel to prevent thermal distortion.

This method has since been applied to the aluminum roof of the OUTLANDER. I have heard that customers like the agility derived from the low center of gravity of these models.

5. Body, chassis, evaluation and analysis

Nishida: Indeed, weight reduction, a low center of gravity and a low moment of inertia are all essential for enhanced dynamic performance of a vehicle. However, simply using aluminum materials causes problems with the rigidity of the body, which has a predominant influence on the vehicle's dynamic performance. We had to work hard to ensure full rigidity of the body in developing the LANCER EVOLUTION X.

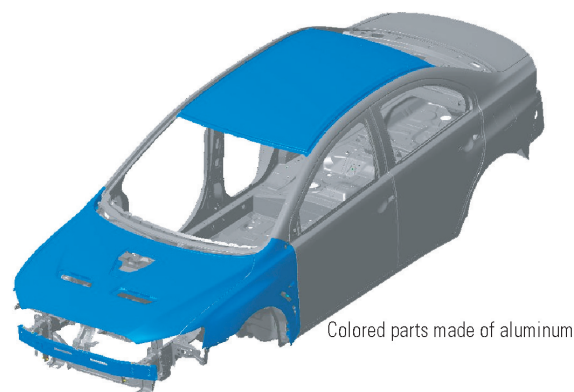


Fig. 3 Body incorporating aluminum (LANCER EVOLUTION X)

We have focused our research on aluminum space-frame body structure technology to reduce vehicle weight. This technology enhances the vehicle's handling and stability, not only because of its weight reducing effect, but also because it increases the rigidity, especially at joints.

Kondo: That's right. As generally stated, the Young's modulus and specific gravity of aluminum are both one third those of steel, which means that its specific rigidity (ratio of stiffness to weight) is also one third that of steel. If aluminum material were simply applied to the body framework for reduced weight, the body would be less rigid. An aluminum space frame structure uses extruded aluminum materials for the main structural members, taking advantage of the material's characteristics to overcome such issues that are characteristic to steel monocoque body structures, such as a loss of rigidity at joints and spot welds. In addition to a low moment of inertia due to reduced weight, the aluminum space frame body provides the type of ride that is not possible with a steel monocoque structure.

Nishida: That is the synergistic effect of reduced weight and high rigidity. When we think about the positive effect of a space-frame structure on stiffness, we can understand how important joining techniques are to a monocoque body.

Kondo: Increasing the number of spot welds is a widely known method of increasing rigidity. At MMC, this method was first employed for the LANCER EVOLUTION IV, followed by the FTO, PAJERO, COLT and other ranges. Today, continuous joining methods such as laser welding are drawing increasing attention as substitutes for spot welding. Furthermore, an increasing number of automaker's are positive about using adhesives in combination with welding.

Funo: A body structure built by using a continuous joining method evidently provides enhanced dynamic performance. One of the clearest pieces of evidence is that a vehicle with such a body structure had a lap time of approximately one second less than predicted on the handling circuit in our proving ground.

Nishida: Unlike tires and suspensions, it is difficult to logically express the impact of body characteristics

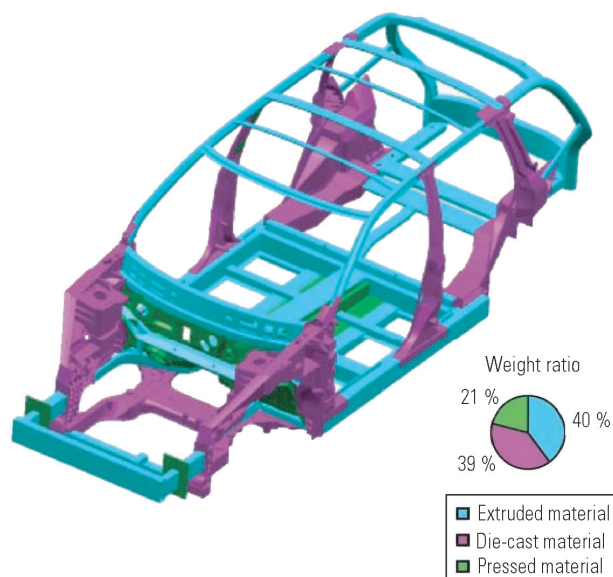


Fig. 4 Aluminum space frame body

on a vehicle's dynamic performance by using mathematical formulae. In actual testing scenarios, staff traditionally use their senses to identify the vehicle's dynamic performance.

It is simple to say "the rigidity of suspension mounts", but it is not simple to define what the phrase means. To begin with, where is the reference point in the coordinates we should use?

Sunouchi: As a member of chassis engineering, I used to focus on increasing the rigidity of suspension members and mounts. I realized, however, that increasing the rigidity of the body framework is crucial. There are areas you cannot enhance no matter how much you intend to increase the suspension stiffness.

Kondo: Flexural stiffness and torsional stiffness are typical values that represent the body's rigidity, but they do not represent everything regarding rigidity. Rigidity is really difficult to express.

Sugimoto: Rigidity of the vehicle's body is difficult to measure. To measure rigidity, the vehicle's body must be fixed in place, but the measurement results obtained from an improperly fixed body may not be what we need. These may represent other things, and you will not understand exactly what you are measuring. We require a method of presenting the force of inertia.

Kondo: It is important to visually confirm the deformation on an actual vehicle body.

In addition to deformation measurement on a body in white (BIW), we used to reproduce the BIW faithfully by using plastic models of individual body parts to see how they deformed. Now, we generally do the same thing on computer screens using CAE technology visually, but the BIW tests were useful to me because I could confirm how those plastic models deformed by physically touching them. It was easy to cause poor structural components to deform by applying a force to them (laughter).

What I have realized about body rigidity is that it cannot be expressed by bending rigidity, torsional rigidity or local rigidity values alone. Unlike collision characteristics or noise, vibration and harshness (NVH) characteristics, the field of handling and stability includes large areas where human sensation plays a part, in other words, intuition. I think it is wrong to examine body rigidity purely by mathematical calculation.

Sugimoto: A well-trained driver testing handling and stability can accurately point out areas of the body that lack rigidity. Currently we are using the software applications that are specially designed for vehicle dynamics analysis but they cannot handle the elastic deformation of the vehicle body.

On the other hand, theoretical interpretations of the effects of suspension geometry and alignment characteristics on the vehicle's handling and stability were established many years ago. Multilink suspension systems, which have been widely employed since the 1980s, are intended to enhance a vehicle's dynamic performance by utilizing their high degree of freedom in designs that incorporate appropriate alignment and compliance characteristics. Large-scale kinematic analysis software was introduced at almost the same time. In software analysis, however, the body was handled as a rigid body. It was not until the 1990s that CAE was applied to deformation of an operating vehicle's body from the viewpoints of the vehicle's handling and stability and riding comfort.

Sunouchi: As a chassis designing engineer, I felt that the body, the foundation of the vehicle, was being left behind (laughter). Geometry control development based on virtual steering axis philosophy and best linkage arrangement of the multilink suspension is worthless without a solid foundation, or body.

Kondo: Today, it is possible to analyze the elastic deformation of an operating vehicle's body by using a combination of multi body analysis and finite element analysis. We need a theoretical analysis of the elastic deformation to find what influence it has on the drivers' senses, as well as on the vehicle's behavior.

Sugimoto: Human senses are extremely delicate, so even today, a driver's assessment during handling and stability testing is often not reflected in the data. Even a difference in data value that is not sufficient to be represented by the width of a line on a graph can represent a great difference for the human senses. However, that amount of difference in human feeling is extremely difficult to use to prompt design changes from designers. In my experience, a designer who tried the vehicle and experienced a distinct difference in feeling criticized us saying, "Why do your data not reflect such a large difference?" Numerical representation of sensory assessment is a big challenge.

6. For the "utmost driving pleasure"

Nishida: Vehicle dynamic control technology can penetrate deeper into areas beyond the ability of the driver, but the ultimate controller is the driver. In this sense, communication between the driver and the vehi-

cle is imperative. Control technology, however, can only work when it is provided with numerical data.

Funo: Vehicle dynamic control technology expands each driver's vehicle control ability and assists with better control. However, it can only do this well when its control logic is tuned to match the vehicle's characteristics as well as the drivers' control habits and expectations. Although the control logic may sometimes be tailored to accentuate an attractive feature of the vehicle, it must at least allow vehicle motion alignment to be fully ensured. Proper feedback of control system operation to the driver should not be perceived as unpleasant, but should rather be perceived as a good thing that provides communication between the driver and the system. However, excessive feedback can generate an unpleasant feel. Feedback must be kept just below the level at which the driver starts perceiving it to be unpleasant.

Equally important is that feedback from the dynamic control system is well balanced with such things as engine response to accelerator operation, even in terms of the quality of sound, as a vehicle is a product of overall balance.

Motoyama: Vehicle systems used to be independently controlled, but are now increasingly integrally controlled. Our goal should be the innovation of individual systems and their integration, to offer enhanced controllability and stability while pushing the limits and also striving towards performance that is harmonized with the drivers' sensation. Control technology should keep a low profile. Even so, it should still be reliable and highly efficient.

An ideal control technology is one that does not give an unpleasant feel because it works as if it were directly linked to the human brain, as if it were intuitively reflecting the driver's intention. I think it will keep growing.



Fig. 5 Driving evaluation

Nishida: After all, the ultimate question should be how control systems can please human senses. Comfort in a vehicle that is responsive to your control will lead to your pleasure in controlling such a vehicle. Some say that younger generations are losing interest in cars while others say that vehicles are only a means of transport. Even if this is true, a vehicle that offers comfort and pleasure should not be a bad means of transport. In this sense, the "utmost driving pleasure" that MMC seeks, is a common goal to be shared by all vehicles, including cars, SUVs, trucks.

Vehicle dynamic control is evolving from a form of independently controlling individual functions to a form of integrally controlling all these functions, which will open up new possibilities. Nevertheless, those areas that are based on sensory assessment, not on numerical data, cannot be easily accommodated in control technology. Anyway, we all understand that no control technology can demonstrate its full capability unless the vehicle's base, namely the specifications, body, suspension and the like, are sound. This is the basis of manufacturing good vehicles.

That's it for today. Thank you everyone.



Improvement of Vehicle Dynamics by Right-and-Left Torque Vectoring System in Various Drivetrains*

Kaoru SAWASE* Yuichi USHIRODA*

Abstract

This paper describes the verification by calculation of vehicle dynamics improvement by means of a right-and-left torque vectoring system in various types of drivetrains. The amount of right-and-left torque vectoring needed for expanding the vehicle dynamics limit is also calculated, and suitable wheels to which the system should be applied for each drivetrain are evaluated. Application to the front wheels is more effective for the front wheel drive (FWD) vehicles, whereas application to the rear wheels is more effective for the rear wheel drive (RWD) and the all wheel drive (AWD) vehicles.

Key words: Drivetrain, Vehicle Dynamics/Torque Vectoring, Torque Distribution

1. Introduction

Since the 1980s, a range of vehicle dynamics control technologies has been released. Among them, direct yaw moment control with brakes, an effective technology for pro-actively preventing accidents, has become widely used today. In 1996, the world's first vehicle with a right-and-left torque vectoring type direct yaw moment control system was developed and released by the authors⁽¹⁾. The system directly controls the yaw moment acting on the vehicle regardless of whether the vehicle is accelerating or decelerating by transmitting torque between the left and right wheels. This feature improves cornering performance at all stages, from normal to critical driving⁽²⁾.

Following on from this system, various torque vectoring systems have been proposed⁽³⁾⁽⁴⁾. There have been a number of reports on improved performance of vehicle dynamics on AWD and RWD vehicles by applying a torque vectoring system to the rear wheels. However, there have been few reports on the effects of a torque vectoring system applied to the front wheels of AWD vehicles or to the rear wheels of FWD vehicles⁽⁵⁾. Furthermore, there has been no report on a possible method for setting up the maximum vectoring torque of a torque vectoring system.

This paper first discusses a range of themes related to the right-and-left torque vectoring system, starting with its functions, and its applicability that even includes non-driving wheels such as the rear wheels of FWD vehicles. The paper then identifies the impact of the system on the vehicle dynamics limit and how to calculate the limit under impact. Then, using the calculation method, the vehicle dynamics limit is evaluated for when the system is introduced only to the front wheels, only to the rear wheels and to both front and rear wheels of FWD, RWD and AWD vehicles. Based on

the evaluation, the most appropriate wheels on which to use the system are discussed for each type of drive system, together with required vectoring torques. Through these works, the paper shows that the calculation method is also useful for determining the maximum vectoring torque required of the system.

2. Right-and-left torque vectoring system

Fig. 1 shows the operation of the right-and-left torque vectoring system. The system works by controlling the direction and magnitude of torque T_v transmitted between the left and right wheels (this is called torque vectoring), which results in driving force T_v/R acting on one wheel and braking force $-T_v/R$ acting on the other wheel. This then generates longitudinal driving force difference ΔD and, as a result, yaw moment M_g acts on the vehicle. When $T_v = 0$, engine torque T_e is equally divided and distributed to the left and right wheels.

This system is capable, by means of torque vectoring, of controlling the difference in longitudinal driving force between the left and right wheels and yaw moment at any time even when engine torque is fluctuating and/or the vehicle is decelerating. This means that the system can be applied not only to the drive wheels but also to the non-driving wheels.

3. Impact of the system on vehicle dynamics limit

The right-and-left torque vectoring system influences vehicle dynamics in two ways. Firstly, the optimum distribution of driving force between the left and right wheels expands the cornering limit. Secondly, the optimum distribution of cornering force between the front and rear wheels also expands the cornering limit.

* Drivetrain Engineering Dept., Development Engineering Office

* Presented at the Society of Automotive Engineers of Japan's Symposium on September 20, 2007.

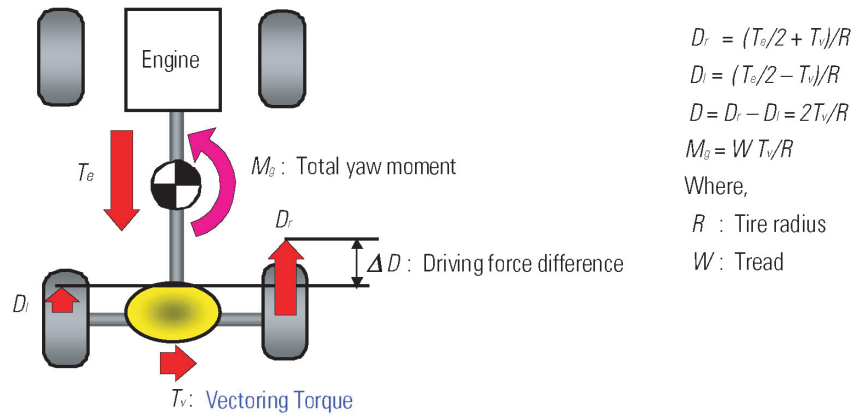


Fig. 1 Definition of right-and-left torque vectoring

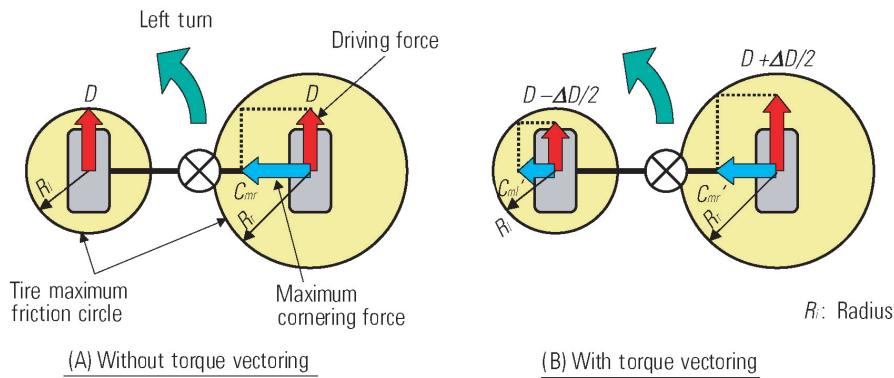


Fig. 2 Effect of torque vectoring #1

Fig. 2 shows the maximum frictional forces of the left and right tires, the driving forces acting on both tires and the maximum cornering force available under these conditions, while the vehicle is turning to the left. In a left turn, due to associated lateral load transfer the frictional force circle of the left tire (R_l) is smaller than that of the right tire (R_r). In the case of (A), which is without left-and-right torque vectoring, the frictional force of the left tire R_l is assumed to be equal to driving force D . The same driving force D that acts on the left tire also acts on the right tire. This driving force D , however, is smaller than the frictional force of the right tire R_r . As a result, only the right wheel is capable of generating the maximum cornering force C_{mr} . In the case of (B), which is with torque vectoring, the left tire, on which driving force $D - \Delta D/2$ acts, is capable of generating the maximum cornering force C_{mr}' . The right tire, on which driving force $D + \Delta D/2$ acts, is also capable of generating the maximum cornering force C_{mr}' . With this, variation ΔC_m in the total maximum cornering force of both tires with right-and-left torque vectoring can be expressed as follows.

$$\begin{aligned}\Delta C_m &= C_{mr}' + C_{mr}' - C_{mr} \\ &= \{R_l^2 - (D - \Delta D/2)^2\}^{1/2} + \{R_r^2 - (D + \Delta D/2)^2\}^{1/2} \\ &\quad - (R_r^2 - D^2)^{1/2}\end{aligned}$$

This equation represents a function where, when ΔD is increased from zero, the maximum value is achieved when:

$$\Delta D = D(R_r - D)/2(D + R_r)$$

This means that right-and-left torque vectoring increases the total maximum cornering force of the left and right tires.

Fig. 3 shows a bicycle model representing a vehicle's steady state cornering. In the case of (A), which is without right-and-left torque vectoring control, the frictional force of the front wheel is assumed to be completely offset by the cornering force C_f (with lateral acceleration: G_y). The vehicle mass is represented by m , the distance between the center of gravity and the front wheel by L_f , the distance between the center of gravity and the rear wheel by L_r , and the cornering force of the rear wheel by C_r . In the case of (B), which is with lateral torque vectoring control, the cornering force of the front wheel is represented by C_f' , the cornering force of the rear wheel by C_r' , and yaw moment by M_g . From the equations of steady turning motion for (A) and (B), the following equations can be derived.

$$\begin{aligned}C_f' &= C_f - M_g/(L_f + L_r) \\ C_r' &= C_r + M_g/(L_f + L_r)\end{aligned}$$

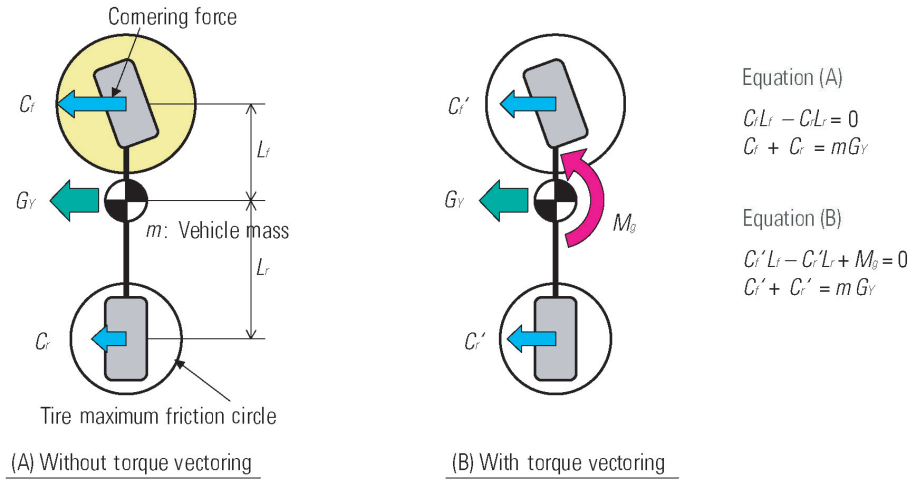


Fig. 3 Effect of torque vectoring #2

This indicates that lateral torque vectoring generates positive (i.e. in the direction of turning) yaw moment on the vehicle, which reduces the distribution of cornering force to the front wheel and thereby expands the cornering limit.

4. Calculation of vehicle dynamics limit

To quantitatively analyze the improvement in vehicle dynamics limit from the application of right-and-left torque vectoring, the equations discussed earlier in this paper were adapted to the dynamic square method for a four-wheel model proposed by Kato et al⁽⁶⁾. Then, using the merged model, a method was developed for calculating front-and-rear driving force distribution, right-and-left torque vectoring on the front wheels and right-and-left torque vectoring on the rear wheels, in order to maximize the vehicle's cornering limit during acceleration and deceleration.

The vehicle model used in the calculation is shown in Fig. 4. As the vehicle accelerates (decelerates) with G_X , load transfer occurs along the longitudinal axis of the vehicle. This load transfer ΔW_X , the magnitude of which is proportional to the vehicle's weight, longitudinal acceleration and the height of the center of gravity, and is inversely proportional to the wheelbase, can be expressed as follows.

$$\Delta W_X = m G_X H_g / L$$

As the vehicle makes a turn with lateral acceleration G_Y , load transfer occurs along the lateral direction of the vehicle. The magnitude of the load transfer is proportional to the vehicle's weight, lateral acceleration and the roll arm length H_s , which is a function of roll stiffness distribution between the front and rear of the vehicle, and is inversely proportional to the treads. With this, the load transfer between the front wheels ΔW_{Yf} and that between the rear wheels ΔW_{Yr} can be expressed as follows.

$$\Delta W_{Yf} = m G_Y \{ H_s / (1 + K_f / K_r - m H_s / K_f) + L_r H_f / L \} / W_f$$

$$\Delta W_{Yr} = m G_Y \{ H_s / (1 + K_f / K_r - m H_s / K_r) + L_f H_r / L \} / W_r$$

With this, the dynamic load distribution between the four wheels can be determined.

By multiplying the dynamic loads for the four wheels by the friction coefficient of the road surface, the maximum frictional force for each wheel as expressed in R_i can be obtained.

Driving force D_i for each wheel can be obtained based on the driving torque from the engine required to achieve G_X , torque distributions T_f and T_r for the front and rear wheels and vectoring torques T_{vf} and T_{vr} between the front wheels and between the rear wheels. The maximum cornering force C_{mi} for each of the four wheels is limited by D_i and R_i , and therefore can be expressed as follows.

$$C_{mi} = (R_i^2 - D_i^2)^{1/2}$$

Taking into consideration the impact of yaw moment on the distribution of cornering force between the front and rear wheels as discussed in section 3 of this paper, the maximum lateral acceleration G_{Yfmax} and G_{Yrmax} of the front and rear wheels can be expressed as follows.

$$G_{Yfmax} = (C_{fl} + C_{fr} + M_y / L) / m_f$$

$$G_{Yrmax} = (C_{rl} + C_{rr} - M_y / L) / m_r$$

When these satisfy both of the following inequalities, the relevant turning with assumed lateral acceleration G_Y is valid. If these fail to satisfy either one of the following inequalities, that turning is not valid.

$$G_{Yfmax} \geq G_Y$$

$$G_{Yrmax} \geq G_Y$$

By conducting loop calculations using the equations discussed above with G_Y as a parameter, maximum lateral acceleration G_{Ymax} with a given G_X , or the vehicle's cornering limit, can be obtained.

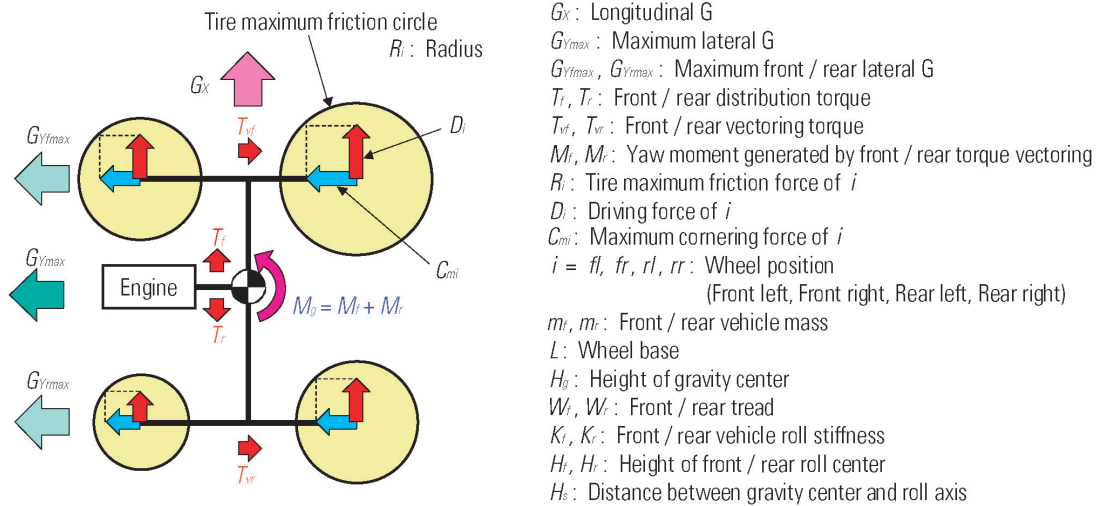


Fig. 4 Four-wheel vehicle model

Table 1 Vehicle dimensions

Front vehicle mass (m_f)	(kg)	900
Rear vehicle mass (m_r)	(kg)	600
Wheel base (L)	(m)	2.6
Height of gravity center (H_g)	(m)	0.5
Front tread (W_f)	(m)	1.5
Rear tread (W_r)	(m)	1.5
Front vehicle roll stiffness (K_f)	(N·m/rad)	70,000
Rear vehicle roll stiffness (K_r)	(N·m/rad)	60,000
Height of front roll center (H_{rf})	(m)	0.05
Height of rear roll center (H_{rr})	(m)	0.12
Tire radius (R)	(m)	0.32

5. Results of calculations for each type of wheel drive

The cornering limit was calculated for each of FWD, RWD and AWD vehicles corresponding in specifications to those of a C-segment sedan shown in **Table 1** to compare the effect of right-and-left torque vectoring.

5.1 FWD vehicle

Fig. 5 shows the calculated effects of right-and-left torque vectoring on the improvement of cornering limit. **Fig. 6** shows the vectoring torque T_{vf} between the front wheels when torque vectoring was applied only to the front wheels. **Fig. 7** shows the vectoring torque T_{vr} between the rear wheels when torque vectoring was applied only to the rear wheels. **Fig. 8** shows the vectoring torque between the front wheels and that between the rear wheels when torque vectoring was applied to both front and rear wheels.

In the longitudinal acceleration region of $0 - 3 \text{ m/s}^2$, the front wheels reach the maximum lateral acceleration limit before the rear wheels do. This is because, on an FWD vehicle, all the driving force is transmitted to the front wheels. In this region, the lateral acceleration limit for the front wheels can be expanded by applying

positive yaw moment to the vehicle by means of right-and-left torque vectoring and thereby reducing the share of the cornering force on the front wheels. The vehicle's cornering limit can be expanded no matter which combination of wheels, front or rear, torque vectoring is applied to. In either case, the required maximum vectoring torque is approximately 500 N·m (**Fig. 6** and **Fig. 7**). However, the extent of improvement is greater when torque vectoring is applied to the front wheels than to the rear wheels. This is because, with the front wheels, it is also possible to optimize the distribution of driving force between them. In fact, the cornering limit with torque vectoring applied to the front wheels is almost equal to that applied to both the front and rear wheels.

In the longitudinal acceleration region of 3 m/s^2 and above, due to lateral load transfer during a turn, the frictional force of the inside front tire is reduced so much as to be offset with only the driving force, and this determines the vehicle's cornering limit. In this case, applying right-and-left torque vectoring control to the rear wheels does not have any effect in reducing the driving force distributed to the inside front tire, and thus has no effect in expanding the cornering limit. On the other hand, applying the control to the front wheels has

a significant effect on improving the vehicle's cornering limit. Even greater improvement can be achieved by applying the control to both the front and rear wheels. However, the required maximum vectoring torque between the rear wheels in that case is almost 800 N·m (Fig. 8). Thus, this option is not efficient, especially in view of the complexity of the associated system.

In the longitudinal deceleration region of 0 to -4 m/s², longitudinal load transfer causes the rear wheels to reach the maximum lateral acceleration limit before the front wheels do. In this region, the lateral acceleration limit for the rear wheels can be expanded by applying negative yaw moment to the vehicle by means of right-and-left torque vectoring. If torque vectoring is applied to the rear wheels, however, the frictional force of the rear wheels is offset with the braking force to generate yaw moment. Therefore, torque vectoring needs to be limited and only a slight improvement in cornering limit is possible. On the other hand, applying torque vectoring to the front wheels not only optimizes the distribution of braking force between the front wheels to improve the front wheels' lateral acceleration limit, but also improves the rear wheels' lateral acceleration limit with negative yaw moment. With this, compared with the acceleration region, the cornering limit can be improved with smaller vectoring torque.

In the longitudinal deceleration region of -4 m/s² and beyond, the frictional force of the inside front tire is offset with only the braking force, and this determines the vehicle's cornering limit. Due to this, applying right-and-left torque vectoring to the rear wheels is not effective at all in improving the vehicle's cornering limit. Applying torque vectoring control to the front wheels optimizes the distribution of braking force, thus improving the front wheels' lateral acceleration limit and the vehicle's maximum lateral acceleration limit. If the control is applied to the front and rear wheels, the negative yaw moment generated by the front wheels is offset by the positive yaw moment generated by the rear wheels. This expands the front wheels' lateral acceleration limit and slightly improves the vehicle's cornering limit.

To summarize, on FWD vehicles, application of right-and-left torque vectoring control to the front wheels effectively expands the cornering limit. The required maximum vectoring torque is approximately 500 N·m.

5.2 RWD vehicle

Fig. 9 to Fig. 12 show the results of calculations for RWD vehicles. In the longitudinal acceleration region of 0 to 0.5 m/s², longitudinal load shift causes the front wheels to reach the maximum lateral acceleration limit before the rear wheels do. Because of this, applying right-and-left torque vectoring to the rear wheels to generate yaw moment improves the vehicle's cornering limit, but only slightly. Then, in the longitudinal acceleration region of 0.5 m/s² and above, the frictional force of the inside rear tire is offset with only the driving force, and this determines the vehicle's cornering limit. Application of torque vectoring control to the front wheels is not effective at all while its application to the

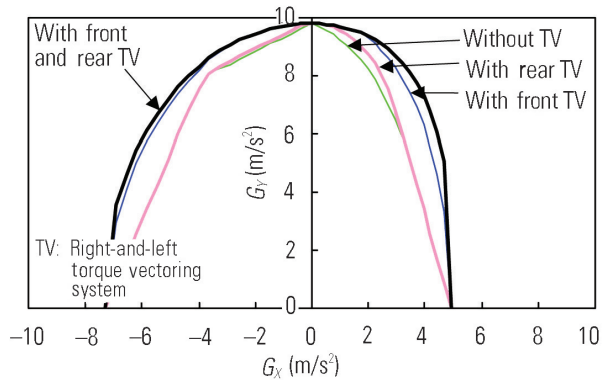


Fig. 5 Vehicle dynamics limit with FWD

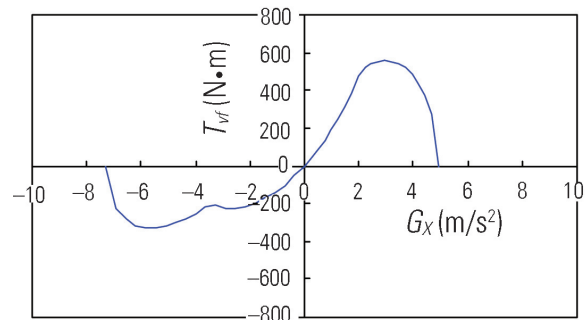


Fig. 6 Front wheel right-and-left vectoring torque

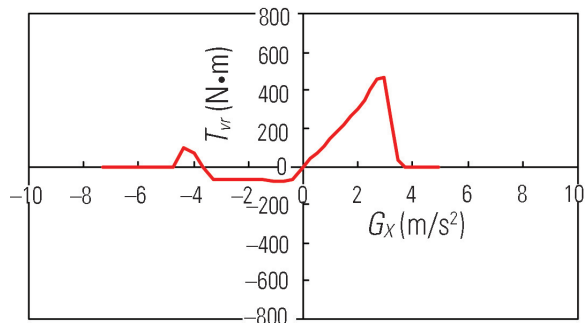


Fig. 7 Rear wheel right-and-left vectoring torque

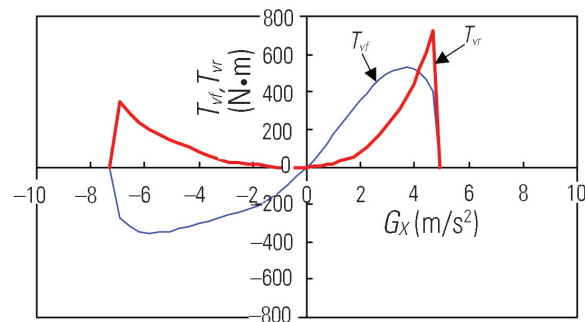


Fig. 8 Front and rear wheel right-and-left vectoring torque

rear wheels is fairly effective. The required maximum vectoring torque in this case is approximately 400 N·m (Fig. 11). With the control applied to the front and rear

wheels, the positive yaw moment generated by the rear wheels, which lowers the lateral acceleration limit for the rear wheels, is balanced by the negative yaw moment generated by the front wheels, improving the vehicle's cornering limit. The required maximum vectoring torque between the front wheels in this case, however, is as much as around 800 N·m (Fig. 12).

In the longitudinal deceleration region of 0 to -0.5 m/s^2 , the rear wheels reach the lateral acceleration limit before the front wheels do and the vehicle's cornering limit can be expanded equally by applying torque vectoring control to either the front or rear wheels. In the longitudinal deceleration region of -0.5 m/s^2 and beyond, the frictional force of the inside rear wheel is offset with only the braking force, and this determines the vehicle's cornering limit. In this case, applying right-and-left torque vectoring control to the front wheels is not effective at all while its application to the rear wheels is effective. Applying the control to the front and rear wheels is more effective, however, this requires a substantial amount of vectoring torque as with the case of accelerating while cornering.

To summarize, on RWD vehicles, application of right-and-left torque vectoring to the rear wheels is effective in raising the vehicle's cornering limit. The required maximum vectoring torque is approximately 400 N·m.

5.3 AWD vehicle

Fig. 13 to Fig. 16 show the results of calculations for AWD vehicles. In each case, the calculations are based on the calculated optimum driving force distribution between the front and rear wheels that achieved the highest cornering limit.

In the longitudinal acceleration region, the front and rear wheels always reach the lateral acceleration limit at the same time due to optimized driving force distribution between the front and rear wheels. As a result, a smooth curve of cornering limit has been plotted. In addition, the cornering limit is expanded across the entire acceleration range no matter which pair of wheels, front or rear, right-and-left torque vectoring control is applied to. The calculations in our study indicate that the control is slightly more effective when it is applied to the rear wheels than to the front wheels. The required maximum vectoring torque is approximately 500 N·m when the control is applied to the front wheels (Fig. 14), and approximately 400 N·m when it is applied to the rear wheels (Fig. 15). Therefore, the cornering limit can be expanded more efficiently by applying the control to the rear wheels. Application of the control to both the front and rear wheels is more effective on AWD vehicles than on FWD and RWD vehicles.

In the longitudinal deceleration region of 0 to -5 m/s^2 , without right-and-left torque vectoring, the rear wheels reach the lateral acceleration limit before the front wheels do. In the deceleration region of -5 m/s^2 and beyond, the front and rear wheels reach the lateral acceleration limit at the same time as in the case of accelerating while cornering. Therefore, as in acceleration, the cornering limit can be expanded throughout

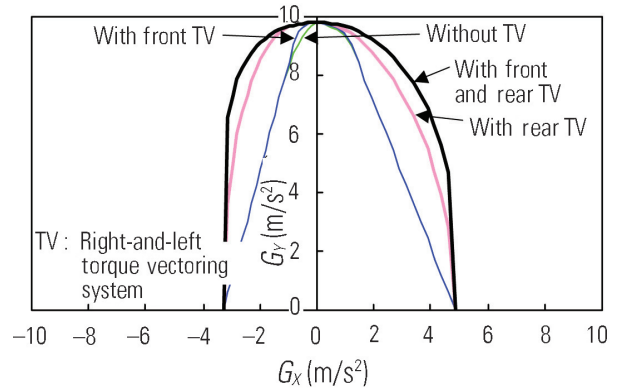


Fig. 9 Vehicle dynamics limit with RWD

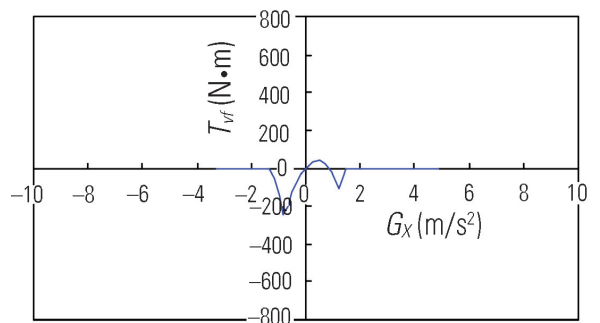


Fig. 10 Front wheel right-and-left vectoring torque

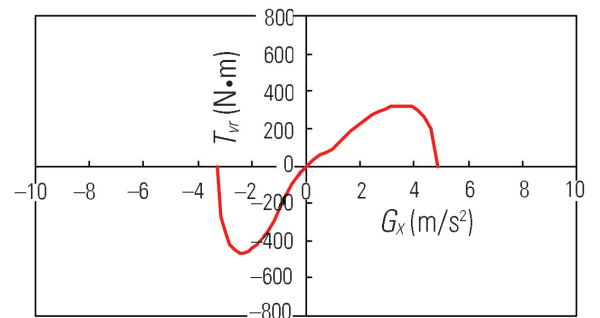


Fig. 11 Rear wheel right-and-left vectoring torque

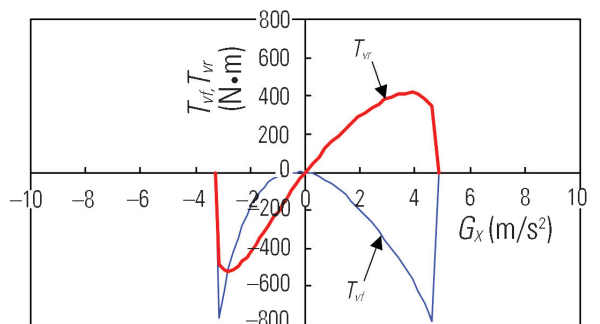


Fig. 12 Front and rear wheel right-and-left vectoring torque

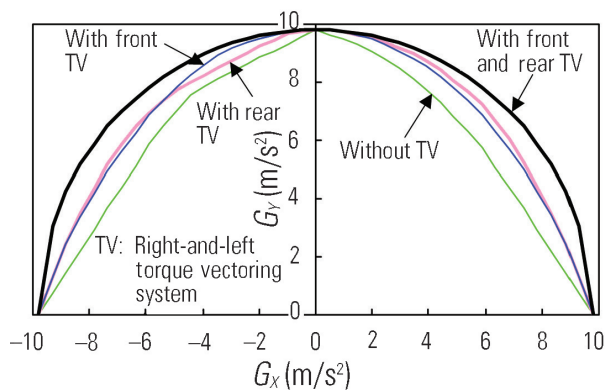


Fig. 13 Vehicle dynamics limit with AWD

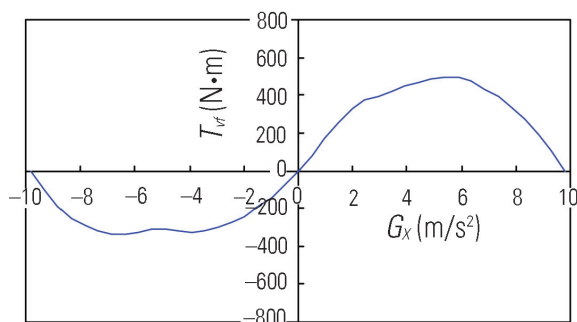


Fig. 14 Front wheel right-and-left vectoring torque

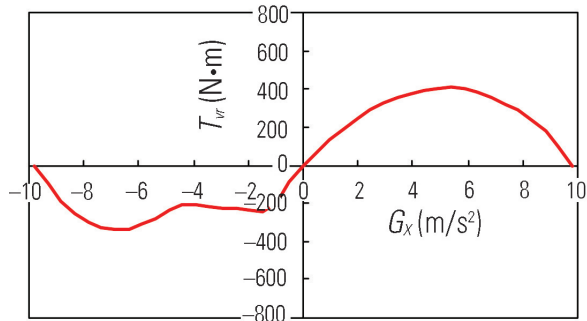


Fig. 15 Rear wheel right-and-left vectoring torque

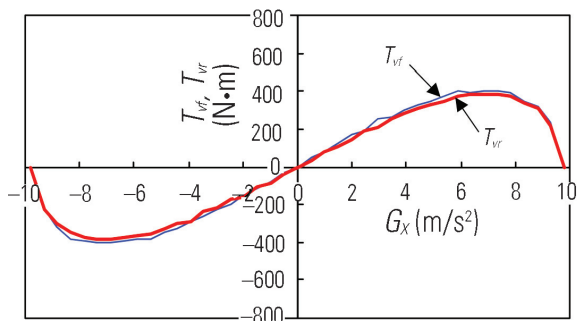


Fig. 16 Front and rear wheel right-and-left vectoring torque

the entire deceleration range by applying right-and-left vectoring control to either the front wheels or the rear wheels. The improvement is substantial when the control is applied to both the front and rear wheels.

To summarize, on AWD vehicles, it is most effective to apply right-and-left torque vectoring control to both the front and rear wheels. If the control is to be applied to either the front or rear wheels in order to avoid system complexity, it is preferable to apply it to the rear wheels, since this results in a greater improvement in cornering limit with a smaller vectoring torque.

6. Summary

This paper discussed equations representing the functions of the right-and-left torque vectoring system, its applicability to non-driving wheels and its effect on the vehicle's cornering limit. The system was adapted to the dynamic square analysis method to calculate its effectiveness in expanding the vehicle's cornering limit for each drive type, and the following results were obtained.

The system is most effective when applied to the front wheels on FWD vehicles and to the rear wheels on RWD and AWD vehicles.

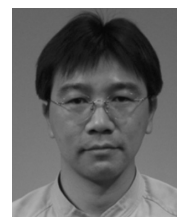
The calculation method used in this study is useful in determining the required maximum vectoring torque for a right-and-left torque vectoring system.

References

- (1) Kaoru Sawase, Application of Active Yaw Control to Vehicle Dynamics by Utilizing Driving/Braking Force, Society of Automotive Engineers of Japan Symposium No. 9702, 9730894
- (2) Ikushima and Sawase: A study on the effect of active yaw moment control, SAE Paper 950303, 1995
- (3) Mohan: Torque vectoring systems: Architecture, stability performance and efficiency considerations, 6th All-Wheel Drive Congress Graz, 2005
- (4) Weals et al.: SUV demonstration of a torque vectoring driveline and new concepts for practical actuation technologies, JSAE annual congress, No. 38-05 194, 2005
- (5) Masatsugu Arai et al., "Development of a Motorized Direct Yaw-moment Control System (1st Report)", JSAE20075252, Preprints of Meeting on Automotive Engineers, 2007
- (6) Kato et al.: Study on vehicle dynamics in marginal condition using dynamic square method, SAE IPC-8, 9531020, 1995



Kaoru SAWASE



Yuichi USHIRODA



Development of Integrated Vehicle Dynamics Control System 'S-AWC'

Takami MIURA* Yuichi USHIRODA* Kaoru SAWASE*
Naoki TAKAHASHI* Kazufumi HAYASHIKAWA**

Abstract

The Super All Wheel Control (S-AWC) for LANCER EVOLUTION X is an integrated vehicle dynamics control system for handling the Active Center Differential (ACD), Active Yaw Control (AYC), Active Stability Control (ASC) and Antilock Brake System (ABS). It is based on the All Wheel Control (AWC) philosophy advocated by Mitsubishi Motors Corporation (MMC). To ensure predictable handling and a high performance margin, the S-AWC system calculates the yaw moment by using the yaw rate feedback control and distributes the yaw moment to each component taking into consideration its characteristics. S-AWC can improve the vehicle cornering performance seamlessly at various driving conditions.

Key words: Four Wheel Drive (4WD), Vehicle Dynamics, Integrated Control

1. Introduction

The All Wheel Control (AWC) is a MMC's four-wheel dynamic control philosophy for maximally exploiting the capability of all four tires of a vehicle in a balanced manner to realize predictable handling and high margin of performance, which in turn yield the driving pleasure and utmost safety that MMC sees as fundamentals in producing vehicles.

The Super All Wheel Control (S-AWC) is an integrated vehicle dynamics control system that combines various components based on the four-wheel drive (4WD) control, and controls all components integrally to embody the AWC philosophy⁽¹⁾.

The S-AWC system on the LANCER EVOLUTION X delivers all of the following functions under integrated control: Active Center Differential (ACD)⁽²⁾, Active Yaw Control (AYC)⁽³⁾, Active Stability Control (ASC)⁽⁴⁾, and Antilock Brake System (ABS). As shown in Fig. 1, by adding braking control to the ACD-AYC combination, which has superior controllability among the currently existing 4WD systems, the S-AWC can control both the driving and braking forces and so handle both longitudinal and lateral behavior of the vehicle. As a result, the S-AWC seamlessly improves the vehicle's dynamic performance for various vehicle operations such as acceleration, deceleration and cornering.

This paper introduces the S-AWC system focusing on the integrated driving and braking force control using the yaw rate feedback control technology, which is the most remarkable feature of the system.

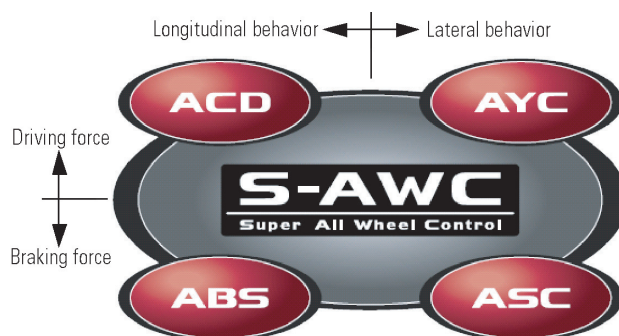


Fig. 1 Components of S-AWC

2. Consideration and selection of system configuration

2.1 Basic control method

The aim of the S-AWC system is to achieve both predictable handling and high margin of performance.

Predictable handling means changing the vehicle direction faithfully according to the driver's intentions, in other words, the vehicle exactly follows the driver's steering operations. High margin of performance, on the other hand, means keeping the vehicle direction without being affected by disturbances, in other words, restraining vehicle's behavioral changes that are not caused by the driver's steering operations.

Although these two characteristics appear different, they are similar in that they both require the vehicle's behavior to match the driver's steering operation, and can be achieved simultaneously by minimizing the difference between the target vehicle behavior calculated from the steering wheel angle and the actual vehicle behavior.

* Drivetrain Engineering Dept., Development Engineering Office

** Chassis Design Dept., Development Engineering Office

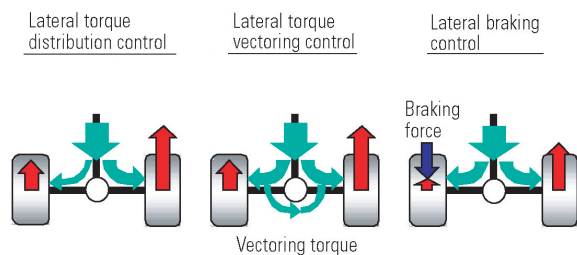


Fig. 2 Various types of direct yaw moment control

To achieve this, the S-AWC system adopts yaw rate feedback control as basic control method, in which the vehicle behavior (target yaw rate) calculated from such parameters as the steering wheel angle is compared with the actual vehicle behavior (actual yaw rate) given by the yaw rate sensor to determine the target amount of control to be provided by the system.

2.2 Components

To make the yaw rate feedback control work effectively, it is necessary to control the yaw moment acting on the vehicle most appropriately under various driving conditions.

The types of control that can generate yaw moment include the following: the steering angle control working on the steering system; the roll stiffness distribution control working on the suspension system; the longitudinal torque distribution control and the lateral torque difference control working on the drive train; and the lateral braking control. The steering angle control can effectively generate yaw moment in the linear region of the tire characteristics, but it cannot generate sufficient moment in the nonlinear region of the tire characteristics. The roll stiffness distribution control can indirectly control the yaw moment, but its effect is limited to the nonlinear region of the tire characteristics. Similarly, the longitudinal torque distribution control is effective only in the nonlinear region of the tire characteristics. On the other hand, the direct yaw moment control that uses the difference in driving and braking forces between the left and right wheels can generate yaw moment in both the linear and nonlinear regions of the tire characteristics⁽⁵⁾.

There are three types of direct yaw moment control technology currently available, as shown in Fig. 2.

The lateral torque distribution control unequally distributes the engine torque to the left and right wheels. The resulting difference in driving torque between the left and right wheels generates the yaw moment. This control, therefore, cannot effectively generate the yaw moment during cruising or deceleration when the engine torque is not large enough.

The lateral torque vectoring control transfers the torque from the left wheel to the right wheel, and vice versa, to generate an amount of braking torque on one wheel while generating the same amount of driving torque on the other wheel. The control of this type,

therefore, can generate the yaw moment at any time regardless of the engine torque. Another merit of this control is that it does not affect the total driving and braking forces acting on the vehicle, which means that the control does not conflict with acceleration and deceleration operations by the driver. Although this control affects the steering reaction force when applied to the front wheels, it does not produce any adverse effects when applied to the rear wheels.

The lateral braking control applies different braking forces to the four wheels independently so as to produce a difference in braking force between the left and right wheels, which generates the yaw moment. As this control uses braking forces, it feels to the driver like deceleration, but the control is effective because it can generate yaw moment under a wide range of conditions of vehicle operation.

In view of the characteristics of these three yaw moment control technologies, a combination of the lateral torque vectoring control applied to the rear wheels and the lateral braking control is the most effective way of providing the yaw rate feedback control seamlessly under varying vehicle driving conditions from acceleration to deceleration. The AYC differential introduced by MMC to its products in 1996 is the world's first component to use lateral torque vectoring control. The braking control can be achieved by using ASC or other existing brake control systems.

For the reasons mentioned above, the S-AWC system consists of ACD, AYC, ASC, and ABS. This configuration is based on the LANCER EVOLUTION IX's system to which the braking control system is added.

3. Configuration and features

Fig. 3 shows the general configuration of the S-AWC system installed into the LANCER EVOLUTION X.

The system has the S-AWC controller, which acts as the master controller. It controls the ACD transfer (longitudinal differential limiting control), AYC differential (lateral torque vectoring control), and brakes integrally by giving commands to the ACD/AYC hydraulic unit and ASC/ABS unit.

For communications between the S-AWC controller and ASC/ABS unit, an independent controller area network (CAN) is used to be able to process large amounts of information at high speed. In addition, the ASC/ABS unit incorporates brake pressure sensors for each of the four wheels and linear valves to ensure smooth and accurate braking control. These ensure precise and highly responsive integrated control.

In addition to the sensors used in the LANCER EVOLUTION IX (steering wheel angle sensor, longitudinal acceleration sensor, lateral acceleration sensor, wheel speed sensors for four wheels, accelerator position sensor, etc.), the yaw rate sensor (integrated yaw and G sensor) is adopted for providing information for yaw rate feedback control. Another feature of the system is the additional sources for such information as the engine torque, engine speed and brake pressure, which all allow the vehicle acceleration and deceleration states

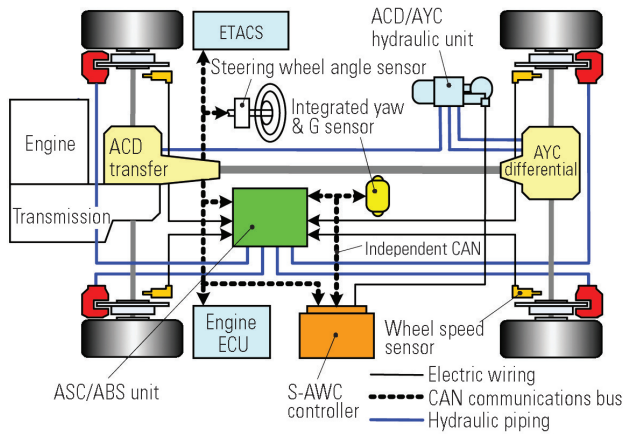


Fig. 3 System configuration

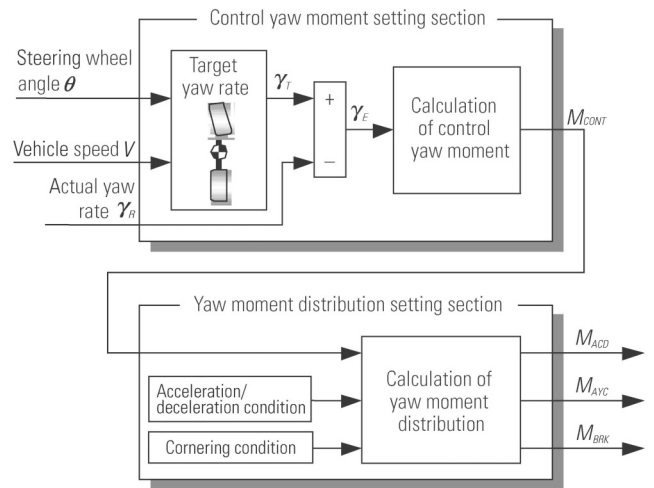


Fig. 4 Control diagram

Table 1 Comparison of component characteristics

		In improving cornering	In restraining cornering
During acceleration	Longitudinal differential limiting control	—	★
	Lateral torque vectoring control	★★★	★★
	Braking control	★	★
During deceleration	Longitudinal differential limiting control	—	★
	Lateral torque vectoring control	★★	★
	Braking control	★★	★★★

★: Control effect

to be quickly and accurately identified, and thus for the control response to be improved.

4. Outview of system control

Table 1 summarizes the characteristics of the longitudinal differential limiting control, lateral torque vectoring control, and braking control. The longitudinal differential limiting control has a stabilizing effect on the vehicle when it is likely to spin, in other words, it can restrain cornering. The lateral torque vectoring control works effectively during acceleration, when loads on the rear wheels increase. It is most effective in improving cornering when the torque is transferred to the outer wheels, on which the load increases. The braking control is most effective in restraining cornering during deceleration where it can provide control effects without causing the driver to perceive excessive deceleration. Seamless and high-quality yaw moment control can be achieved by appropriately combining these control effects based on their characteristics. The control logic shown in Fig. 4 is designed in line with this concept.

The control yaw moment setting section in the fig-

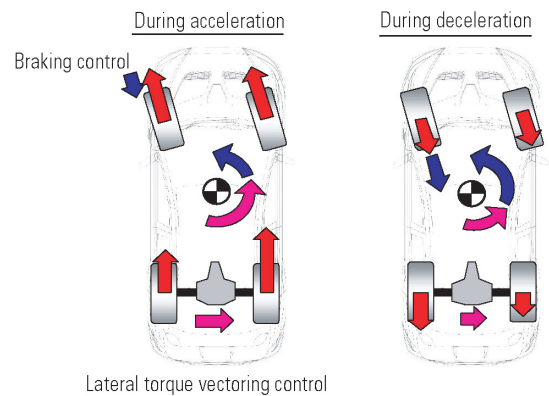


Fig. 5 Yaw moment distribution in improving cornering

ure uses a linear two-wheel model to calculate the target yaw rate γ_r from the steering wheel angle θ and vehicle speed V , and the control yaw moment M_{CONT} to be applied to the vehicle is determined based on the difference γ_e of the target yaw rate γ_r and the actual yaw rate γ_a .

The yaw moment distribution setting section, on the other hand, apportions the control yaw moment M_{CONT} among the longitudinal differential limiting control yaw moment M_{ACD} , lateral torque vectoring control yaw moment M_{AYC} , and the braking control yaw moment M_{BRK} according to the condition of acceleration, deceleration and cornering. For example, when the vehicle's cornering motion is improved, the section increases the distribution of yaw moment to the lateral torque vectoring control during acceleration, whereas it increases the distribution of yaw moment to the braking control during deceleration (Fig. 5). When the vehicle's cornering motion is restrained, on the other hand, the section first increases the distribution of yaw moment to the braking control and then to the longitudinal differential lim-

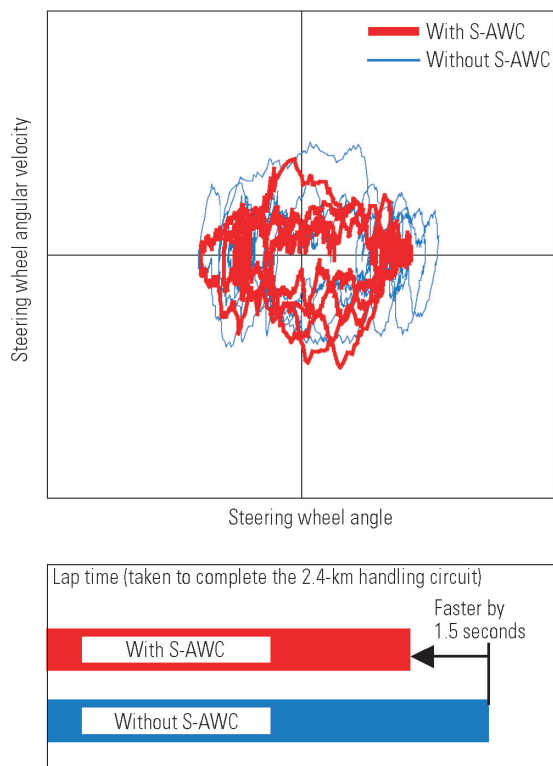


Fig. 6 Result of sporty driving on dry handling circuit

iting control.

Like this example, the system achieves an integrated vehicle dynamics control using the yaw rate feedback by apportioning the yaw moment among the longitudinal differential limiting control, left-right torque vectoring control and the braking control most appropriately according to the characteristics listed in **Table 1**.

5. Vehicle performance

This section describes how the S-AWC demonstrates its effect in an actual vehicle using an example. This example compares the dynamics control results derived from the tests on the same vehicle when it is equipped with the S-AWC (called "With S-AWC" hereafter) and when it is equipped with a control system that simulates the LANCER EVOLUTION IX's system (called "Without S-AWC").

Fig. 6 shows the steering wheel angles and the steering wheel angular velocities plotted on the same graph for when the vehicle was put in sporty driving on a 2.4-km dry handling circuit. It shows that the With S-AWC presented smaller values for both the steering wheel angle and steering wheel angular velocity and that the lap time of the With S-AWC was about 1.5 seconds shorter than the Without S-AWC.

Fig. 7 shows the steering wheel angles and steering wheel angular velocities plotted on the same graph for when the vehicle was turned around a 15-m radius circle as fast as possible on a snow packed road. It shows that the With S-AWC presented substantially smaller

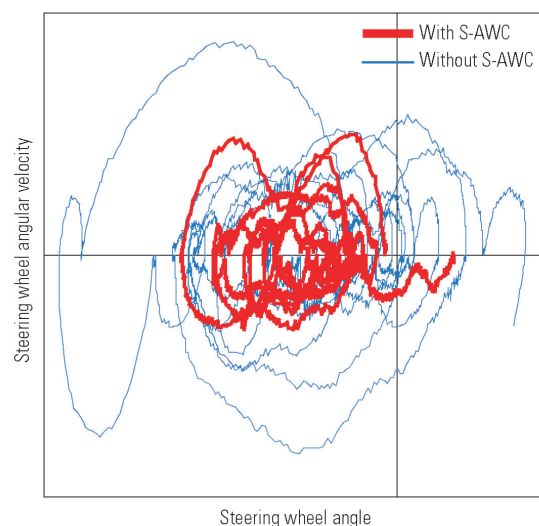


Fig. 7 Result of cornering on a snow packed road

values in both the steering wheel angles and steering wheel angular velocities than the Without S-AWC.

These test results clearly show that the S-AWC improves the vehicle's response to operation of the steering wheel regardless of the road surface conditions and helps drive the vehicle reliably at faster speeds with less operation of the steering wheel. In other words, the S-AWC system improves the cornering performance, stability and controllability of the vehicle.

6. Conclusion

With the integrated vehicle dynamics control capability realized using the yaw rate feedback control as the base technology, the S-AWC system on the LANCER EVOLUTION X has succeeded in dramatically improving the vehicle dynamics performance under various driving conditions, thereby achieving both predictable handling and high margin of performance.

MMC will continue to evolve the S-AWC system by adding novel components and improving the control logic, aiming to improve the dynamics performance of our products even further.

References

- (1) Kaoru Sawase, Yuichi Ushiroda, Takami Miura, "Left-Right Torque Vectoring Technology as the Core of Super All Wheel Control (S-AWC)", Mitsubishi Motors Technical Review, No. 18, pp. 16 – 23, 2006
- (2) Kaoru Sawase, et al., "Development of Center-Differential Control System for High-Performance Four-Wheel Drive Vehicles", Mitsubishi Motors Technical Review, No. 13, pp. 61 – 66, 2001
- (3) Kaoru Sawase, et al., "Development of the active yaw control system", Journal of Society of Automotive Engineers of Japan, Vol. 50, No. 11, pp. 52 – 57, 1996
- (4) Shunzo Tanaka, et al., "Development of Vehicle Cornering Control System Utilizing Driving/Braking Force Differences between Right and Left Wheels", Mitsubishi Motors Technical Review, No. 9, pp. 32 – 43, 1997

- (5) Sumio Motoyama, Keiji Isoda, Masayoshi Osaki, "Study on quantitative evaluation method for yawing control potential", Journal of Society of Automotive Engineers of Japan, Vol. 50, No. 11, pp. 95 – 99, 1996



Takami MIURA



Yuichi USHIRODA



Kaoru SAWASE



Naoki TAKAHASHI



Kazufumi HAYASHIKAWA



New 4B11 Turbocharged Engine

Yoshihiko KATO* Kenta TOHARA* Hiromi AKEBO*

Abstract

Mitsubishi Motors Corporation (MMC)'s newly developed inline 4-cylinder turbocharged engine for the LANCER EVOLUTION X is introduced. This new 4B11 turbocharged engine (2 L) attained the 12.5 kg weight reduction thanks to an aluminum die-cast cylinder block and direct-acting valve train. A variable valve timing device MIVEC (Mitsubishi Innovative Valve-timing Electronic Control System) is equipped not only at the intake side but also at the exhaust side in this engine. This makes it possible to set the best valve timing for overall engine speed and improve performance, fuel economy and exhaust emissions. Furthermore, the low- and middle-speed torque and the response are dramatically improved by reducing pressure drops in the intake and exhaust systems and by revising the turbocharger specifications. Regarding environmental aspects, this engine achieved the 50 % reduction level (3☆) requirements of Japan's 2005 Emission Standard by means of a high-performance metal catalyst, etc.

Key words: Gasoline Engine, MIVEC, Turbocharger, J-ULEV

1. Objectives of the development

The main objective set forth for the development of the 4B11 engine was creating a new turbocharged engine that is excellent in performance while meeting the needs of the times for environmental compatibility. In line with this objective, an aluminum die-cast cylinder block was newly developed with the aim of reducing the weight of the engine. The cylinder block in development also featured a rear exhaust layout, which is the first of its kind to be introduced for MMC turbocharged engines. The measures employed for better fuel economy included the Mitsubishi Innovative Valve-timing Electronic Control System (MIVEC) and a high-efficiency alternator. Started by setting "superiority of performance in the motor sports field" as one of the concepts to be embodied in the engine, the development had generous technical feeds from the motor sports know-how or DNA that MMC had cultivated and accumulated through World Rally Championship (WRC) experiences. This know-how was incorporated into this production engine.

2. Major specifications

Table 1 compares the major specifications of the two MMC turbocharged engine models, the new 4B11 and the previously developed 4G63.

3. Features

The following part of this section introduces the technologies and components adopted to attain the above-mentioned objectives of the development. Many of the technology and component items contribute to two or more improvements as shown in **Table 2**.

3.1 High performance engine consuming less fuel

The technologies adopted to undertake the challenge of creating a high performance engine consuming less fuel included the MIVEC system applied to both intake and exhaust valve mechanisms (this configuration of the MIVEC system was first employed in the 4B1 model engines) and optimization in the shape of the intake manifold as well as of the intake and exhaust ports. Adoption of these technologies provided the effect of distributing an equal amount of air to every cylinder, which in turn enabled the idling speed to be lowered without compromising the high-speed performance of the engine. In addition, the use of an aluminum die-cast cylinder block with improved cooling efficiency made it possible to further advance the ignition timing and consequently to reduce the fuel consumption rate. Also, the friction-caused loss of energy was reduced by the use of full-floating piston pins and through-holes made in the bulkhead of the cylinder block to lower pressure in the crankcase. Another improvement adopted for higher fuel economy was the use of a high-efficiency alternator, the first of its kind to be used by MMC. On the one hand, while it brought about higher vehicle performance, the application of these improvements, on the other hand, successfully achieved a fuel economy level equivalent to or higher than that of the LANCER EVOLUTION IX MR, despite the LANCER EVOLUTION X being 100 kg heavier than the former model.

Fig. 1 shows the performance curves of the engines on these two vehicle models.

3.2 Weight reduction and durability

The 4B11 engine has an aluminum die-cast cylinder block of reduced weight. The biggest challenge with regard to the employment of this aluminum die-cast

* Engine Designing Dept., Development Engineering Office

Table 1 Major specifications

		LANCER EVOLUTION X	LANCER EVOLUTION IX MR (Reference)
		4B11 (2.0 L)	4G63 (2.0 L)
Displacement	(cc)	1,998	1,997
Cylinder bore	(mm)	86	85
Stroke	(mm)	86	88
Stroke/bore (S/B) ratio		1.00	1.04
Bore to bore pitch	(mm)	96	93
Big-end to small-end length of connecting rod	(mm)	143.75	150
Compression ratio		9.0	8.8
Red zone speed/over-revolution fuel cut speed		7,000 / 7,600	
Fuel used		Unleaded premium gasoline	
Turbocharger		TD05HA-152G6-12T Titanium-aluminum alloy turbine wheel and aluminum alloy compressor wheel combination	TD05HRA-155G6C-10.5T Titanium-aluminum alloy turbine wheel and aluminum alloy compressor wheel combination
	Option	TD05H-152G6-12T Inconel turbine wheel and aluminum alloy compressor wheel combination	TD05HRA-155G6mC-10.5T Titanium-aluminum alloy turbine wheel and magnesium alloy compressor wheel combination
Cylinder block material		Aluminum die-casting	Cast iron
Camshaft drive		Silent chain-driven	Timing-belt-driven
Valve train		Direct-acting DOHC, 16 valves, continuously variable MIVEC applied to both intake and exhaust systems	Roller rocker arm DOHC, 16 valves, continuously variable MIVEC applied to intake system
Balancer shaft		None	Secondary balancer
Exhaust system layout		Rear exhaust	Front exhaust
Maximum torque	(N·m/min ⁻¹)	422 / 3,500	400 (GSR), 407 (RS) / 3,000
Maximum output	{kW(PS)/min ⁻¹ }	206 (280) / 6,500	206 (280) / 6,500
Compliance with exhaust emissions control standard		50 % reduction level (3☆) requirement of Japan's 2005 Emissions Standard	Japan's 2000 Emissions Standard
Engine weight reduction		△12.5 kg*	Base weight

* Reduction in weight of engine main body (not including intake and exhaust system parts)

Table 2 Adopted technologies and their purposes

Technology/component	High performance, low fuel consumption	Compactness, light weight	Low emissions	Low NVH	High reliability
Aluminum die-cast cylinder block		○			
Four-bolt fastened bearing cap	○				○
Semi-closed deck design	○				○
Continuously variable valve timing system (MIVEC) on intake and exhaust sides	○		○	○	
Equal-length, short-port aluminum intake manifold	○	○			
Rear exhaust engine layout	○	○	○		
Compact-size, large capacity, fine spray injector	○		○		
Disuse of balancer shaft		○			
Fuel system refinement (optimization of control fuel pressure)	○		○		
Use of long-reach M12 ignition plug	○				○
High-efficiency alternator	○			○	
High-performance metal catalyst	○		○		

cylinder block was to ensure strength sufficiently durable against operational stress while reducing the weight. The first measure to make this possible was fastening each of all the five bearing caps to the cylinder block with four bolts to assure strength enough to withstand high output operation of the engine. The second measure was the application of a semi-closed

shape top deck with bridges to the cylinder block to minimize the bore deformation of the cylinders under stress of high-output operation. Furthermore, a ladder frame structure was applied to the cylinder block, which greatly contributed to the reduction in noise, vibration and harshness (NVH). **Fig. 2** shows the structure of the cylinder block.

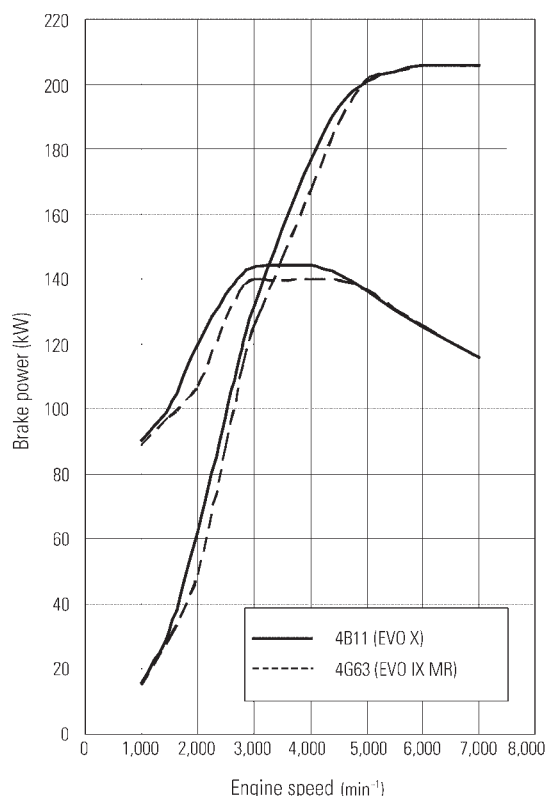


Fig. 1 Engine performance

In addition to the above, other weight reduction measures were also applied, examples of which are the adoption of a direct-acting valve train and the disuse of balancer shafts. As a result, the weight of the new engine mechanism could be successfully reduced by as much as 12.5 kg compared with the 4G63 turbocharged engine.

3.3 Low exhaust emissions

The technologies adopted for simultaneously satisfying high performance and low exhaust emission requirements were compact-size fine spray injectors and optimization of fuel line pressure. Application of these technologies enabled improved fuel atomization while maintaining necessary fuel flow rate during high-output operation and eventually ensured clean exhaust emissions while the engine stayed capable of delivering high power. Using these technologies in combination with the rear exhaust layout and a high-performance metal catalyst featuring a shorter activation time, the new engine successfully reduced exhaust emissions of the EVOLUTION X to a level as low as less than 1/4 of the EVOLUTION IX, achieving the 50 % reduction level (3☆) requirements of the Japan's 2005 Emission Standard.

3.4 Improved engine response

An engine's "high performance" is most often represented by large maximum output and torque. In the motor sports field, the engine response is another important performance factor. The 4B11 engine incorporates such improvements as an optimally shaped tur-

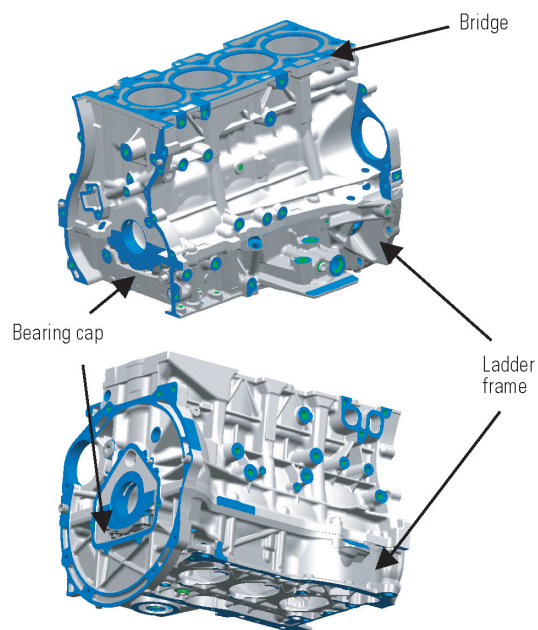


Fig. 2 Cylinder block structure

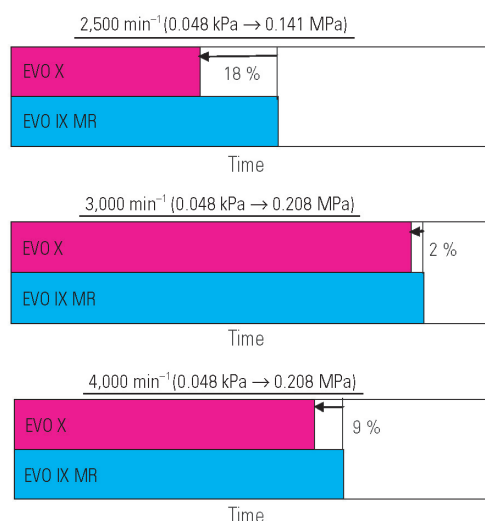


Fig. 3 Engine response

bocharger compressor wheel, a straight type intake system and large diameter exhaust system piping featuring heightened response performance which is up to 18 % faster to respond to accelerator operation than the 4G63 turbocharged engine. **Fig. 3** compares the engine response characteristics of the LANCER EVOLUTION X and LANCER EVOLUTION IX MR. **Fig. 4** shows the details of the compressor wheel improvement.

3.5 Higher reliability

Unlike the 4G63 turbocharged engine which uses M14 long-reach spark plugs, the 4B11 turbocharged engine uses M12 long-reach spark plugs that enable the water jackets around the combustion chambers to be expanded for more efficient cooling. This, coupled with the highly heat-conductive aluminum cylinder block,

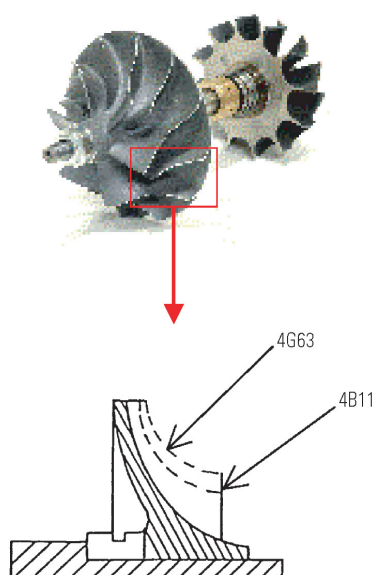


Fig. 4 Compressor wheel improvement

lowers the fire-contact surface temperature of the new engine by approximately 50 °C compared with the 4G63 engine, greatly reducing the thermal load upon the cylinder head. Fig. 5 shows cross sectional views of the cylinder head.

4. Conclusion

Exhaust emissions, fuel economy and other environmental performances of the engine will further increase their importance in the future. The situation will thus certainly impose a challenge of simultaneously nurturing to a still higher level two contradicting factors, namely high performance and environmental compatibility in order for us to make the next evolutionary step in engine development.

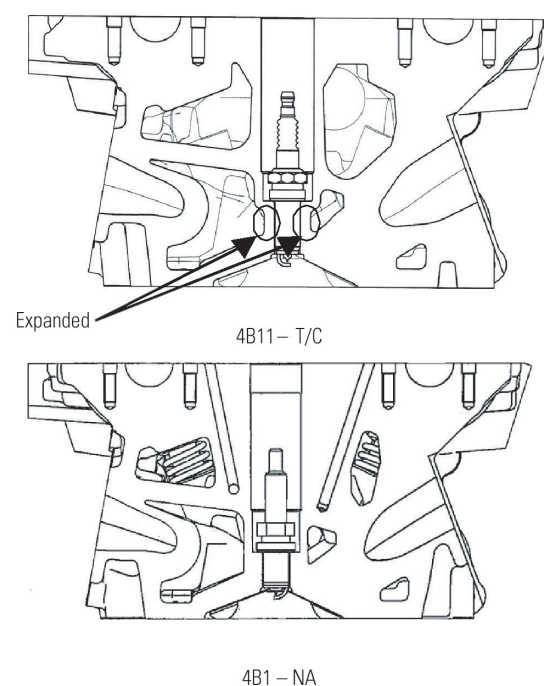
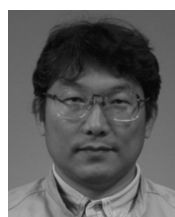


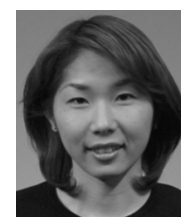
Fig. 5 Cylinder head cross section



Yoshihiko KATO



Kenta TOHARA



Hiromi AKEBO



Newly Developed Twin Clutch SST (Sport Shift Transmission)

Takao KIMURA* Takashi SASAKURA* Kunishige HAYASHI*

Abstract

This paper describes the newly developed Twin Clutch Sport Shift Transmission (TC-SST) used in the LANCER EVOLUTION X. In the Twin Clutch SST (the first transmission of its kind to be used by Mitsubishi Motors Corporation (MMC)), a six-speed automated manual transmission in which two automatic clutches are used to realize (a) quick gearshifts and a concomitantly good acceleration feeling and (b) highly efficient torque transmission and concomitantly good fuel economy. MMC plans to include the TC-SST in the transmission lineups of future front-engine, front-wheel-drive passenger cars.

Key words: Transmission, Power Train, Clutch, Hydraulic System

1. Objective of the development

The Twin Clutch Sportronic Shift Transmission (hereinafter referred to as TC-SST) was developed with the following as key concepts:

- (1) Quicker gear shifting than conventional automatic transmissions (A/Ts) with the same or better gearshift smoothness
- (2) Fuel economy as good as in manual transmissions (M/Ts)
- (3) Off-the-line acceleration performance as good as in M/Ts

For each of these concepts, the objectives for achievement in the development were set based on the needs and benchmarks of the vehicles that were slated to be equipped with the TC-SST.

The TC-SST has two electro-hydraulically controlled clutches; one connects to an odd-number gear set, i.e., the 1st, 3rd and 5th gears and the other to an even-number gear set, i.e., the 2nd, 4th and 6th gears. Either of these two clutches is used at any given time to connect power to a selected gear. Before the working clutch is switched from one to the other, the control system determines the gear to be used next and engages that gear (pre-shift gear engagement). The system then disengages the first clutch and engages the second clutch at the most appropriate timing while controlling the engine torque so that the gear shifting will take place most smoothly and the fuel economy and off-the-line acceleration performance will be made high enough to be comparable to or better than those offered by five-speed M/Ts (Table 1).

2. Basic structure

Table 2 compares the specifications of the TC-SST and those of the five-speed A/T used in an MMC vehicle model. Despite its larger coupled engine's torque compared with the five-speed A/T, the TC-SST is shorter in overall length and lighter in weight, meaning that it has

Table 1 Adopted technologies and their purposes

Items \ Purpose	Shift Q up efficiency	High fuel	Driveability up weight	Small or light	NVH decrease
Cooperation with engine	Yes	Yes	Yes		
Wide gear spread		Yes	Yes		
Short length with multi shaft				Yes	
Use ball or roller bearing as much as possible		Yes	Yes		
Floating of center bearing of the shaft supported with 3 points		Yes	Yes		
Press fit of gear and shaft				Yes	Yes
Variable control of line press		Yes			
Use many linear solenoids	Yes				
Optimization of clutch slip control	Yes				Yes
Optimization of Pre-shift	Yes				
Precise adaptive control of the piston engagement point or pre-filling	Yes	Yes			

improved characteristics for installation on vehicles.

Fig. 1 shows a cross-sectional view of the TC-SST. Fig. 2 is a skeleton diagram of the TC-SST.

There are two hydraulically controlled, wet type multiple-disc clutches of the same diameter. They are coaxially arranged, the one being installed on a hollow shaft that drives the odd-number gears and the other on a solid shaft that drives the even-number gears. Compared with A/Ts and continuously variable transmissions (CVTs) using torque converters, the TC-SST gives less feel of slip and offers direct response to accelerator operations comparable to M/Ts.

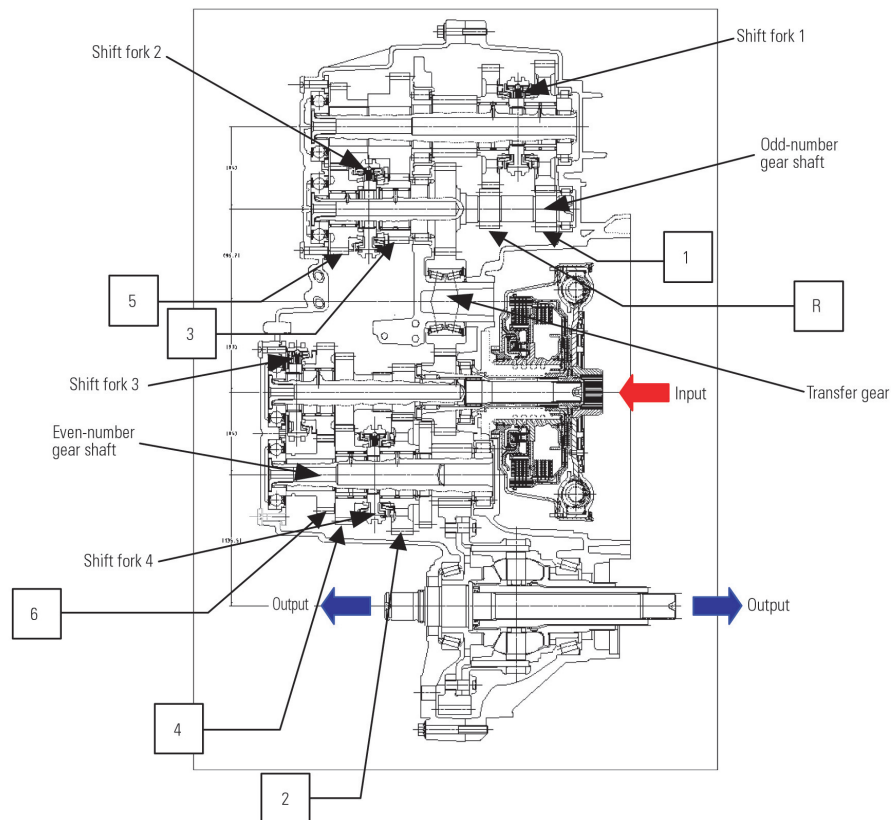
Another feature of this clutch system is the use of long-travel damper springs. By properly setting the inertia working on both ends of the springs, the clutches operate smoothly with low vibration noise.

The gear unit of the TC-SST has a total of six speed gears; the three (1st, 3rd and 5th) of them and the reverse gear are installed on the odd-number gear shaft

* Drivetrain Engineering Dept., Development Engineering Office

Table 2 TC-SST specifications

Model name		W6DGA (TC-SST)	W5A5A (A/T for LANCER EVO wagon MR)
Overall length (mm)		385	418
Power transmission system (Engine to transmission)		Wet multiple-disc clutch (two clutch sets)	Torque converter
Coupled engine's torque (N-m)		422	343
Gear ratios	1st	3.655 (14.848)	3.789 (12.633)
	2nd	2.368 (9.621)	2.057 (6.860)
	3rd	1.754 (7.127)	1.421 (4.737)
	4th	1.322 (5.372)	1.000 (3.333)
	5th	1.008 (4.097)	0.731 (2.437)
	6th	0.775 (3.148)	—
Final reduction ratio		4.062	3.333
Mass (dry) (kg)		98	108

**Fig. 1 TC-SST cross-sectional view**

and the remaining three gears (2nd, 4th and 6th) are installed on the even-number gear shaft, forming a combination of two three-speed M/Ts. This arrangement with the odd-number speed gears installed on a shaft different from the shaft for the even-number gears with a transfer gear in between significantly reduces the overall length of the transmission. Like conventional M/Ts, a synchromesh mechanism using the shift fork to slide the synchronizer sleeve is employed for shifting gears. The shift fork is operated hydraulically through the hydraulic pistons on both of its ends.

Conventional A/T systems have the control unit

located inside the cabin, separately from the A/T unit. With the TC-SST, the control unit forms an integral part of the TC-SST unit together with various sensors, solenoids and its hydraulic valve body. This contributes to substantial reduction in physical wiring. Furthermore, this makes it possible for the control unit to undergo the process for calibrating the clutch strokes and other unit specific characteristics before the TC-SST leaves the transmission manufacturing factory, which significantly helps to ensure the stable gearshift feeling of the TC-SST (Fig.3).

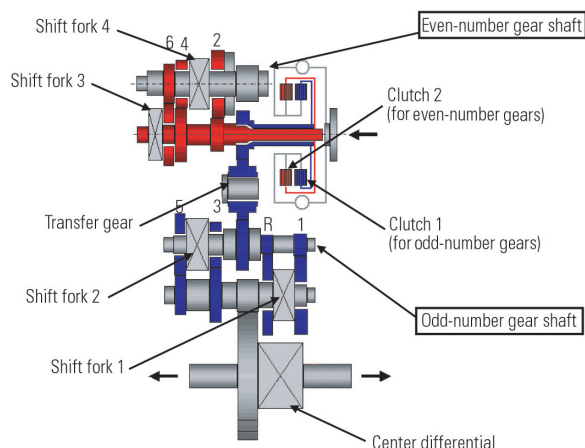


Fig. 2 TC-SST basic structure (1)

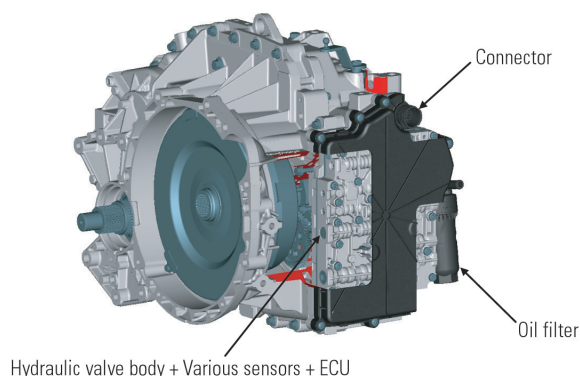


Fig. 3 TC-SST basic structure (2)

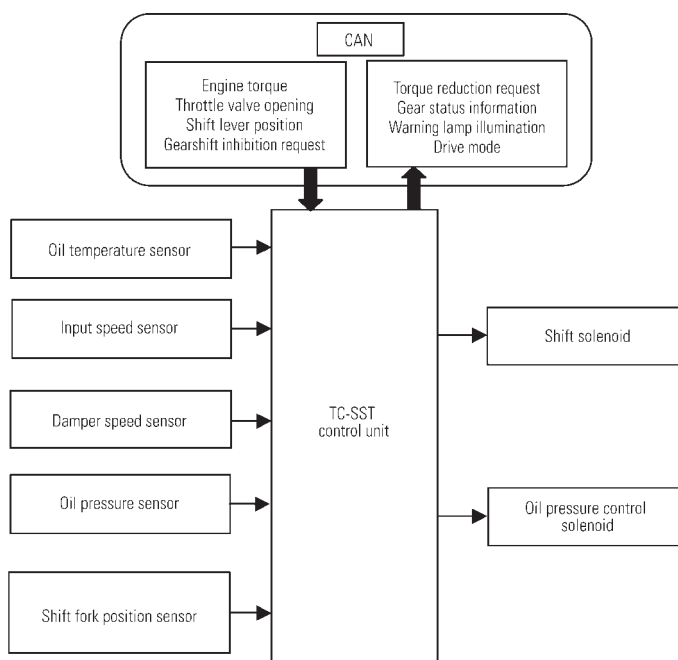


Fig. 4 Control system

3. Outline of TC-SST operation

When the vehicle is to be started in 1st, for example, the 1st gear is brought in mesh with the output shaft by the synchromesh mechanism and then the odd-number gear clutch is engaged to cause the engine torque to be transmitted to the output shaft through the 1st gear. While this process is taking place, the 2nd gear on the even-number gear shaft is brought in mesh with the output shaft by the corresponding synchromesh mechanism. When the conditions for shifting up to 2nd are met, the even-number gear clutch is engaged simultaneously with the disengagement of the odd-number gear clutch in such a way that transmission of engine torque is not interrupted. Likewise, before a shift from 2nd to 3rd takes place, the synchromesh mechanism causes the 3rd gear to mesh with the output shaft while the vehicle is running in 2nd and the 2nd to 3rd gearshift completes when the odd-number gear clutch is engaged simultaneously with disengagement of the even-number gear clutch.

4. Electronic control system

Fig. 4 is a block diagram showing the control system of the TC-SST. Vehicle and engine status data are transmitted through the control area network (CAN), an international standard intra-vehicle communication network, to the TC-SST control unit. The control unit uses these data together with TC-SST internal data to control the TC-SST in a way most suitable for the vehicle condition. When controlling the TC-SST, the control unit adjusts the supply of hydraulic pressures to the four shift forks and two clutches to make these shift forks and clutches operate most appropriately in order to ensure both smooth gear change and quick gearshifts without causing interruption of engine torque transmission.

(1) Creep control

Like A/Ts with a torque converter, the TC-SST allows the vehicle to creep through minute control of the clutch pressure to create a slip-engagement state. The TC-SST control unit makes this control in coordination with the engine control to prevent engine stalls.

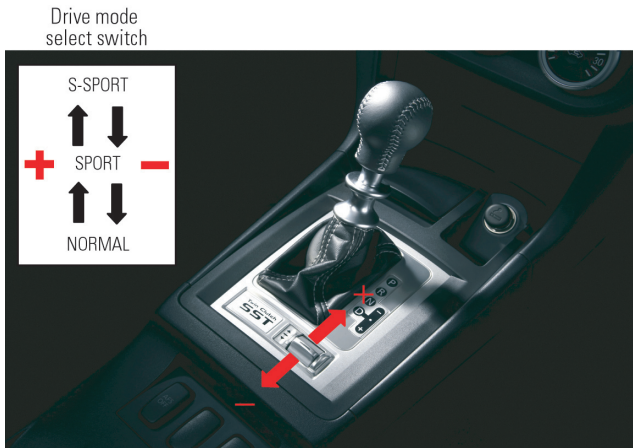
The control unit also takes control to reduce the torque transferred through the clutch to the minimum while the driver is stepping on the brake pedal. This control is effective to improve fuel economy and reduce clutch engagement shock that would result from shift lever operation.

(2) Variable control of line pressure

The TC-SST uses a variable line pressure control system that allows it to precisely adjust the line pressure to the minimum levels necessary for the control of the clutches, as well as lubrication of the clutches and control of gear shifting, while also adjusting it according to oil temperature and other similar conditions. This control keeps the total energy loss of the transmission to a minimum and contributes to

Table 3 TC-SST control modes

Mode	Gear change timing	Gear change time	Accelerator response
Normal	At low engine speed	Standard	Moderately responsive
Sport	At medium engine speed	Short	Responsive
S-Sport	At high engine speed	Very short	Very responsive

**Fig. 5 TC-SST control modes**

improvement in fuel economy.

(3) Clutch slip control

The TC-SST is capable of controlling the clutch slip speed using the selected drive mode, vehicle speed, accelerator position and other factors as parameters. By employing this control, the TC-SST can simultaneously satisfy such contradicting requirements as fuel economy, direct response to accelerator operation and reduced vibration noise.

(4) Pre-shift control (bringing a gear in mesh before clutch engagement)

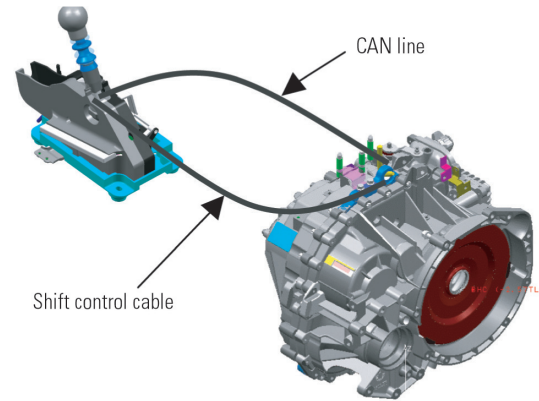
Pre-shift control is programmed in a way consistent with the gearshift characteristics intended by each drive mode. The control logic reflecting the result of the analysis on the data collected through a series of test drives has enabled a natural and quick shift response of the transmission.

(5) Other control features

The TC-SST control incorporates a function of automatically memorizing the best clutch engagement points through learning. This function offsets the unit specific deviation resulting from part variations, thereby ensuring the TC-SST's original high gearshift quality. It also includes a function of pre-pressurizing a clutch hydraulic piston circuit under certain conditions for quicker gear shifting.

5. Control modes

In the case of the TC-SST used in the LANCER EVOLUTION X, three drive modes, i.e., "Normal," "Sport" and "Super Sport" can be selected using the TC-SST

**Fig. 6 Communication with shift lever**

control mode select switch located next to the shift lever. The timing of a gear change as well as how quickly the gear change takes place and how the gear change is responsive to accelerator operation is made different between the control modes so that the user can enjoy driving in all scenes (Table 3 and Fig. 5).

6. Shift lever

The shift lever system of the TC-SST accommodates CAN communications and is the first of its kind to be used by MMC. Shift lever position data, TC-SST control mode select switch status data and paddle shift data are transmitted through the CAN line from the shift lever control unit to the TC-SST control unit. The use of the CAN communication system substantially reduces the amount of in-vehicle wiring (Fig. 6).

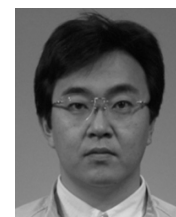
7. Conclusion

In the development and production of the TC-SST, the latest simulation technologies are applied to a variety of analyses that are conducted, digital modeling technologies are used extensively and latest types of production equipment are introduced, all to assure the highest possible quality of the new transmission.

Using this opportunity, we wish to extend our sincere thanks to all of those who helped make this development possible.



Takao KIMURA



Takashi SASAKURA



Kunishige HAYASHI



LANCER EVOLUTION X Chassis Technologies

Masaru OHUCHI* Takeshi YAMAMURA* Hiroshi OIKAWA*

Abstract

For the kind of driving pleasure targeted by Mitsubishi Motors Corporation with the LANCER EVOLUTION X, the platform was updated and new chassis technologies were developed. The suspension was fundamentally revamped in terms of layout and structure and was combined with wider treads* and 18-inch wheels, resulting in exceptional roadholding at all four tires and in concomitantly improved cornering performance and a high-quality ride befitting the new-generation LANCER EVOLUTION. In addition, larger-diameter brakes were adopted for superior stopping power and fade resistance and a superior pedal feel.

*: 30 mm wider than LANCER EVOLUTION IX

Key words: Sport Car, Motor Sports, Chassis, Vehicle Dynamics, Steering System, Stability, Suspension System, Shock Absorber, Damping, Wheel Alignment, Brake, Tire, Wheel, Handling, Ride Comfort

1. Introduction

The LANCER EVOLUTION was developed as the base vehicle for rallies and other competitions, and has continued to evolve to the present. In recent years, however, there have arisen demands not only for high driving performance, but also for high-quality riding performance as well.

This time, along with the renovation of the platform, the entire chassis has been newly developed, aiming at the simultaneous realization of enhanced handling stability and high-quality riding.

2. Suspension

The suspension was designed with the aim of increasing the rigidity of each part and also optimizing the geometry for secure positioning of wheels. Also, a highly rigid, lightweight suspension was developed by selecting the right material for the right place and optimizing its construction. In addition, the road holding performance was increased in order to maximize the effectiveness of the Super All Wheel Control (S-AWC) integrated vehicle dynamics control system.

2.1 Front suspension

The front suspension was newly developed along with the evolution of the MacPherson strut which used the proven inverted strut (Fig. 1).

To cope with the increased various inputs and the improved cornering performance due to the adoption of 18-inch low-profile tires, steps were taken to increase the size of the hub unit bearings, increase the stiffness of the upper insulator that supports the strut, and also extensively increase the stiffness of the sub-members which correspond to the framework structure of the suspension (Fig. 2 and Fig. 3).



Fig. 1 Front suspension

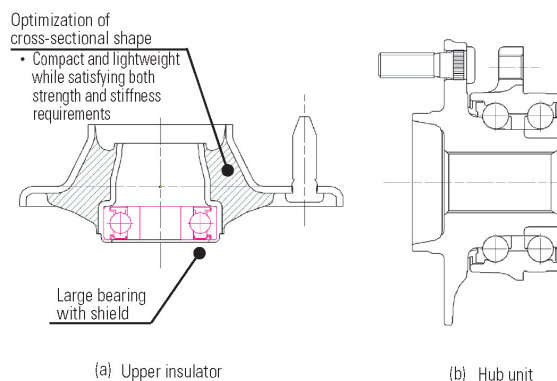


Fig. 2 Front stiffness-enhancing component

* Chassis Design Dept., Development Engineering Office

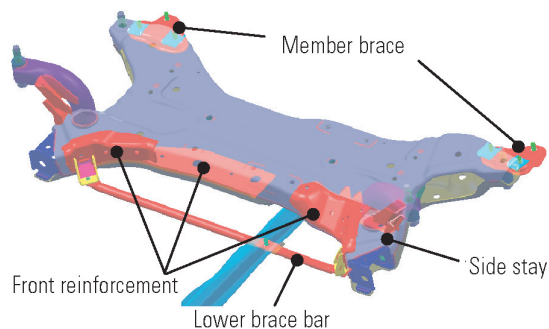


Fig. 3 Front stiffness-enhancing component



Fig. 4 Rear suspension

2.2 Rear suspension

A completely new suspension was developed which has a sub-member conforming to the new platform while following the design of the proven multi-link type used on the LANCER EVOLUTION IX.

The sub-member was connected securely to the body at six points, and the sub-member itself was also of a high-stiffness construction (Fig. 4).

Regarding the suspension arms, the support span between each arm was enlarged, the length and layout of the arms were made appropriate, and the high stiffness and change of alignment were optimized (Fig. 5 and Fig. 6). The hub unit bearing was also enlarged, resulting in greater stiffness (Fig. 7).

Excellent road holding performance was realized by increasing the number of places where pillow balls were used and also by changing the mounting position of the rear damper from the lower arm to the knuckle (Fig. 4 and Fig. 7).

By thus optimizing the construction of the suspension and increasing its stiffness, the handling stability - consisting of cornering limit, response and so on - and the riding performance - consisting of straight stability, riding comfort and so on - were simultaneously realized with relatively little compromise.

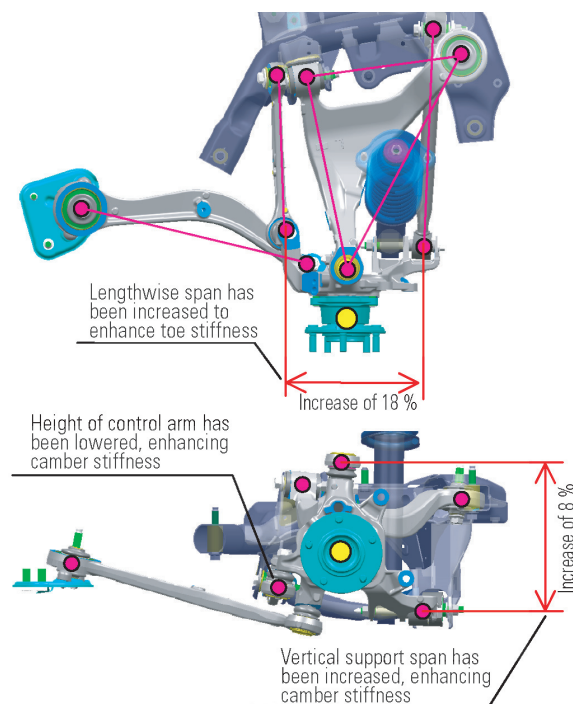


Fig. 5 Rear arm layout

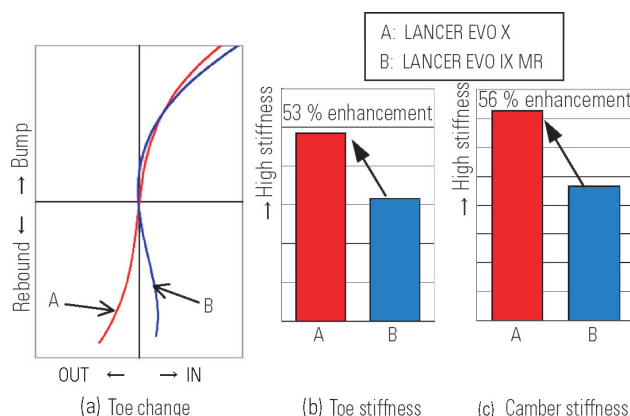


Fig. 6 Rear suspension characteristics

2.3 Power steering system

A hydraulic assist system was employed. By optimizing the assist characteristics and the steering gear ratio, a quick and high quality steering feeling was realized.

3. Tires and wheels

3.1 Tires

245/40R18 low-profile wide tires were used. The necessary performance factors for high performance tires, consisting of handling stability, braking performance, wet performance, and quietness, were well-balanced against each other due to the newly developed asymmetrical tread pattern and the optimized inner structure.

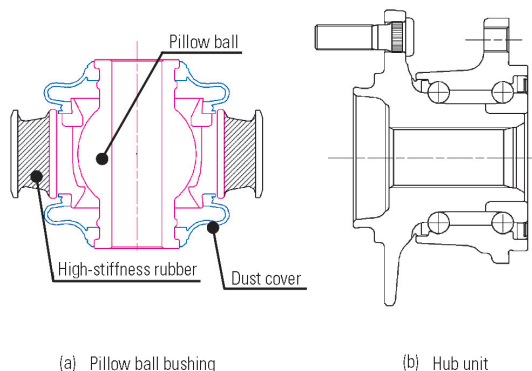


Fig. 7 Rear stiffness-enhancing component

3.2 Aluminum wheels

The rims of the aluminum wheels were processed by spinning process for increased material strength while reducing their thickness and weight. In addition, the rim shape and location of the spokes were optimized for highly rigid and lightweight wheels.

4. Brakes

4.1 Wheel brakes

The front brakes were 18 inches and the rear brakes were 17 inches, 1 inch larger than those for the LANCER EVOLUTION IX. The outer diameter of the rotor was set to ϕ 350 mm for the front brakes, and ϕ 330 mm for the rear brakes, thus increasing the fading resistance and effectiveness of brakes (**Fig. 8**). In addition, the caliper mounting rigidity and the characteristics and shapes of the pad and rotor were optimized for the reduction of squealing and judder (**Fig. 8**).

4.2 Highly rigid vacuum booster

Aiming at improving biting feeling at the initial braking stage, a linear increase in braking force, and enabling of an increase in the braking force when the brake pedal is depressed further in the high G deceleration zone, a through-bolt type 10-inch vacuum booster was adopted together with improving the wheel brake performance. By reducing the internal sliding resistance due to the adoption of a single booster and by suppressing the shell deformation due to the use of a through-bolt, reduced friction feel, reduced pedal effort at high fluid pressure, and higher rigidity were realized, enhancing the braking control performance (**Fig. 9**).

5. High performance items for MR grade

In order to realize higher performance, Bilstein dampers, Eibach coil springs, and 18-inch two-piece front disc rotors, were made available as MR grade.

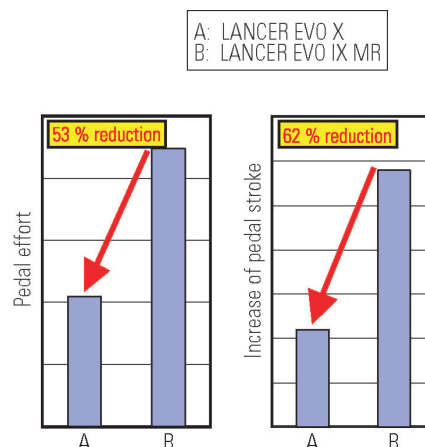


Fig. 8 Fade resistance during sport driving

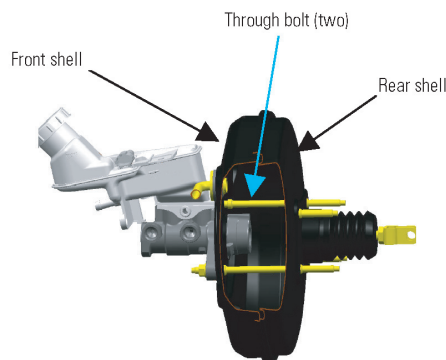


Fig. 9 High-rigidity vacuum booster

5.1 Bilstein dampers and eibach coil springs

The reputable Bilstein monotube permits fine tuning of damping characteristics from the ultra-low speed range. Furthermore, coupled with the Eibach coil spring, it realizes a pliable suspension with good road holding performance (**Fig. 10**).

5.2 Two-piece disc rotor

It is a two-piece construction consisting of a separate friction rotor and hub mounting bell. Compared to a single piece construction, the weight of each rotor has been reduced by 1.3 kg. A floating construction in which the rotor and the bell are bolted together via a spacer is employed, and also the shape has been optimized, minimizing coning angle of the friction surface at high temperature and realizing good braking stability (**Fig. 11**).

6. Summary

It is expected that in the future demands will continue to be made for further increases in the level of chassis technology for the LANCER EVOLUTION, concerning which high targets have been set and realized for each generation.



Fig. 10 Bilstein damper, Eibach coil spring



Fig. 11 Two-piece disc brake rotor

The LANCER EVOLUTION is Mitsubishi Motors' leading car. To ensure that it also remains a leading car in the automobile industry, efforts aimed at technical innovation will continue to be made in the future.



Masaru OHUCHI



Takeshi YAMAMURA



Hiroshi OIKAWA



Aerodynamics for LANCER EVOLUTION X

Satoshi KATAOKA* Norimasa HASHIMOTO* Masahiro YOSHIDA*
Tomio KIMURA* Naoki HAMAMOTO*

Abstract

Aerodynamics technology for the LANCER EVOLUTION X was developed not only to reduce drag but also improve lift and cooling performance. The applied aerodynamics technology includes the nose shape like that of a shark, the cooling, the rear spoiler shape, etc. As a result, the drag coefficient (C_D) and lift coefficient (C_L) values are less than that of the LANCER EVOLUTION IX. This paper describes the aerodynamics technology for the LANCER EVOLUTION X and also introduces the Under Floor Air Guide, a new aerodynamic device.

Key words: Aerodynamics, Fluid Dynamics, Aerodynamic Devices, Cooling

1. Introduction

Since the appearance of the first-generation model, the LANCER EVOLUTION has been continually improved to excel in various motor sports by outstanding driving performance superior to competitors. A lot of model tests, CFD analyses, and tests using actual vehicles have been performed (Fig. 1) that aims not only to reduce the drag coefficient (C_D), but also to reduce the lift coefficient (C_L) and enhance cooling performance. The resulting aerodynamically shaped bodies offered a sophisticated combination of riding comfort and body design. In developing the LANCER EVOLUTION X, additional efforts have resulted in lower C_D and C_L compared to the LANCER EVOLUTION IX. Particularly, the C_L value is world-leading for this class of vehicle. The development work is summarized below (Fig. 2).

2. Aerodynamic development of the LANCER EVOLUTION X

In the aerodynamic development of the LANCER EVOLUTION X, first the entire body was optimized aerodynamically, and then the specific aerodynamics parts shown in Fig. 3 were optimized. The shapes of the body have been optimized through repeated studies to combine the low drag coefficient styling with impressive design of the EVOLUTION – for example, shark nose, the over-fenders which gently incline along the length, and the rear combination lamps with sharp edges. The wheel arch air dam and the shape of the bottom edge of the bumper actively separate the air flow, creating negative pressure which reduces the lift of the body. For cooling, the hood inlet, based on the NACA scoop shape, and hood outlet which have adopted from LANCER EVOLUTION IX, and the new fender outlets located at suitable positions on the body surface enhance the cooling performance for the engine compartment. Details of the rear spoiler, the

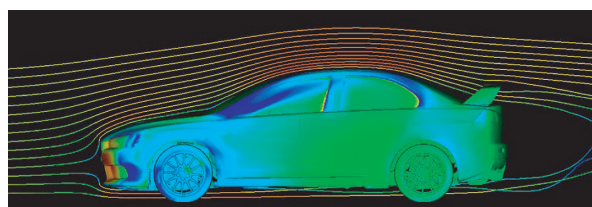


Fig. 1 Pressure distribution and air flow trace line

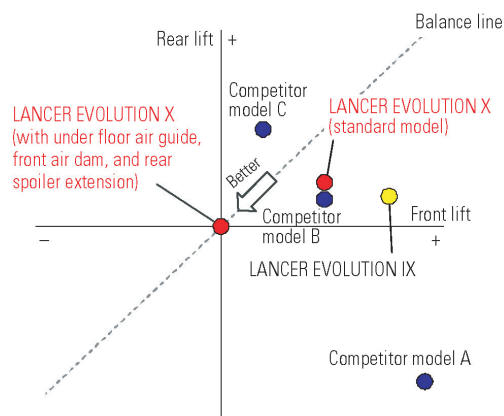


Fig. 2 Comparison of lift coefficient (C_L)

under floor air guide (optional part), and the cooling air intake construction with effective opening are described below.

3. Development of a new shape (twisted wing) rear spoiler

In the case of a sedan body, the flow separated at the C pillar is drawn in above the rear window, resulting in a pair of vortices (Fig. 4). As a result of these vortices, the downflow angles at the center and the outside

* Testing Control Dept., Development Engineering Office

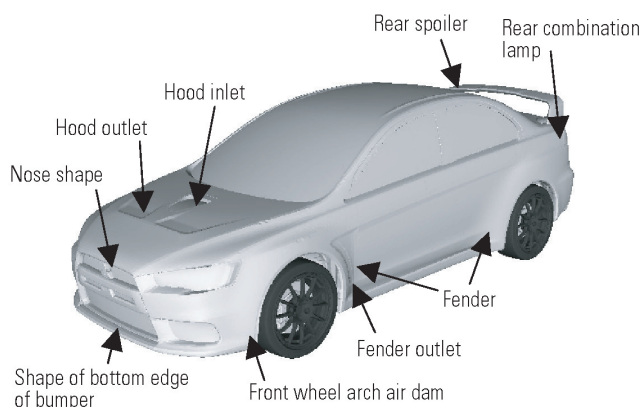


Fig. 3 Body shape with aerodynamic functions

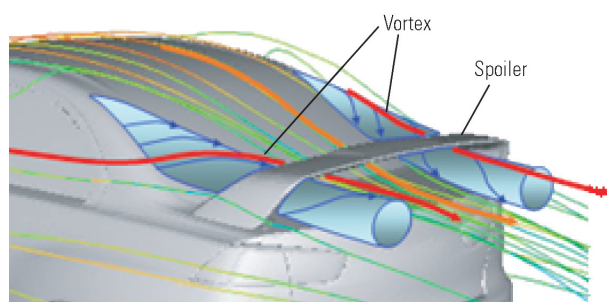


Fig. 4 Air flow on rear of vehicle

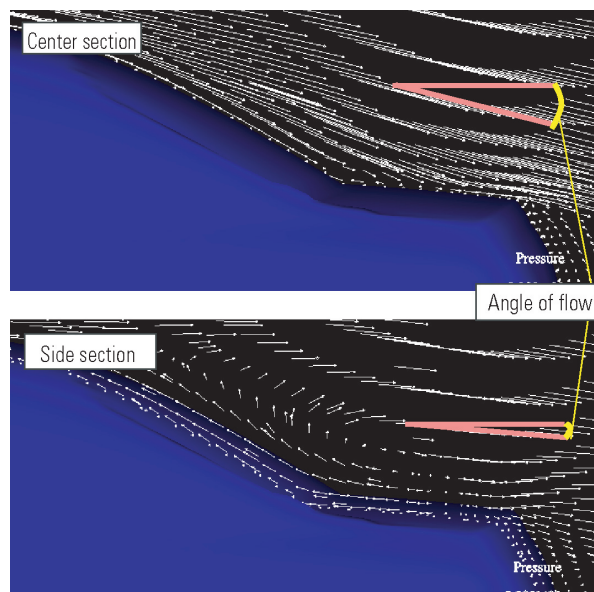


Fig. 5 Angle of flow at each position

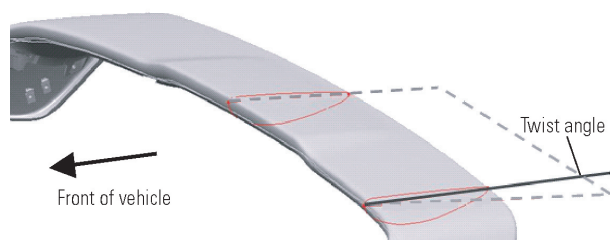


Fig. 6 Twisted wing

of the body are different from each other (**Fig. 5**), which could cause the following problems with the conventional wing.

- (1) Where the downflow angle is deep, the angle of attack of the wing is excessively large, and the flow separates at the trailing edge side.
- (2) Where the downflow angle is shallow, the angle of attack of the wing is excessively small, reducing the full performance of the spoiler.

To overcome these problems, the wing angle of the LANCER EVOLUTION X differs at the center and the outside of the vehicle body (**Fig. 6**). As the wing performance is enhanced, the increase in drag is curbed and the lift is significantly reduced (**Fig. 7**). The height of the spoiler, its position in the lengthwise direction, and the shape of the wing cross-section were also optimized by wind tunnel tests.

4. Under floor air guide

The under floor air guide which effectively reduces lift has been newly developed as an optional part for the LANCER EVOLUTION X (**Fig. 8**). This device is the fins installed under the floor to diffuse the airflow from the under floor to the outside of the body, thus increasing the flow velocity at the center section of the under floor. This high-velocity airflow and the vortices created the lower pressure region at the under floor behind the fins and this area contributes to reduce the lift of

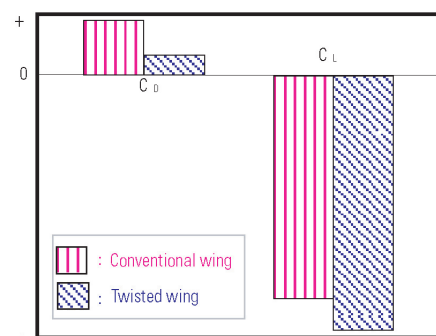


Fig. 7 Comparison of twisted wing and conventional wing

the body.

Fig. 9 shows the results of a model test performed with a pair of air guides installed on a flat plate simulating an under floor of the vehicle. The top half of the figure shows the change in the surface pressure when the air guides are installed. The blue area indicates the region in which the pressure falls (reducing lift), and the red area indicates the region where the pressure rises. These results reveal that the maximum pressure reduc-



Fig. 8 Under floor air guide

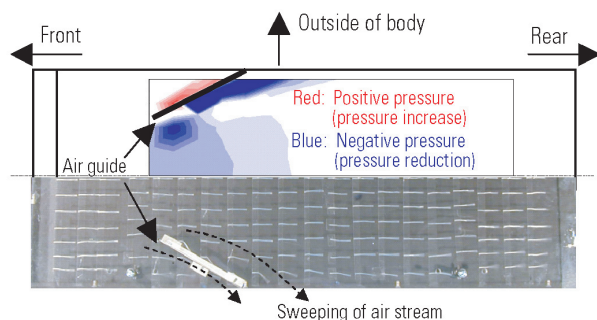


Fig. 9 Model test results of under floor air guide

tion occurs downstream of the air guide, and also that pressure is reduced even at the center of the body between the left and right air guides. Although there is a red region where the pressure rises upstream of the guides, it is smaller in area than the blue region where the pressure falls. The bottom half of the figure shows the results of a flow visualization test of the under floor using tuft method. It can be seen that the flow is diffused to the outside of the vehicle and vortices are created behind the air guides. The flow at the center part of the vehicle is thought to be drawn toward the outer part by the negative pressure of these vortices, that accelerate the flow velocity at the center part and thus reducing pressure of the under floor.

Fig. 10 shows the pressure distribution obtained by CFD analysis performed both with and without the air guides on an actual under floor model. The image also shows that the air guides have increased the area of the negative pressure region (blue area).

A lift reduction device represented by a front air dam and a rear spoiler are normally effective in reducing the lift at the front or the rear alone. The remarkable feature of the new air guide is that it reduces both the front and rear lift in a well-balanced manner depending on where it is installed (Fig. 11). In the LANCER EVOLUTION X, the air guide was set in the optimum position in consideration of the balance between the front and rear lift of the standard model.

5. Optimization of cooling performance by redesigning the body structure

Extensive development work on engine cooling was carried out in order to obtain the maximum perfor-

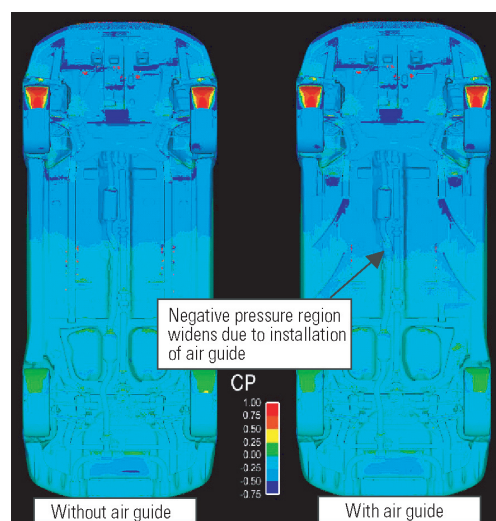


Fig. 10 Effect of under floor air guide

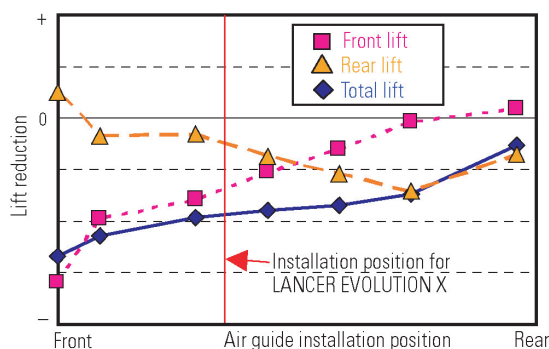


Fig. 11 Change of lift in relation to position of under floor air guide

mance from the LANCER EVOLUTION X. As an example of enhanced cooling performance, the structure for guiding air to the twin clutch SST oil cooler and the engine oil cooler is described below. Fig. 12 shows the front view of the vehicle. In order to efficiently cool the oil, the air taken from the center opening is guided via an air duct to the oil coolers (Fig. 13).

Fig. 14 shows the CFD results of the flow for cooling. It can be seen that the cooling air enters the duct from the center opening and passes through it then flows into the oil coolers. Fig. 15 shows measurements of actual air flow velocity; the air flow velocity has increased by about 50 %.

6. Conclusion

The LANCER EVOLUTION X employs a newly developed rear spoiler and under floor air guides on the body which harmonize dynamic design and aerodynamic characteristics. As a result, the performance far surpasses that of the previous EVOLUTION models not only the reduction of aerodynamic drag but also the lift



Fig. 12 Openings for cooling

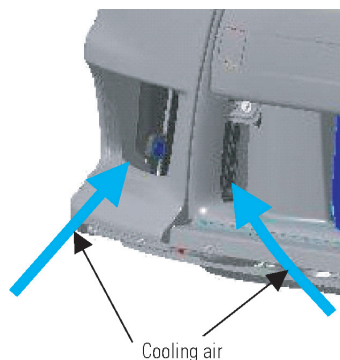


Fig. 13 Oil cooler opening and air duct at center opening

which greatly affects the steering stability. With this excellent aerodynamic balance, the LANCER EVOLUTION X will uphold the reputation of its predecessors in motor sports such as rallies.

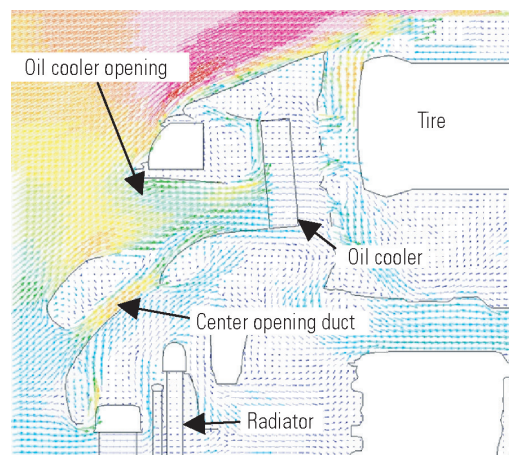


Fig. 14 Velocity vector in air duct (horizontal section)

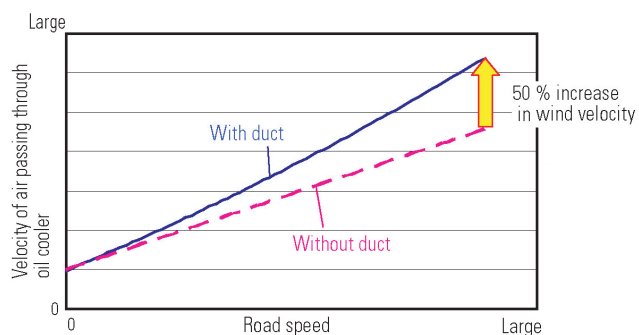
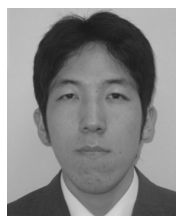


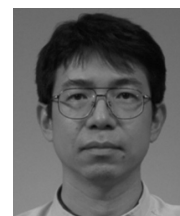
Fig. 15 Comparison of wind velocities through oil cooler



Satoshi KATAOKA



Norimasa HASHIMOTO



Masahiro YOSHIDA



Tomio KIMURA



Naoki HAMAMOTO



Electrical-System Design for LANCER EVOLUTION X

Morihiro SHIOTANI* Youichi SENOO* Tsukasa ITO*

Abstract

With the LANCER EVOLUTION X, Mitsubishi Motors Corporation (MMC) adopted its first ever trunk-mounted battery with a view to delivering superior performance through a reduction in the proportion of vehicle weight borne by the front wheels. Since the battery is the central part of the power-supply circuitry, changing its location had a significant effect on the electrical systems. Nevertheless, MMC was able to mount the battery in the trunk while ensuring component commonality with the GALANT FORTIS (the vehicle on which the LANCER EVOLUTION X is based). An overview is given in this paper.

Key words: Electric Equipment, Battery, Wiring Harness (W/H), New Model

1. Introduction

To improve the motion performance of the LANCER EVOLUTION, it was considered essential to reduce the load at the front of the vehicle. One solution was to use an aluminum cylinder block for the engine to reduce its weight, and another was to relocate the battery to the trunk. Combined, these measures reduced the proportion of vehicle weight borne by the front wheels and thus improved the front-rear vehicle weight balance (by 2 to 3 % compared with the predecessor model). This paper outlines the technologies used for relocating the battery to the trunk, and the development of the wiring harnesses necessitated by the relocation.

2. Relocation of battery to trunk

2.1 Technologies to counter flammable gas from battery⁽¹⁾

The first challenge in installing the battery in the trunk was to deal with flammable gas emanating from the battery.

Charging a lead acid battery causes electrolysis to occur in the water of the electrolyte, producing oxygen gas at the positive plates and hydrogen gas at the negative plates. As a result, the quantity of the electrolyte decreases. This hydrogen gas is not a problem when the battery is in the engine compartment, because it escapes to the open air through openings such as gaps around the engine hood. If the battery is installed in the trunk, however, hydrogen gas will be trapped inside and could cause an explosion if it ignites.

To prevent the risk of explosion, a valve regulated lead acid (VRLA) battery is used with a hose added for draining gases. **Fig. 1** shows the VRLA battery together with relevant information. The VRLA battery is a sealed unit with a gas-pressure regulating valve as a vent to the outside. Oxygen gas is produced at the positive plates earlier than the hydrogen gas at the negative plates, so it can be fed to the negative plates to make it

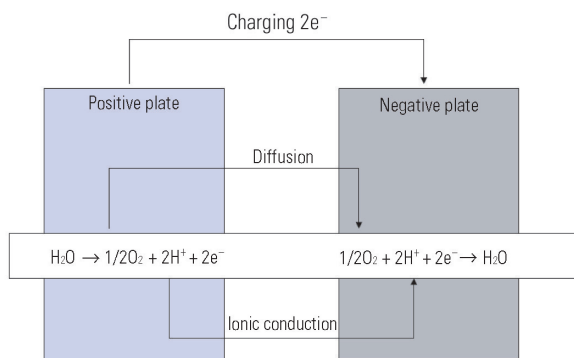
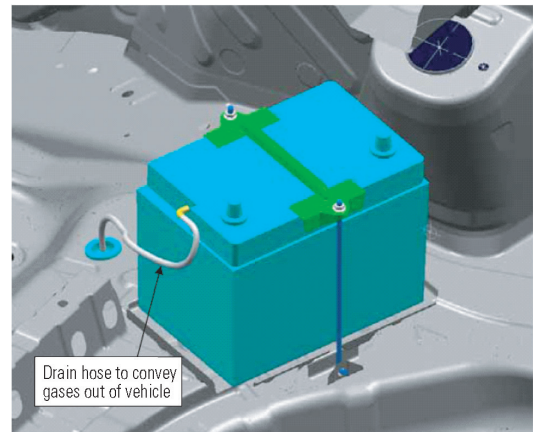
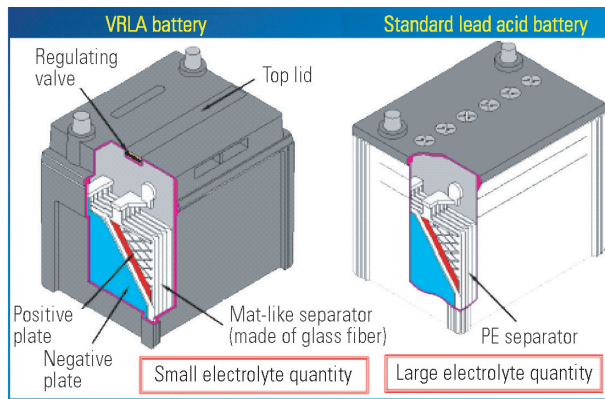
recombine with the hydrogen produced there to form water, thus preventing the generation of hydrogen gas and loss of electrolyte. This process is known as "oxygen absorptive reaction on negative plates" and takes places with 100 % probability, so no gases are released to the outside. However, if an overcharge or over-voltage state occurs due to a malfunctioning alternator or other causes, part of the oxygen gas cannot be absorbed at the negative plates, so hydrogen gas is produced at the negative plates and the quantity of electrolyte decreases as a result. The resulting gas pressure forces the regulating valve to open the way out of the battery. The drain hose connected to the valve and installed passing through the trunk floor can then convey the gas from the vent to the outside.

Another candidate means of preventing the accumulation of hydrogen gas in the trunk was to use a sealed box to house the standard lead acid battery. However, the VRLA method was finally selected rather than the sealed box method because of the following difficulties of the latter: If the wiring from the battery is routed on the floor, the battery harness constituting the wiring makes it impossible to keep the box hermetically sealed. On the other hand, if the wiring is routed under the floor, the box can be kept completely sealed but the hydrogen gas trapped inside the box could cause an explosion.

2.2 Battery protection and maintenance considerations

A plastic trim is used from a practical viewpoint to protect the battery from the potential impact with moving baggage during sudden braking. The trim has a lid opening that is needed when replacing the battery, disconnecting the battery cable before servicing electrical components and connecting the cable to the negative terminal as the final process before shipping the vehicle from the factory, whereas a maintenance-free battery does not require any access through the trim for inspecting the electrolyte level and replenishing it.

* Electronics Engineering Dept., Development Engineering Office



Oxygen absorptive reaction on negative plate

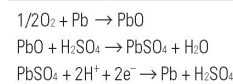


Fig. 1 VRLA battery

In addition, a booster cable connection terminal is provided at the joint terminal block inside the engine compartment for convenience in case of a dead battery.

3. Effects of trunk-mounted battery on electrical components

3.1 Differences from the conventional vehicle

Due to the trunk-mounted battery, it was necessary to split the battery positive cable between the starter and battery into two harnesses, i.e., the starter harness and battery harness. The joint terminal block for connecting them is provided in the engine compartment. The LANCER EVOLUTION X shares the same power supply circuit with the OUTLANDER and GALANT FORTIS by using the same relay box and junction block.

3.2 Effects of trunk-mounted battery on engine starting performance and charge-discharge balance

The trunk-mounted battery requires longer cables, which increases the wiring resistance. This disadvantage for engine starting performance was compensated for by specifying the use of a low-viscosity engine oil, resulting in engine starting performance equivalent to the LANCER EVOLUTION IX.

However, the increased resistance of the wiring between the battery and alternator might have caused false sensing of the battery voltage and ultimately an incorrect charge-discharge balance. Therefore, to con-

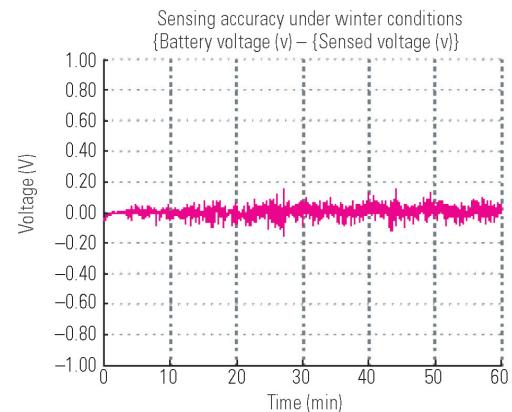


Fig. 2 Results of charging and discharging verification test

firm the actual effect of the increased wiring resistance on the vehicle, charge-discharge balance tests were conducted under both winter and summer conditions. The results showed that the difference between the sensed and actually measured battery voltages was 0.1 V on average and 0.5 V at maximum. Thus, the sensed battery voltage was sufficiently accurate to prevent over-charging and over-discharging (Fig. 2).

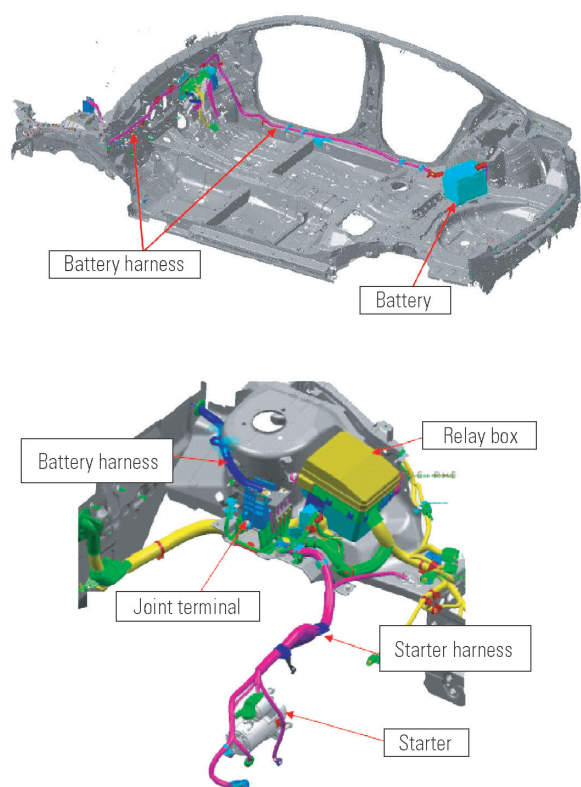


Fig. 3 Layout of wiring harness

3.3 Battery harness

3.3.1 Battery harness layout

The battery harness is routed inside the cabin and connected to the starter harness at the joint terminal block located on the transmission mounting at the left side of the engine compartment (Fig. 3).

Table 1 compares the merits and demerits of the in-cabin and under-floor battery cable layouts. The initially considered under-floor layout of the battery harness was replaced by the in-cabin layout due to the following problems with the under-floor layout.

- (1) With the under-floor layout, it takes a longer time to install the battery harness than is available in the manufacturing process.
- (2) A battery harness divided into two portions must have connections at locations exposed to mud and water, increasing the chance of added electrical resistance due to secular change.
- (3) A harness installed under-floor could be damaged by flying stones and heat, and the cables could be caught by obstacles and become detached.
- (4) The under-floor layout forces the battery harness to cross the dash panel, which requires a drastic change from the common platform model in the layout of the engine compartment components, which is too costly.
- (5) The under-floor layout requires plastic protectors which are too large for delivery boxes to accommodate them, causing problems in parts handling.

A battery harness installed inside the cabin must not adversely affect the appearance of such interior furnish-

Table 1 Battery harness layout comparison

	In-cabin	Under-floor
Workability at factory	○	×
Number of battery harness portions	2	3
Susceptibility to damage by flying stones and heat	○	△
Shared use of parts (cost effectiveness)	○	△
Increase of radio noise	△	△
Handling of parts	○	×
Adaptability to dirt racing (anti-ground-contact merit)	○	△

○: There is no problem △: There may be a problem ×: There is a problem

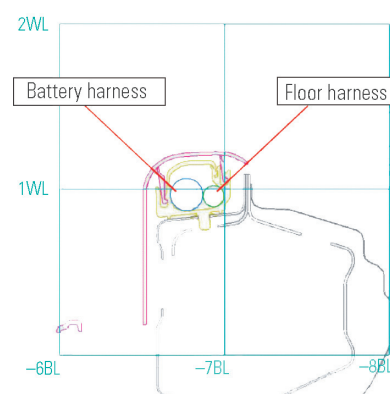


Fig. 4 Cross-sectional view of side sill

ings as the trim and carpet. This requirement was dealt with by limiting the equipment specifications to make the floor harness thinner and changing the sectional shapes of the trim and harness clips to enable the battery harness to be installed on the side sill (Fig. 4).

3.3.2 Radio noise

A battery installed in the engine compartment absorbs ripple noise from the alternator as it serves as a capacitor. This effect was not expected with a trunk-mounted battery and, furthermore, the noise that would be radiated from the battery might cause additional radio noise. However, actual drive tests showed that the cabin-installed harness had little effect on the radio noise and caused no practical problem. This is thought to be due to the relatively large separation between the harness and antenna feeder cable.

3.3.3 Safety considerations

The battery harness as well as the starter harness forms a battery-voltage circuit without any fuse, so it needs appropriate protection against short-circuits especially in the event of a collision. One measure taken to prevent short-circuit was to install the harnesses in a location where body deformation was the least likely in the event of a collision. The other measure was to provide full-length protection to the harnesses with corrugated or plastic protectors. Also, the joint terminal block for connecting the battery and starter harnesses was located on the transmission mounting where deformation was least likely in a collision, and plastic protec-

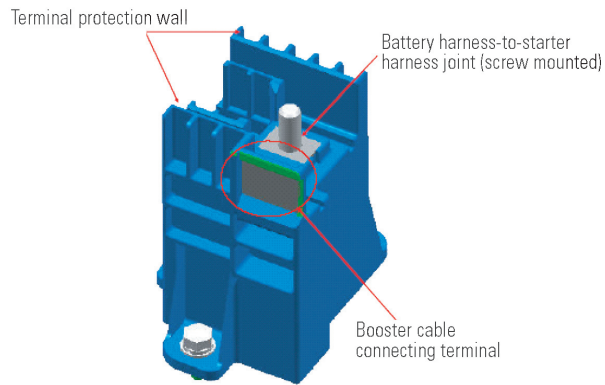


Fig. 5 Joint terminal

tion walls were provided there to prevent short-circuits at the connection (**Fig. 5**).

4. Conclusions

The trunk-mounted battery helped achieve the remarkable improvement in the motion performance of the LANCER EVOLUTION X over the predecessor model. There were various related problems during the development such as the engine starting performance and manufacturing requirements at the factory, but all of them could be solved successfully to complete the development. We sincerely thank Panasonic Storage Battery Co., Ltd. and all others concerned for their cooperation in the development.

References

- (1) Japan Storage Battery edition, Latest practical secondary battery (Chapter 6, Mechanism and characteristics of lead acid batteries), 1995



Morihito SHIOTANI



Youichi SENOO



Tsukasa ITO



Design Concept for LANCER EVOLUTION X

Hiroaki MATSUNOBU* Norihiko YOSHIMINE**
Kei HAMADA** Chigusa YASUI**



Abstract

With the LANCER EVOLUTION X, Mitsubishi Motors Corporation (MMC) used the GALANT FORTIS global strategic model, which combines sportiness with comfort, as the basis of a next-generation high-performance sedan that incorporates MMC's proprietary cutting-edge technologies. Since the LANCER EVOLUTION X is Mitsubishi's flagship car, MMC carried forward the long-popular sporty look of the LANCER EVOLUTION series but shifted the styling toward greater refinement and combined it with outstanding functionality as a way to express a higher dimension of performance.

Key words: Development, Concept, Styling, Aerodynamics

1. Introduction

In this project, the point to which most attention should be paid is the fact that from the initial stage the designers and the engineers always shared the evolution and carried out development while cooperating with each other. The designers fully understood the functional requirements for realizing a higher dimension of performance reflecting driver intent in real time, the problems were thrown back and forth between the designers and the engineers, and as a result the design and functions were successfully combined at a sophisticated level.

Design was aimed at the pursuit of higher quality styling, handling ability, and material selection, in order to satisfy not only the current LANCER EVOLUTION users but also the customers who desire high quality and high performance as well.

2. Design concept

This LANCER EVOLUTION marks the fourth generation model. For the project, three themes were established as design concept. The first theme was modeling without loss of function. Concerning the exterior, the designers aimed for a solid, tight form that was hitherto unavailable in a sedan, by carrying out design after obtaining a complete understanding of the dimensions for superior road performance accumulated by the company's participation in motor sports (Fig. 1).

The second theme was the necessity to continue evolution. In this development work, wind tunnel tests were carried out repeatedly from the initial stage, and the concept of aerodynamics was incorporated into the basic design. Each aerodynamic device was optimized and then the body was designed, realizing high quality functional beauty with a sense of unity. Regarding the interior, with the difficult task of ensuring the suitability for normal, comfortable driving and the capability of withstanding extreme driving conditions at the same

* Design Dept., Design Office

** Design Promotion Dept., Design Office



Exterior image sketches (final)

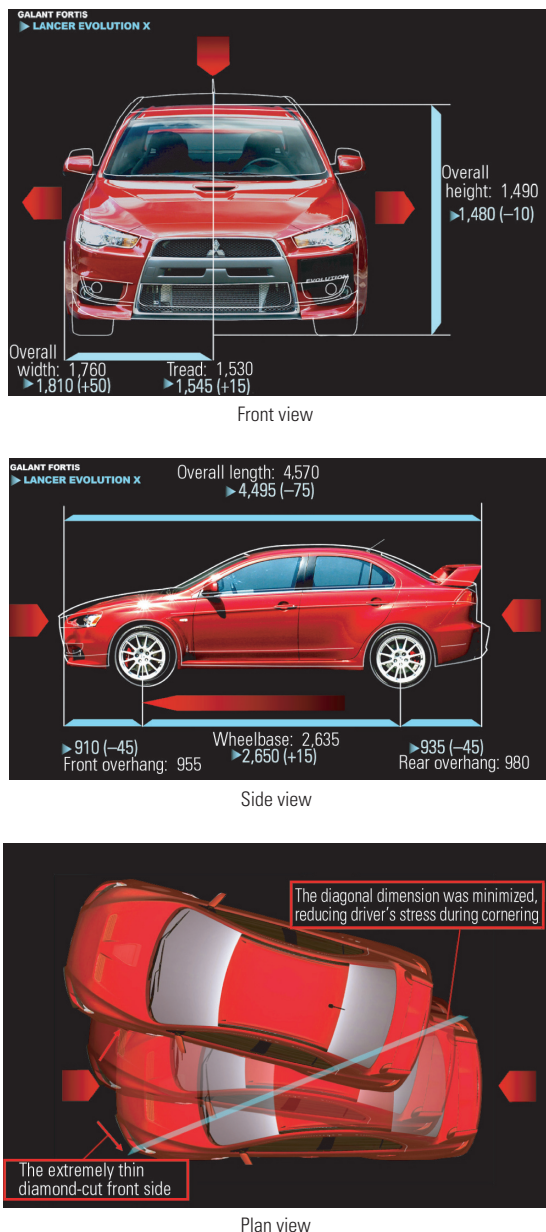


Fig. 1 Dimensional comparison with GALANT FORTIS

time, the development was carried out in cooperation with test drivers.

The third theme was the necessity for the design to be attractive to people. In addition to refining function-



Fig. 2 Modeling in wind tunnel

al beauty, fat was trimmed away, and emphasis was placed on achieving surface quality, materials, and coloring that provide a feeling of fastidiousness.

3. Exterior design

3.1 Construction of an aerodynamic form

Dimensions for superior road performance and aerodynamic requirements were essential items for representing the LANCER EVOLUTION's functional beauty. In order to avoid as much as possible an impression that the aerodynamic device was later attached onto the basic design, aerodynamic processing was studied from the initial stage. The results of these studies were also incorporated in the GALANT FORTIS, which was being developed simultaneously, resulting in further performance enhancement of the LANCER EVOLUTION X which is based on the GALANT FORTIS. The normal styling work had not started at the stage of the initial study on the 1:1 size model, and instead a long-term aerodynamic study in the wind tunnel was carried out (Fig. 2). In order to determine all of the styling related to cooling performance, an FRP hood and bumper were fabricated based on the scanned data obtained from intermediate stage models. These parts were installed on a prototype vehicle, and cooling tests were performed, resulting in the realization of the styling based on the optimum cooling requirements (Fig. 3).

There was no end to the functional beauty created as a result of these tests: the large trapezoidal grille that efficiently cools the radiator and the inter-cooler, the NACA duct on the hood and the pickup shape of the front part of the wheel arch, the fender outlet that helps to release hot air from the engine compartment and also reduce resistance, and the blister fenders that transport the side air streams rearward without separation. The shape of the rear diffuser which efficiently discharges the air stream from under the floor was realized by using a position and angle proposed by aerodynamic engineers. It was indeed a shape that was created empirically (Fig. 4). The large rear spoiler, which is also a symbol of the LANCER EVOLUTION, adopts an airfoil section and the twisted shape with different attack angles at the center and outside parts, and the use of aluminum core material realized a refined and sporty 3D shape that retains high strength.



Fig. 3 FRP bumper and hood for tests



Fig. 6 Creation of refined surface by skilled craftsmen

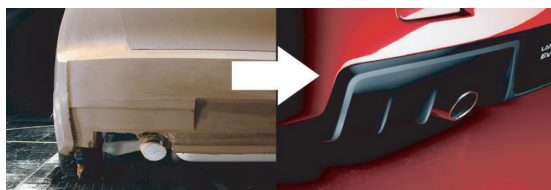


Fig. 4 Rear diffuser and cooling outlet resulting from wind-tunnel testing



Fig. 7 Communication model

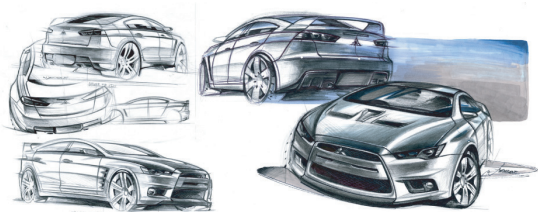


Fig. 5 Sketches for refinement of model

3.2 True design beauty created together with function

Even after aerodynamic performance was incorporated into styling, surface constructions were refined and functional areas and parts were integrated while sketching work was repeated (Fig. 5). In order to simultaneously realize the limit of moldability using aluminum material aimed at expressing the muscularity and solidness of the blister fender while realizing lightness in weight, and the requirements of the pedestrian protection performance, measures were repeatedly devised in cooperation with sheet metal engineers, and the results were incorporated into clay models. In this way, the surfaces were progressively tuned (Fig. 6). In order to realize a more beautiful form, coordination was carried out with the body engineers, and a completely no-compromise design that included detailed parts was realized without loss of function. These were made possible as a result of discussions held with the developers, including the persons in charge of engineering and testing, from the initial stage. And integrated with the body refined by the hands of modelers and digital designers, the successful creation of uncompromised design beauty was realized.

3.3 Styling incorporating responses from inside and outside the company

The development of the design identity (inverted slant nose + trapezoidal grille) first adopted for the GALANT FORTIS, and the sporty exterior which follows this identity was started three years prior to putting the LANCER EVOLUTION on the market. In 2004, a communication model was made (Fig. 7) in order to confirm the directionality of the design. A high evaluation was obtained from inside and outside the company, and based on this the technical specifications related to styling were progressively determined. A concept car was made to gauge the reactions from the domestic and overseas markets (Fig. 8). At the 2007 North American International Auto Show, a concept car that approximated the final form was exhibited (Fig. 9). As a result, fine tuning was carried out while opinions were gathered from the domestic and overseas markets, leading to the establishment of the front identity and styling befitting a sporty sedan that holds its own in the world.

4. Interior design

4.1 Interior design that increases concentration on driving

Design development of the interior of the "Concentration" – LANCER EVOLUTION X was promoted aiming at the creation of a functional cockpit that reduces the burden on the driver, and facilitates concentration on driving.

Previously, when the word "sports car" was mentioned, one would conjure up the image of a tight internal space. However, the interior of the LANCER EVOLUTION X was designed to provide as comfortable an



Fig. 8 Concept X



Fig. 9 Prototype X

interior space as possible, to create a condition that makes it easier to concentrate on driving. The instrument panel was basically arch-shaped to locate the center operation panel which is frequently accessed close to the driver, and to increase the distance between the panel and the front passenger seat occupant larger toward the outside. This realized both a readily accessible operation panel and a generous leg space (Fig. 10). This clear arch form and the construction with fine details were adopted from the GALANT FORTIS, the base vehicle of the LANCER EVOLUTION X. More precisely, because these two models were developed in the same period, they were allowed to affect each other so that they could be refined into good shapes in order to realize the ideal forms of premium sport sedans that take into account a wide range of driving conditions from extreme sports driving to everyday use.

4.2 Unique interior parts for the LANCER EVOLUTION X designed in the pursuit of reliable handling and quality worthy of a premium sports car

4.2.1 Steering wheel

The steering wheel, which has a diameter 10 mm less than that of the GALANT FORTIS, has an S-AWC mode toggle switch (or audio switch) on the spoke part, enabling the vehicle to be handled reliably without any need to remove hands from the wheel while driving. The grip is made of smooth genuine leather which feels good to the touch and the seaming edges of the leather are sewn together using parallel stitches, enabling the steering wheel to slide in the hands without resistance during rapid steering maneuvers. This finish also expresses sportiness (Fig. 11).

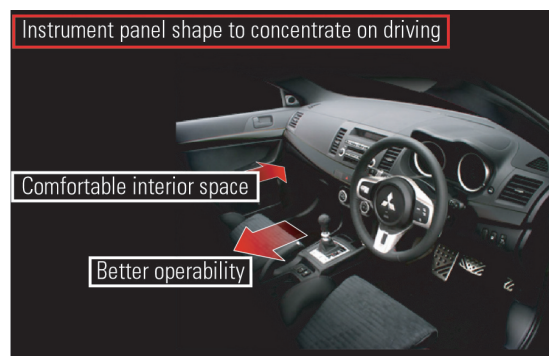
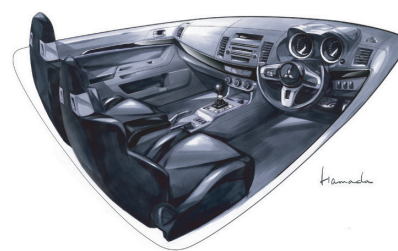


Fig. 10 Instrument panel shape



Interior sketch (final)

4.2.2 Shift indicator panel (twin clutch SST)

The shift panel of the newly developed twin clutch SST (Sport Shift Transmission) high performance transmission uses a shift knob of the same shape as that for the manual transmission and a leather-like boot intended to express "operation reflecting driver intent in real time" (Fig. 12). The shift indicator panel has bright finish on it to give the appearance of silver painting or chrome plating, and expresses high quality befitting a premium sports car. At the back of the boot is a toggle type twin clutch SST mode switch, which makes for reliable handling during driving.

4.2.3 Meters

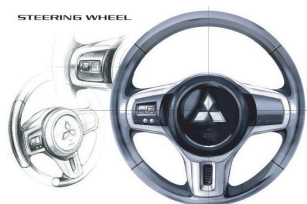
The dedicated meter panel of the LANCER EVOLUTION X uses high contrast meters for good legibility. The meter graphic is specially designed, and the figure font enables the driver to accurately read the meters in an instant during sports driving. The zero (0) position of the scale graduation is at the bottom of the meter, and the maximum engine speed range (6,000 – 7,000 rpm) is at the top, enabling the graduations between these two points to be spread out and thus permit minute changes in engine speed to be seen clearly. The use of precision meter scales and a dot graphic at the center part expresses the sophistication of the vehicle (Fig. 13).

4.2.4 Recaro seats

The front seats are full bucket seats made by the reputable company, Recaro GmbH. In this development, the designers aimed at having as many customers as possible enjoy the comfort of this high performance sports sedan rather than placing emphasis on the seat supportability based on the assumption of sports driving as was previously the case. In other



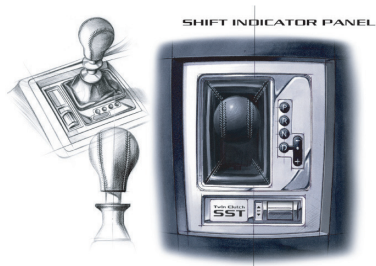
Fig. 11 Steering wheel (for LANCER EVOLUTION X)



Sketch (steering wheel)



Fig. 12 Shift panel (Twin clutch SST)



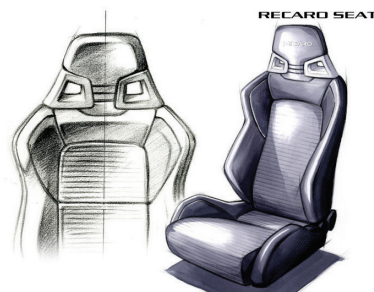
Sketch (shift panel)



Fig. 13 High-contrast meters (for LANCER EVOLUTION X)



Fig. 14 RECARO seat (GSR)



Sketch (front seat)

words, this vehicle has evolved into one that is also intended for ease of use in everyday situations. The designers strove to simultaneously alleviate the feeling of constriction, make it easier to get in and out of the vehicle, and improve the shift lever operability, without any reduction of the seat supportability, and carried out tests repeatedly until a satisfactory feeling was obtained (Fig. 14).

5. Color and material

5.1 Phantom black for the new generation model

To express the functional beauty of the LANCER

EVOLUTION X more attractively right down to the finest details, the designers searched for a body color that could express the beauty and strength of the design.

The new colors developed were red metallic and the unique color of "phantom black (pearl)".

The idea of developing "phantom black (pearl)" came from the change in the color of steel seen during a forging process, which is one of the processes used to manufacture the wheels, for example. This color appears black at first glance, however when light is reflected off a vehicle body painted in this color, the body emits orange light reminiscent of forged steel that contains heat. It was selected as the body color (Fig. 15) because it directly expresses the high performance hidden inside the vehicle.

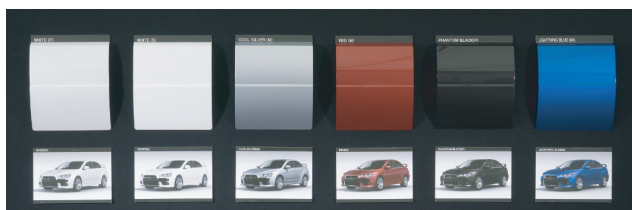
"Red (metal)" was the result of aiming for a red that



Fig. 15 Image (Phantom Black Pearl)



Fig. 16 Image (Red Metallic)



Body colors

was brilliant and very eye-catching, and directly conjured up the image of passionate driving. By changing over from solid red, which was used on previous models, to deep, brilliant metallic red, the body color has evolved into a communication color that enables the sport DNA fostered by Mitsubishi Motors in the rally field over many years to widely infiltrate the market (Fig. 16).

5.2 Seat material discussed many times with test drivers

In the development of the seat material, importance was placed on the function of supporting the driving position. At the development stage, test drivers repeatedly checked the feeling during driving tests under extreme conditions, and fed back their impressions concerning the seat material. As a result, two kinds of seat materials were developed.

One of these is a suede-like knit material which has high gripping performance over the entire seat surface and thus satisfies the needs of drivers who are interested primarily in motor sports (Fig. 17).

The other material is a combination of leather and Glanluxe (suede-like artificial leather consisting of ultra-fine fibers) which is intended for drivers who wish to enjoy quality and comfortable driving in a powerful vehicle. This material, which is a combination of functionality and premium quality, not only grips the body firmly, but also demonstrates the quality of a well-built vehicle (Fig. 18).

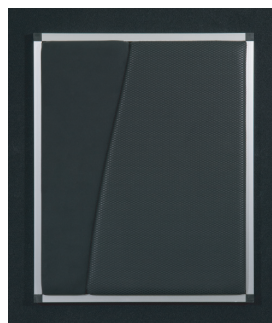


Fig. 17 Knit (suede)

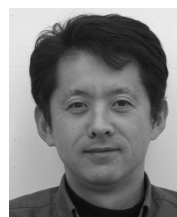


Fig. 18 Leather and Glanluxe

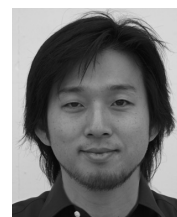
6. Conclusion

This project was concentrated on incorporating functions into shapes while repeatedly carrying out concrete tests and discussions from the initial stage. Many of these shapes were created not from styling but rather from functions, to a greater degree than in previous projects. However, the designers were not too content with this, and spent a considerable amount of time in order to find the best compromise between functions and styling. The designers created a test vehicle for measuring the cooling performance without waiting for the construction of a normal test vehicle, and carried out numerous enhancements, such as the building of a concept car over two fiscal terms, during the course of development. The background of this development is the precondition that the LANCER EVOLUTION must undergo continuous evolution as Mitsubishi Motors' flagship car.

The authors would like to take this opportunity to thank the persons who provided valuable cooperation in carrying out the difficult task of refining styling without allowing any loss of function.



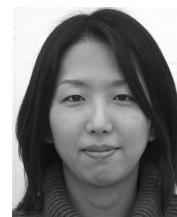
Hiroaki MATSUNOBU



Norihiko YOSHIMINE



Kei HAMADA



Chigusa YASUI

Development of i MiEV Next-Generation Electric Vehicle (Second Report)

Takashi HOSOKAWA* Koji TANIHATA* Hiroaki MIYAMOTO*

Abstract

Mitsubishi Motors Corporation (MMC) recently developed the i MiEV—an electric vehicle (EV) utilizing the ultimate eco-friendly zero-emission driving based on the “i” minicar. With the i MiEV, MMC addressed the shortcomings of earlier electric vehicles using revolutionary technologies such as high-performance lithium-ion batteries and compact, high-performance motors. MMC is verifying the i MiEV’s real-world practicality by means of on-road running tests.

Key words: *Electric Vehicle (EV), Environment*

1. Introduction

As global warming has become a serious concern in recent years, there is a growing need to reduce the environmental burden caused by energy utilization. In response, in autumn 2006 MMC started to develop an advance test model of its next-generation electric vehicle (i MiEV) using revolutionary technologies such as high-performance lithium-ion batteries and compact high-performance motors, and has carried out various tests. In March 2007, MMC started a joint research project with Tokyo Electric Power Company and Kyushu Electric Power Co., Inc. on marketing the electric vehicle (EV). Together with Chugoku Electric Power Co., Ltd. which joined in June 2007, the project is now testing practical characteristics such as per-charge range and electricity consumption, mainly assuming the EV will be used for commercial applications. Compatibility with the quick chargers currently being developed by various electric power companies is also being tested. During the one year after completion of the advance test model, the project has verified the per-charge range, electricity consumption and charge time of the EV, which are the key issues of EVs. The project has clarified actual performance compared with development targets, and identified new issues with the EV. This paper reports on these results.

2. Issues concerning EVs to date

Ten years have passed since Toyota Motor Corporation started mass-producing the PRIUS, and hybrid .s (HEVs) have been spreading year by year as other manufacturers enter the hybrid market. However, EVs are limited to a very few business and governmental applications, and there are many challenges to be addressed before they can be sold to general consumers.

MMC started developing EVs as early as 1971, when Japan established its first agency governing environ-

mental affairs, the then Environment Agency of Japan, to address air pollution and photochemical smog that were major problems at the time. At the height of Japan’s rapid economic growth, EVs were considered the solution to air pollution and automakers competed to develop EVs. MMC started out by developing the MINICA VAN EV and the MINICAB EV under commission by an electric power company and 108 units were delivered.

MMC continued to develop EVs, producing the DELICA EV in 1979 and the MINICA ECONO EV in 1983 in response to the oil crisis and air pollution. In the 1990s, demand grew for protecting the ozone layer and addressing global warming. In this period, MMC developed the LANCER VAN EV and the LIBERO EV, which were delivered to an electric power company. This period also saw a surge in EV development by major automakers seeking to meet the requirements of the California Zero Emission Vehicle (ZEV) Program. Although MMC was not among the automakers designated by the Program and thus had a relatively long time for developing products conforming to the ZEV requirement, the company actively improved its EV technologies, developing in 1998 the FTO-EV which was powered by a large-capacity lithium-ion battery that could cover a much longer distance per charge, followed in 2001 by the ECLIPSE EV (Fig. 1).

However, using electricity as the energy source introduces various problems that have prevented automakers’ electric vehicles from being marketed widely. The three major problems are: 1) vehicle performance, including too short per-charge range and too long charge time; 2) component technologies, such as the batteries and motors being too heavy, bulky and costly; and 3) battery charging infrastructure.

The per-charge range is no more than 100 km for currently marketed EVs, and even the new types currently being developed by various automakers have a range of only about 160 km. The battery, which determines the performance of the vehicle, is produced in

* MiEV Engineering Dept., Development Engineering Office

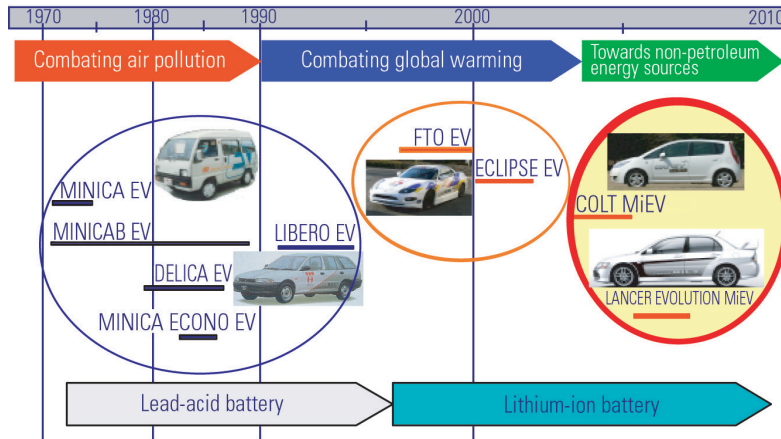
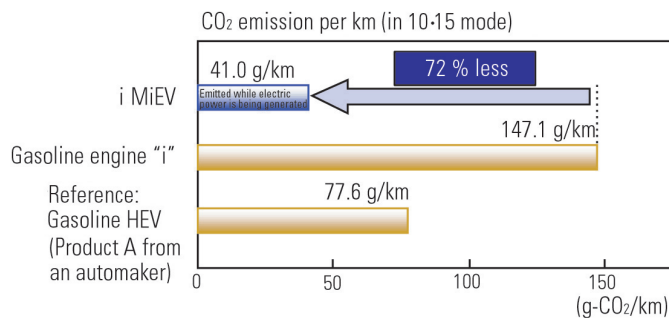


Fig. 1 History of electric vehicle development

Table 1 Overall energy efficiency

Vehicle type	Well to Wheel		Total energy efficiency
	Well to Tank	Tank to Wheel	
EV	Refining, power generation, electricity transmission 43 %*	On-the-vehicle efficiency 67 % (Including charging efficiency of 83 %)	29 %
Diesel engine vehicle	Refining, transportation 88 %	On-the-vehicle efficiency 18 %	16 %
Gasoline HEV	Refining, transportation 82 %	On-the-vehicle efficiency 30 %	25 %
Gasoline engine vehicle		On-the-vehicle efficiency 15 %	12 %

*: The above figures are based on Japan's average composition of energy sources for power generation.

Fig. 2 CO₂ emissions

small quantities and so, like the vehicle, is expensive. The advantage of the battery is that it can be recharged using a household power outlet and no new infrastructure is required. On the other hand, the per-charge range is short, and it takes between four to eight hours to fully charge the battery. For EVs to spread among general users, recharging stations with quick chargers are needed. The EV itself does not emit exhaust gases while it is running and produces little noise and vibration. However, if it uses electricity produced by a thermal power plant, the plant has produced CO₂ in large quantities, causing doubt about the EV's environmental performance.

3. Benefits of EVs

EVs score highly on environmental performance as they emit no exhaust gases during running and provide a route for moving away from fossil fuels. In terms of total energy efficiency, CO₂ emission and energy economy, EVs rank above all other types of powered vehicles in all of these respects. The total energy efficiency data⁽¹⁾ shown in **Table 1** are based on a "well to wheel" analysis (covering the total energy path from fuel production and supply to consumption on the vehicle). Here, the efficiencies of a vehicle's energy sources are compared in terms of the "well to tank" (from fuel production and supply to tank filling) and "tank to wheel" (from tank filling to driving) analyses, which are the two analytic segments of the "well to wheel" analysis. In terms of the "well to tank" segment, the oil refining efficiency is generally estimated to be 82 % for gasoline and 88 % for diesel fuel. As for electricity, the refining efficiency is generally rated at 43 % when based on the average energy source composition in Japan (the refining efficiency varies with the composition of the energy sources used for power generation). Comparing the on-the-vehicle efficiency of the same energy sources in terms of the "tank to wheel" analysis assuming that vehicles are operated in 10-15 mode, the efficiency of gasoline engine vehicles is rated at approximately 15 % and that of gasoline HEVs at 30 %. Diesel engine vehicles show a better on-vehicle energy efficiency than gasoline engine vehicles but are still around only 18 %. In contrast, the on-the-vehicle energy efficiency of EVs is 67 % even when counting the loss during charging; this value is far higher than the other two energy sources. When compared in terms of the overall "well to wheel" analysis, the energy efficiency is rated at

25 % for gasoline HEVs, 16 % for diesel engine vehicles, and 29 % for electric vehicles. The results indicate that EVs are the most energy efficient in total. MMC is now striving to develop EVs that can achieve a total energy efficiency of 32 % by improving their on-the-vehicle energy efficiency. **Fig. 2** compares total CO₂ emission values of vehicles for three types of energy source in terms of "well to wheel" analysis⁽¹⁾. The EV (i MiEV) produces 72 % less CO₂ than the base gasoline engine vehicle ("i"), and 47 % less than the gasoline HEV now available in the market. Furthermore, EVs emit CO₂ only during electricity generation in the power plant and not while driving. The EV (i MiEV) also outperforms gasoline or diesel fueled internal combustion engine vehi-

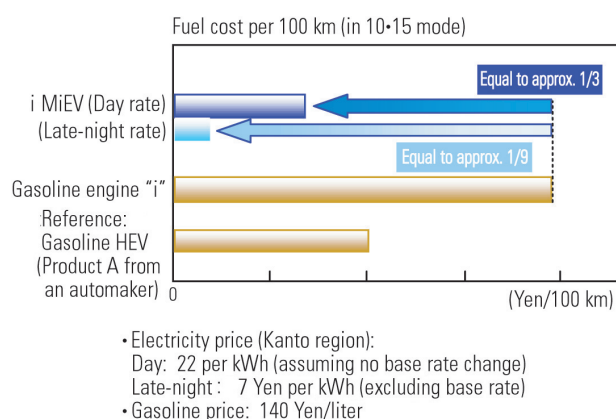


Fig. 3 Energy economy



Fig. 4 i MiEV

cles in both energy economy and fuel cost (Fig. 3). To cover a distance of 100 km, the EV costs just 270 Yen, which is approximately one third that of an "i" gasoline engine vehicle. Furthermore, using the late-night electricity billing rate in Japan, the cost falls to only 84 Yen, or 1/9th that of the gasoline engine vehicle.

The i MiEV newly developed by MMC incorporates innovative technologies including lithium-ion batteries and a compact high-performance motor. In the ongoing joint research with electric power companies, MMC is verifying the i MiEV's practicality by means of on-road experimental test (fleet monitoring).

4. Features of the newly developed i MiEV

4.1 Technical features of the i MiEV

The i MiEV (Fig. 4) directly inherits the advantages of its base model "i", which means that few modifications were required to turn the base model into an EV. The i MiEV is designed to offer an adequate per-charge range for daily use as well as sufficient power performance for sport-like driving. The major specifications of the i MiEV are listed in Table 2.

Table 2 Major specifications

Overall dimensions (L x W x H)	(mm)	3,395 x 1,475 x 1,600
Vehicle weight	(kg)	1,080
Seating capacity	(persons)	4
Maximum speed	(km/h)	130
Per-charge range (10·15 mode)	(km)	160*
Motor	Type	Permanent magnet synchronous motor
	Maximum output (kW)	47
	Maximum torque (N·m)	180
Drive system		Rear wheel drive
Batteries	Type	Lithium-ion
	Total voltage (V)	330
	Total wattage (kWh)	16

*: MY 2007 fleet test target value

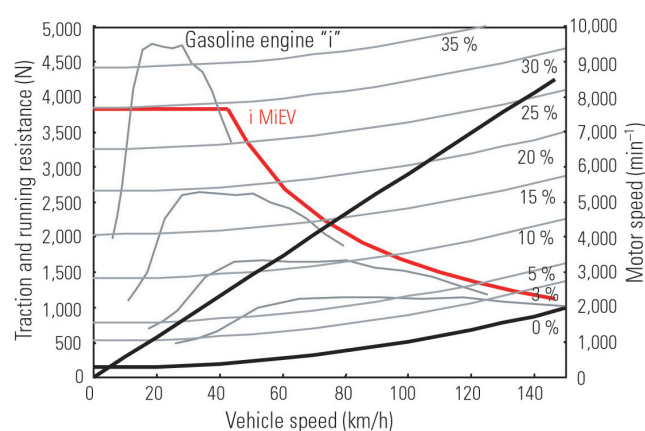


Fig. 5 Running performance curves

4.2 Higher power performance than the base model

The i MiEV uses a compact, high-performance, permanent magnet synchronous motor instead of an engine. This motor can deliver the maximum torque even from 0 min⁻¹ speed and, unlike internal combustion engine vehicles, can cover the entire range of driving speed without any transmission system. A motor with a maximum output of 47 kW and maximum torque of 180 N·m combined with a reduction gear covers the entire traction performance available from the base model (Fig. 5).

4.3 Extended per-charge range

The i MiEV uses lithium-ion batteries as the driving power source. These compact, high-performance batteries have a per-weight energy density at least four times that of conventional lead-acid batteries. Lithium-ion batteries offer excellent output performance because of their internal resistance that stays low irrespective of the level of discharge, thus ensuring stable power performance right down to the discharge limit (Fig. 6).

The per-charge range of the i MiEV with the current battery system is 130 km in 10·15 mode. In preparation for the MY2008 fleet test, MMC is improving the running

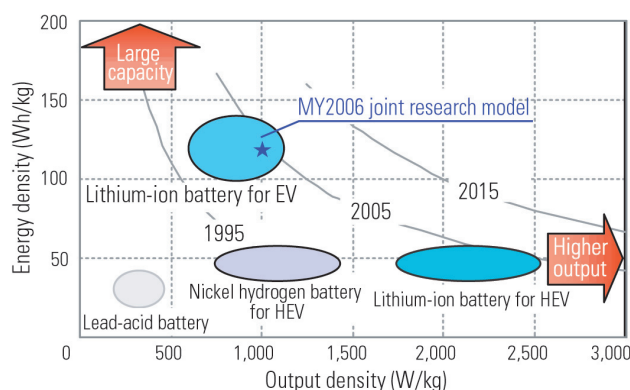


Fig. 6 Lithium-ion batteries

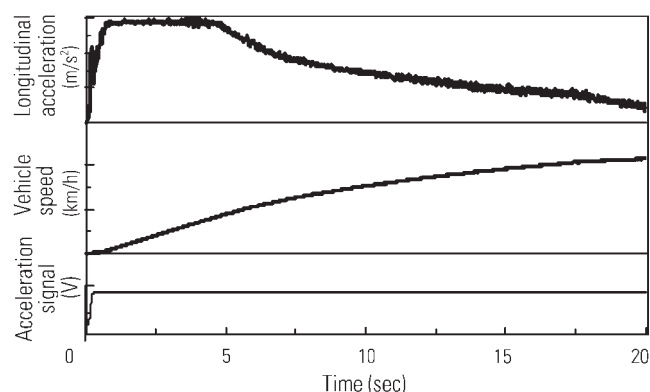


Fig. 7 Dynamic performance (acceleration and speed)

Table 3 Rapid charging and household charging

Type	Power source	Charge time
Quick charge (80 % charge)	3-phase 50 kW/200 V	Within 30 minutes
Household outlet charge (Full charge)	200 V (15 A)	Approx. 7 hours
	100 V (15 A)	Approx. 14 hours

efficiency as well as the battery performance of the EV aiming at a per-charge range of 160 km.

4.4 Quick charge and normal charge from 100 V/200 V household outlets

The battery system can be charged by either quick charge or normal charge from a 100 V/200 V household outlet for enhanced convenience (Table 3). The quick charger is a stand-alone type and can charge the battery to 80 % state of charge (SOC) in 30 minutes, which will be useful for quick charging when away from home. The home charger is an onboard equipment and compatible with both 100 V and 200 V household outlets. It charges the battery system to full SOC in 14 hours when using a 100 V/15 A power source, and in seven hours when using a 200 V/15 A power source. This assumes overnight charging at cheaper late-night electricity rates in a household garage.

5. Results of verification test of the i MiEV

5.1 Power performance

The i MiEV does not have any transmission system; the motor is directly connected to the drive wheels. Since the motor has a high torque response, the driver can accelerate the vehicle immediately after pressing the accelerator pedal even from a standing start and raise the speed continuously to the top speed.

In addition, unlike an internal combustion engine, the motor of the EV can generate the maximum output

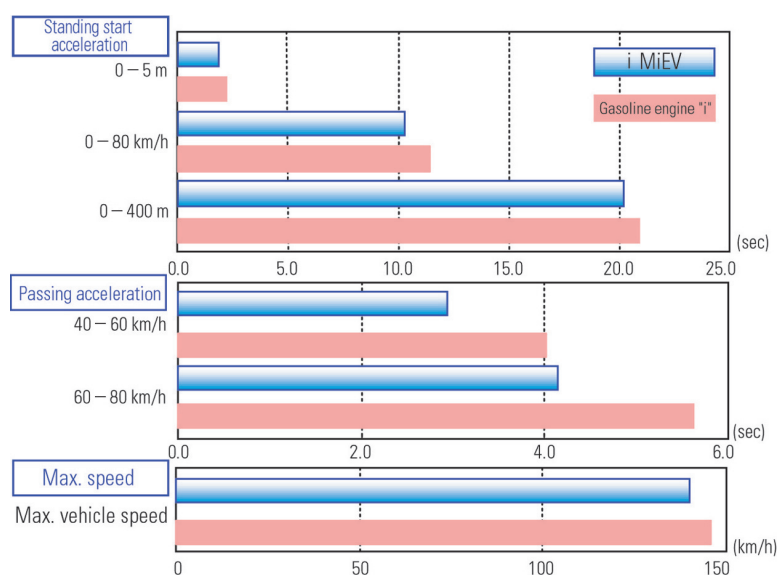


Fig. 8 Test results (dynamic performance)

over a wide range; when the accelerator pedal is fully depressed, the motor's output quickly reaches the maximum power, so the vehicle accelerates quickly, smoothly and powerfully, because the motor is free of the torque interruptions that are common with a gasoline engine due to air intake delay or gear shifting (Fig. 7). This advantageous characteristic of the EV becomes more noticeable at higher vehicle speeds. The passing acceleration performance of the i MiEV both from 40 to 60 km/h and from 60 to 80 km/h is 30 % better than that of the gasoline engine model (Fig. 8).

These characteristics compensate for the surplus weight over the gasoline engine "i" of the i MiEV, resulting in an even higher performance than a normal gasoline engine vehicle. With high vehicle performance as well as the acceleration feel specific to EVs, the i MiEV offers true driving pleasure.

5.2 Drivability

EVs do not require a transmission, so the drive train from the motor is directly connected to the wheels.

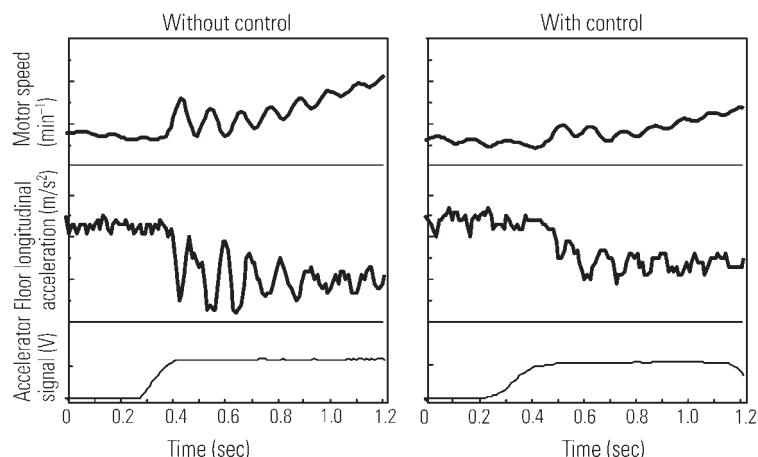


Fig. 9 Driveability improvement

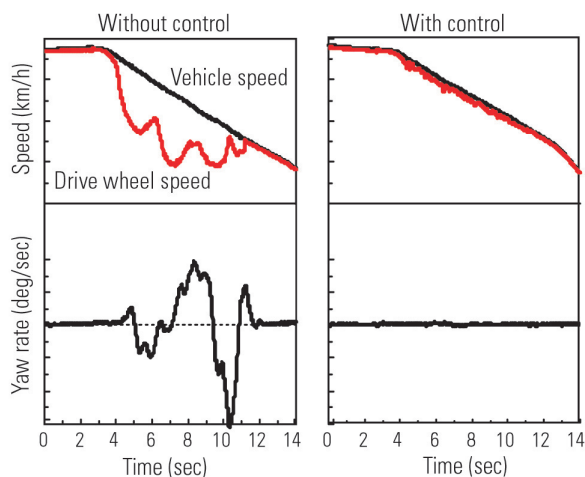


Fig. 10 Vehicle stability

This, together with the output characteristics of the motor, ensures a rapid response to the driver's control. However, this also means that EVs do not have a cushioning medium to absorb torque fluctuations; when the transmission of torque to the body is stopped, the body may resonate, resulting in large shock and vibration. This is also true with the i MiEV. When the motor operation switches from the regeneration to drive phase, the direction of the torque is reversed. This releases the twist energy that has been absorbed in the motor mounting and drive shaft and then these components reabsorb the twist energy now acting in the reverse direction. The resulting momentary interruption of torque transmission at this point constitutes a vibration source. Without any protection, the generated shock would cause the body to resonate and vibrate. In the i MiEV, the torque from the motor is controlled during the changeover from the regeneration to drive phase in order to mitigate shock, and also phase control is used to rapidly dampen vibration. This produces a smooth acceleration feel without spoiling the rapid response that is characteristic of the motor (Fig. 9).

5.3 Vehicle stability

The i MiEV is a rear-wheel-drive vehicle, so if the drive wheels spin during acceleration, the body posture may become unstable. To prevent this, traction control using the rapid response of the motor is applied to the drive wheels to ensure stability and standing start performance. The traction control is also used to prevent unstable vehicle body posture during regeneration. Regenerating energy during deceleration is a feature specific to EVs, not available with gasoline engine vehicles. However, the vehicle body could become unstable on a surface with a low coefficient of friction (μ) if the braking effect resulting from regeneration is great. The traction control ensures that the vehicle remains stable from acceleration to deceleration (Fig. 10).

5.4 Power consumption and per-charge range

The electricity consumption and effect of the running environment on consumption were investigated by driving the i MiEV on specified general roads in addition to performing a 10-15 mode driving test. Two courses were selected for electricity consumption evaluation: an urban course and a mountainous road

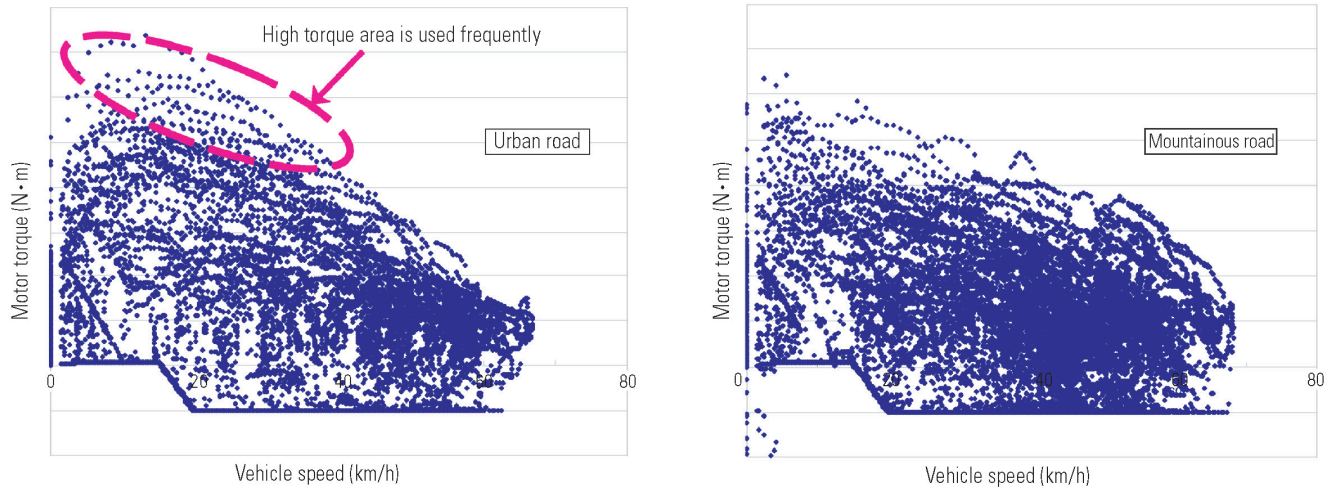


Fig. 11 Torque range differences due to running conditions

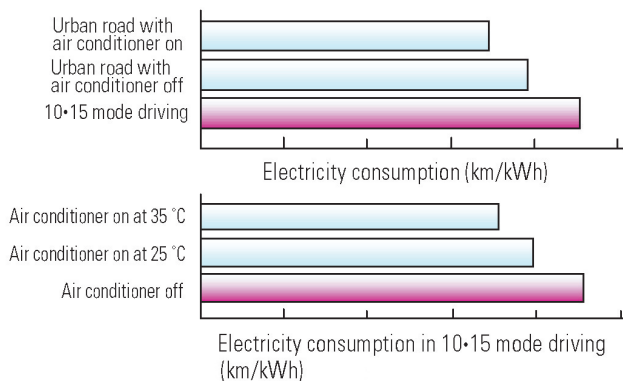
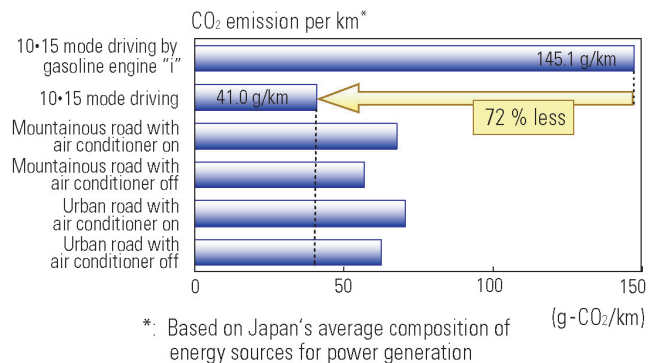


Fig. 12 Power consumption in typical conditions

course. The result of the running test on the urban course showed that the electricity consumption was increased by about 14 % on average compared with the 10·15 mode driving because of the traffic situation specific to the course such as frequent stopping and starting caused by congestion and traffic lights, but that a distance of at least 80 km could be covered per charge. On the running test on the mountainous road, the driving conditions were severer than those in the urban area with acceleration and deceleration due to slopes and curves, but the overall electricity consumption was less than that on the urban road because there was less stopping and starting at traffic lights (Fig. 11).

Next, the vehicle was driven in midsummer on an urban course with the air conditioner turned on and with it turned off, and the difference in electricity consumption between the two cases was studied. The increase in electricity consumption due to the use of the air conditioner was between 15 and 25 %. From this result, the typical per-charge range in urban areas should be between about 70 and 90 km (Fig. 12).

The average distance traveled per day by an average passenger car driver is approximately 30 km, so it has been confirmed that the i MiEV can satisfy typical

Fig. 13 CO₂ emissions in typical running conditions

usage patterns for daily life.

5.5 Effectiveness in reducing CO₂ emissions

The per-kilometer CO₂ emission involved in battery charging was calculated from the average values of electricity consumption obtained from the urban road and mountainous road tests (Fig. 13). In calculating the amount of CO₂ emitted, the proportions of the power generation methods (atomic power, thermal power, wind power, etc.) were estimated from Japan's average composition of energy sources for power generation announced at the JHFC* seminar. Including the cases where the air conditioner is not used, driving the i MiEV on urban and mountainous roads emits more CO₂ than 10·15 mode driving, but the CO₂ emission of the i MiEV is far smaller than that of the gasoline engine "i", showing that the EV has high environmental performance.

*: Japan Hydrogen & Fuel Cell Demonstration Project

5.6 Energy efficiency

The energy efficiency of the i MiEV in terms of battery charging cost was calculated from the per-100 km average electricity consumption obtained from the urban and mountainous road tests (Fig. 14). The elec-

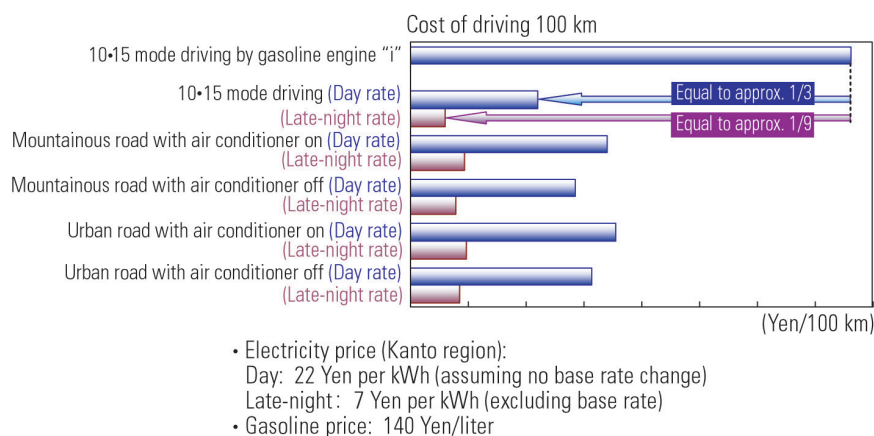


Fig. 14 Energy economy in typical running conditions

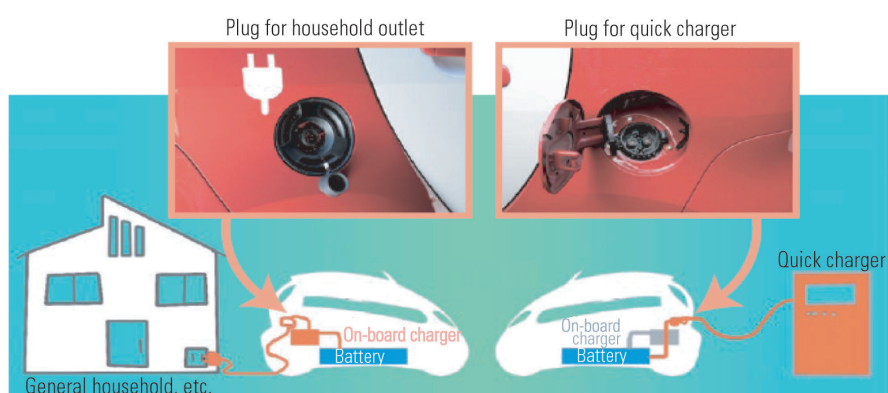


Fig. 15 Charging systems

Electricity prices used in the calculation are shown below the figure but in reality, each power company has its own electricity price plans and may levy a special basic charge as part of the late-night use charge. Although the energy efficiency in both the urban road and mountainous road driving is inferior to the 10·15 mode driving regardless of whether the air conditioner is used, the i MiEV offers significantly better economy than the gasoline engine "i".

5.7 Quick charge and normal charge from household outlets

The quick charger is a stand-alone type. It is connected to the dedicated quick charger plug on the i MiEV, and exchanges data with the i MiEV via a dedicated communication line in order to control charging according to commands from the i MiEV. The 100 V/200 V charger for normal charging from a household outlet is an on-board device. When the on-board charger plug is connected to a household power outlet, the charger automatically distinguishes between 100 V and 200 V before it starts charging (Fig. 15).

A charging test with the quick charger was performed on the i MiEV. Quick charging is con-

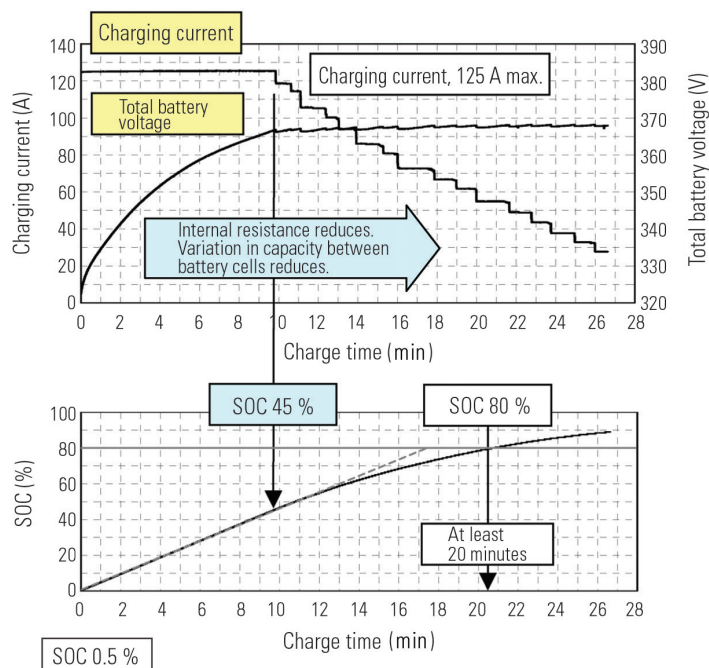


Fig. 16 Results of rapid charging test

trolled such that constant-current charging at a maximum of 125 A takes place as soon as charging starts, and when the voltage of the driving battery system reaches the specified value, the charging mode switches over to constant-voltage charging. When this is expressed using the state of charge (SOC), the constant-current charging initially takes place until approximately 45 % SOC is reached, and then constant voltage charging follows. It takes just 20 minutes to quick-charge the battery system to 80 % SOC (Fig. 16).

A test of normal charging from a 100 V/200 V household outlet was also performed on the i MiEV. Normal charging is controlled such that it begins with constant-power charging to ensure that the power capacity of the household outlet is not exceeded and when the voltage of the driving battery system reaches the preset value, constant voltage charging follows. The initial constant-power charging takes place at approximately 6 A and 2 kW for a household outlet of 200 V, and at approximately 3 A and 1 kW for a household outlet of 100 V. The charging mode then shifts to constant voltage charging late in the charging process. The normal charging takes about 6 hours with 200 V, and about 16 hours with 100 V (Figs. 17 and 18).

In the case of normal charging from household outlets, the charge time may be longer because of the larger proportion of power consumed by a vehicle's accessory loads.

Although the battery charge time is one inherent disadvantage of EVs, the i MiEV uses compact, high-performance lithium-ion batteries for the driving battery system to shorten the charging time. For the future development of EVs, it is important to improve the convenience, including building battery charging infrastructure, to enable the battery to be charged easily at any time, anywhere and by anyone.

6. Conclusion

EVs have seen two booms in the past. The current boom is the third one and started 10 years after the second boom. As a result of technical innovations during the last decade, EVs now offer almost practical running performance and per-charge range. Also, general users are becoming increasingly interested in the environment rather than focusing on vehicle performance, due to rising public awareness of the environment and the recent rise in oil prices. Although various challenges remain for the practical use of EVs, MMC will address these and improve the i MiEV to the level where EVs can be widely used as the ultimate eco-car by general users.

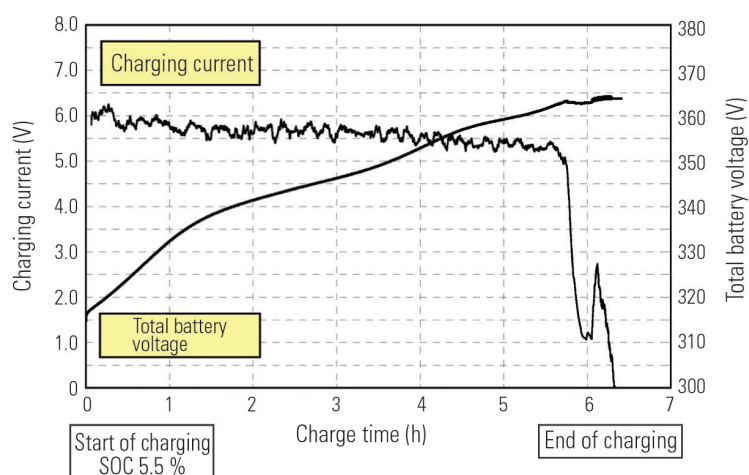


Fig. 17 Results of household 200 V charging test

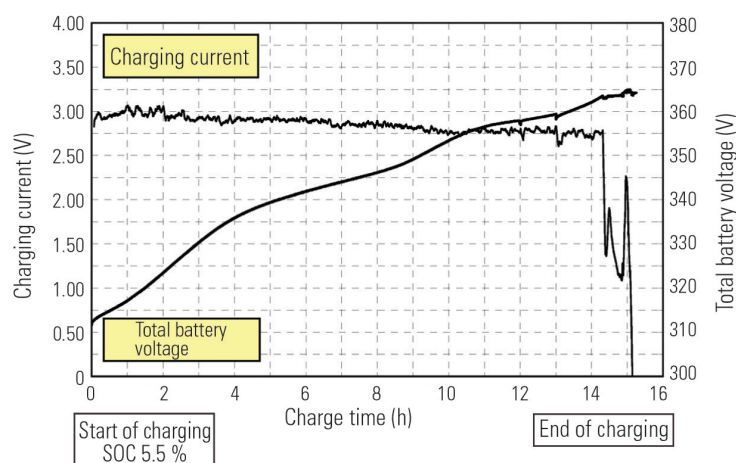


Fig. 18 Results of household 100 V charging test

Reference

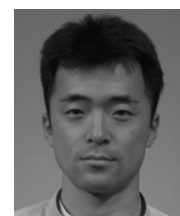
- (1) Kazunori Handa, Hiroaki Yoshida, "Development of Next-Generation Electric Vehicle "i MiEV", " Mitsubishi Motors Technical Review, No. 19, 2007



Takashi HOSOKAWA



Koji TANIHATA



Hiroaki MIYAMOTO

Development of Technology for Detection of Approaching Objects Using Noseview Cameras

Keiji UEMINAMI* Takahiro MAEMURA* Hirokazu TANIUCHI*
Takashi SHIMIZU* Shigeya SASANE**

Abstract

Mitsubishi Motors Corporation (MMC) recently developed a system that warns the driver when an object is approaching. The system uses the results of processing of images from noseview cameras in calculation of the time until the approaching object and the system-equipped vehicle cross each other's paths. (Noseview cameras help a driver check for safety to the left and right when moving forward into intersections where visibility is poor.) The newly developed system uses monocular cameras and a three-dimensional reconstruction algorithm adapted by MMC to calculate the time to crossing (TTC; the time until an approaching object traverses the camera position). The system showed itself capable of delivering appropriate information to the driver as it could calculate the TTC approximately 2 seconds or more earlier than the crossing with the approaching object. Further, it was verified as robust with respect to typical disturbance that affects detection of an approaching object and calculations of the TTC in real-world conditions. It was thus confirmed as being capable of correctly calculating the TTC in an environment containing disturbance.

Key words: *Intelligent Vehicle, Safety, Electric Equipment, Comfort, Human-Machine-Interface, Intelligent Transport Systems (ITS)*

1. Introduction

Data on traffic accidents in 2006 show that, in terms of the total combined number of reported deaths and injuries by type of accident, collisions at intersections rank second after rear-end collisions, accounting for more than a quarter of all injuries/deaths. Looking specifically at fatalities from vehicle-to-vehicle accidents in 2006, collisions at intersections topped the list of accident types with 36 % of the total. Of all collisions at intersections, 75 % of them occurred in urban areas, half of which were at intersections without traffic lights^{(1) (2)}. Against this background, MMC has developed a vehicle-mounted system that detects objects (vehicles, bicycles, etc.) approaching the vehicle from the left and/or right at an intersection with obstructed visibility, then calculates the time it will take for the vehicle and detected object(s) to intersect, and then provides the driver with appropriate information according to the circumstances.

2. Outline of the system

The system uses noseview cameras. It captures the monitor screen images, and processes them to detect approaching vehicles, bicycles and other objects. The noseview cameras, mounted on both sides of the front of the vehicle, capture images of the areas to the left and right at an intersection with obstructed visibility as the vehicle is entering the intersection, and the captured

images are displayed on the monitor to help the driver check the safety. Today, many vehicles, especially minivans, come equipped with similar systems (Fig. 1).

Fig. 2 shows the view angles of the noseview cameras currently on the market, the driver's field of view and displayed images. Images captured on both sides of the vehicle are shown on a monitor in the cabin as the vehicle enters an intersection.

This detection system primarily consists of an existing noseview camera system and an added image-processing electronic control unit.

3. System requirements

In the process of developing this system using noseview cameras to support driving, we first reviewed the system requirements.

Unlike millimeter wave radar technology for warning and control systems designed to assist driving, camera image processing technology has limited robustness against darkness, rain, snow, fog and other similar conditions. Therefore, this project is aimed at developing a system that provides the driver with information appropriate for the conditions of the moment, not a system that automatically applies the brakes.

The primary location for using the system was assumed to be urban intersections, with vehicles and bicycles traveling at 20 – 60 km/h as detection targets. The typical scenario envisioned for system utilization was as follows: A vehicle equipped with the system

* Electronics Engineering Dept., Development Engineering Office

** MCOR Co., Ltd

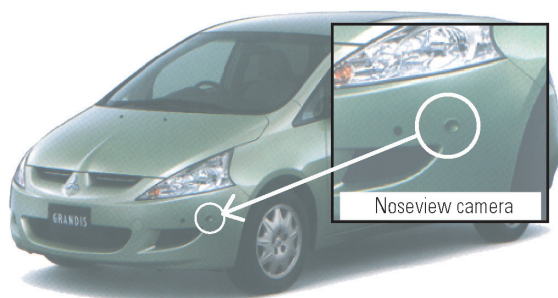


Fig. 1 Noseview camera (external appearance)

briefly stops in front of an intersection before entering it. The vehicle then starts to enter the intersection without noticing the approaching object(s). The system should then provide information to the driver, taking the driver's response time and other factors into account, at least two seconds prior to possible collision.

Price is one factor that influences the marketability of any safe driving support system. While efforts are being made to popularize driving support systems including collision mitigation brake systems and lane-keeping systems, to date these systems have only been fitted on high-end vehicles. To help achieve an attractive price for our system, it was decided to use existing monocular cameras and to develop an algorithm with low calculation cost, which affects the performance of the microprocessor used.

The time taken for an object to reach the monocular camera was defined as Time to Crossing (TTCR) (Fig. 3). An algorithm that enables a 32-bit 400 MHz microcomputer to calculate TTCR every 100 ms was developed.

4. Moving object detection algorithm

4.1 Outline

The existing systems for detecting traveling vehicles are generally designed to measure traffic flows by processing images captured by monitoring cameras installed along the roadside. In such systems, an inter-frame difference technique with relatively light calculation load was widely used for real-time image processing. Today, with ever-increasing processor speeds, optical flow algorithms have come to be used⁽³⁾⁽⁴⁾. Although camera movement does not need to be considered for measuring traffic flow using fixed cameras, it must be considered for systems that use on-board cameras.

In this study, to satisfy the system requirements of providing appropriate driver information with limited calculation cost, an algorithm to estimate TTCR defined earlier was developed by applying a three-dimensional reconstruction algorithm for monocular cameras (Fig. 4).

Noseview camera images (640 x 480 pixels) as shown in Fig. 2 are fed into the system as 256 gray-scale images, and then divided into left and right segments before being compressed to 1/4 of the original sizes for calculation. The left and right images are then analyzed

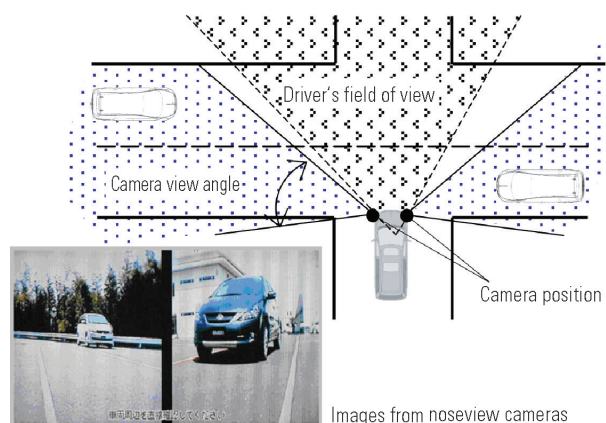


Fig. 2 Noseview camera images and driver's field of vision

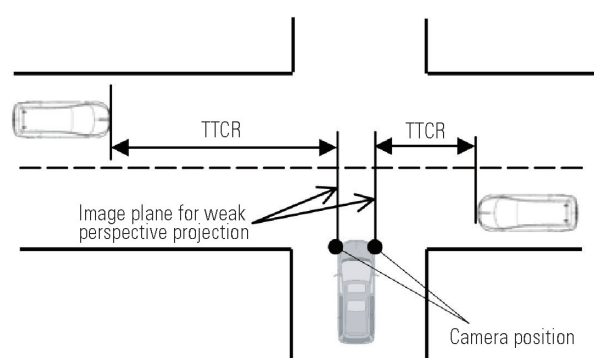


Fig. 3 Definition of TTCR

to extract feature points of approaching objects. Specifically, from among the characteristic values on the small-window space gradient matrix of the images, those which resemble polygonal angles are derived⁽⁵⁾⁽⁶⁾. In addition, a pyramid Lucas-Kanade algorithm⁽⁷⁾, known for its stable and low-load numerical calculation, is used to track feature points. Furthermore, the tracked feature points are filtered to remove noise, then subjected to three-dimensional reconstruction⁽⁸⁾⁽⁹⁾ and clustering processes before being used to calculate crossing angle and TTCR.

It is relatively easy to extract feature points and calculate optical flows around these features. However, optical flows are only apparent phenomena and cannot be used to calculate the actual position and speed of an object approaching a camera mounted on a vehicle in the real world. Thus, optical flows cannot clearly indicate how many seconds remain before an approaching object will get closest to the vehicle, and therefore are not appropriate for a driving support system that provides information appropriate for various levels of danger. Therefore, this system uses a three-dimensional reconstruction algorithm to calculate TTCR.

4.2 Three-dimensional reconstruction algorithm

To build a three-dimensional reconstruction algorithm, the noseview cameras were treated as a weak perspective projection camera (Fig. 5). In the three-

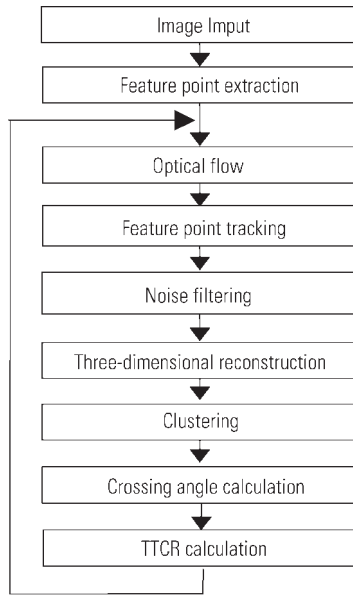


Fig. 4 Outline of algorithm for detection of approaching object

dimensional space at time t_f , the position of the camera is represented by $\mathbf{p}(t_f)$, and the attitude of the camera is represented by three orthogonal unit vectors, $\mathbf{i}(t_f)$, $\mathbf{j}(t_f)$, $\mathbf{k}(t_f)$.

The position of the feature point i in real space is represented by $\mathbf{S}_i = (X_i, Y_i, Z_i)^T$. The distance between the camera and the hypothetical image plane is represented by $z(t_f)$.

The following matrix \mathbf{W} was established for three-dimensional reconstruction. At time t_f , the location of the feature point i on the image plane is represented by $(x_i(t_f), y_i(t_f))$, the number of frames for tracking feature points is represented by F , and the total number of feature points is represented by P , where t_1 is the time at which tracking starts and t_f is the time for the current frame.

$$\mathbf{W} = \begin{bmatrix} x_1(t_1) & \cdots & x_P(t_1) \\ \vdots & \ddots & \vdots \\ x_1(t_f) & \cdots & x_P(t_f) \\ y_1(t_1) & \cdots & y_P(t_1) \\ \vdots & \ddots & \vdots \\ y_1(t_f) & \cdots & y_P(t_f) \end{bmatrix} - \begin{bmatrix} \bar{x}(t_1) \\ \vdots \\ \bar{x}(t_f) \\ \bar{y}(t_1) \\ \vdots \\ \bar{y}(t_f) \end{bmatrix} [1 \quad \cdots \quad 1] \quad (1)$$

The center of gravity for all feature points at time t_f is represented by $(\bar{x}(t_f), \bar{y}(t_f))$.

In a three-dimensional reconstruction using a weak perspective projection camera, the distance $z(t_f)$ between the camera and the hypothetical image plane can be highlighted by placing the hypothetical image plane at the center of gravity for all feature points. The matrix \mathbf{W} in equation (1) can be divided into a move-

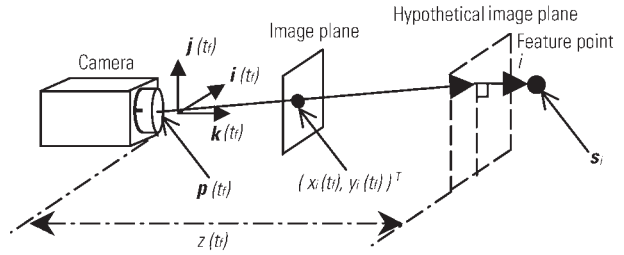


Fig. 5 Weak perspective projection camera model

ment matrix \mathbf{M} for showing relative movement between the camera and feature points and a shape matrix \mathbf{S} for showing the shape of an object based on the locations of the feature points⁽⁸⁾⁽⁹⁾.

$$\mathbf{W} = \mathbf{M}\mathbf{S} = \begin{bmatrix} m(t_1)^T \\ \vdots \\ m(t_f)^T \\ n(t_1)^T \\ \vdots \\ n(t_f)^T \end{bmatrix} [\mathbf{s}_1 \quad \cdots \quad \mathbf{s}_P] \quad (2)$$

$$\text{where } m(t_f) = \frac{\mathbf{i}(t_f)}{z(t_f)}, \quad n(t_f) = \frac{\mathbf{j}(t_f)}{z(t_f)}$$

To solve the above equation for a complete three-dimensional reconstruction, a constraint condition must be met that the coordinates of the center of gravity of feature points at a given time are known. However, in reality the coordinates are not known. With this, by assuming that the distance $z(t_f)$ is equal to α at a given time, the relationship between calculated distance $z(t_f)$ and actual distance $\hat{z}(t_f)$ (true value) can be expressed as

$$\hat{z}(t_f) = A \cdot z(t_f) \quad (3)$$

where A is a positive constant.

Equation (3) indicates that the distance $z(t_f)$ between the camera and the object (the center of gravity of feature points) that is calculated per frame multiplied by a constant A equals the true distance $\hat{z}(t_f)$. Then, considering the time at which the object crosses the image plane $x - y$ with respect to the above relationship between calculated time-series distance $z(t_f)$ per frame and true distance $\hat{z}(t_f)$, it is established that when $z(t) = 0$, then $\hat{z}(t) = 0$, irrespective of the value of constant A . Hence, TTCR can be derived by interpolating time-series calculations and predicting the time at which the true distance $\hat{z}(t_f)$ becomes zero (Fig. 6).

The object's crossing angle at the center of gravity of feature points can be derived as a movement vector $\Delta \mathbf{s}$ of difference in the location (X_f, Y_f, Z_f) of the center of gravity of feature points calculated per frame.

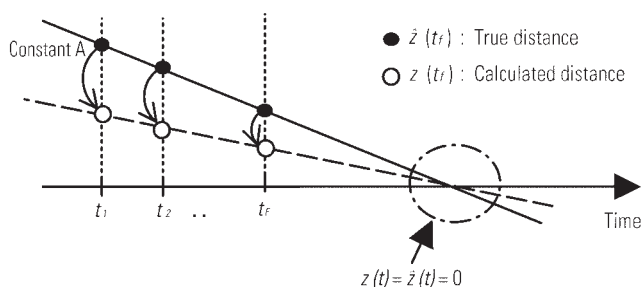


Fig. 6 Derivation of TTCR

$$\Delta s = (X_f, Y_f, Z_f) - (X_{f-1}, Y_{f-1}, Z_{f-1}) \quad (4)$$

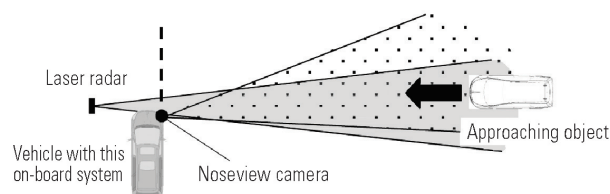
This crossing angle calculation greatly helps to eliminate noise not perpendicular to the image plane $x - y$, as the filters' crossing angle thresholds are calculated using the method. The three-dimensional reconstruction algorithm is not dependent on parameters related to the camera, such as view angle and focal length, in calculations of TTCR and crossing angle.

5. Evaluation of basic performance

Experiments were carried out to extract feature points and calculate TTCR using the noseview camera images (640 x 480 pixels) shown in Fig. 2, of lower resolution than that achieved with 256 gray-scale. These experiments were conducted during the daytime to evaluate the basic performance of the developed algorithm. Fig. 7 (a) shows the arrangement of the experiments, and Fig. 7 (b) and (c) respectively show a camera image of an approaching bicycle and vehicle. For comparison, a laser radar was also used. TTCR detected by the laser radar was compared with that calculated based on on-board noseview camera images.

Fig. 8 (a) to (f) show the results of various experiment sessions, with the vertical and horizontal axes representing TTCR and time respectively. Each of the sessions (a) to (f) is described below.

Fig. 8 (a) shows the result for an approaching bicycle. Calculations of TTCR became available at 2 seconds prior to crossing. TTCR calculations were not available during the period of 2.0 – 1.5 seconds prior to crossing, but became available again at 1.5 seconds prior to crossing. Fig. 8 (b) to (e) show the result for a vehicle approaching at 20, 40, 60 and 80 km/h respectively. Calculations of TTCR became available at approximately 2 seconds or even earlier prior to crossing at all speeds except 80 km/h. Fig. 8 (f) shows the results of simulation of a vehicle entering an intersection. The vehicle with the on-board noseview camera system accelerated to 6 km/h and moved by 2 m as it entered the intersection while another vehicle was approaching at 40 km/h. TTCR calculations were not available during start off due to the influence of the noise filters eliminating abnormal movement of feature points associated with start off, but became available again 0.5 seconds later.



(a) Experiment layout



(b) Bicycle



(c) Vehicle

Fig. 7 Basic performance evaluation experiment

In all sessions, TTCR was not available near 0 second, because the object went out of the camera view angle.

6. Robustness

6.1 Noise filters

For the system's image processing performance to be stable in real-world applications, feature points for three-dimensional reconstruction must be free of noise and accurately represent approaching objects. For that reason, the system processes the results of feature points tracking using noise filters, as discussed earlier, to improve robustness. The noise filters were developed by focusing on the following optical flow characteristics of feature points of an approaching object:

- The flow is moving in a specific direction.
- The flow is moving straight ahead.
- The flow is extending.

Each of the filters is described below.

Regarding flow direction, the relevant filter distinguishes approaching objects from the background based on the direction of flow vectors of the feature points. This is based on the principle that, with the noseview cameras mounted on the sides of the vehicle, approaching objects captured by the left camera move to the right while those captured by the right camera move to the left (Fig. 9 (a)). Regarding straight-ahead travel and extension, the relevant filters remove noise based on the principle that approaching objects have a series of flows that stay within a certain range of angles (straight-ahead travel) and that these flows extend with time (extension) (Fig. 9 (b)).

In real-world applications, the system's detection performance can be influenced by external disturbance such as rain, snow and other weather conditions as well as the disturbance of an approaching object's behavior caused by irregularity of the road surface.

Rain drops, snow flakes and other weather-related objects can be picked up by the system as feature

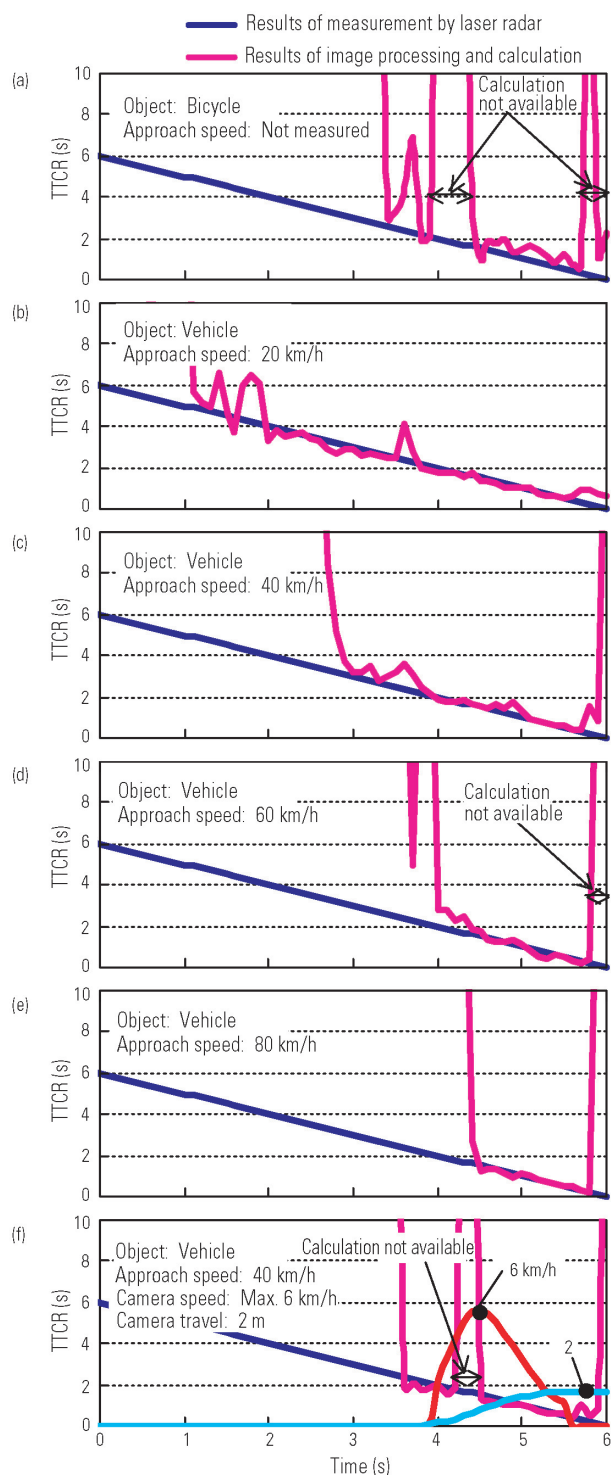
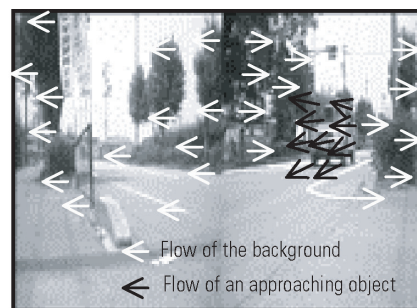
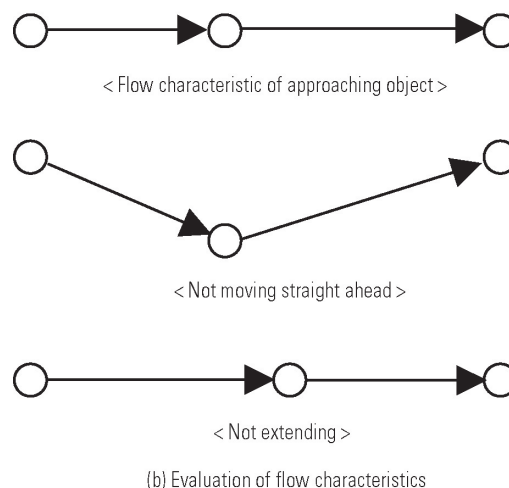


Fig. 8 Results of basic performance evaluation

points, increasing the ratio of false detection. However, these are efficiently removed by the noise filters discussed above. However, these filters can also remove feature points of approaching objects as noise when their behaviors are disturbed. The robustness of the system against these weather- and behavior-related disturbances was evaluated using computer graphics (CG) and other technologies, as discussed in the following paragraphs.



(a) Removal of the background



(b) Evaluation of flow characteristics

Fig. 9 Outline of noise filter

6.2 Robustness against weather-related disturbance

While robustness against weather-related disturbance should ideally be evaluated under real-world conditions, this may be difficult in terms of reproducibility and quantitative analysis requirements. Therefore, composite images, consisting of simulated CG images of rain and snow and real images captured by the noseview cameras, were used for evaluation. Composite images of snow (Fig. 10 (a)) were compared with images free of snow disturbance to determine the difference in processing performance (Fig. 10 (b)). The horizontal and vertical axes represent time elapsed and TTC respectively. For additional comparison, TTCs measured by a laser radar are also shown on the graphs.

With snow disturbance, the system showed a slight delay in the start of detecting an approaching object and had a slightly greater TTCR error than a laser radar. However, the system offered TTCR calculations at 2 seconds and earlier prior to crossing. Therefore, the noise filters efficiently removed snow disturbance.

6.3 Robustness against disturbed behavior of approaching object

6.3.1 Object behavior analysis

To evaluate the system's robustness against disturbed behavior of approaching objects, an actual vehicle was mounted on a four-wheel oscillation test device

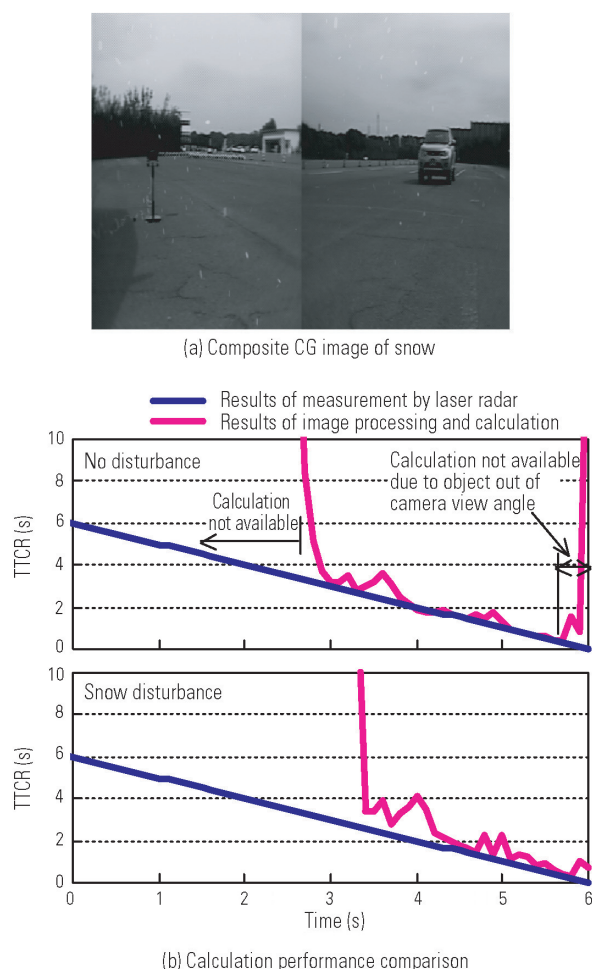


Fig. 10 Results of evaluation of robustness with respect to environmental disturbance

to simulate its behavior under actual road conditions. The oscillation device is capable of independently oscillating the four plates on which the four tires of a test vehicle are placed. Simulated oscillation waveforms typical of those caused by actual road surfaces are fed into the device to reproduce vehicle behavior caused by actual roads. During the analysis using the device, oscillation waveforms typically experienced on ordinary roads in urban areas were fed into the system and resultant vertical displacement was measured by four laser displacement gauges, two of which were placed on both sides of the lateral axis running through the vehicle's center of gravity and the other two placed on both sides of the longitudinal axis, to analyze the vehicle's bouncing, pitching and rolling behaviors (Fig. 11).

The oscillation waveforms used were those typically experienced when traveling at 40 km/h on slightly rough roads in urban areas. Road surface displacement that was actually measured was used as the waveforms to reproduce slightly rough roads in urban areas for vertical vehicle acceleration. Fig. 12 shows the power spectral density distribution of the oscillation waveforms. The test vehicle had a relatively high center of gravity to produce slightly greater amounts of oscillation-caused behavior than normal.

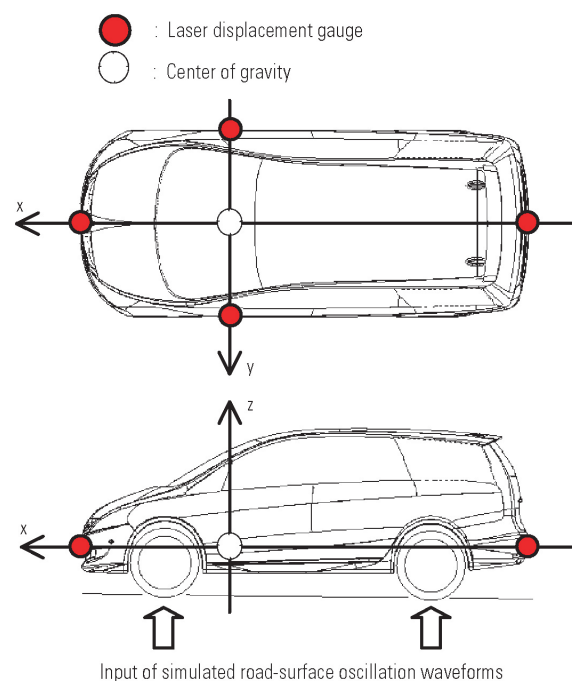


Fig. 11 Behavior analysis experiment using four-wheel oscillation test device

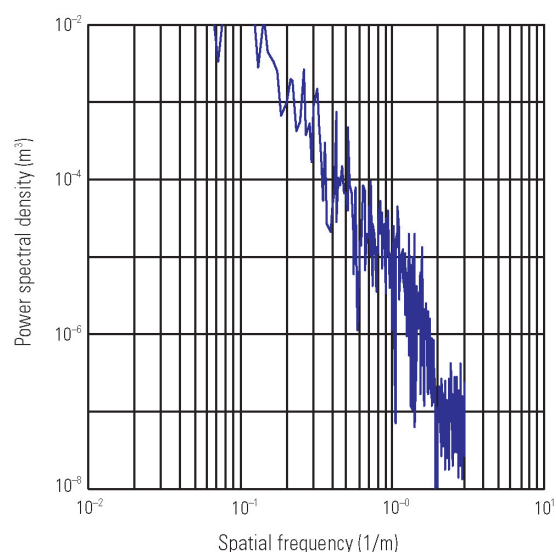


Fig. 12 Power spectrum distribution of oscillation waveform

The amount of bounce, or the displacement along the Z-axis running through the vehicle's center of gravity, was obtained by averaging the measurements of the left and right gauges. The pitch angle, or the rotational angle on the Y-axis, was obtained based on the difference in measured displacement between the front and rear gauges. The roll angle, or the rotational angle on the X-axis, was obtained based on the difference in measured displacement between the left and right gauges. The vertical displacement of the front of the vehicle, which is caused by the composite effects of bouncing and pitching and has the most influence on

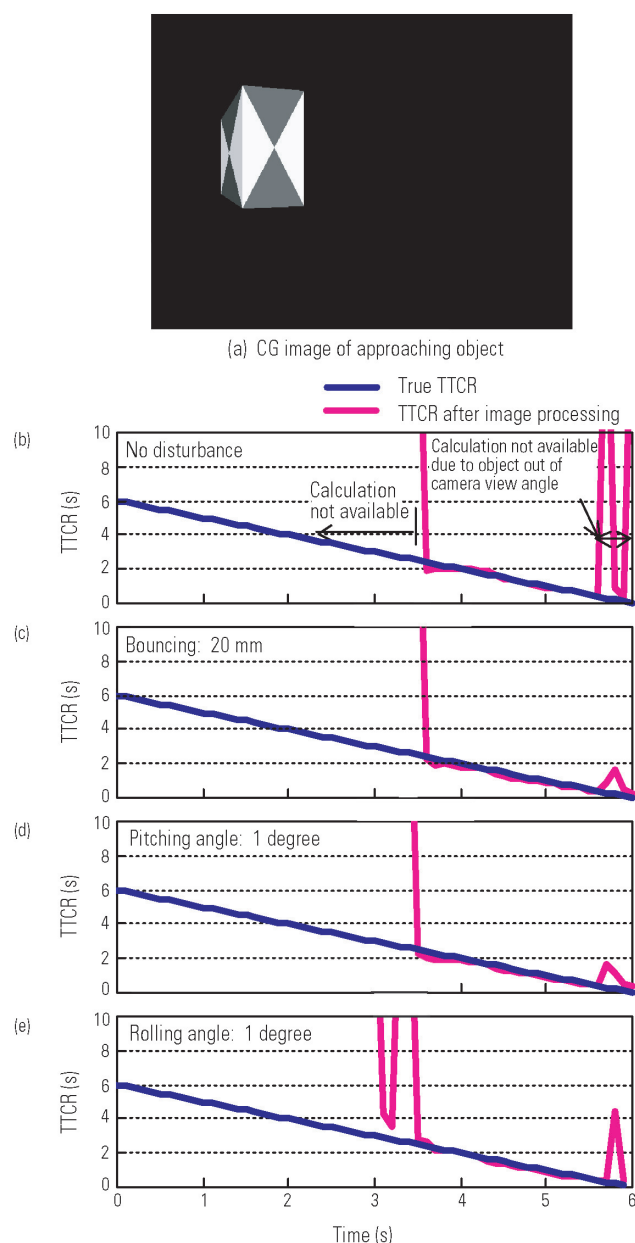


Fig. 13 Results of verification of robustness with respect to behavior of approaching vehicle

object detection performance, was obtained based on the displacement at the front of the vehicle. Assuming that the frequency distributions of these parameters are normal, the 3σ values, which represent 99.7 % of the frequencies, were as follows: bouncing = 10.1 mm, pitch angle = 0.36 degrees, roll angle = 0.73 degrees, and vertical displacement at the front of the vehicle = 17.9 mm. Then, the detection performance of the system was evaluated within the areas of the 3σ specified above.

6.3.2 Verification of robustness using CG

As with the evaluation of robustness against weather-related disturbance, it is difficult to evaluate robustness against disturbed behavior of approaching objects under real-world conditions. Therefore, simulated CG images of objects were used to evaluate robustness against vehicle behavior (Fig. 13 (a)).

Fig. 13 (b) to (e) show the results of image processing, with (b) not experiencing vehicle behavioral disturbance and with (c), (d) and (e) experiencing the disturbance of bouncing, pitching and rolling, respectively. The approaching speed was set at a constant 40 km/h. The vertical displacement at the front of the vehicle, which was the composite result of bouncing and pitching, was approximated by bouncing. The results indicate that TTCR calculations were not influenced by the 3σ of any parameter obtained in the analysis of vehicle behavior on actual roads. To identify performance limits, vehicle behavior was magnified until it started to affect the calculation. The results were: 50 mm for bouncing, 20 degrees for pitch angle and 5 degrees for roll angle. These results are twice or larger than the corresponding values when driving at 40 km/h on slightly rough roads in urban areas.

7. Summary

Using existing monocular noseview camera technology, an algorithm capable of detecting objects approaching a vehicle equipped with the technology and calculating TTCR has been developed. It has been proven that the algorithm has the basic performance capable of calculating TTCR approximately 2 seconds before an approaching vehicle traveling at 20 – 60 km/h crosses the camera mounted on the vehicle, although the system needs to be improved for reliable detection of bicycles. This shows that the system can provide the driver with appropriate information for safe driving.

The algorithm enables the system to process data at high speed and with lower calculation cost, which is essential for wide acceptance in the market. The noseview camera system can calculate TTCR every 100 ms or at even shorter intervals with only one high-performance microcomputer as commonly used in navigation and other systems.

The robustness of the system was evaluated under real-world conditions. In a verification of robustness against weather-related disturbance using composite CG and noseview camera images of rain and snow, the system's noise filters were shown to efficiently remove external disturbance. Behavioral ranges of approaching vehicles under real-world conditions were established by feeding a four-wheel oscillation device with oscillation waveforms typical of city driving. In a related experiment using simulated CG images of approaching vehicles, it was shown that disturbance-caused vehicle behavioral disturbance under real-world conditions did not influence the calculations of TTCR. The system was thus proven to be robust against weather-related disturbance as well as disturbed behavior of approaching vehicles caused by road surface irregularities, and to be capable of accurately calculating TTCR.

The system is expected to be efficient under real-world conditions in preventing accidents at intersections resulting from the driver's failure to notice approaching objects (bicycles and vehicles) when starting off after pausing at an intersection.

References

- (1) Traffic Bureau, National Police Agency, Traffic accidents situation, 2007
- (2) Institute for Traffic Research and Data Analysis, ITARDA Information No. 69, 2007
- (3) Heitou Zen et al., "Road Traffic Sensing by Multi-view Monitoring", Proceedings of 11th Symposium on Sensing via Image Information, A-6, pp. 21 – 24, 2005
- (4) Yoshiaki Oki et al., "Opposing Lane Vehicle Information System", Journal of Society of Automotive Engineers of Japan Vol. 61, pp. 68 – 72, 2007
- (5) Yasushi Kanazawa, Kenichi Kanatani, "Detection of Feature Points for Computer Vision", The Journal of the Institute of Electronics, Information, and Communication Engineers Vol. 87, No. 12, pp. 1043 – 1048, 2004
- (6) Jianbo Shi, Carlo Tomasi: Good features to track, IEEE Computer Vision and Pattern Recognition, pp. 593 – 600, 1994
- (7) Bruce D. Lucas, Takeo Kanade: An iterative image registration technique with an application to stereo vision, Proceedings of Imaging Understanding Workshop, pp. 121 – 130, 1981
- (8) Conrad J. Poelman, Takeo Kanade: A paraperspective factorization method for shape and motion recovery, Technical Report CMU-CS-92-208, CMU, 1992
- (9) Takeo Kanade, Conrad Pollman, Toshihiko Morita, "A Factorization Method for Shape and Motion Recovery", Transactions of the Institute of Electronics, Information and Communication Engineers D-II, Vol. J76-D-II, No. 8, pp. 1497 – 1505, 1993



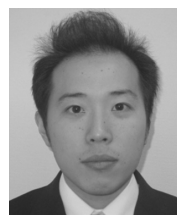
Keiji UEMINAMI



Takahiro MAEMURA



Hirokazu TANIUCHI



Takashi SHIMIZU



Shigeya SASANE

Study of Fuel Economy and Exhaust Emission Reduction by Intake Flow Control

Katsuhiko MIYAMOTO* Masayuki YAMASHITA* Kenji GOTO*
Naoto FUJINAGA* Akira MIKITA**

Abstract

With the increasing demand for car engines with higher power and lower fuel consumption, this research was focused on a variable intake flow system as a promising technique that attains both targets. Using computational fluid dynamics (CFD) simulation and testing, the authors investigated the effect of an intake manifold that blocked a certain portion on combustion and fuel consumption. Subsequently, an engine with this system was installed in a car in order to verify the fuel consumption reduction. Regarding exhaust gas, the reduction of hydrocarbon (HC) emission during cold start was addressed, with particular focus on the relationship between after-radiation distribution representing fuel droplets burning up and HC emission. The results showed that the deviation in liquid fuel was relatively large and that considerable HC was emitted when part of the intake manifold was blocked. It was also found that after-radiation and HC decreased when an adequate intake flow prevented fuel droplets from adhering to the wall.

Key words: Gasoline Engine, Intake System, Combustion

1. Introduction

In recent years, global warming has become one of the most pressing environmental issues. Ever since the Industrial Revolution, humankind has taken out thermal energy from carbon resources trapped underground to produce motive power, but while emitting carbon dioxide (CO₂) into the atmosphere. In the 100 years following the Industrial Revolution, atmospheric CO₂ concentration has risen dramatically, causing the heat generated by solar radiation during the daytime to be absorbed by CO₂ and other greenhouse gases in the atmosphere. This process is thought to be causing the steady rise in the surface temperature of the earth.

In Japan, the transportation sector accounts for approximately 25 % of total CO₂ emissions in the country, making it the second largest polluter after the civil affairs sector. At the same time, political instability in the Middle East has been delayed the supply of crude oil, and price has risen suddenly. Against this background, car manufacturers have come under increasing pressure to further reduce the fuel consumption of their cars. For example, in Japan the 2015 fuel economy standards require reductions of approximately 30 % from the 2010 levels, and in Europe efforts are being made to introduce legislation that would limit CO₂ emissions from cars to 120 g/km.

In addition to these requirements, car manufacturers are also expected to improve engine power, which is a major part of the "driving pleasure".

Engine-related efforts are being made to reduce fuel consumption, such as improved combustion by intensi-

fied in-cylinder flow, reduced pumping loss by exhaust gas recirculation (EGR) and timing retard of closing the intake valves, and reduced friction with low-tension piston rings and low-viscosity oil.

To achieve intensified in-cylinder flow and power at the same time, valves that control the intake air flow are increasingly being employed. During low-speed, low-load driving, the valves are closed to partially block the intake ports. This deflects the air flow, increasing in-cylinder tumble or swirl and thereby improving combustion and fuel economy. During high-speed, high-load driving, the valves are opened to send full of air into the cylinders (**Fig. 1**).

This paper discusses the valve that controls the flows of intake air (intake flow control valve (IFCV)), focusing on how the location and extent of blocking affect tumble characteristics, fuel consumption, and emissions reduction performance.

2. Specifications of test engine including variable valve train (VVT)

Table 1 shows the specifications of the engine used in the test. The VVT system uses controls a cam phase for the intake and exhaust valves independently.

3. Influence of tumble plate location on tumble ratio in constant flow

At first, in a constant air flow test setup, the valve location was varied to identify any influence on tumble ratio. In the test, a plate was used in place of the IFCV.

* Advanced Powertrain Development Dept., Development Engineering Office

** Mitsubishi Automotive Engineering Co., Ltd.

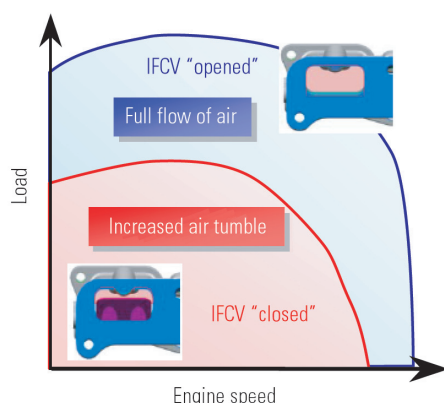


Fig. 1 Example of IFCV operation

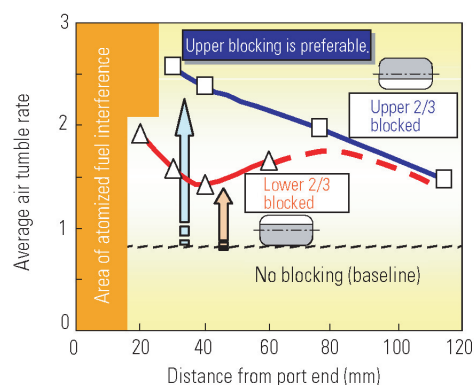


Fig. 2 Tumble plate location and tumble intensity

Table 1 Engine specifications

Fuel injection type / No. of cylinders	Port injection / 4	
Displacement	2.4 L	
Compression ratio	10.5	
Cam type	DOHC	
VVT actuator	Variable phase vane type	
VVT operation angle	Intake	50° CA
	Exhaust	50° CA

Table 2 Specifications of constant flow test

Throat diameter	31 mm
Cylinder used	#2
Liner differential pressure	4.05 kPa

The test conditions are shown in Table 2 and Fig. 2.

With the upper portion blocked, the tumble ratio increased as the tumble plate was moved closer to the cylinder head (C/H). In case of the lower portion blocked, the tumble ratio reached a minimum when the tumble plate was located at 40 mm upstream of C/H and then increased as the plate was moved further towards C/H. To find out the reasons for this, CFD simulation was carried out using STAR-CD by alternating the valve location up and down (Table 3). As shown in the left-hand graph in Fig. 3, the average tumble ratio relative to the valve location in the CFD simulation resembles the patterns identified in the constant air flow test (Fig. 2), with higher ratios achieved in upper blocking and a “dip” existed in lower blocking.

The middle and right-hand images in Fig. 3 show flow lines in the intake port and cylinder.

With the upper portion blocked, air flow was deflected downward and continued along the nearly-straight bottom surface of the port down to the intake valve. The air flow then passed directly above the valve face towards the ignition plug. This flow pattern intensifies tumble flow.

With the lower portion blocked, air flow was deflect-

Table 3 CFD conditions for constant flow test

Test conditions	Valve lift: 9 mm
Cell type	Rectangular
Boundary layer	3 layers x 0.5 mm
No. of cells	765158 – 906849
Computational conditions	Incompressible constant flow analysis
Difference scheme	MARS (Monotone Advection and Reconstruction Scheme)
Turbulence model	RNG k-ε

ed upward and then dispersed by the protruding injector mount. The flow line was thus disturbed and insufficient tumble flow resulted.

Then the injector mount protrusion was removed so that the air flow would not be disturbed. The result is shown in Fig. 4. Air flow was no longer dispersed and instead, ran along the upper surface of the port, resulting in strong tumble flow.

The above experiment showed that, irrespective of which side of the port is blocked with the valve, the port surface must have smooth contours at least where air flow is deflected so as not to disturb it.

4. Reduction of fuel consumption with tumble plate

Fuel consumption was evaluated using various blocking locations, extents and resultant intensities of tumble flow, and by varying EGR ratios under partial load (Fig. 5). Without EGR, intensification of tumble flow by partial blocking of the intake port hardly affected the fuel consumption. This is because the improvement of combustion recognized by retarded MBT ignition timing is nearly offset by the pumping loss caused by blocking and increased thermal loss from the higher maximum in-cylinder gas temperature due to improved combustion.

In relation with the introduction of EGR, without blocking, the improvement of the fuel consumption ceases at an EGR ratio of just 5 %. In contrast, with blocking, the EGR ratio at the same IMEP fluctuation reaches approx. 25 %, enabling the fuel consumption to

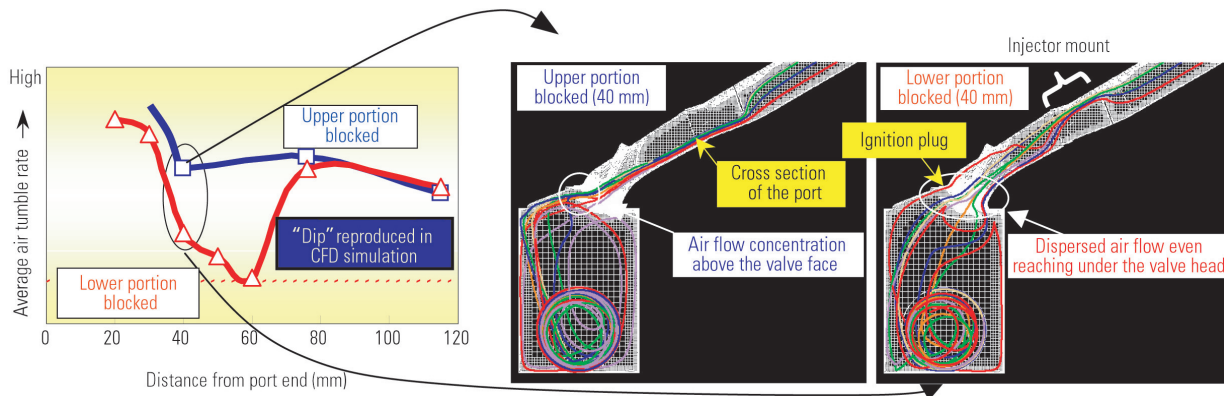


Fig. 3 CFD result of constant flow test

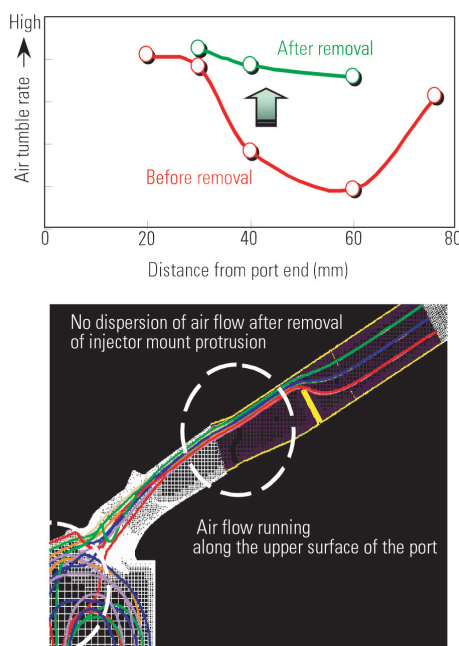


Fig. 4 Effect of modified injector installation area

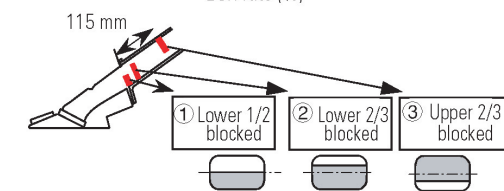
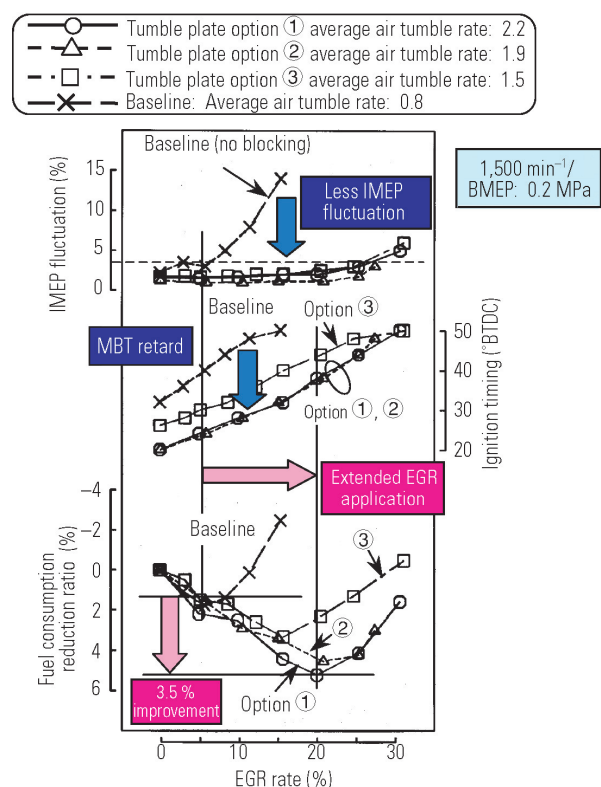


Fig. 5 Fuel consumption reduction by tumble plate

be greatly improved by the large amount of EGR. The greater the tumble ratio, the better the fuel economy. The average tumble ratio of 2.2 reduces fuel consumption by approximately 3.5 %. In addition, the introduction of EGR with tumble intensified improves combustion, which helps prevent excessive advancing of the ignition timing and minimizes the difference in ignition timing from other driving conditions, thus making the engine run more smoothly. This is another benefit of intensified tumble flow.

5. Performance evaluation of intake manifold with IFCV

5.1 Bench testing with constant flow

Bench testing was conducted in a constant air flow using an intake manifold based on the results of the previous testing discussed above. The results, averaged

over the four cylinders, are shown in Fig. 6.

The average coefficient of air flow with IFCV was 3.8 % lower than that of the standard intake manifold. The average tumble ratio with IFCV was almost 2, this was near the target. Fig. 7 shows the reduction of fuel consumption by the closed IFCV under partial load.

Combustion was more stable even at high EGR rates with IFCV closed than with IFCV opened. With IFCV closed, MBT ignition timing was more retarded than

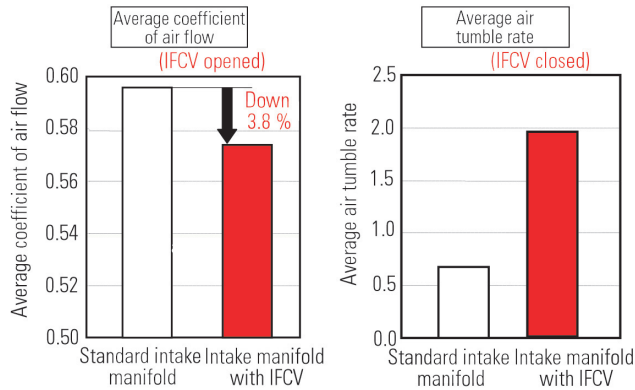


Fig. 6 Constant flow test results for intake manifold with IFCV

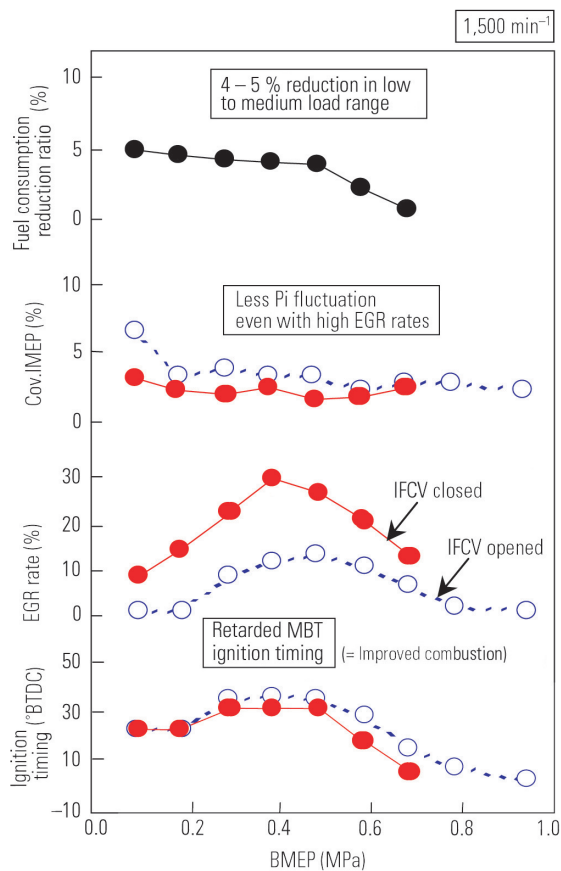


Fig. 7 Fuel consumption reduction by IFCV

that with IFCV opened. These facts indicated that the combustion was remarkably improved. A fuel consumption reduction of 4 to 5 % was obtained from the low to medium load range, and this trend continued until BMEP 0.7 MPa.

Fig. 8 shows the IFCV control strategy. As air flow rate increases with IFCV closed, more power is lost during air intake, thus offsetting the improved combustion. However, the operation area of improved fuel economy covers a wide region of practical driving range. The 10-15 and JC08 mode cycles can be driven with IFCV closed.

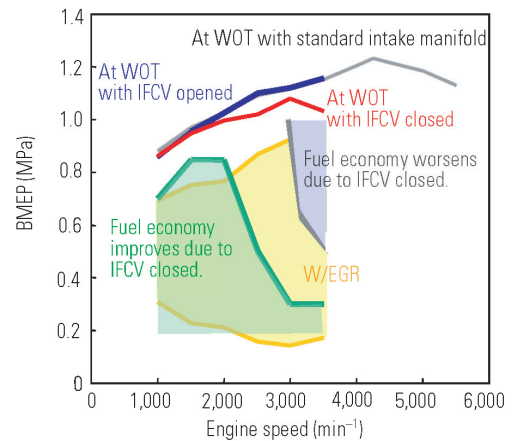


Fig. 8 IFCV control and region of fuel consumption reduction

Table 4 Fuel consumption reduction ratio in 10-15-mode cycle and JC08 (hot) mode

10-15	JC08 (HOT)
3.5 %	2.6 %

5.2 Actual vehicle fuel consumption in driving mode cycles

With the IFCV-equipped intake manifold mounted on OUTLANDER of Japanese specifications, fuel consumption was measured in 10-15 and JC08 (HOT) mode driving, with IFCV opened and closed. Fuel consumption reductions of 3.5 % and 2.6 % were confirmed in 10-15 and JC08 (HOT) mode driving cycles respectively (Table 4). The reductions were in part attributable to improved combustion leading to the retardation of MBT ignition timing, on low-speed, low-load operation near the MBT ignition timing range.

Fig. 9 shows fuel consumption reduction ratios and contribution ratios for the 10-15 mode driving cycles. The steady phase is the top contributor to the reduction with 42 %, followed by the acceleration phase with 30 %. The reduction ratio of the steady phase exceeds 5 %, which resembles the results in the bench testing. The reduction rate of the acceleration phase is just above 2 %, which is due to high engine load during the mode driving. The deceleration phase has a significant reduction ratio, which is due to improved combustion enabling the ignition timing to be set near MBT.

6. Reduction of HC at cold start

The startability of the engine using low volatility fuel can be improved by closing IFCV (Fig. 10).

This is because the intake air flow after the first combustion is accelerated by closing IFCV, improving the transport efficiency of fuel injected into the intake port. Based on this, with closed IFCV, the same level of startability as that with opened IFCV can be obtained using less fuel. Then, using a test unit of which fuel control is

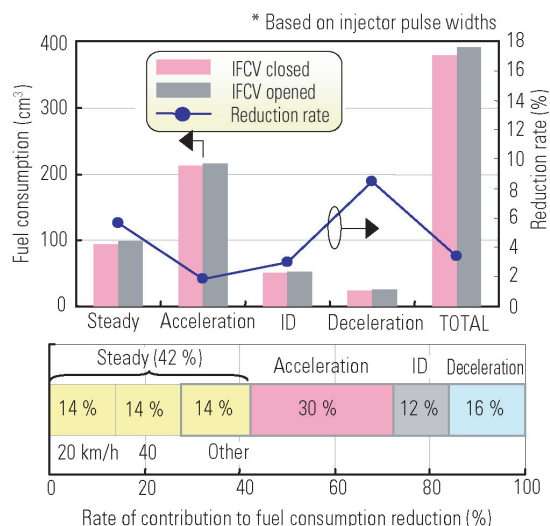


Fig. 9 Fuel consumption reduction ratio in 10-15-mode cycle and contribution ratio of each driving mode

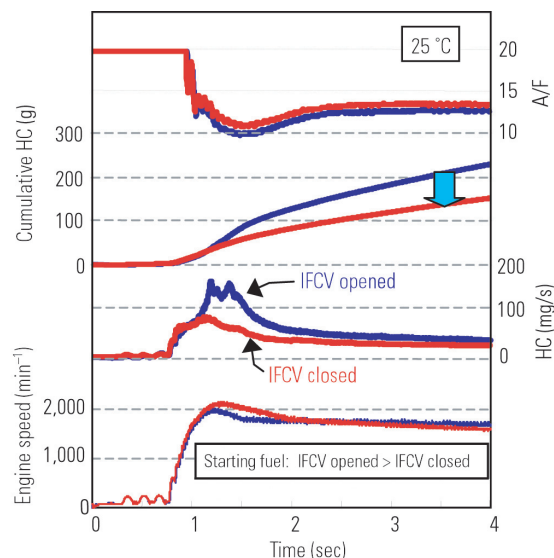


Fig. 11 HC reduction during cold start (with the same startability as that using low-volatility fuel)

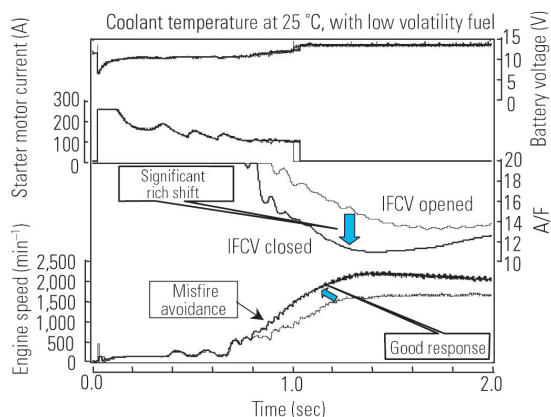


Fig. 10 Effect of IFCV on cold startability with low-volatility fuel

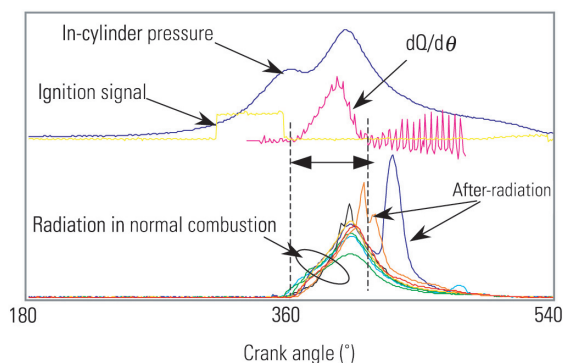


Fig. 12 Definition of after-radiation

set to assure the startability having an acceptable start feel under the condition with low volatile fuel and with IFCV closed, HC at engine start was measured using standard fuel. The results are shown in **Fig. 11**. There is less HC emission with closed IFCV than with opened IFCV.

7. Distribution of in-cylinder fuel droplets and HC emission at engine start with closed IFCV

To find out whether it would be possible to further reduce HC emission with closed IFCV, we attempted to indirectly analyze the distribution of fuel droplets in the cylinder. For this, a Visio knock of AVL, a combustion radiation measuring device, was used⁽¹⁾. The device's 8-direction sensing unit was installed onto the spark plug to observe combustion radiation in radial directions during engine start.

In normal combustion, the profile of signals from

the combustion radiation sensor resembles that of heat release rates ($dQ/d\theta$). In cold starting, however, signal spikes may be observed after heat release. This is assumed to be due to radiation that is generated when fuel droplets, after entering the cylinder, come into contact with flames and burn. With this, the ratio of the height of signals in normal combustion to that of spikes was defined as the intensity of after-radiation⁽²⁾. Then, assuming that the distribution of fuel droplets in the cylinder can be determined by observing the orientation of after-radiation intensity, the following experiments were carried out (**Fig. 12**). HC emission from the cylinder to which the Visio knock sensing unit was installed was measured using a high-speed HC meter.

Fig. 13 shows the intensities of after-radiation, measured with the IFCV opened and closed, and with the center of the port blocked. **Fig. 14** shows HC measurements with a high-speed meter.

With the IFCV closed, the intensity of after-radiation was stronger and concentrated on the intake side. With equal amounts of fuel injected, HC emission was

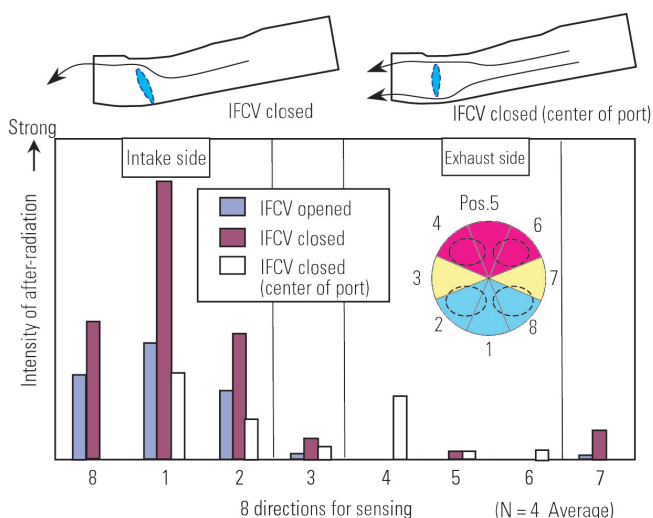


Fig. 13 Intensity of after-radiation

greater with closed IFCV than with opened IFCV. With the IFCV opened, the intensity of after-radiation was less strong and was more evenly distributed. Also, HC emission was less than IFCV closed test. It is thus considered that HC emission is greater with the IFCV closed because the air flow speed on the opposite side of the deflected intake air flow slows down, allowing more fuel to enter the cylinder as droplets.

With the center of the intake port blocked, both the intensity of after-radiation and HC emission were less severe. It is considered that the center blocking generated the rapid air flow near both the upper and lower portions of the intake port wall, which prevented fuel droplets from adhering on the lower surface of the port as happened with closed IFCV.

This suggests that HC could be reduced further by better controlling the intake air flow.

8. Summary

- (1) Using IFCV, which partly blocks the intake manifold, intake air was controlled to intensify tumble flow, thereby enabling high EGR rates. This reduced fuel consumption by 3.5 % in the 10-15 mode driving cycle and 2.6 % in the JC08 (HOT) driving cycle.
- (2) The IFCV system improved startability with low volatility fuel. Furthermore, the system also reduced HC emission at engine start with standard fuel.
- (3) The relationship between intake air control at engine start and HC emission was analyzed by measuring combustion radiation. Where there is air flow in the cylinder that has been slowed down by intake air control, after radiation is seen, which suggests

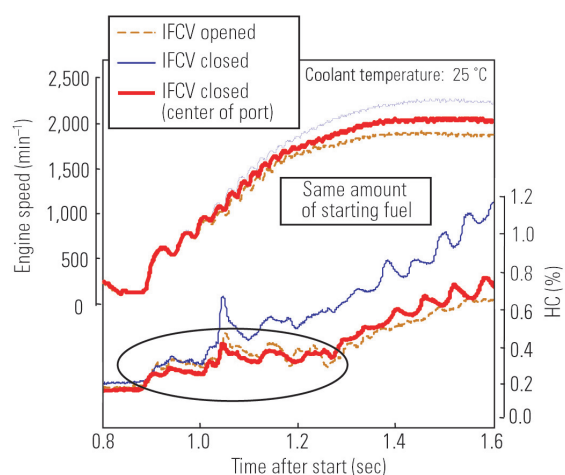


Fig. 14 Relationship between HC emissions and IFCV position

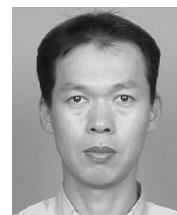
adherence of fuel droplets. This indicates that HC emission could be further reduced by better blocking the intake manifold.

References

- (1) Hiroshi Yoshimura, Akio Yoshimatsu, Kazuyoshi Abe, Shigematsu Isaka, "Effects of Mixture Homogeneity to DISI Engines on Knock Characteristics", Preprints of Meeting on Automotive Engineers, No. 132-05, pp. 13 – 16, 2005
- (2) Katsuhiko Miyamoto, Hiroshi Tanada, Masayuki Yamashita, Ken Tanabe, "Development of Technology for Super Low Emission Vehicle", Preprints of Meeting on Automotive Engineers, No. 154-07, pp. 19 – 24, 2007



Katsuhiko MIYAMOTO



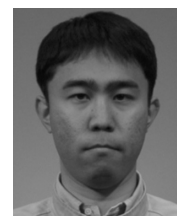
Masayuki YAMASHITA



Kenji GOTO



Naoto FUJINAGA



Akira MIKITA

Development of Vibration Calculation Code for Engine Valve-Train

Taizo KITADA* Masato KUCHITA*

Abstract

A vibration calculation code for an engine valve-train was developed. This code can be used in a similar manner to Mitsubishi Motors Corporation (MMC)'s engine performance simulator⁽¹⁾ with which MMC engineers are very familiar. The code quickly predicts how the valve lift curve obtained by using the engine performance simulator affects the valve-train vibration. The calculation results help engineers to understand the valve-train vibration characteristic and to take appropriate countermeasures.

Valve-train vibration calculation is somewhat difficult because of nonlinear elements such as valve clearance, but this code ensures a stable calculation by employing finite difference calculus with the implicit method. The code also has some useful auxiliary software. For example, the data is input by mouse operation and the spring vibration can be observed as an animation. All operations can be done on Windows' applications.

Key words: CAE, Vibration, Valve Train

1. Introduction

Computer progress has lead to our engine performance simulator easily predicting the engine performance once inlet and exhaust systems and valve timing are defined. Although the best valve lift curve for good engine performance can be obtained, the lift curve sometimes can not be used because of the unfavorable valve-train condition. Recently the valve-train mechanism has been changing from a type of shifting intake and exhaust valve timing for bringing out better engine performance to another type of VVT (Variable Valve Timing) system which also shifts a valve lift continuously by using a multi-link system. And this evolution can not be stopped. Considering the trend, a vibration prediction technique is desired in order to obtain maximum valve-train performance.

A retro styled valve-train vibration analysis is one that the amplitude of vibration at each order is calculated with Fourier series expansion and the valve-train natural frequencies which are strongly influenced by the amplitude around high engine speeds are marked for designing. Nowadays MMC is trying a full FEM valve-train vibration calculation with commercially available LS-DYNA™ and a multi-dimensional vibration calculation with also commercially available ADAMS/Engine™⁽²⁾. But these codes take many hours to compose their input data, so these are really not design tools which can be used to calculate many cases. Our original valve-train vibration calculation code was therefore developed with the aim of being used like our engine performance simulator which MMC engineers are very familiar with. The overview and calculation examples are introduced in this report.

2. Overview of vibration calculation code for valve-train

2.1 Vibration calculation code for valve-train and auxiliary software

The vibration calculation code for valve-train and auxiliary software are shown in **Fig. 1**. In the operating environment, all calculations can be done on Windows' applications. The input models are made with MSNpre (④), the valve lift curves are made with ValveLift (③) and the calculations are run with MSnetwork (①). When making input data, FnSpring (②) is used to make the multi mass model for the valve spring. The calculation result graphs are quickly drawn in the window by using GraphMaker (⑤) to help analyze the phenomena without loss of time. Also, the spring motion can be observed in the animation by using MSNanime (⑥). This series of software is completely made by MMC.

In addition, MSNpre enables the user to compose a one dimensional vibration system model interactively with mouse and button operations. As an element representing mass, the fixed point or lifted point is selected with a button and allocated on the sheet of the software. A spring element is defined by the mouse drag from the knob of an element to the knob of another one. The input data can be provided for the element with the dialog which is opened by clicking the mouse right button.

ValveLift, a share code with our engine performance simulator, generates a polynomial valve lift curve, a combined sine and parabola, and a combined sine and oval.

MSNanime enables the display of the spring vibration on the screen from the calculation results about

* Advanced Powertrain Development Dept., Development Engineering Office

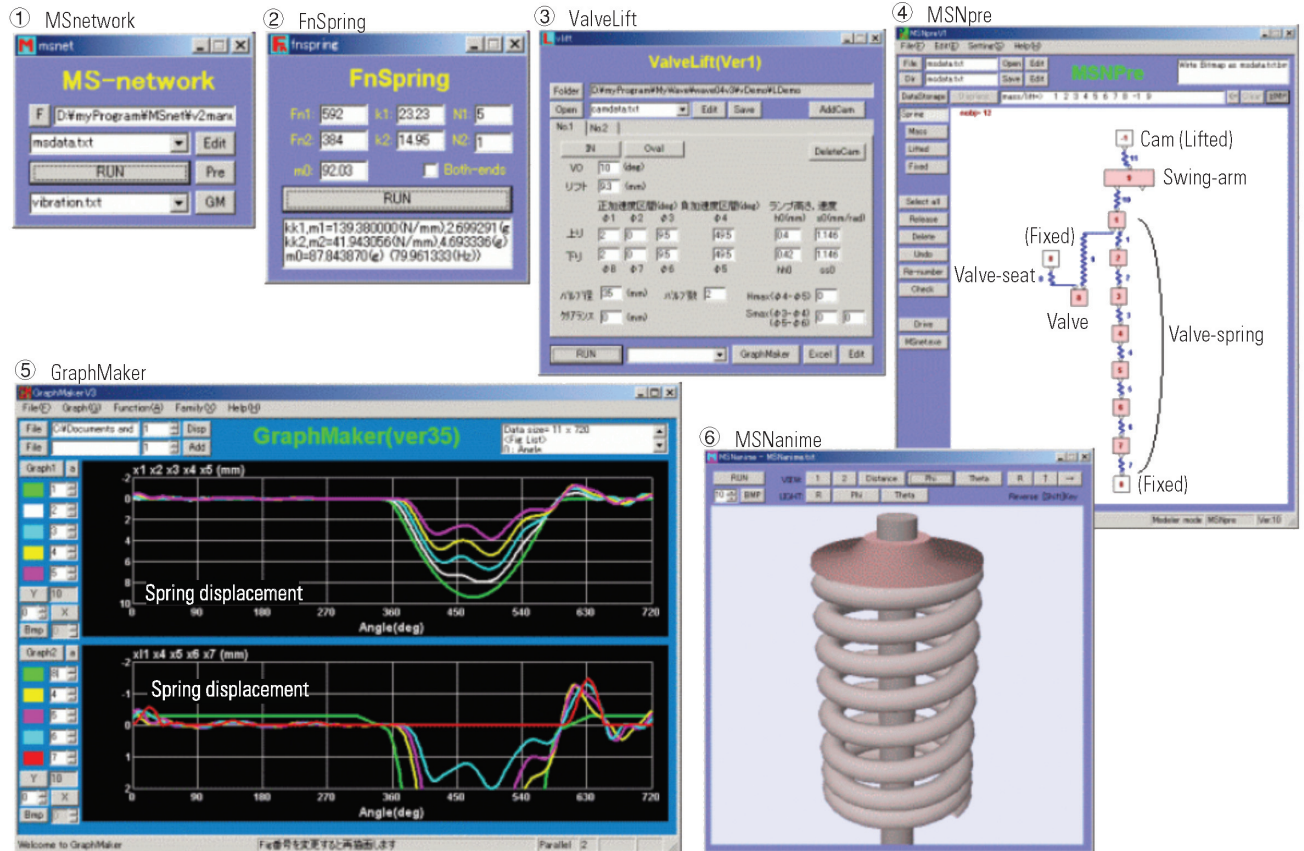


Fig. 1 Valve-train calculation code (MSnetwork) and auxiliary software

mass displacement with only providing the text style input file in which the spring descriptions such as wire diameter, coil diameter, the number of coils and so on are written. Because it has three dimensional display data in it, it can be observed from different view points and angles. In addition, it has a function making a Bitmap file from the picture on the screen at each crank angle previously defined. An animation is also made by compiling these Bitmap files.

2.2 Method of valve-train vibration calculation

2.2.1 One dimensional vibration model

This code handles a one dimensional vibration model. To be specific, the connection of the model is defined by way of describing what boundary element (such as mass, fixed or lifted) is placed at both ends of the spring in the input data. At first glance, a whole vibration model showed in Fig. 2 looks like a quite simple spring-mass model, but there are some difficult phenomena peculiar to valve-trains from the discontinuities such as valve clearance, valve sitting on the sheet, the jump which is said that the tappet leaves from the cam phase during a valve lift period at high engine speed, and a spring wire collision which is when a portion of the spring wire collides with another portion at higher engine speed. In other words, the sudden spring constant switching happens everywhere in the model.

In addition, almost all valve springs have a portion

of a so called close coil, a closer winded portion of the coil, in order to restrain its vibration. This portion is usually closed, but when the vibration becomes larger at the valve sitting timing, the portion turns to be open and switches the spring constant to change the natural frequency of the valve-train. The natural frequency of the valve-train used here means the value defined from the spring constant and the mass including a tappet, a retainer, a valve and some of a spring.

Therefore in valve-train vibration calculations, a suitable algorithm which can be running stably without divergence whenever such a sudden change of the spring constant happens is required to be chosen.

2.2.2 Algorithm of vibration calculation

A complete implicit method was adopted to ensure stability for the vibration calculation. This method uses an iteration loop in which the presumed mass displacement at current time is gradually adjusted until all displacement becomes a suitable value without discrepancy.

Taking a valve-train with two masses in Fig. 2 for example, the dynamic equations around mass 1 and mass 2 are described as equations (1) and (2) respectively:

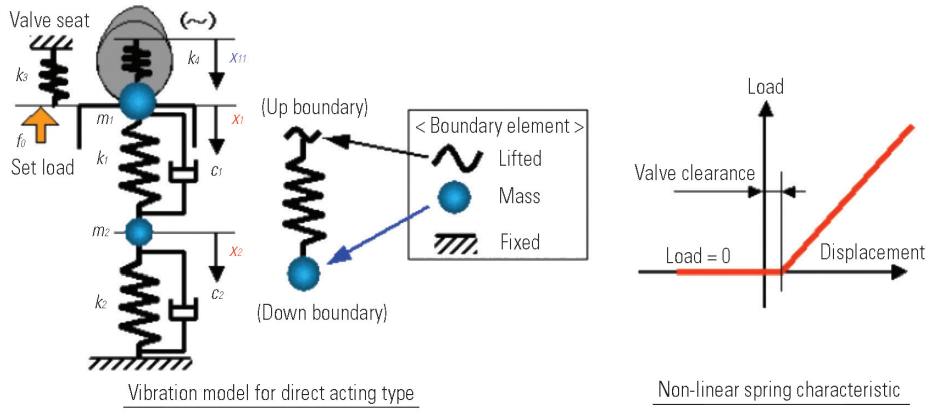


Fig. 2 Details of vibration calculation code for valve-train

$$m_1 \frac{d^2 x_1}{dt^2} = k_1(x_2 - x_1) - k_3 x_1 + k_4(x_{11} - x_1) + c_1 \left(\frac{dx_2}{dt} - \frac{dx_1}{dt} \right) - f_0 \quad (1)$$

$$m_2 \frac{d^2 x_2}{dt^2} = k_1(x_1 - x_2) - k_2 x_2 + c_1 \left(\frac{dx_1}{dt} - \frac{dx_2}{dt} \right) - c_2 \frac{dx_2}{dt} \quad (2)$$

m : mass,
 x : displacement,
 k : spring constant,
 c : damping coefficient,
 t : time,
 f_0 : load,
 suffix: 1, 2, 11 show their ID-numbers.

Applying the 2nd order one side difference⁽³⁾ at the time direction, its acceleration and velocity are expressed as equations (3) and (4) respectively.

$$\frac{d^2 x}{dt^2} = \frac{2x^n - 5x^{n-1} + 4x^{n-2} - x^{n-3}}{dt^2} \quad (3)$$

$$\frac{dx}{dt} = \frac{3x^n - 4x^{n-1} + x^{n-2}}{2dt} \quad (4)$$

The superscripts show time steps (n ; current, $n-1$; 1 step before, $n-2$; 2 step before, $n-3$; 3 step before).

Substituting these equations (3) and (4) into equations (1) and (2), the m_1 and m_2 displacement can be showed as discrete equations (5) and (6) below.

$$x_1^n = \frac{\frac{m_1}{dt^2} (5x_1^{n-1} - 4x_1^{n-2} + x_1^{n-3}) + k_1 x_2^n + k_4 x_{11}^n + \frac{3c_1}{2dt} (3x_2^n - 4x_2^{n-1} + x_2^{n-2} + 4x_1^{n-1} - x_1^{n-2}) - f_0}{\frac{2m_1}{dt^2} + k_1 + k_3 + k_4 + \frac{3c_1}{2dt}} \quad (5)$$

$$x_2^n = \frac{\frac{m_2}{dt^2} (5x_2^{n-1} - 4x_2^{n-2} + x_2^{n-3}) + k_1 x_1^n + \frac{3c_1}{2dt} (3x_1^n - 4x_1^{n-1} + x_1^{n-2} + 4x_2^{n-1} - x_2^{n-2}) + \frac{3c_2}{2dt} (4x_2^{n-1} + x_2^{n-2})}{\frac{2m_2}{dt^2} + k_1 + k_2 + \frac{3c_1}{2dt} + \frac{3c_2}{2dt}} \quad (6)$$

Now observing the current notation superscript n , it can be understood that x_1^n is solved with x_2^n and adversely x_2^n is solved with x_1^n . That means an iteration is required to find the solution where the x_1^n and x_2^n are compromised without discrepancy. But all displacement solved here is compromised without contradiction, so the calculation can be run with good stability whenever any spring constant change occurs suddenly.

Another merit is that the calculation time step is able to be fixed to one degree of the crank angle because the constraint of the calculation is not very strict. Although the time interval for actual calculations is extremely different through the engine speed, thanks to the implicit method the calculation can be run without any problems.

2.2.3 Validation of calculation

In a simple spring model with one mass, the mass is offset by certain distances and vibrated, so its damping is observed in order to validate the accuracy of the finite difference algorithm. The calculation results are posted in Fig. 3 (a). The results of the highly accurate 4th order Runge-Kutta method has little damping for 0.1 second, and on the other hand, that of the 2nd order

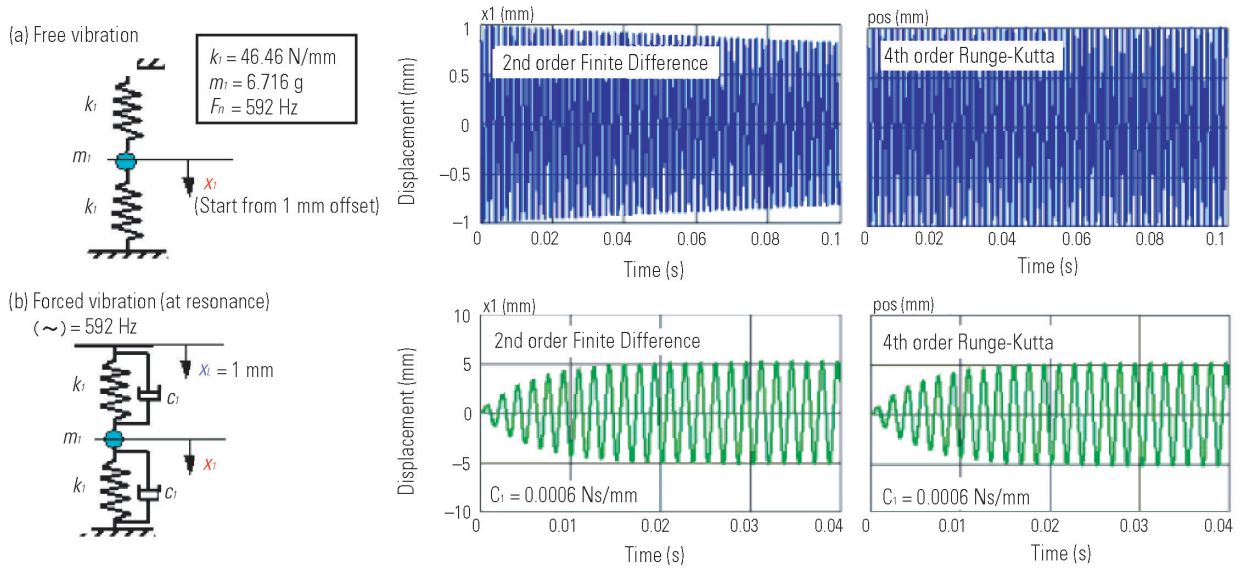


Fig. 3 Precision of calculus of finite difference with second-order accuracy

finite difference method has about 20 % damping of the amplitude during the same period because of the artificial viscosity generated from the residual error.

Fig. 3 (b) shows an example when the mass displacement is observed under a forced oscillation at the resonant frequency on the end of the spring. An adequate damping coefficient is provided here. It is found that the amplitude of the vibration of the 2nd order finite difference method is almost the same as that of the Runge-Kutta method under this condition. Since this level of the damping coefficient is usually provided on the spring element, it is considered that the 2nd order finite difference method will not create any problems in actual use.

The 1st order finite difference method can be also provided for a pre-calculation when the adequate damping coefficient is not sure. Using the 1st order method, the calculation is able to be run without setting the damping coefficient because the artificial viscosity made from the residual error acts adequately.

2.3 Multi-mass modeling for valve spring

Special software (FnSpring) is provided to make a multi-mass model for a valve spring. If only the spring constant, natural frequency and the number of masses are defined, the dispersed masses are solved in this software. And it also supports a spring with some close coils. This software also adjusts the valve-train mass (m_1 at Fig. 4 (c)) because the part of the spring mass included in its mass is slightly changed.

The dispersed masses are calculated through this procedure. A flexibility matrix is composed with influence coefficients, and the matrix is solved with the iterative solution method⁽⁴⁾. In case of dividing the spring showed in Fig. 4 (a) into some masses, the matrix and the influence coefficients are written bellow.

$$\begin{pmatrix} x_1' \\ x_2' \\ x_3' \end{pmatrix} = \omega^2 \begin{pmatrix} a_{11} & a_{12} & a_{13} \\ a_{21} & a_{22} & a_{23} \\ a_{31} & a_{32} & a_{33} \end{pmatrix} \begin{pmatrix} x_1 \\ x_2 \\ x_3 \end{pmatrix} \quad (7)$$

$$a_{11} = \frac{m_1}{k_1 + 1 / (1 / k_2 + 1 / k_3 + 1 / k_4)} = \frac{3m}{4k} \quad (8)$$

$$a_{21} = a_{11} \frac{1 / (1 / k_2 + 1 / k_3 + 1 / k_4)}{1 / (1 / k_3 + 1 / k_4)} = \frac{2}{3} a_{11} \quad (9)$$

$$a_{31} = a_{11} \frac{1 / (1 / k_2 + 1 / k_3 + 1 / k_4)}{k_4} = \frac{1}{3} a_{11} \quad (10)$$

$$a_{22} = \frac{m_2}{1 / (1 / k_1 + 1 / k_2) + 1 / (1 / k_3 + 1 / k_4)} = \frac{m}{k} \quad (11)$$

$$a_{12} = a_{22} \frac{1 / (1 / k_1 + 1 / k_2)}{k_1} = \frac{1}{2} a_{22} \quad (12)$$

$$a_{32} = a_{22} \frac{1 / (1 / k_3 + 1 / k_4)}{k_4} = \frac{1}{2} a_{22} \quad (13)$$

Here the influence coefficient a_{ij} represents the affection of how the displacement of the mass point i (x_i) is influenced by the mass m_j . For instance, a_{21} shows how strong the mass m_1 influences the displace-

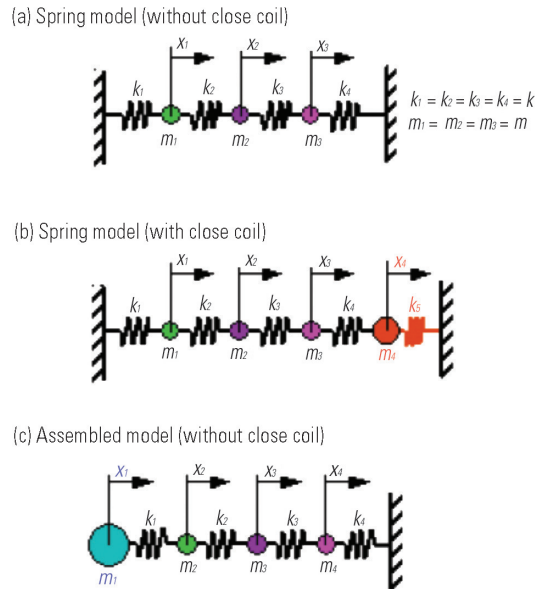


Fig. 4 Multi-mass calculation model for valve spring

ment of the mass point 2 (x_2).

ω is the natural angular frequency. The coefficients $a_{13} - a_{33}$ are omitted because they are the similar equations as $a_{11} - a_{31}$.

The iterative solution method carries out the following procedure. At first the matrix of equation (7) is composed after the influence coefficients are made. Then adequate initial values set in $x_1 - x_3$, and $x_1' - x_3'$ are solved with the matrix. After that, this calculation replacing $x_1' - x_3'$ with $x_1 - x_3$ is repeated until both will be the same value.

In this case, since the targeted natural frequency is sought through modifying mass m , the tentative values placed initially are modified repeatedly through the above procedure until the target natural frequency will be obtained.

The mass (m_4 at Fig. 4 (b)) in the close coil and the adjusted valve-train mass (m_1 at Fig. 4 (c)) are solved in the same way with the mass solved here.

3. Examples of calculation

3.1 In case of direct acting valve-train

3.1.1 Valve-train vibration at maximum engine speed

A calculation example of a so called direct acting valve-train which directly pushes the tappet by the cam and opens the valve is shown here. This vibration model has a valve spring with six masses including the close coil, and the spring constants of the cam and the valve sheet with the valve clearance between them. The valve spring is also given the set load (f_0).

Fig. 5 shows an example around the limited engine speed (7,500 min⁻¹). A lift with the clearance generating an external force is set at the cam. The valve-train load, the valve acceleration multiplied by the valve-train mass, is designed to have enough margin against the

spring static load. But because the spring is excited well at this speed, it is a concern that some periods when the spring force can not sustain the valve-train load will emerge above this engine speed. A close coil (k_7) placed at the bottom of the spring makes the portion contact and non-contact repeatedly during the valve seating, and reduces the spring vibration. Some impact force is observed when the spring coils contact each other. And it is also observed that the spring loads (k_1 , k_7) at both ends are vibrating by the opposite phase.

3.1.2 Valve jump simulation

A so called jump happens when the engine is driven over a certain engine speed. This means the phenomenon that a tappet leaves the cam-face at the timing when the spring no longer can sustain the valve-train load.

The valve-train behaviour at the start of jumping is showed in Fig. 6. The calculation conditions are the same as those of Fig. 5. The distance between the cam lift and the valve lift (displacement for m_1) is uncertain at the top figure in which the both are superimposed. This is enlarged in the figure below. It is seen here that two small jumps happen around the top lift. These jumps occur at the timing when the valve-train load can not be sustained by the spring force because of its vibration. The jump can be clearly simulated because the spring element of the cam has a constraint not to generate force, or to switch the spring constant into zero, at tension. Look at the cam load (k_9). It is observed that some impact loads happen just at the moment that the jumping tappet returns to the cam-face. And it is seen from the enlarged valve lift curve that the bounce, although tiny, happens and it is gradually reducing. The bounce means the phenomenon that the valve sits on the seat with velocity (ramp velocity), and if the impact force can not be absorbed around the seat, the valve rebounds.

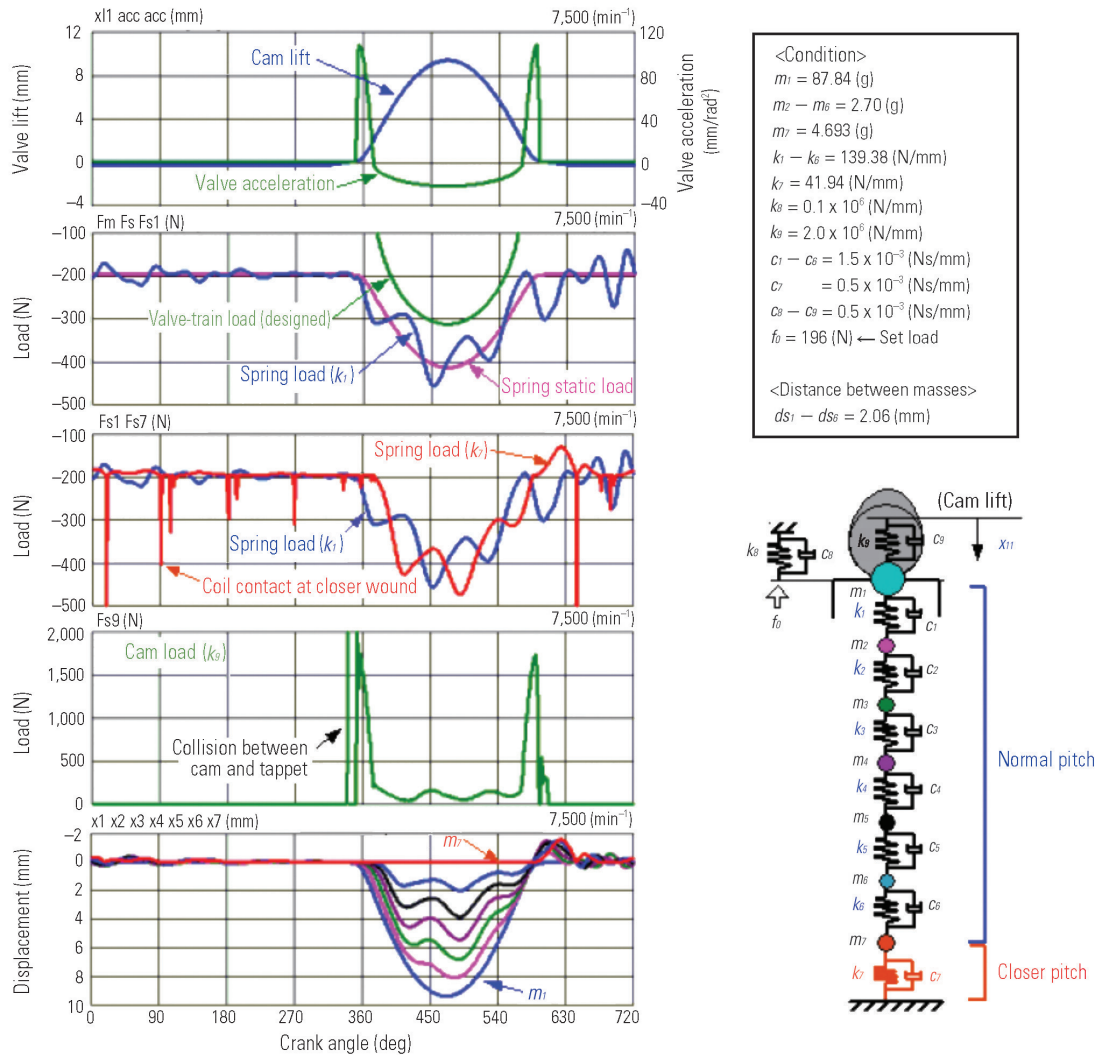


Fig. 5 Example of direct-acting valve-train calculation (7,500 min⁻¹)

3.1.3 Spring coil contact simulation

When the engine speed is increasing, the spring force is not able to sustain the valve-train load anymore and a big jump which is much bigger than the cam-lift curve occurs as shown in Fig. 7. If it comes, a big bounce also occurs because the valve is not able to move according to the designed valve lift and the valve is sitting on the seat at a much higher speed than the ramp velocity. This bounce is gradually damped but continues during the valve seated period.

If such a big jump happens, the increased valve lift presses the spring more than expected, correlating with the inner spring vibration, and spring coil contact happens, which means some portions of the coil contact with each other everywhere.

Fig. 7 shows that some coil distances reach zero and the impact force occurs by the coil contact.

Switching to the large spring constant is carried out when the distance between the masses is smaller than defined in order to simulate the coil contact.

3.2 In case of valve-train with swing arm

This software has a unique function that handles an element with a rocker ratio like a swing arm. A calculation example of a valve-train with a swing arm whose rocker ratio is 1.4 (constant) is shown in Fig. 8. This vibration model includes the valve stem as a spring element and the valve head as a mass element.

This valve lift is rocker ratio times higher than the cam lift in the figure. And the load during positive acceleration at the cam side of the swing arm is also rocker ratio times higher than that at the valve side.

The valve clearance between the cam and the swing arm, and a nonlinear spring constant (k_{11}) between the cam and the swing arm and another nonlinear spring constant (k_{10}) between the swing arm and the valve, are placed to transfer the load at compression. That enables a simulation as the swing arm moves up and down in the clearance when the valve is seated.

The valve stem is affected by the spring set load as tension when the valve is seated, and by the load which the valve acceleration multiplied by the valve head

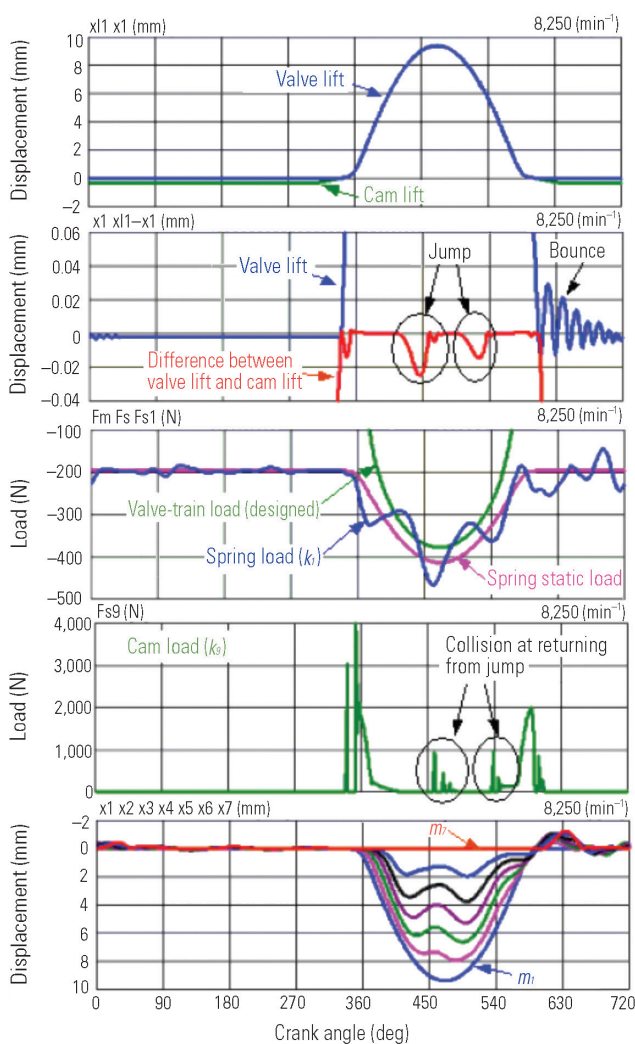


Fig. 6 Example of direct-acting valve-train calculation (8,250 min⁻¹)

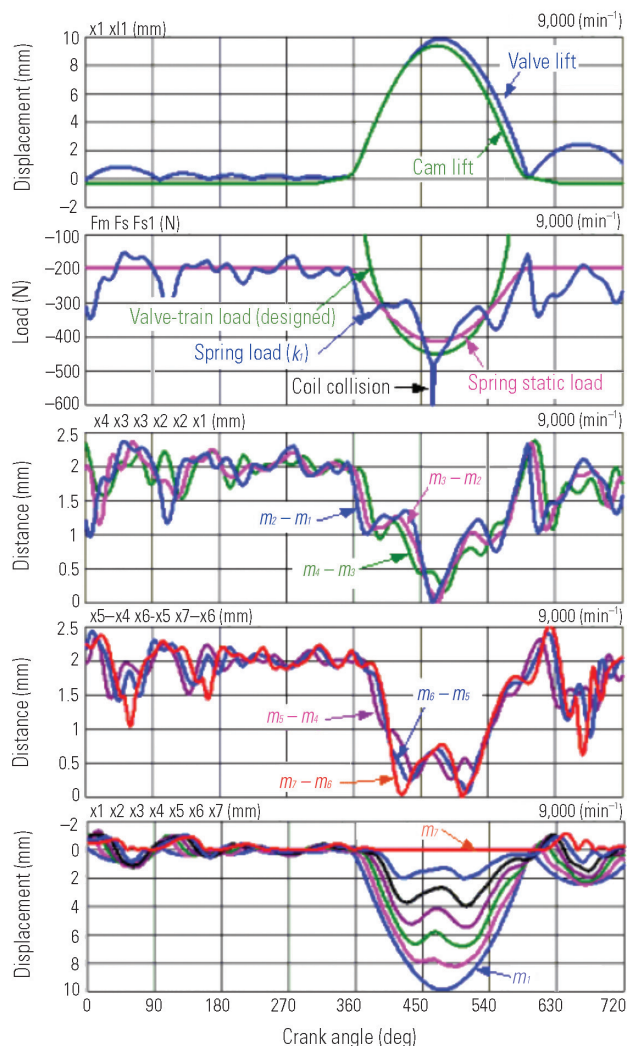


Fig. 7 Example of direct-acting valve-train calculation (9,000 min⁻¹)

mass is equal to when the valve is lifted. And at the moment that the valve sits on the seat, it is observed that the spring set load is larger by the impact force.

3.3 Animation display of spring vibration

It is difficult to have an image of how the spring coil is vibrating from a figure drawn of the mass displacement along with the crank angle as the x-axis. Therefore animation software displaying the spring vibration is prepared to make users understand the phenomena visually.

Fig. 9 shows the valve spring motions at 7,500 min⁻¹ of a direct acting valve-train in 3.1.1. From the pictures of the spring in this figure, it is observed that the bottom end coil of the spring is compressed earlier when the valve is being lifted and the top end coil of the spring is opened earlier when the valve is being returned. Then it also can be observed that the close coil which is usually closed opens a little after the valve closed timing.

4. Summary

Although many nonlinear elements like valve clearance and so on have to be handled in the valve-train calculations, the implicit algorithm used in this calculation code enables stable calculations. This report shows that this calculation method is able to handle any valve jumps, bounces and spring coil contacts. And this code is arranged to be used in the same sense as our engine performance simulator which users are very familiar with.

Because vibration calculations are not more difficult than fluid dynamics calculations, it is anticipated that if the damping coefficient is chosen well from experimental results, it is possible to develop a valve-train without making a prototype.

As computers progress, whole engine vibration calculations including a valve-train, engine main moving and timing parts has come into sight and this is one of our targets. In addition, since both side pressures of an engine valve calculated by our engine performance simulator are known, the advanced vibration calculation

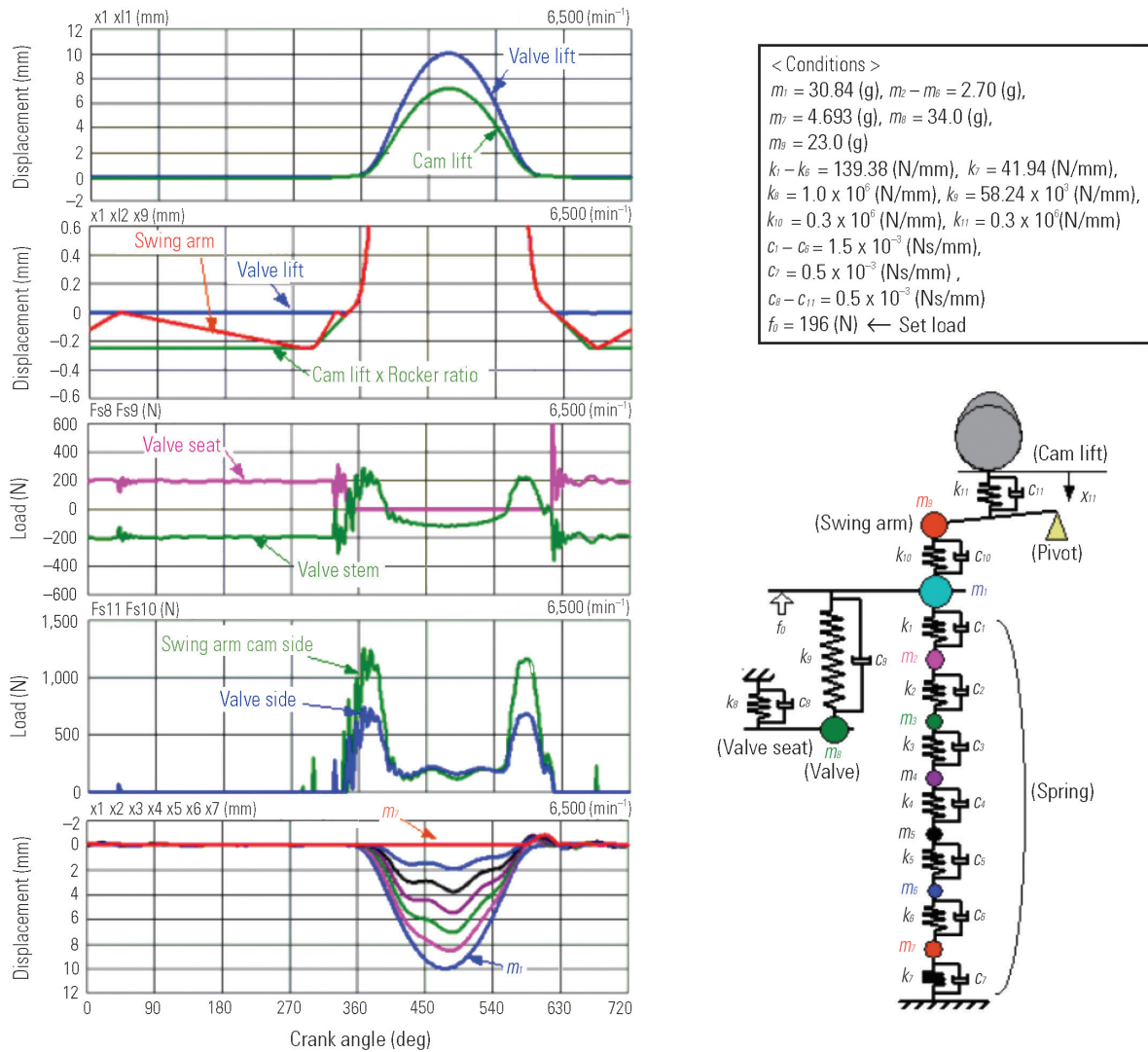


Fig. 8 Example of swing-arm-type valve-train calculation (Rocker ratio 1.4)

including the affect of these pressures is being considered.

5. After word

Since many kinds of commercial software have been available, the CAE job has changed from developing CAE software to applying CAE software to our development process. From this change, sometimes the results are misled because the engineer does not have enough knowledge about dynamic equations of the calculation target or the calculation algorithm itself. To avoid this bad situation, if CAE software can be made in a relatively easy algorithm, we dare to continue developing software ourselves in the future.

Mr. Fujimoto and Mr. Ohsawa in Advanced Powertrain Dept. gave a hand to verify the precision of this software in the developing process.

References

- (1) T. Kitada, M. Kuchita, T. Ohashi: Mitsubishi Motors Technical Review No.11, P. 29, 1999
- (2) A. Fujimoto, H. Higashi, M. Osawa et al.: Mitsubishi Motors Technical Review No.19, P. 19, 2007
- (3) The Japan Society of Mechanical Engineers, Numerical Simulation of Flow, P. 58, Korona-sya, 1988 (Japanese)
- (4) K. Kitasato, M. Tamaki: Mechanical Vibration (Basic and application), Kougaku-tosyo, p. 84, 1980 (Japanese)

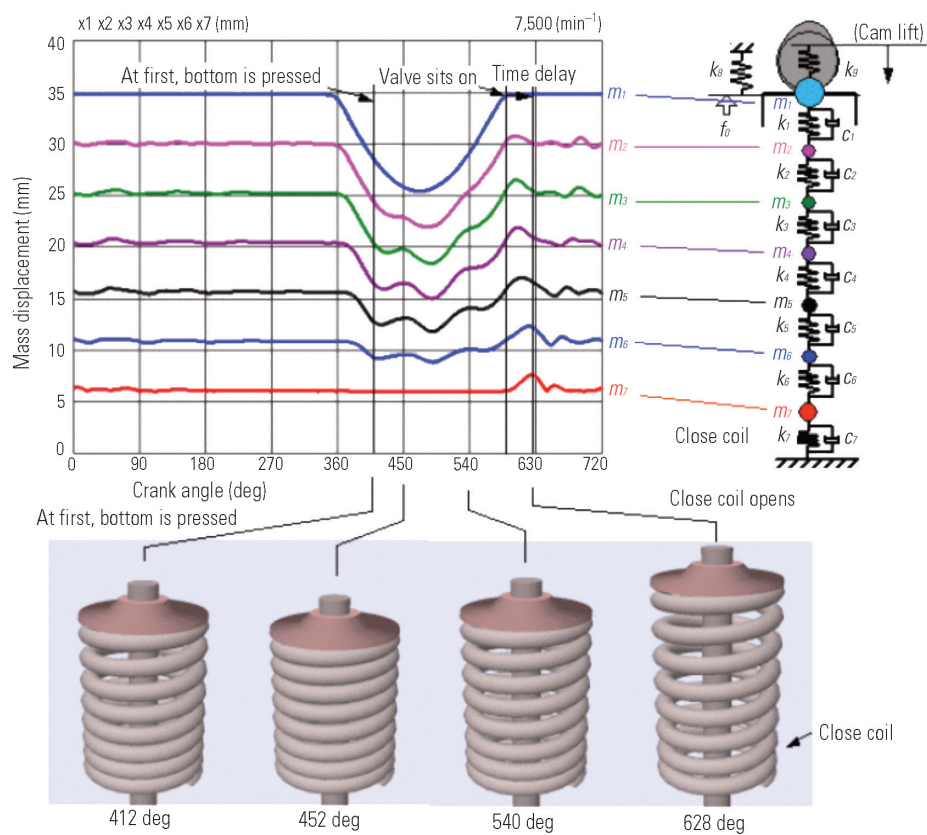


Fig. 9 Spring movement animation (Direct-acting type at 7,500 min⁻¹)



Taizo KITADA



Masato KUCHITA

Inexperienced Drivers' Behavior, and Control Technology that Adapts Powertrain Behavior to Drivers

Kazuhide TOGAI*

Abstract

For a vehicle to move as desired, it must be driven by a person. Some drivers are more skilful drivers than others, and good driving requires a certain amount of experience. Mitsubishi Motors Corporation (MMC) recently created a driver model and applied it to a speed tracking simulation. The results showed that the experience-linked level of skill was dictated by the ability to read the road ahead and by the accuracy of the internal model of vehicle behavior. With the powertrain, which produces driving force, it was found that non-linearity and response lags were significant and that disturbance caused output fluctuations other than those caused by driver inputs. By employing control technologies to improve these factors, MMC made it possible for inexperienced drivers to drive without being troubled by discrepancies between driver inputs and vehicle responses.

Key words: *Driving Behavior Modeling, Driving Agent, Emission Test Cycle, Disturbance Compensation, Powertrain Control*

1. Introduction

A passenger car is a high-tech machine with dozens of microcomputers on board. Its function is to transport people between locations on the road. However, it cannot function at all without a driver. A washing machine is more sophisticated than a car as an automatic machine – it automatically washes and even dries clothes once they are put in. A tool performs best when it is adapted to the physical characteristics of its user. As examples of this tool-human relationship, some scissors and kitchen knives are specially designed to fit the dominant hand of the user, and violins for children are available in different sizes to match the sizes of the children's fingers. Pianos, which were developed much later, feature uniformly sized keys and fixed tone intervals, and the player's physical characteristics will influence his/her performance levels.

Depressing the accelerator pedal accelerates the vehicle and depressing the brake pedal decelerates the vehicle. However, due to the mechanisms of the engine and transmission of the vehicle, the driving force created by, or the response of the vehicle to, the same depression of the accelerator pedal is not constant. When operating the accelerator pedal and brake pedal, a driver uses his/her body as an integrated sensor and actuator to follow his/her intended target (track and speed).

When investigating a vehicle's behavior, it must be based on the tracking system including a human (driver)⁽¹⁾. For this purpose, a driver operation model which consists of structure (prediction of targets, lags of response and operation, experience and other factors are defined as elements) and parameters was devel-

oped. On the vehicle response side, powertrain (static and dynamic), control techniques and external disturbance characteristics were reviewed. This type of analysis of a human-machine system involving driver inputs and vehicle responses can facilitate the designing of easy-to-operate automobiles⁽²⁾.

2. Driver input characteristics (speed tracking)

2.1 Driver inputs at different skill levels

Using a chassis dynamometer, driver behavior was observed under the 10-15 mode, a Japanese test cycle for measuring fuel efficiency and exhaust gas emissions. Two drivers participated in the test: one (the first timer) was going through the test cycle for the first time while the other was totally familiar with both the test and vehicle used. Pedal strokes and target tracking performance for each driver were measured. The results are shown in Fig. 1.

2.2 Tracking performance factors

On the very first session, the first timer did not have any prior experience in target speed changes of the test cycle and therefore could not predict and prepare for accelerator pedal and brake pedal operations at the target speed change points. The first timer neither knew how much the vehicle would accelerate nor decelerate in response to varying degrees of pedal strokes, and therefore could not figure out correct initial pedal strokes at start points for acceleration or deceleration. Faced with actual speed deviations, the first timer then made corrective maneuvers. As humans generally are not very good at making an immediate feedback

* Advanced Powertrain Development Dept., Development Engineering Office

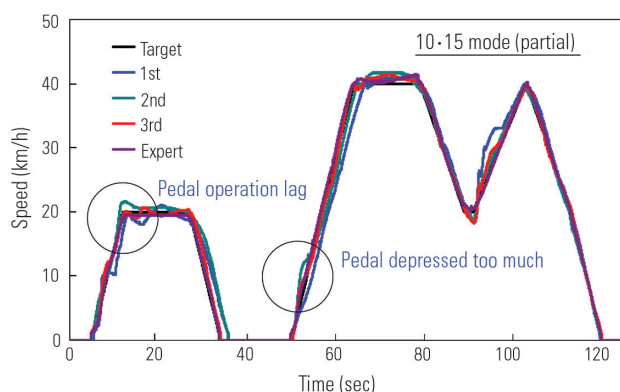


Fig. 1 Target speed tracking behavior in a test cycle

response, it took a rather longer time for correction. In the second and subsequent sessions, however, the first timer showed gradual improvement in initial pedal operation timing (less lag) and pedal stroke for the feed-back operation^{(3)–(5)}.

3. Driver model

3.1 Recognition, judgment and operation

To understand human driving patterns, a driver model was developed that is clearly structured and uses parameters to enable individual settings based on skill levels. Prior to model designing, human driving behavior was analyzed. Findings suggested that human driving behavior when preparing for the next action at the change of the target speed or when taking a corrective action upon noticing the deviation between actual speed and target speed consists of three stages: recognition (of difference between the current and target (future) speeds); judgment (of the required accelerator or brake pedal stroke); and operation (of foot). These are the primary functions of the driver model. **Fig. 2** shows the flow of information between these functions⁽⁶⁾.

Where:

$V(t)$: Current speed

$V'(t)$: Recognized speed
(with lag taken into account)

$a(t)$: Estimated acceleration error

$f(t)$: Pedal force

ε : Additional error at each stage
(Suffix: R = recognition, E = evaluation,
A = action)

τ : Lag
(Suffix: R = recognition, E = evaluation,
A = action)

3.2 Operation amount control

Vehicle speed is controlled by operating the accelerator pedal and brake pedal. Braking power is generated from the depressing force of the brake pedal, which is augmented by a brake booster (master vac) and a hydraulic system. When a driver decides to apply

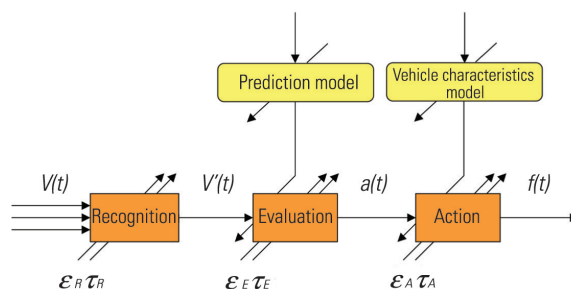


Fig. 2 Driver model and information transfer

brakes, he/she first moves his/her foot (e.g. from the accelerator pedal) to the brake pedal, and the initial action is completed when he/she feels a certain reaction force of the pedal. Then the driver depresses the brake pedal until a certain degree of braking power is established (feed-forward), and next regulates the pedal depressing force while evaluating the difference between the current and target speeds.

The accelerator pedal requires much less effort to operate than the brake pedal (10 N·m for 50 mm stroke, which is 1/20 of the brake pedal force), making it easy to finely adjust the pedal stroke. **Fig. 3** shows typical relations between pedal strokes and forces.

3.3 Reading the road ahead

When negotiating a curve, the driver looks not near, but ahead, in correspondence to vehicle speed and starts maneuvering the steering wheel early to ensure that, upon entering the curve, the wheels are already being steered at appropriate angles. This also applies to acceleration and braking. The driver looks ahead (both in distance and time) and starts operations early taking into consideration the time required to switch from one pedal to another and vehicle response time. In these conditions, beginners tend to look too close to the vehicle. How far ahead to look and how early to start maneuvering can be learned by experience.

3.4 Formation of vehicle response model in driver

When driving an unfamiliar vehicle, no driver knows exactly how much to depress the accelerator or brake pedal to achieve target acceleration or deceleration. Improper pedal operation, however, will be corrected as the driver becomes familiar with the vehicle. This indicates that the driver forms a vehicle response model within him/herself.

A driver cannot drive proactively or make feed-forward foot maneuvers unless he/she has integrated a relationship (knowledge) between the accelerator/brake pedal stroke and the acceleration/deceleration rate in his/her recognition-evaluation system. Accelerator pedal stroke and its reaction force have a linear relationship. As shown in **Fig. 5**, however, accelerator pedal stroke and engine torque have a linear relationship only up to around 20 % (depending on engine speed) of the pedal stroke, beyond which engine torque almost completely saturates. In case the drive system includes the

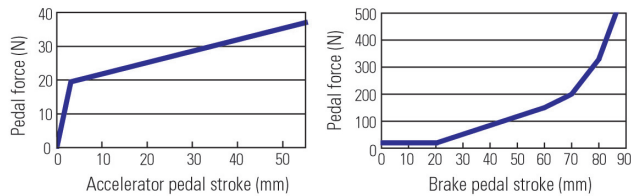


Fig. 3 Pedal force vs. stroke – accelerator and brake pedals

gears and a torque converter, another parameter, i.e. speed, is further added to the relationship between accelerator pedal stroke and driving force.

Beginner drivers often have just basic knowledge such as “depressing the brake pedal increases the braking power and depressing the accelerator pedal increases the driving force”. On the other hand, skilled drivers appear to have built a fairly accurate knowledge about driving force and braking power in their evaluation systems. For braking power, its response with the brake pedal operation works fairly well because the pedal depressing force is directly applied to the brake discs (drums) via hydraulic circuits. Outside the normal operation range where required pedal force becomes substantially great, it is difficult for beginner drivers to perform fine operations of a brake pedal.

The relation between the driving force and the accelerator pedal depressing force is not like engine output information, but the information is just how much the vehicle accelerates with varying accelerator pedal depressing force. This may be similar to the gradient of driving force relative to accelerator pedal inputs. Except for electric vehicles, this gradient is different for each gear ratio even on the same vehicle, and it takes a while to master every gradient. In addition, any delay in driving force response, except that of a torque converter, is too small in comparison to the human motion capability, and it therefore can hardly be developed into a model in driver.

3.5 Driver model

Recognition stage: The driver recognizes the locus of the target speed and the current speed. Based on the target speed, the driver anticipates pedal switching and other substantial operational changes. The driver also recognizes whether the vehicle is currently accelerating or decelerating, or needs substantial corrective inputs. With this, recognized information consists of current speed and acceleration, recognition error and time lag. In addition, the driver predicts speed in the near future based on the recognized acceleration.

Judgment stage: The driver decides whether it is time to switch pedals. If the pedal is to be switched, the driver establishes initial pedal stroke. The driver also increases or decreases accelerator or brake pedal force in accordance with speed deviation from inputs. Based on recognized information, the driver evaluates the difference between target and current vehicle speeds and determines target (corrective) pedal stroke.

Operation stage: The driver moves his/her foot from

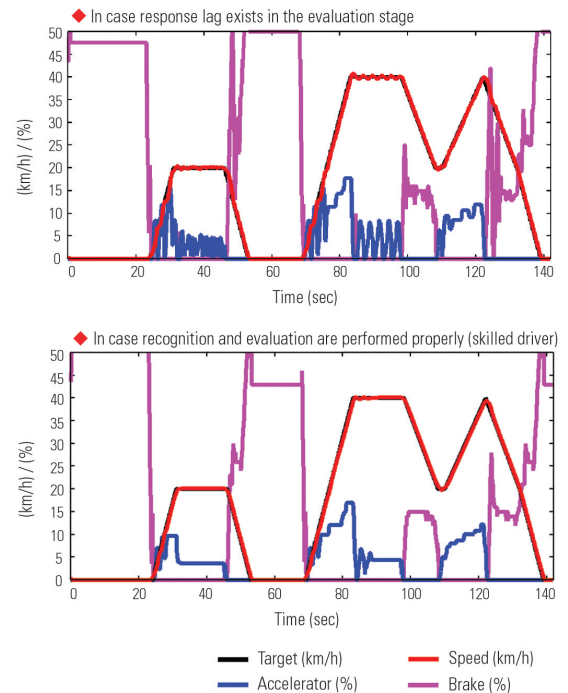


Fig. 4 Test cycle driving with an experienced agent

one pedal to the other. The movement is completed when the foot has been moved over a distance determined by the driver's body coordinate system and the target pedal has been sensed. This movement, however, is not included in the agent. The driver then depresses the pedal until the initial pedal force determined by the driver is reached. The driver may continue to depress or release the pedal based on the determined value. This is localized bodily feedback control.

The driver acknowledges the relationship between the pedal stroke and acceleration based on his/her inner vehicle model. Based on it, the driver determines initial pedal stroke.

In a continuous acceleration or deceleration situation, the driver classifies the amount of difference between target and actual accelerations to some ranges and applies the required correction based on the classified range.

3.6 Unskilled driver behavior clarified by simulation

Fig. 4 shows the measurement results of 10-15 test cycle sessions performed by a prepared driving agent. As indicated, speed tracking performance improves with experience. There are two reasons for this: less delay in making decisions in the recognition stage, and correct initial pedal force in anticipation of vehicle response. This is evident on the acceleration side while, on the deceleration side, the agent showed good tracking performance from the beginning. This appears to be because driver inputs and braking power are in a linear relationship and (in that relationship) there is little response lag that humans can sense. With this, it can be said that the time lag in the recognition stage and knowledge about vehicle response (internal vehicle

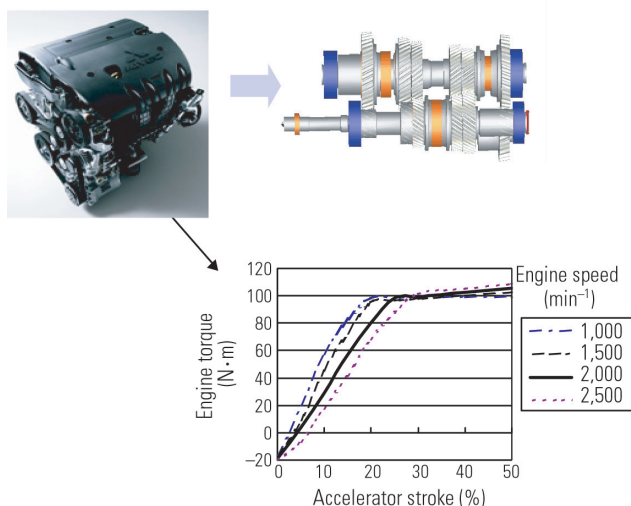


Fig. 5 Engine torque and accelerator pedal stroke

model) both effect driving skills. This also applies to a steering maneuver for lateral position tracking control.

3.7 Target track and tracking requirements

Driving a vehicle means following a target track envisioned on a two-dimensional surface. Primary rules to observe in this case are: not to deviate from the road (lateral position control), not to collide with a vehicle (object) ahead and to stop at traffic signals. Speed tracking control such as in an emissions test cycle is not very easy to perform due to the nature of human capability and vehicle response. Then, why has there been no major problem? That is because target track setting in traveling direction, as well as other tracking requirements (as a measure for evaluation), are not very strict.

4. Vehicle response

4.1 Engine torque response to accelerator pedal input (Fig. 5)

Vehicle response characteristics depend on powertrain characteristics and vehicle weight. Take, for example, the powertrain consisting of a gasoline engine and an automatic transmission (with a torque converter). Acceleration is controlled by the accelerator pedal operation. Gasoline engine output is actually controlled by the throttle valve opening. On current passenger cars, there is no mechanical cable linkage between the accelerator pedal and the throttle valve. Instead, a position sensor (which in many cases is a potentiometer) detects accelerator pedal stroke (distance from the home position), based on which a target throttle valve opening is determined. Then a motor is used to open the throttle valve to the target position. The accelerator pedal yields a reaction force in proportion to the pedal stroke and the driver utilizes this reaction force when operating the accelerator pedal. Of course, the driver also needs a certain amount of positional change (pedal stroke). As with a braking maneuver, acceleration involves preparatory actions. The driver moves his/her

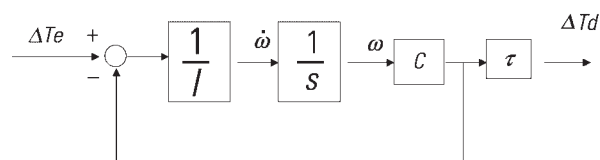


Fig. 6 Torque converter transfer function

foot (over a certain distance) on to the accelerator pedal and, from the pedal reaction force, ensures that the pedal is in the correct initial position. The pedal force determined in the judgment stage is fed forward to achieve the corresponding pedal position and then there is an adjustment of pedal force in response to the speed deviation. Feed-forward amount itself has a complex element which is determined based on the feedback on the difference between expected and actual reaction forces. Thus, the driver's experience contributes to obtain the correct feed-forward amounts.

When a person needs to perform fine maneuvers while sensing force (and position change), it is important that he / she understands the range of that operation (in terms of position and force) and the orientation of that operation relative to the body. Operation becomes more accurate in proportion to the amount of exercise made⁽⁶⁾. A pedal, which is too heavy, is difficult to operate accurately. With fine operation by hand, some are good at pushing while others are good at pulling. Accurate positioning can be achieved by the rotary motion with the palm fixed.

4.2 Driving force response including that of the transmission

Accelerator pedal input and vehicle acceleration are not in a linear relationship. For the first, engine torque stops increasing beyond a certain throttle valve opening. At the speed range of an emissions test cycle, this occurs at the throttle opening of 1/3 or less. In relation to this, the gear ratio change takes place to increase power for more driving force. Secondly, many of the new vehicles in Japan are equipped with a torque converter, which typically is designed to operate from right after start-up until reaching around 20 km/h. A torque converter transmits torque that is proportional to the square of engine speed, and therefore is a great contributor to the non-linear relationship mentioned above. Structurally and in principle, engine output has time lags behind a change in the throttle valve opening (accelerator pedal operation) (Fig. 6).

In Figure 6, ΔT_e is the engine torque increment, ΔT_d is driving torque increment, ω is engine speed, I is moment of inertia, C is the torque converter capacity coefficient and τ is torque ratio.

Given the above, what differentiates skilled drivers from beginners on acceleration is how much the driver knows the characteristics of the vehicle.

4.3 Brake system response

Braking power is proportional to brake pedal force (and stroke) independent from driving conditions (Fig. 3). Response lag is negligible. As long as there is sufficient master vacuum, pedal effort is small and it is easy to operate.

5. External disturbance and control technologies

External disturbance is an unexpected change in vehicle behavior that occurs independently of driver inputs. When the air conditioning compressor operates, less power is available to drive the vehicle. When the air conditioning compressor stops, power available to drive the vehicle increases, which may sometimes be felt as acceleration shock.

Vibration can be a disturbance. When driving at a slow speed, abrupt accelerator pedal depression causes the drive shaft to generate torsional vibration (tip-in shock), which can be annoying⁽⁸⁾⁽⁹⁾.

5.1 Torque fluctuation

It takes a maximum of around 10 N·m to drive an air conditioning compressor, which corresponds to 20 % or even more of the available power depending on the running conditions of the engine. That is neither based on driver input nor can be predicted, and can cause annoying shock by sudden deceleration or acceleration.

To prevent this, the engine control unit has the following control functions: timing for load change is delayed to prevent it from occurring simultaneously with other important events; by detecting the increase or decrease of the compressor load by monitoring air conditioning control and compressor pressure, engine output is increased or decreased to offset the compressor load.

The alternator and (hydraulic) power steering system also cause load fluctuations. The alternator, however, only generates a mild fluctuation, and the alteration by power steering system is less noticeable as it is accompanied by the steering operation. There is also a control function to keep the load fluctuation caused by the alternator mild.

5.2 Gear shift

Shifting the transmission from neutral to D or R range brings the driving force up to the tires. Gearshifting causes torque to change. A poor gearshift (clutch engagement) control leads to shock interference (described later). Even it is not going to become such a condition, delayed clutch engagement is confusing for a driver who has selected D and expects instant torque availability.

With the clutch completely engaged and the accelerator pedal fully released (the engine running at idle), there should be a certain amount of torque that can be felt by the driver in order to ensure positive vehicle response to driver input. This torque is not the same as that required for creeping.

With automatic transmissions (and automated man-

ual transmissions (AMT)), generally the greater the accelerator pedal stroke, the greater the gear ratio (lower gear) selected. Gear shift points can be located anywhere within the engine speed range. While these shift points are determined to meet target fuel economy and exhaust gas emissions requirements, it is necessary for an easy acceleration maneuver to establish an appropriate relationship, including hysteresis, between the accelerator pedal stroke change (ΔA_c) and drive shaft torque increment (ΔT_d).

With a gear shift ratio control system of a continuously variable transmission (CVT), depending on the parameter setting for the hydraulic feedback control, self-excited vibration can occur in conjunction with driveline torsional vibration⁽⁷⁾. Phenomena of this type can compromise the consistency of vehicle response that all drivers expect from their vehicle.

5.3 Road slope and surface

On slopes, where vehicles are subjected to gravitational acceleration, the same accelerator pedal operation (driving force / engine braking) and brake pedal force (braking power) as on horizontal terrain do not produce the same acceleration or deceleration. With the widespread use of automatic transmissions, vehicles of today are increasingly capable of detecting slopes. And along with the widespread use of electronically controlled throttle valves (and electronically controlled diesel engines), it may be possible to perform the engine output control and gear ratio control for optimum engine braking with the slopes under consideration. However, slopes of more than certain gradients can be recognized by the driver visually or based on the relationship between the accelerator pedal stroke and the vehicle speed/acceleration, and therefore they cannot be called external disturbance. What is worse, simply overcoming slopes with torque control can confuse the driver (because of different vehicle behavior from that expected from his/her internal vehicle model) and may let the vehicle come too close to the preceding vehicle depending on accelerator pedal operation. Therefore, torque correction is a subject that should be discussed carefully. On the deceleration control side, one technique has been widely used in which lower gears (with greater reduction ratios) are automatically selected to secure engine braking power appropriate for the negative gradient. A gear selected may lead to engine braking of a certain magnitude so that the driver feels too aggressive; however, the system has been generally accepted for safety reasons as it substitutes for the foot brake which should not be used too much when going downhill.

On wet or icy roads with extremely low coefficients of friction, tires slip, failing to transmit driving force onto the road surface and making driving difficult. A driver who unexpectedly encounters this type of low-friction road or who has little experience in such conditions can make excessive acceleration, braking and/or steering maneuvers, making the vehicle unstable beyond control. While antilock brake systems (ABS) are installed on almost all cars, an increasing number of

vehicles are equipped with an active stability control system (ASC), which maintains torque below the level permitted under the prevailing coefficient of friction.

5.4 Vibration interference

In principle, a vehicle is made up of masses connected with each other by springs and is extremely easy to vibrate. Because of this, a vehicle is susceptible to resonance (e.g. vibration experienced when the transmission is in D and the engine is running at idle, and also gear rattle) that results from specific vibration input, and body vibration (e.g. acceleration shock) that is caused by stepped input. These can be annoying especially when they are not intended or expected by the driver. Among them, acceleration/deceleration (tip-in/tip-out) shock is caused when the driver rapidly depresses the accelerator/brake pedal at low to middle speed. This is caused by stepped change in engine torque, which then generates torsional vibration on the driveline, and it is then transmitted via the powertrain mounts and suspensions into the cabin. This can be counteracted by active vibration damping technique based on engine torque control, and has been offered with electronic control of the throttle valve^{(8)–(10)}.

Due to the torque converter characteristics, the vehicle may cause self-excited vibration during creep off accompanied by driveline torsional vibration. This vibration dampens as the vehicle gains speed, and is difficult to control electronically⁽⁷⁾.

6. Easier driving

Easier driving can be defined as when the driver can easily make the actual vehicle follow the target behavior (speed, acceleration and position) in the driver's mind. More sophisticated compensation, by which the vehicle decides and follows the most appropriate target behavior based on the driver's ambiguous target behavior, is not under consideration.

6.1 Linearity and agility of vehicle response

Linear response to driver's input is extremely important. As previously discussed in this paper, humans form a vehicle response model in themselves. Linearity is important for the driver to quickly form the vehicle model (learn the characteristics of the vehicle). At least smooth uniformity is necessary.

Humans have difficulty forming a delayed response model, such as that of a torque converter. It is therefore preferable to minimize response lags that can be sensed by humans. For pedal switching, including the operational delay, it can be managed by prediction and decision.

6.2 Minute operation and operation force

Just depressing the pedal and performing fine-adjustment on the pedal is quite different. You can kick the pedal if massive force is needed, however, if fine adjustment is needed, the relationship between the pedal position and the applied force is important. Braking power can be finely adjusted thanks to engine

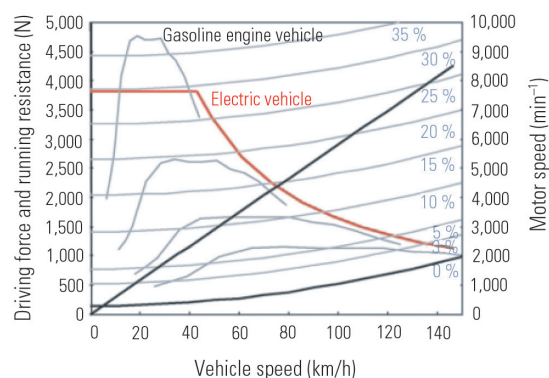


Fig. 7 Electric vehicle driving force characteristics

vacuum and hydraulic boosting whereby light pedal force is amplified to generate greater braking force. Without this amplification, an accurate braking maneuver is difficult.

The accelerator pedal is equipped with a light spring while the throttle valve with a heavy return spring is driven by an electric motor. Compared with a mechanical system, this offers better controllability with lighter pedal force and more appropriate pedal stroke.

6.3 Smooth acceleration

Stepped (conventional) automatic transmissions perform upshifts as the vehicle accelerates, with each gearshift giving a jerk. Torque converters, normally coupled to an automatic transmission, transmit torque that is proportional to the square of the engine speed. Therefore, output torque does not increase significantly until engine speed increases sufficiently, offering a kind of torque response resembling the time lag of the first order. The output torque reaches its peak at a certain speed and then drops off monotonously. Today, electronic engine control technology is available that curbs torque fluctuation during gear shifting. Attempts have been made to use a multi-disc clutch in place of a torque converter and electronically control it to limit acceleration response lag and peak acceleration drop.

Electric vehicles show completely different torque output characteristics, offering constant torque up to a certain speed with almost no torque output delay typical of a combined system of an internal combustion engine and torque converter. The linear and swift torque response to accelerator pedal input enables the driver to quickly learn the characteristics of the vehicle. Fig. 7 shows typical torque characteristics of electric vehicles⁽¹¹⁾.

6.4 Maintaining constant speed

When a petrol-powered vehicle is driven with the throttle valve kept at a certain position, torque output decreases as engine speed increases. In addition, its running resistance increases with speed as the vehicle experiences aerodynamic drag corresponding to the square of vehicle speed. As a result, a stable equilibrium is established at a certain speed. On diesel-pow-

ered vehicles, depending on the characteristics of the governor used, it has been reported that the vehicle causes self-excited vibration when running with a constant speed maintained⁽¹²⁾.

6.5 Deceleration, stopping and creeping

As previously discussed, braking power shows good linearity and response to brake pedal depressing force. This must be maintained until immediately before the vehicle comes to a halt in order to make the vehicle decelerate smoothly and stop at exactly the intended spot. On the other hand, the driver may encounter difficulty in stopping the vehicle if the frictional properties of the brake system rapidly changes at creeping speed, causing a sudden increase in braking power and leading to an unintended hard stop. If a brake judder occurs, the driver is subjected to cyclic interference in the reaction to the brake pedal force.

Vehicles are not equipped with gear ratios that directly connect the engine to the wheels and enable the vehicle to creep at idle engine speed. To creep that way, the driver needs to operate both the accelerator and clutch pedals at the same time, but that is hardly easy for beginners. For the driver, vehicle speed and position can be controlled accurately and easily if constant torque converter output, at least greater than that causing engine stall, is controlled by braking.

6.6 External disturbance control and correction

Let us assume that a vehicle, which stopped on an uphill slope, is now starting off again. The vehicle may go backward as the driver is switching pedals, which can be a big concern and lead to risk, unless he/she uses both feet, one for the brake pedal and the other for the accelerator pedal (a convenient and safe feature of automatic transmissions). This can be addressed on a vehicle with a torque converter by designing the converter to have a large creeping capacity. This, however, can lead to increased fuel consumption. Some of the vehicles with an AMT or other type of automatic clutch feature a type of clutch control, which detects slopes and prevents rolling down. This technique, however, also leads to increased fuel consumption.

6.7 Extended driver assistance technologies

Many driver assistance technologies are on progress, such as collision avoidance or vehicle distance control, or even entire automatization of driving maneuvers including recognition and judgment stages. This is too extensive to be covered in this paper and is appropriate for discussion in separate papers.

7. Conclusion

Skilled drivers have a highly refined sense of recognition and are capable of extremely accurate operation, which even sophisticated machines cannot emulate. However, this cannot be expected of inexperienced drivers. This raises the subject of how much machines can be adaptive to human inputs of various skill levels.

What clearly differentiates between a skilled driver

and a beginner is the ability to track targets. This difference is due not to bodily response (motion capabilities) but to recognition and judgment processes.

We divided human driving maneuvers into recognition, judgment and operation stages and defined these stages as input, knowledge (environment) and output in that order. Based on this, we then created a driver model.

A driver improves his/her skills by learning to quickly recognize any chance in the target, judging how to operate the vehicle to address the change and refining his/her knowledge (driver model) about the characteristics of the vehicle.

The expanding applications of electronic control together with other new technologies are making it far easier to drive a vehicle. On the other hand, vehicle response lag and non-linearity to driver inputs still exist and, along with external disturbance, need to be tackled further. Along with this, controllability can drastically change when switching from one technology to another, as has been seen in the electric vehicle response to driver inputs where an electric motor is used as the power plant in place of an internal combustion engine.

This paper has discussed vehicle response, external disturbance and control technologies to assist drivers by especially focusing on the powertrain. The discussion can also be applied in principle to the other parts of the vehicle.

Technology-assisted easy driving leads to enhanced safety and also less fuel consumption and emissions. The human-machine interface has traditionally focused on visibility and the design of controls. In the future, this field is expected to see more studies on the behavior of human-operated vehicles and related corrections.

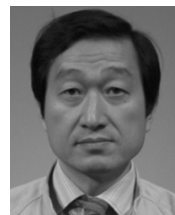
8. Acknowledgment

The drive agent mentioned in this paper is based on a joint study with Professor Hisashi Tamaki of Kobe University Graduate School. I would like to thank Mr. Shimizu of the graduate school for calculations of driver behavior.

References

- (1) Tatsuya Suzuki, "Analysis of Human Factor in Driving Situation: Driver as a Controller", *Journal of the Society of Instrument and Control Engineers*, Vol.45, No.3, pp. 231 – 236, 2006
- (2) Masayuki Sato, "Controller Design for Variable Maneuverability and Disturbance Rejection for Vehicles", *Transactions of the Society of Instrument and Control Engineers*, Vol. 32, No. 8, 632/640, 2007
- (3) Ichiro Kageyama, Yukiyo Kuriyagawa, Mieko Ohsuga, Yoshinori Horie, Osamu Shimoyama, "Study on Evaluation of Driver's Behavior at Running on Narrow Road", *Preprints of Meeting on Automotive Engineers*, pp 5 – 10, 2005
- (4) A. Pellicchia, C. Igel, J. Edelbrunner, & G. Schoner: *Making Driver Modeling Attractive*, IEEE IEEE INTELLIGENT SYSTEMS, 1541 – 1672/05, 2005

- (5) Ichiro Kageyama, Yukiyo Kuriyagawa, "Construction of Driver Model for Analyzing Driver Behavior", JSAE20075284, Preprints of Meeting on Automotive Engineers, 2007
- (6) Kazuhide Togai, Hisashi Tamaki, "Emission test cycle drive agent and improvement in behavior", JSAE20075814, Preprints of Meeting on Automotive Engineers, 2007
- (7) Kazuhide Togai, Tadashi Takeuchi, "CVT Drive Train Vibration Analysis and Active Control System Design", Mitsubishi Motors Technical Review, No.17, 2005
- (8) Kazuhide Togai, Kyounggon Choi, Tadashi Takeuchi: Vibration Suppression Strategy with Model Based Command Shaping: Application to Passenger Car Powertrain SICE02-0607 SICE annual conference 2002, 2002
- (9) Tadashi Takeuchi, Kyoung-Gon Choi, "Sensibility Analysis of Vibration Transfer Path and Control of Input Force for Reduction of Acceleration and Deceleration Shock", Mitsubishi Motors Technical Review, No.15, 2003
- (10) Seiji Kuwahara, Katsumi Kono, et al., "Toyota's New Integrated Drive Power Control System", JSAE20075624, Preprints of Meeting on Automotive Engineers, 2007
- (11) Kazunori Handa, Hiroaki Yoshida, "Development of Next-Generation Electric Vehicle "i MiEV"", Mitsubishi Motors Technical Review, No.19, 2007
- (12) Kazutoshi Mori, "The Previous Stage to Electronic Control for Diesel Engine", Journal of the Society of Instrument and Control Engineers, Vol.45, No.3, pp. 231 – 236, 2006



Kazuhide TOGAI

Development of Plant-Based Plastics Technology, 'Green Plastic'

Isamu TERASAWA* Kazunori TSUNEOKA*
Akihiro TAMURA* Mitsutaka TANASE**

Abstract

It's very important to make effective use of sustainable resources, as the reduction of carbon dioxide is urgent for the prevention of global warming. We note a wide variety of plant-based material and name 'Green Plastic' (Fig. 1) for these technologies generically and promote developments of new materials considering environment. We have already developed a new automotive interior board made from a composite of plant-based polybutylene succinate resin and bamboo fiber and a floor mat using polylactic acid resin, and used them to vehicles. And also, we are developing several kinds of plant-based materials and car parts using them. The overview of these technologies is introduced.

Key words: Composite Material, Plastic, Environment, Interior

1. Introduction

According to the IPCC Fourth Assessment Report released in February 2007, the average temperature of the earth's surface rose by 0.74 °C over the 100 years from 1906 to 2005 and the rate of temperature increase over the latter 50 years of that period is about twice the rate over the entire 100 years. The report also states that the temperature on average will rise at the rate of at least 0.2 °C/decade⁽¹⁾. The Japan Agency for Marine-Earth Science and Technology in August 2007 announced that satellite monitoring had confirmed that the area of ice in the Arctic Ocean had dwindled to the lowest level since observations began in 1978⁽²⁾. Global warming has been progressing much faster than forecast, and the IPCC Fourth Assessment Report strongly suggests that global warming is caused by increased emissions of greenhouse gases (CO₂ etc.) from human activities including the burning of fossil fuels, agricultural operations and changing land utilization⁽¹⁾.

In addition, there is concern that oil and other fossil-fuel resources will be seriously depleted if major industrial powers and rapidly developing countries continued to consume them in such large quantities.

Against this background, Mitsubishi Motors Corporation (MMC), with the aims of helping to arrest global warming, reduce the consumption of fossil-fuel resources and protect forest resources, has been studying the development of automobile parts made from sustainable resources, namely, plant-based materials such as plant-based plastics and fibers. Thus far, MMC has developed polybutylene succinate (PBS) bamboo-fiber board, and floor mat made from polylactic acid (PLA) fibers^{(3) - (5)}. Samples of these parts were displayed at the Frankfurt Motor Show 2007 from September 13 to 23, 2007, in Frankfurt, Germany, together with an injection-molded PLA part and three



Fig. 1 MMC Green Plastic logo

fiber-based parts which were still under development.

As explained above, these resin and fiber parts are made from plants. That is, they are carbon neutral, which means that burning them does not add extra CO₂ to the atmosphere, because the plants from which they were made absorbed CO₂ in the atmosphere during the process of photosynthesis as they grew (Fig. 2).

This paper introduces these plant-based parts.

2. PBS bamboo-fiber board

2.1 Selection of reinforcing fiber

One of the shortcomings of PBS resin is its low elasticity. In order to improve its stiffness and increase the plant-based content, we examined the possibility of using plant fiber as a reinforcing material. Among various plant fibers, bamboo fiber was selected for the following reasons.

Firstly, while its density is low, bamboo fiber has an extremely high modulus of elongation (stiffness). Table 1 shows the characteristics of major plant fibers⁽⁶⁾⁽⁷⁾. Secondly, bamboo fiber is environmentally friendly and readily available. Bamboo takes only 2 to 4 years to grow enough for harvesting, and has long been used as an eco-friendly resource. Furthermore, bamboo is found extensively throughout the world, including Japan, countries in Southeast Asia and China, and thus is readily available. Thirdly, with increasing imports of

* Material Engineering Dept., Development Engineering Office

** Advanced Vehicle Engineering Dept., Development Engineering Office

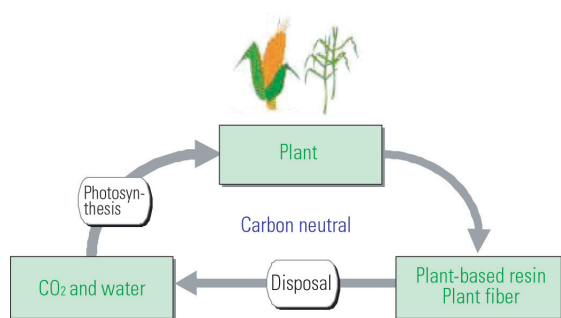


Fig. 2 Carbon neutral

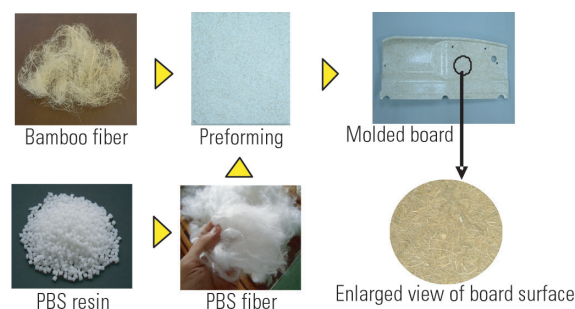


Fig. 3 Manufacturing process of PBS bamboo-fiber board

Table 1 Characteristics of plant fibers⁽⁶⁾⁽⁷⁾

Type	Density ⁽⁶⁾ (g/cm ³)	Modulus of elongation ⁽⁶⁾ (GPa)	Tensile strength ⁽⁷⁾ (MPa)
Hemp	1.50	12.7	—
Flax	1.30	13 – 26	344
Jute	1.50	19 – 35	393
Kenaf	1.50	15 – 37	—
Sisal	1.45	16 – 37	510
Ramie	1.50	—	—
Bamboo	0.9 – 1.2	21 – 38	391 – 713
Mousou bamboo	1.20	21.1	—
Banana	1.35	27 – 32	—
Coconut	1.45	13.7	—
Cotton	1.50	11	—
Glassfiber (for comparison)	2.50	70	3,400

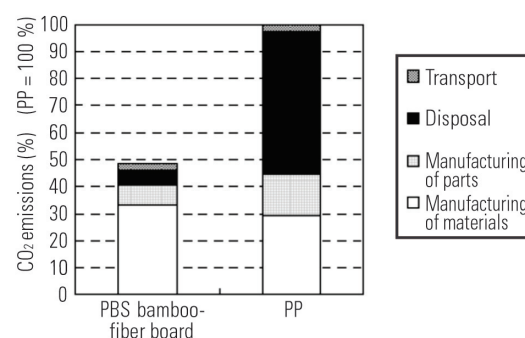


Fig. 4 LCA of PBS bamboo-fiber board

4). It was found that the PBS bamboo-fiber board emits approximately 50 % less CO₂ than PP resin.

2.4 Emissions of VOCs and organic acids

Emissions of volatile organic compounds (VOCs), and those of organic acids which are a major component of odors, were measured on the PBS bamboo-fiber board. Fig. 5 and Fig. 6 compare these measurements relative to corresponding measurements of conventional wood fiber hardboard indicated as 100 %.

It was found that the PBS bamboo-fiber board emits at least 90 % less VOCs, including formic aldehyde, than wood fiber hardboard. The board was also found to emit approximately 60 % less acetic acid and its emissions of formic acid were below the detection threshold.

Wood fiber hardboard contains VOC-rich phenol resin as a binder, whereas the PBS bamboo-fiber board contains no VOC-rich binders, hence the substantially lower emissions of VOCs in the test. Lignin, cellulose and hemicellulose that compose plant fiber are hydrolyzed into aldehydes and organic acids. Hydrolysis temperature varies among these components: lignin at around 130 °C, cellulose at 240 °C and hemicellulose at 160 °C⁽⁸⁾. With the PBS bamboo-fiber board, PBS resin melts for molding at a lower temperature than these, which is another reason for the lower emissions of VOCs and organic acids than from wood fiber hardboard.

low-priced Chinese edible bamboo shoots and the use of plastic products in place of bamboo products, the bamboo industry in Japan has been in serious decline. As a result, bamboo forests are left unattended and underground roots are invading residential areas and agricultural fields, causing serious problems. PBS bamboo-fiber board may be a new application for the domestic bamboo industry and provide an opportunity to rejuvenate rural towns where bamboo is grown, while also helping to solve the problem of underground bamboo roots.

2.2 Manufacturing processes

Fig. 3 shows the manufacturing processes of the PBS bamboo-fiber board. Using a special machine, PBS fiber is mixed with bamboo fiber to make the preformed mixture. The preformed mixture is then hot-press molded to melt the PBS resin and finally allowed to cool.

2.3 CO₂ emissions

CO₂ emissions throughout the lifecycle of the PBS bamboo-fiber board from harvesting to disposal were calculated based on the Life Cycle Assessment (LCA) criteria, and the results were compared with the corresponding CO₂ emissions of conventional PP resin (Fig.

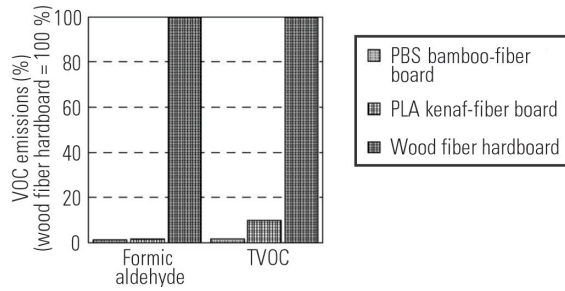


Fig. 5 VOC emissions from boards

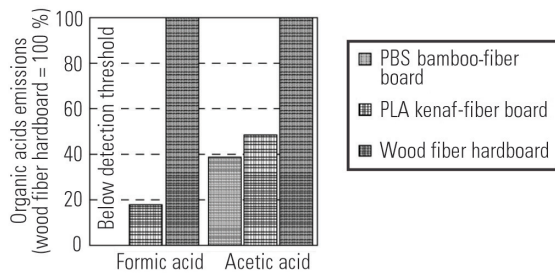


Fig. 6 Organic acid content of boards

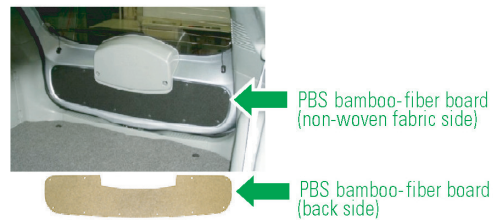


Fig. 7 PBS bamboo-fiber board used in i MiEV fleet monitor vehicle

2.5 Other characteristics

Table 2 shows the general properties of the PBS bamboo-fiber board. PBS resin is hydrolyzable, so a hydrolysis inhibitor is added to the PBS bamboo-fiber board to improve its hydrolysis resistance (which means resistance to hydrothermal aging). The PBS bamboo-fiber board has a deflection temperature of 109 °C under load, and thus can be used in environments up to 100 °C. Its impact resistance and bending modulus of elasticity are equal to or better than those of conventional materials.

In addition, as the PBS resin in the PBS bamboo-fiber board acts as a binder, a skin can be adhered onto the board as it is being hot-press molded. This eliminates the need for adhesive, which normally contains solvent, a source of VOCs. Table 3 shows the performance of the PBS bamboo-fiber board complete with the skin. As indicated, the board satisfies a range of test items for use as interior materials, and in fact has been used on the environmentally-friendly i MiEV fleet monitor vehicles released in the autumn of 2007 (Fig. 7).

Table 2 General properties of PBS bamboo-fiber board

Evaluation items	PBS bamboo-fiber board	Wood fiber hardboard	Recycled PP + PE + PET	PLA kenaf-fiber board
Density (g/cm ³)	1.20	1.00	1.19	0.62
Deflection temperature under load (°C)	109	170	76	60
Bending modulus of elasticity (MPa)	53.2	31.8	37.5	24.6
Izod impact resistance (kJ/m ²)	15.5	13.6	15.0	26.6
Coefficient of water absorption (%)	3.8	38.6	—	52.5

Table 3 Component performance of PBS bamboo-fiber board

Evaluation items	Result	Evaluation items	Result
Flammability	Passed	Stapling	Passed
Shrinkage factor	Passed	Thermal insulation	Passed
Warpage	Passed	Air permeability	Passed
Epidermal peeling	Passed	Odor	Passed
Impact resistance	Passed	Chemical resistance	Passed
Sound absorbing coefficient	Passed	Accelerated lightfastness (non-woven fabric side)	Passed
Resistance to hydrothermal aging	Passed	External appearance (non-woven fabric side)	Passed

3. PLA fiber floor mat

3.1 Resistance to hydrothermal aging and wear

The PLA fiber floor mat uses PLA fiber in the pile surface. PLA resin is hard and brittle, and thus has poor wear resistance. Its resistance to hydrothermal aging (hydrolysis resistance) is also low, as with PBS resin. To overcome this, its molecular structure was optimized to improve its hydrolysis resistance. However, the improved version still showed lower hydrolysis and wear resistance than conventional products. Therefore, doubled and twisted thread using PA6 fiber, which is flexible and wear resistant, and PLA fiber are used to improve resistance to hydrothermal aging and wear (Fig. 8).

3.2 CO₂ emissions

Fig. 9 compares the developed PLA fiber floor mat and a conventional product (PA6 fiber) in terms of CO₂ emissions of the pile surface throughout their life cycles. As indicated, the PLA fiber floor mat emits

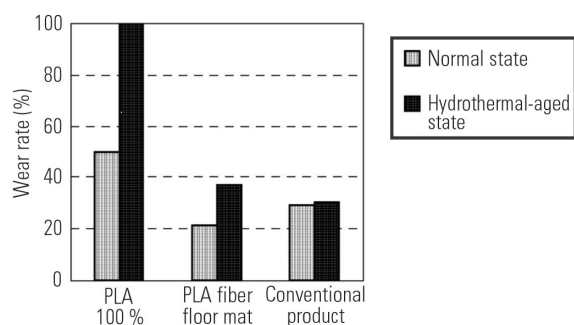


Fig. 8 Hygrothermal aging and abrasion resistance of floor mats

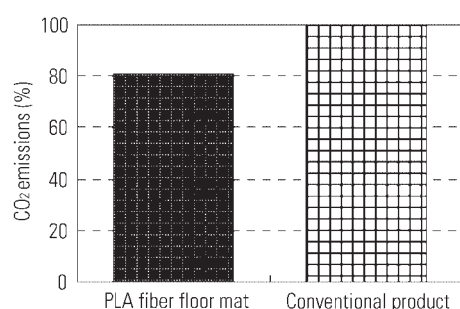


Fig. 9 LCA of floor mats

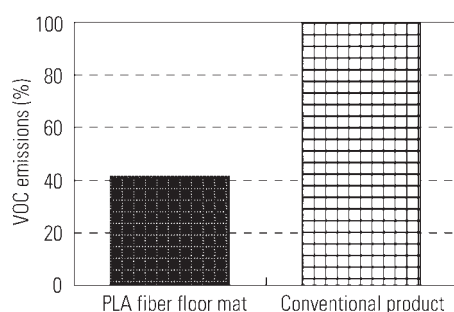


Fig. 10 VOC emissions from floor mats

Table 4 General properties of developed floor mats

Evaluation items	PLA fiber floor mat	Conventional product
Tensile strength (N/25 mm)	562 (longitudinal) x 486 (lateral)	284 (longitudinal) x 252 (lateral)
Tear strength (N/25 mm)	114 (longitudinal) x 108 (lateral)	131 (longitudinal) x 113 (lateral)
Pile pull strength (N)	21.6	24.6
Heat shrinkage (%)	0.2	0
Wear resistance	Passed	Passed
Accelerated lightfastness	Passed	Passed
Thermal aging resistance	Passed	Passed
Cold resistance	Passed	Passed
Odor	Passed	Passed
Weight resistance	Passed	Passed
Resistance to hydrothermal aging	Passed	Passed
Flammability	Passed	Passed

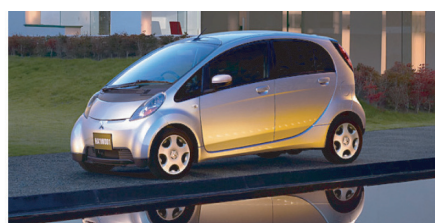


Fig. 11 PLA fiber floor mat used to i 1st anniversary edition

approximately 20 % less CO₂ than the conventional product.

3.3 VOC emissions

In addition to using PLA fiber to reduce CO₂ emissions, the PLA floor mat uses materials that do not include VOCs, and employs hot melt PP (polypropylene) resin instead of adhesive to bond the surface layer to the lining. As a result, it emits approximately 60 % less VOCs than a conventional product (which includes latex as an adhesive) (Fig. 10).

3.4 Other characteristics

Table 4 shows the general properties of the PLA fiber floor mat. As indicated, the PLA fiber floor mat has equivalent quality to the conventional product. The floor mat is used on the 1st anniversary edition of the "i" released in January 2007 (Fig. 11).

4. Parts display at the Frankfurt Motor Show 2007

MMC displayed samples of the two parts discussed above, together with samples of the following four parts which then were still under development, at the Frankfurt Motor Show 2007 from September 13 to 23, 2007, in Frankfurt, Germany. (Fig. 12)

- ① Door trim fabric (PLA fiber)
- ② Quarter upper trim (injection-molded PLA)
- ③ Floor carpet (PLA fiber)
- ④ Pillar garnish (flocked PLA fiber)

Table 5 shows the features of these parts as well as the areas still needing improvement. Those parts listed above that use PLA fiber require higher durability than the PLA fiber floor mat, so they use modified PLA fiber to improve hydrolysis resistance. However, they still

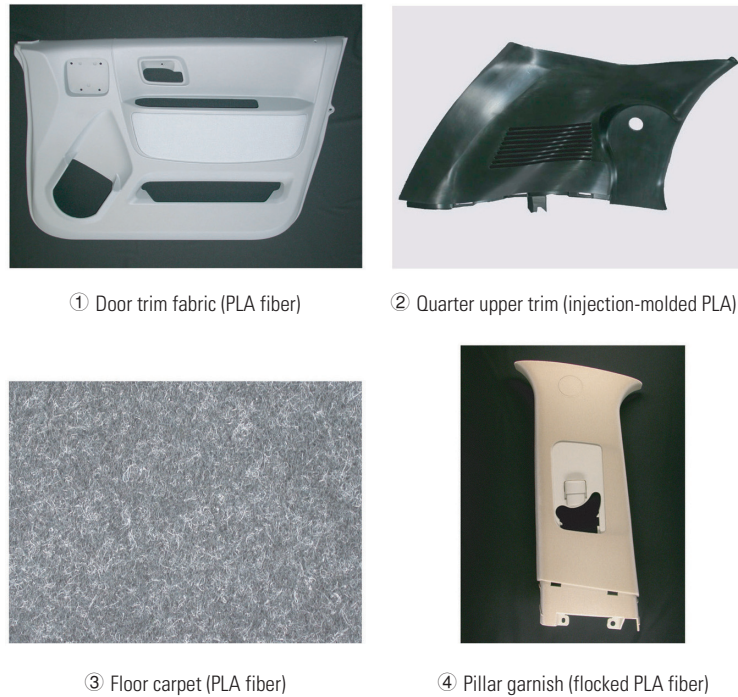


Fig. 12 Exhibits at 2007 year Frankfurt Motor Show

Table 5 Characteristics and problems of exhibits at 2007 Frankfurt Motor Show

Parts	Door trim fabric	Quarter upper trim	Floor carpet	Pillar garnish
Structure / Material	Modified PLA fiber	Injection-molded modified PLA	Modified PLA fiber – non-woven fabric	Flocked modified PLA fiber
Feature	Hydrolysis resistance Lightfastness	Hydrolysis resistance Heat resistance Impact resistance	Hydrolysis resistance Wear resistance	Hydrolysis resistance Wear resistance Aesthetic appearance
Area for improvement	Durability Cost	Durability Moldability Elongation Cost	Durability Formability Cost	Durability Cost

need to be improved in areas such as durability, moldability and cost. The heat resistance of injection-molded PLA has been improved by means of natural fiber (jute), and a new crystal nucleation agent; in impact resistance by means of polyallylate fiber; and in hydrolysis resistance by means of hydrolysis inhibitor. The quarter upper trim still needs to be improved in terms of lower cost and a good balance between durability, moldability and elongation. All of these parts will be refined for commercialization.

5. Future challenges

To encourage the use of plant-based material in automobile parts, the following challenges must be addressed:

- (1) Development of plant-based materials with sufficient heat and impact resistance for use in instrument panels and other interior parts
- (2) Development of plant-based materials with sufficient durability for use in exterior and other parts

that are exposed to moisture, solar radiation and heat at the same time

- (3) Price reduction to the same levels as PP resin and other conventional materials

6. Conclusion

The reduction of CO₂ emissions is an urgent issue for humankind to curb the progress of global warming. The PLA floor mat that MMC has developed, although a small step toward that goal, would, if used in 1000 "i" vehicles, offset the equivalent of the CO₂ emitted from 224 households on one day.

MMC will continue to develop CO₂ reduction technologies for application to plastic and rubber materials for automobiles. We will explore new applications for PLA resin, PBS resin and bamboo fiber while actively investigating the use of materials such as plant fibers, wood, cellulose, lignin, natural fats and natural rubber.

The PBS bamboo-fiber board was developed with extensive cooperation from the Aichi Industrial Technology Institute while the PLA floor mat was the

result of collaboration with Toray Industries, Inc. We would like to thank all those involved in these developments.

References

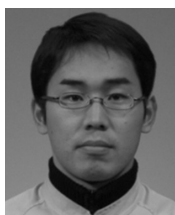
- (1) Ministry of Education, Culture, Sports, Science and Technology et al., "Intergovernmental Panel on Climate Change (IPCC) Fourth Assessment Report: Climate Change 2007, Working Group I Report "The Physical Science Basis"", 2007
- (2) Total area of sea ice in Arctic Ocean smallest since observations began – Much faster ice melting than IPCC's forecast, Sankei WEB, August 16, 2007
- (3) Kazunori Tsuneoka et al., "Development of Automotive Interior Board Made from Polybutylene Succinate Resin and Bamboo Fiber", Preprints of Meeting on Automotive Engineers, Vol. 50-07, p. 13, 2007
- (4) Isamu Terasawa et al., Application of Plant-based Materials to Automobiles, the 18th Annual Meeting of the Japan Society of Polymer Processing Presentation Papers, p. 35, 2007.
- (5) Akihiro Tamura, Development of PLA Resin Floor Mat, the Society of Automotive Engineers of Japan Kansai Branch News No. 30, p. 1, 2007.
- (6) Kazuo Kitagawa, "Biodegradable Resin – Biodegradation by Soil Organism and Resin-Biomass Fiber Composite", Seminar Text, the Technical Information Institute Co., Ltd., 2003.
- (7) Toru Fujii, Advanced Application of Bamboo – Full Utilization of Bamboo as a Sustainable Renewable Natural Resource, Processing Technology Vol. 42, No. 4, p. 233, 2007
- (8) Publication of Patent Applications, 2004-278160



Isamu TERASAWA



Kazunori TSUNEOKA



Akihiro TAMURA



Mitsutaka TANASE

Development of EPS+ (Electric Power Steering Plus)

Sumio MOTOYAMA*

Abstract

A new control algorithm called EPS+ was developed for electric power steering and adopted in the 2008-model "i". It improves the steering feel and vehicle stability.

Key words: Steering System, Electric Power Steering

1. Introduction

The use of electric power steering (EPS) systems is spreading rapidly thanks to their fuel efficiency compared with hydraulic systems. As a result, the steering feeling of EPS, which was a weakness, has been improved almost to the level of hydraulic steering systems. Nevertheless, research is underway to improve the steering feeling further by using the high degree of control freedom that is characteristic of EPS systems⁽¹⁾⁽²⁾.

Our newly developed "EPS+" is an EPS control algorithm for improving the steering feeling while assuring vehicle motion stability. This paper introduces aspects of the EPS+ in the 2008 model Mitsubishi "i".

2. EPS+ control

Fig. 1 shows an outline of the EPS+ control. To the assist control provided by the previous type of EPS, the EPS+ adds two new controls: self-alignment estimation control and vehicle motion estimation control (**Fig. 1**).

2.1 Self-alignment estimation control

The self-alignment estimation control uses both the EPS sensor information and internally programmed EPS control information to estimate the self-alignment torque that is generated between the vehicle's tires and the road surface. The self-alignment torque thus estimated is used to add a steering torque corresponding to the torque by means of an electric motor. This control allows the driver to feel the self-alignment torque clearly through the steering wheel, and so the steering feels more natural. **Fig. 2** schematically shows how the effects of this control are produced.

2.2 Vehicle motion estimation control

The vehicle motion estimation control uses the steering angular velocity information internally programmed in the EPS system to estimate how the vehicle is likely to turn. According to the estimation, the control adds as much steering torque as necessary to suppress the likelihood of changes in direction. This control helps improve yaw damping of the vehicle at high speeds, so the driver needs to make fewer adjust-

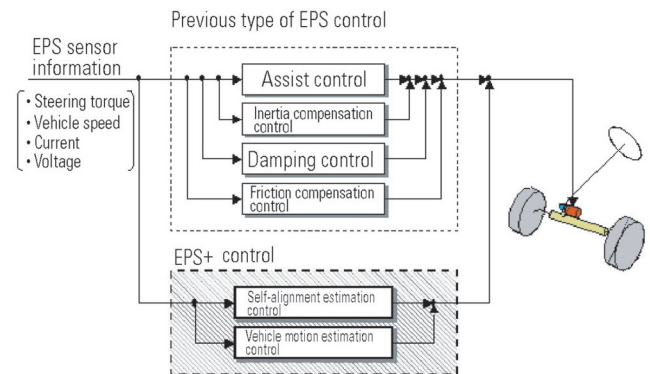


Fig. 1 Outline of EPS+ control

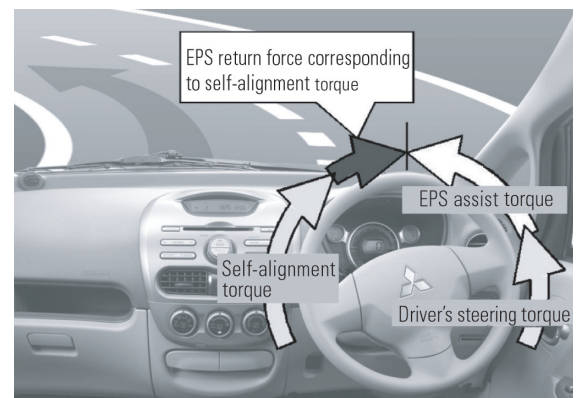


Fig. 2 Effect of self-alignment estimation control

ments to the steering wheel. **Fig. 3** schematically shows the effect of this control.

2.3 Assist control

To maximize the effects of these two new controls, the assist control has been completely retuned. Specifically, the assist current relative to each steering torque is set lower compared with the conventional setting to give a slightly heavier steering feeling, while lowering the setting of the damping control current to give a more responsive steering feeling.

* Advanced Vehicle Engineering Dept., Development Engineering Office

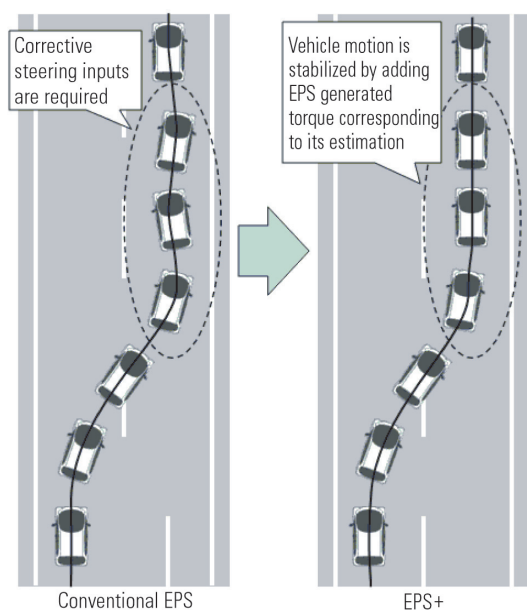


Fig. 3 Effect of vehicle motion estimation control

3. Effects of the EPS+

Fig. 4 shows the results of the steering wheel self-aligning (returning to neutral) test at low speeds. It shows that the additional torque of the self-alignment estimation control provided by the EPS+ offsets part of the friction in the steering system and so enhances the self-aligning of the steering wheel.

Fig. 5 shows the results of the free steer stability test conducted at a vehicle speed of 100 km/h. As is evident from the figure, the conventional EPS suffers greater yaw oscillation after releasing the steering wheel than EPS+, in which the torque added by the vehicle motion estimation control effectively suppresses changes in vehicle motion and thus improves damping of the yaw oscillation.

4. Conclusion

Application of EPS+ to the Mitsubishi "i" has improved the light steering feeling that is common to midship engine vehicles and increased the vehicle's motion stability at high speed. In future we will focus on applying the EPS+ to more Mitsubishi Motors Corporation models, and on developing harmonized control of the steering and other systems.

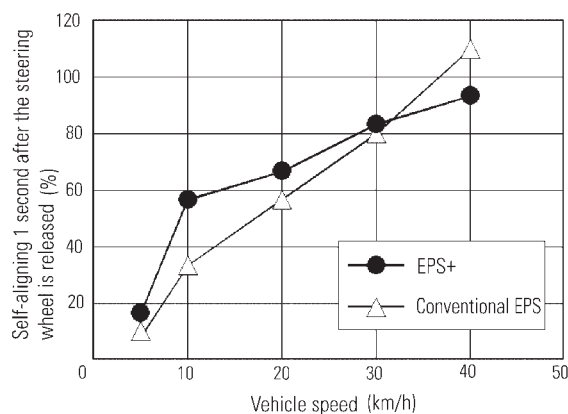


Fig. 4 Improvement of steering returnability

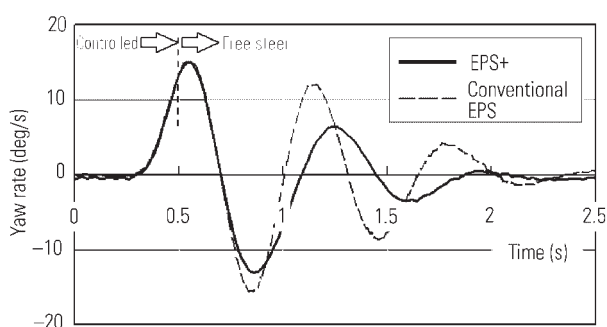
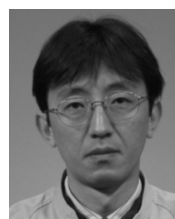


Fig. 5 Improvement of free steer stability

References

- (1) Tanaka et al.: The Torque Controlled Active Steer for EPS, AVEC'04, pp. 501 – 506
- (2) Kubota et al.: Influence of Transient Steering Assist Characteristics on Motion of Vehicle, Proceedings of JSAE Symposium, No. 75-05, pp. 9 – 14, 2005



Sumio MOTOYAMA

Development of a Rain-Light Sensor

Shinichi KATO* Toshinori YAGI*

Abstract

Mitsubishi Motors Corporation (MMC) has developed a rain-light sensor that controls the auto-light system and the rain-sensitive wiper system. It is installed in the new GALANT FORTIS. The rain-light sensor controls the headlamps and windshield wipers, sending an activation request to ETACS⁽¹⁾ (Electronic Time and Alarm Control System). This data consists of vehicle information from ETACS, ambient light intensity, front light intensity and raindrop detection. Regarding the auto-light function, the rain-light sensor distinguishes between entering a tunnel and passing under a bridge, using front and ambient illumination sensors. It prevents the headlamps from blinking when the vehicle passes under a bridge. The rain-sensitive wipers have newly designed lenses to ensure uniform distribution of sensitivity for raindrops and improve the timing for the first wipe when there are fewer raindrops on the windshield glass.

Key words: Rain-Light-Sensor, Auto-Light, Rain Sensitive Wiper, Electronic Control, Convenience

1. Foreword

Automatic lighting and rain-sensitive wiper systems are commonly found even in B-segment vehicles in Europe, to relieve drivers from having to frequently operate lighting and wiper controls when driving at high speed on roads with many tunnels at short intervals, for example. In addition to increasing comfort in this manner, they also improve safety by making the vehicle more recognizable to other vehicles in the twilight.

In Japan, the auto-light system has recently become popular, but the rain-sensitive wiper system is not yet widespread. This paper introduces the rain-light sensor developed by MMC for its new GALANT FORTIS as a comfort-oriented device that increases driving pleasure and safety by making the vehicle more visible to other vehicles.

2. System configuration

The rain-light sensor forms an ECU that integrates both automatic lighting and rain-sensitive wiper functions into a single unit. It is directly mounted on the windshield glass surface as shown in **Fig. 1**. This device consists of the sensor that works as a control unit and the optical coupler bonded to the glass. The control unit has two raindrop sensors and two light sensors for the automatic lighting function. **Fig. 2** and **Fig. 3** show the appearances of the rain-light sensor and optical coupler, respectively.

Fig. 4 is a block diagram of the rain-light sensor system. The rain-light sensor constitutes a slave node in the local interconnect network (LIN) that has the Electronic Time & Alarm Control System (ETACS) as the master node and performs the following functions: It transmits requests for turning the auto-light on and off

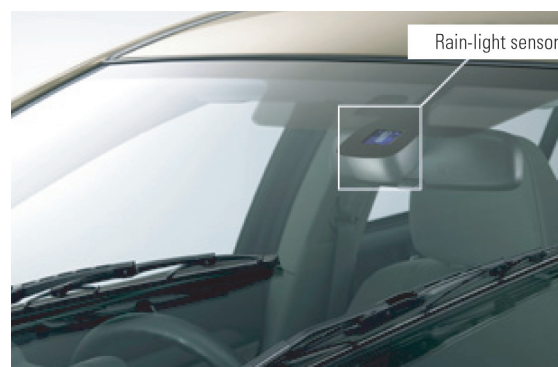


Fig. 1 Location of rain-light sensor

and activating the rain-sensitive wiper to the ETACS based on data provided by ETACS such as the vehicle speed, outside temperature and vehicle specifications, including destination, and also based on signals from the lighting and wiper switches on the steering column switch that works as another slave node. Based on these requests, the ETACS controls the operation of the headlamps, other exterior lamps and windshield wipers.

The GALANT FORTIS' rain-light sensor uses the vehicle speed data that is transmitted by an anti-lock brake system (ABS), whereas it receives the meter-calculated outside temperature data via the ETACS, both transmitted through the in-vehicle communications network and the gateway function⁽²⁾ provided by the ETACS. The ETACS also retains and supplies data coding information⁽³⁾, which includes the destination and other vehicle specification information, to the sensor. Via the ETACS, the auto-light customization information to be displayed for the user on the navigation screen is also supplied.

* Electronics Engineering Dept., Development Engineering Office



Fig. 2 Appearance of rain-light sensor

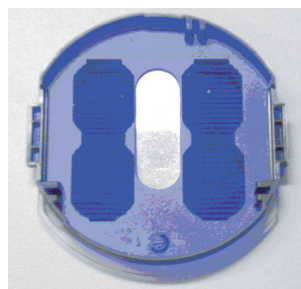


Fig. 3 Appearance of optical coupler

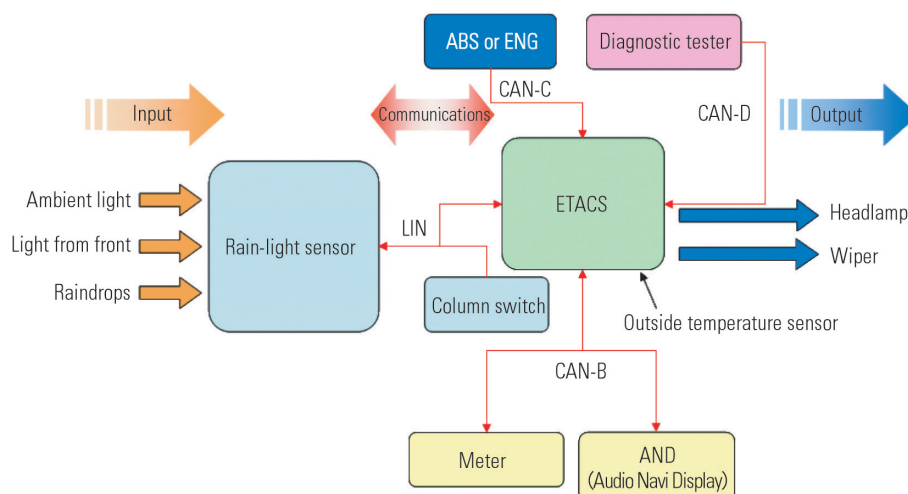


Fig. 4 Structure of rain-light sensor system

The rain-light sensor obtains all necessary data through this communications network, using only three harnesses that are for its power supply, grounding and LIN communications. This configuration allows the system to be applied easily to those models that share the same electronic platform as the new GALANT FORTIS.

3. Rain-light sensor functions

3.1 Automatic lighting function

(1) Basic function

The automatic lighting function turns on and off the headlamps and other exterior lamps according to the intensity of ambient light when the lighting switch is in the AUTO position and the ignition switch in the ON position. The function also allows the user to advance the light-on time in two steps and retard it also in two steps using the customization function on the navigation screen.

The light-on timing in the twilight for the headlamps is set different from the other exterior lamps on models for the Japanese market, whereas the headlamps and other exterior lamps are set to light up simultaneously on models for other markets.

(2) Improvements over the conventional automatic lighting system

The conventional auto-light sensor, which detects

only the ambient light intensity, used to respond to momentary dips in light intensity such as when passing under a bridge, and so a distance and time filter was incorporated to ignore signals showing rapid changes in light intensity. However, this filter caused a delay in illumination of the headlamps when the vehicle entered a tunnel.

With the rain-light sensor on the new GALANT FORTIS, the automatic lighting function detects not only the ambient light intensity but also the intensity of the light ahead of the vehicle, as schematically indicated in Fig. 5 by the blue line and red line, respectively. By processing these two light intensity data together, the automatic lighting function determines whether the vehicle has entered a tunnel, in which case it immediately turns on the headlamps, or simply has passed under a bridge, in which case the function does not trigger the headlamp-on control. Being also able to distinguish the conditions for lighting the headlamps upon entering a tunnel from those in the twilight, this logic enables the new automatic lighting function to cause the headlamps to turn on earlier in the twilight and thus the vehicle to be more recognizable for other drivers than with the conventional function, while preventing momentary illumination of the headlamps in the shade of trees and under bridges.

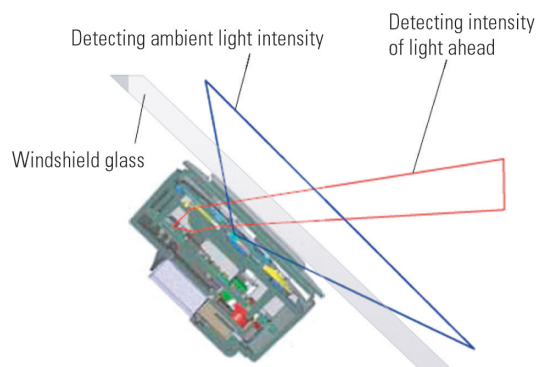


Fig. 5 Outline of light detection

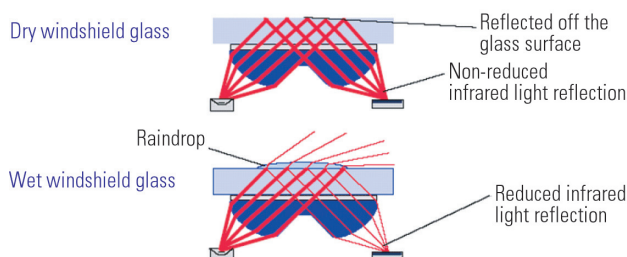


Fig. 6 Outline of raindrop detection

3.2 Rain-sensitive wiper function

(1) Basic function

The rain-sensitive wiper function causes the wipers to operate intermittently or in the low- or high-speed mode according to the amount of raindrops on the windshield when the wiper switch is in the AUTO position and the ignition switch in the ON position. The driver can vary the sensitivity to raindrops using the dedicated knob.

(2) Improved raindrop sensing

Fig. 6 shows how the rain-sensitive wiper function detects raindrops. A light emitting diode emits infrared light beams. A photodiode receives the reflection of the light beams from the windshield glass surface. If there are raindrops on the glass surface, the amount of infrared light reflected off the surface decreases, so the raindrops can be detected.

The problem with the conventional raindrop sensing system was that it did not have a sufficiently large sensing area or uniform sensitivity. The new rain-light sensor overcomes this problem thanks to an improved lens structure of the glass-attached part that enlarges the sensing area as shown in Fig. 7. Particularly, the peak sensitivity spot (the red colored area in the right part of Fig. 7), which was at the center of the sensing area with the conventional lens mechanism, is now widened to nearly the boundary of the sensing area, so that the high-sensitivity zone (the yellow area in the photos in the right part of Fig. 7) is substantially expanded. This improves the sensitivity of the system, enabling the wiper to start wiping more responsively at the beginning of rainfall. This eventually widens the

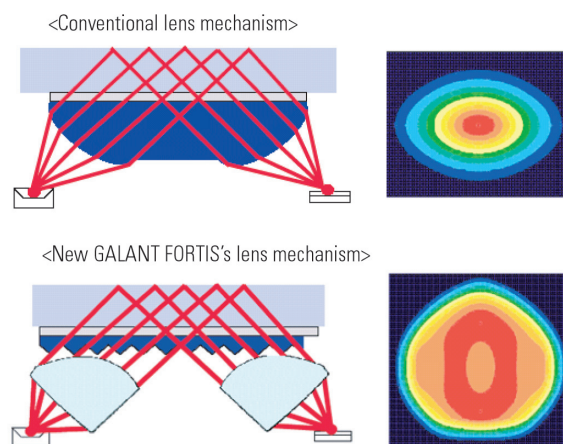


Fig. 7 Optimized lens shape

range available for the user to adjust the sensitivity of the system during rainfall according to preference.

The raindrop sensing area is, however, only a part of the entire windshield glass surface and does not necessarily correspond to the user's field of view. To accommodate possible discrepancies between the driver's field of view and system-controlled wiper operation, a feature has been added that allows the wipers to be operated manually once if the driver operates the knob for a high raindrop sensitivity setting.

Another function of the system uses outside temperature data to prohibit operation of the wipers when starting the engine under very low temperature conditions to prevent the risk of damage to the wiper blades due to freezing on the windshield.

The rain-sensitive wiper system must sense only raindrops accurately while ignoring both the wiper blade moving past the sensor and the water collected by the wiper blade. The new GALANT FORTIS's system does this by using the wiper blade-position sensing signal from the ETACS provided via the LIN. To overcome the problem of the signal transmission interval of the LIN communications being 50 ms at the shortest, the on/off signal of the wiper auto stop switch is transmitted with a time stamp (showing the time elapsed after the on/off change).

3.3 Variations of the system

The Japanese market and European market models of the GALANT FORTIS are different in the automatic light-on timing and mode specifications. It is also necessary to change the parameter about the glass type, because the difference in light-on timing resulting from differences in light transmission characteristics of the glass used must be eliminated. The parameter showing the positional relationships between the location of the rain-light sensor and moving wipers is used for the determination to correct the movement of the wiper blade over the sensor.

The rain-light sensor can adapt itself to any of these different specifications by receiving the following data from the ETACS through the LIN communications system:

- Destination-dependent automatic lighting specifications information
- Automatic light-on timing adjustment information
- Glass type information
- Wiper movement vs. on-glass sensor location parameter

3.4 Fault detection function and diagnostics function

Each rain-light sensor needs to be calibrated when the power is first turned on in order to store in memory the amount of infrared light reflected off the surface of a dry windshield glass. When the power is turned on, therefore, the sensor must already have been installed on the windshield glass. In case the initial calibration fails to complete due to turning on the sensor power before the sensor is installed on the production line, the diagnostic system includes an arrangement to store such incomplete calibration as a fault that can be detected later using the diagnostic tester. The diagnostic system also stores fault codes if the automatic lighting function and rain-sensitive wiper function cannot be properly controlled due to a fault.

Each individual rain-light sensor unit is given a unique serial number, and specific software and hardware version information to enable future traceability.

4. System evaluation on actual vehicles

Through drive tests, the functionality of the rain-sensitive wiper and automatic lighting system has been evaluated by drivers in terms of the following items.

Evaluation points of rain-sensitive wiper function

- Wiper operation in light, medium, and heavy rain
- Wiper operation upon entering and exiting a tunnel during rainfall
- Wiper operation when driving in and out of a multistory parking lot during rainfall
- Wiper operation during snowfall (under low temperature)
- Dry wiping action in non-rainy weather

Evaluation points of automatic lighting function

- Headlamp on and off operations upon entering and exiting a tunnel
- Headlamp on and off operations when driving in and out of a multistory parking lot

- Non-operation of headlamps when driving under a bridge or overpass
- Light-on timing in the twilight (according to customized setting)

5. Conclusion

The new capability to sense both the intensities of ambient light and the light from the front has successfully enabled the automatic lighting function of the rain-light sensor system to prevent momentary operation of the headlamps under a bridge, while advancing the illumination timing of the headlamps in the twilight.

As to the rain-sensitive wiper function of the system, the new lens design has significantly raised the rain-drop sensitivity of the sensor to start the wiping action. This allows the driver to select the sensitivity level for automatic wiper operation from a wider range of options.

We intend to develop a more advanced system that offers even greater comfort and safety by using the features of the communications network and the body system electronic controller ETACS that are now embodied in the new GALANT FORTIS.

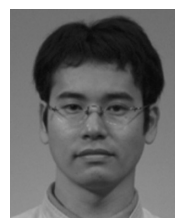
Finally, the authors sincerely thank the people concerned at KOSTAL and all others who contributed greatly to this development project.

References

- (1) Takeo Nagamori et al., "ETACS Functionality Development for the OUTLANDER", Mitsubishi Motors Technical Review, No. 18, 2006
- (2) Hiroki Fukatsu et al., "Development of a Next Generation Electronics Platform", Mitsubishi Motors Technical Review, No. 18, 2006
- (3) Hiroki Takimizu et al., "ECU Variant Coding System", Mitsubishi Motors Technical Review, No. 18, 2006



Shinichi KATO



Toshinori YAGI

Newly Evolved Electronic Time and Alarm Control System (ETACS) of 2008 eK WAGON

Naoki KAWASHIMA* Toshihide TANAKA**
Masashi OGINO** Shuuhei ISHIKAWA**

Abstract

Mitsubishi Motors Corporation (MMC) greatly evolved the ETACS of the eK WAGON for the 2008 model. The improved ETACS has greater customer appeal owing to new functionality that includes the first driver's-door-only unlocking function among minicars; greater customizability of functions to accommodate customer preferences; and stronger fault-diagnosis functions.

Key words: *Electronic Control, Electric Equipment, Multiplexing, Diagnostics*

1. Introduction

The Electronic Time and Alarm Control System (ETACS) provided the preceding generation eK WAGON with a variety of useful functions that go beyond the mini-car level by controlling the vehicle body's various electric/electronic functions and equipment through a multiplex communication network working on 8-bit microcomputers⁽¹⁾. The ETACS on the 2008 model eK WAGON has even greater functionality and performance, thanks to upgraded electronic components including 16-bit microcomputers. In addition to the new components, this paper also introduces the ETACS software that incorporates the latest control logic and allows for future system expansion.

2. Overview of the new ETACS

2.1 System configuration

The vehicle body electronic control system of the 2008 model eK WAGON is configured using the MMC original Smart Wiring System (SWS) as the communications bus and three control units (ECUs), i.e., the ETACS that works as a master control node and the column switch and power window switch ECUs that work as slave nodes. The loads connected to the system include the headlamps, tail lamps, an anti-theft alarm horn, turn signal lamps, wipers, interior lamps, centralized door locks, power windows, electrically retractable door mirrors and various indicators. The ETACS forms an integral part of the junction block that collectively contains power circuit components (fuses, relays, etc.), and it centrally controls the flasher and door lock circuits, keyless entry receivers and antenna. There is no significant difference in system configuration and input/output devices between the ETACS of the new and preceding model eK WAGONS. **Fig. 1** shows an external view of the ETACS and **Fig. 2** shows a block diagram of the system.



Fig. 1 Appearance of ETACS unit

2.2 Communication specifications

Communication control of the SWS is handled by the column switch ECU that performs control using its internal communication ICs and also by the ETACS and power window switch ECU that control communications by means of the software programmed in their microcomputers.

The ECUs form a decentralized control type network and operate under the following specifications:

- Transmission cycle of 40 ms, at which there is practically no delay in switch response
- Transmission rate of 5 kbps, at which noise radiated from communication lines can be suppressed
- Bit synchronizing Manchester code that requires no high-accuracy clocks

Table 1 shows the details of the communication protocol for the SWS. Like with the system configuration referred to in section 2.1, the communication protocol of the 2008 eK WAGON's SWS is similar to that of the preceding model.

However, there are two features that characterize the 2008 model eK WAGON's system: one is that the SWS has an increased data communication capacity, and the other is that the system is capable of bilateral communication with the Multi-Use Tester III (MUT-III), a

* Electronics Engineering Dept., Development Engineering Office

** Mitsubishi Automotive Engineering Co., Ltd.

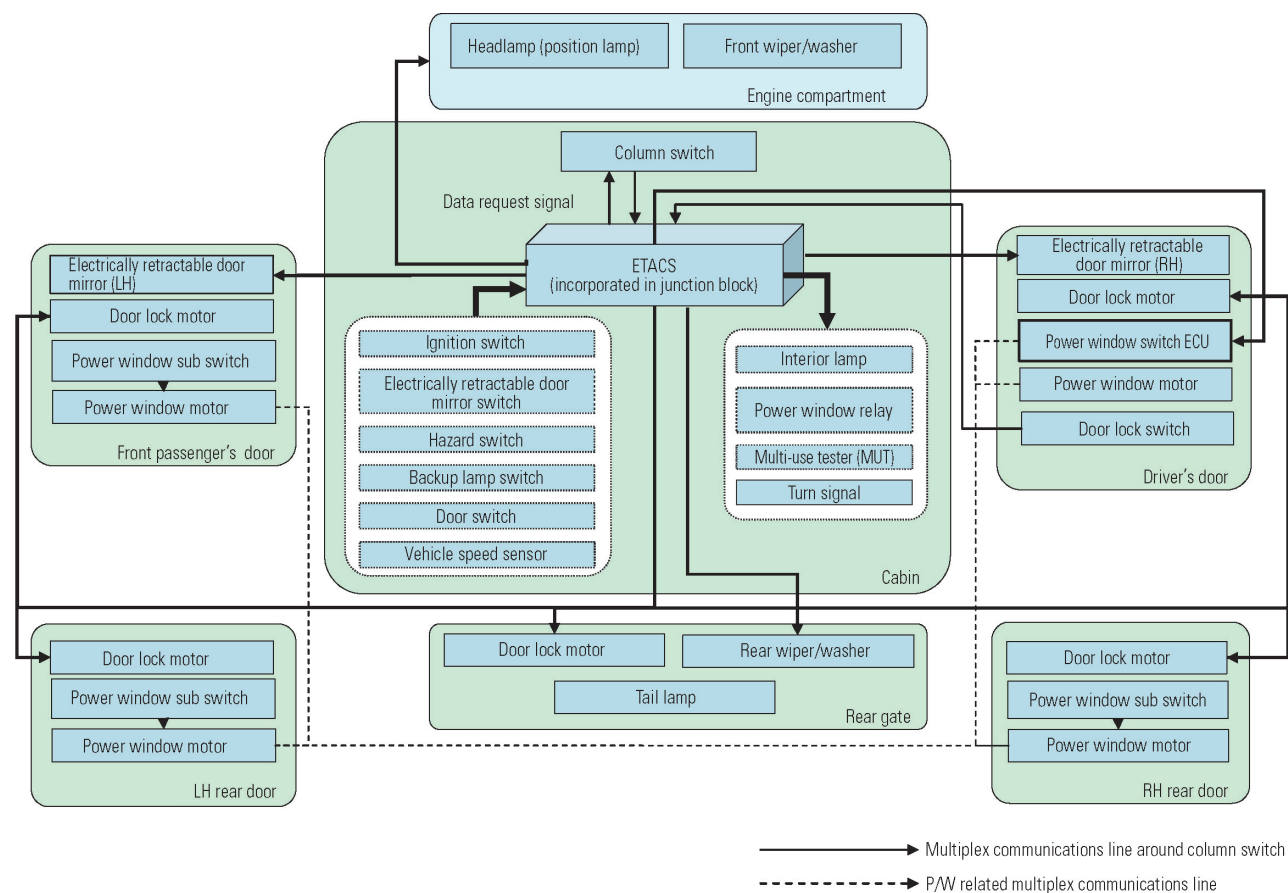


Fig. 2 Overview of system

Table 1 Communication protocol

	Item	Specification
Physical layer	Network configuration	Bus type topology
	Transmission medium	CAVS line
	Transmission speed	5 kbps
	Code type	Bus phase (Manchester Code)
	Transmission type	Single wire voltage transmission
	Maximum number of nodes	8
Data link layer	Synchronization method	Asynchronous
	Frame configuration	SOM: 1
		Data: 4 – 16 (variable length)
		CRC: 5 bits
		EOM: 1
	Error detection	CRC, frame length check

fault diagnosis tool used by dealers. Thanks to this capability, the new model can be customized to an even greater level. The 2008 model eK WAGON is called “08 eK WAGON” hereafter in this paper.

3. New functions

The 08 eK WAGON has ten new functions (Table 2) and a total of 19 functions available for vehicle cus-

tomization (Table 3), thus greatly boosting product appeal in the market. Since the MUT-III can also be used for customization, dealers can now install any of these functions easily at the customer’s request.

Broadly classified, the newly added functions consist of convenience-oriented functions, such as the comfort flasher used in the latest MMC vehicles and the electrically retractable door mirrors with remote control; safe driving functions such as the vehicle speed-

Table 2 Function comparison chart

		08 eK	Previous model eK
Warning buzzers and indicators	Backup buzzer	○	○
	Security alarm buzzer	○*	
	Ajar door alarm buzzer	○*	
	Key reminder buzzer	○	○
	Light monitor buzzer	○	○
	Customization adjustment function buzzer	○	○
	Auto-light manner function buzzer	○*	
	Turn signal buzzer	○*	
Comfort flasher		○*	
Front wiper		○	○
Rear wiper		○*	○*
Reverse-interlocked rear wiper (A/T model)		○	○
Rear wiper washer		○	○
Power window key-off timer		○*	○*
Electrically retractable door mirror key-off timer		○*	
Lighting (headlamp, tail lamp)		○	○
Headlamp auto-cut function		○*	○*
Centralized door lock	Driver's-door-only unlocking function	○*	
Key-left-in-switch prevention function		○	○
Multi-mode keyless entry system	Opening/closing of power window	○*	○*
	Deployment/retraction of electrically retractable door mirror	○*	
Dimming interior lamp		○*	○*
Answerback function of keyless entry system		○*	○*
Opening/closing of power slide door		○	○
Customization function using MUT-III		○	
Function of adjustment by special operation		○	
SWS communication	Communication with MUT-III possible	○	
	Communication with MUT-III impossible		○
Fault diagnosis related functions	Input check function	○	○
	SWS diagnosis code output	○	○
	Transmission of switch input signal status	○	
	Transmission of analog input signal status	○	
	Transmitter switch status data transmission	○	

*: customization items available

sensitive front wipers and intermittent rear wiper that can be switched for continuous operation at the single touch of the control; and anti-theft functions such as the security alarm and driver's-door-only unlocking system. Many of these new functions offer detailed settings that can be selected according to the customer's preference. The body electrical equipment/function control system of the 08 eK WAGON provides a super mini-car level functionality. The major new functions are described in the following paragraphs.

3.1 Driver's-door-only unlocking function

The driver's-door-only unlocking function refers to an additional keyless entry function that allows only the driver's door to be unlocked whereas the traditional keyless entry system unlocks all door locks simultaneously. Specifically, when the UNLOCK switch of the keyless entry transmitter is pressed once, only the dri-

ver's door is unlocked, and when pressed twice, all doors are unlocked. This function is already fitted on MCC vehicles for the North American market to meet the demand for security (to prevent entry by intruders from the passenger side when the driver is the only occupant of the vehicle). The same demand is increasing in Japan, particularly among female drivers who often use the vehicle alone, and so this function was adopted in the 08 eK WAGON. It is the first of its kind to be used in mini-cars, and is one of the most appealing features of the 08 eK WAGON (**Fig. 3**).

3.2 Security alarm function

This function gives an alarm by sounding the horn and making the hazard warning lamps flash when any of the doors (including tailgate) is opened by a method other than the keyless entry transmitter. The system includes an LED indicator inside the cabin, which con-

Table 3 Function customization chart

Equipment	Function available for customization	Setting	08 eK	Previous model eK
Keyless entry system	Signaling of door lock operation by flashing of hazard warning lamps when door is locked/unlocked using remote control switch	a. No flashing	○	○ Only settings "a" and "b" are selectable
		b. 1-time flashing for locking/2-time flashing for unlocking		
		c. 1-time flashing for locking/No flashing for unlocking		
		d. No flashing for locking/2-time flashing for unlocking		
		e. 2-time flashing for locking/1-time flashing for unlocking		
		f. 2-time flashing for locking/No flashing for unlocking		
		g. No flashing for locking/1-time flashing for unlocking		
	Control of power window and door mirror operation using remote control switch	a. Not activated	○	○ Mirror cannot be operated
		b. Power window: Opening and closing Door mirror: Deployment and retraction		
		d. Power window: Closing Door mirror: Deployment and retraction		
	Time till door is automatically locked after pressing UNLOCK switch on remote control switch	a. 30 seconds	○	×
		b. 60 seconds		
		c. 120 seconds		
		d. 180 seconds		
	Door location(s) that can be unlocked when UNLOCK switch on remote control switch is pressed once	a. All doors	○	×
		b. Only driver's door		
Door mirror	Conditions for automatic retraction and deployment of electrically retractable door mirror	a. Deployment at approx. 30 km/h	○	×
		b. Retraction and deployment interlocked with starter switch position		
		c. Retraction and deployment upon locking and unlocking of doors		
		d. No automatic retraction and deployment		
Wiper	Wiper operation after spray of washer fluid	a. Yes	○	×
		b. No		
	Rear wiper intermittent operation interval	a. 4 seconds; continuously operating mode also available	○	×
		b. 8 second; continuously operating mode also available		
		c. 16 second; continuously operating mode also available		
		d. 0 second; continuous operation only		
		e. 4 seconds		
		f. 8 seconds		
		g. 16 seconds		
Headlamp	Headlamp automatic cut-off (automatic turning off)	a. Headlamps automatically turn off	○	×
		b. Headlamps do not automatically turn off		
	Position of light switch at which headlamps can be used for illumination after getting off the vehicle	a. Functional only in headlamp-on position	○	×
		b. Functional in headlamp-on and position-lamp-on position		
Interior lighting	Time till interior light goes out after all doors and tailgate are closed (delayed turning off function)	a. On for 7.5 seconds	○ Default value "b" selectable	○ Default value is "c". "b", "c" or "g" are selectable
		b. On for 15 seconds		
		c. On for 30 seconds		
		d. On for 1 minute		
		e. On for 2 minutes		
		f. On for 3 minutes		
		g. No dimming		
Audible alarm	Security alarm activation/deactivation	a. Functional	○	×
		b. Non-functional		
	Warning by buzzer when running with door ajar	a. Buzzer sounds for set time	○	×
		b. Buzzer does not sound		
Power window	Time for which power window can be opened and closed after starter switch is turned off (timer function)	a. 0 second	○	×
		b. 30 seconds		
		c. 3 minutes		
		d. 10 minutes		
	Door window location(s) that can be opened and closed using driver's control during time set by key-off timer after starter switch is turned off	a. Can be opened and closed at all window locations	○	×
		b. Can be both opened and closed only at driver's window (can be only closed at front passenger's and rear windows)		
	Door window location(s) that can be opened and closed using driver's control with lock switch ON	a. All windows (operation of all other windows permitted)	○	×
		b. Driver's window only (operation of all other windows inhibited)		
Turn signal lamp	Three-time flashing for signaling a lane change	a. Functional	○	×
		b. Non-functional		
	Lever operation time till three-time flashing function is activated for signaling a lane change	a. Standard setting	○	×
		b. Longer setting		
	Tone(s) of buzzer that sounds intermittently while turn signal lamps are flashing	a. High- and low-pitch tones	○	×
		b. Low-pitch tone		
	Starter switch position at which turn signal lamp can operate	a. Only at ON	○	×
		b. At ON or ACC		

The shading indicates factory settings.

○: Available for customization

×: Not available for customization

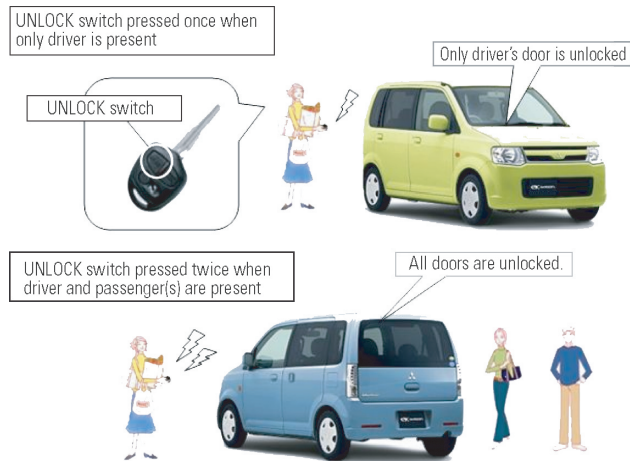


Fig. 3 Driver's door limited unlocking function

tinues to flash during parking to deter unauthorized entry.

3.3 Electrically retractable door mirrors

The electrically retractable door mirrors have three automatic operation modes, any of which is selectable. The mode (3), for example, gives the driver reassurance about safety because he/she can check that all the doors are locked.

- (1) The mirrors automatically deploy from their retracted position when the vehicle reaches a speed of 30 km/h.
- (2) The mirrors retract when the driver gets off the vehicle (turns off the ignition switch and opens the driver's door), and deploy when the driver gets on the vehicle (turns on the starter switch).
- (3) The mirrors retract when the doors are locked with the keyless entry transmitter and deploy when the doors are unlocked.

3.4 Ajar door warning

The most common type of warning given to the driver when any of the doors or tailgate is left open (or "ajar" as expressed elsewhere in this paper) is the illumination of the door indicator in the combination meter. The door warning system of the eK WAGON causes the door indicator to flash and also a buzzer to sound if the vehicle is in motion (at 8 km/h or faster) with a door ajar. These simultaneous visual and audible warnings can minimize the chance of moving off without the driver realizing that a door is open.

3.5 Comfort flasher

The comfort flasher is a function that makes the turn signal lamps flash three times consecutively when the turn signal lever is operated for a short time. As this function eliminates the need to move the lever back to the original position, it reduces the workload on the driver when changing lanes.



Fig. 4 MUT-III

4. Ease of service

By connecting the diagnosis tester MUT-III (Fig. 4) to the vehicle, the following servicing tasks can be performed.

4.1 Customization of vehicle

The previous model eK WAGON could be customized through special operation of the steering column switch but this was complicated, and there were not enough functions that could be customized to meet customers' varied preferences. For this reason, the number of functions available for customization has been substantially increased in the 08 eK WAGON and customization at the dealership using the MUT-III is now much easier.

4.2 Service data

The MUT-III can display useful diagnosis data (see Table 4) such as SWS communication line data, ETACS input data on hard wire switch ON/OFF status, and physical conversion values of ETACS processed data. This improvement helps to diagnose the 08 eK WAGON more precisely and quickly.

5. Conclusions

In recent years, vehicle electrical systems have become ever more sophisticated and complicated, and are now called "electronic platforms"⁽²⁾. Meanwhile, for the communication protocol, it has become commonplace to use a controller area network (CAN) and local interconnect network (LIN) which are the standard in the industry. In the 08 eK WAGON, which features minor changes over the previous model, the ETACS was innovated not by making extensive changes to the electronic platform but by changing mainly the internal electronic components and software, in order to greatly improve the body-related electrical functions. As a result, the new model has many additional functions that appeal to customers, such as the driver's-door-only unlocking function. The new functions also include an upgraded fault diagnosis function that is advantageous to dealers. Also, the remarkably improved reception

Table 4 Service data list

Function	Setting	Output ECU	Item name (MUT displayed)	Switch status
Wiper	INT	Steering column ECU	INT wiper SW	ON
			LO wiper SW	OFF
			HI wiper SW	OFF
			Mist wiper SW	OFF
			Front washer SW	OFF
	LO	ETACS	Ignition switch ACC	ON
			Wiper INT time	Time T
			INT wiper SW	OFF
			LO wiper SW	ON
			HI wiper SW	OFF
Lighting	LO	Steering column ECU	Mist wiper SW	OFF
			Front washer SW	OFF
	HI	ETACS		OFF
			Ignition switch IG1	ON
			HD lamp auto cut	OFF
Security alarm	Security alarm	Steering column ECU	Headlamp SW	ON
			Dimmer SW	ON
			Passing SW	OFF
Security alarm	Security alarm	ETACS	Ignition switch IG1	ON
			HD lamp auto cut	OFF
Security alarm	Security alarm	ETACS	Security alarm	ON

performance and operational response of the keyless entry system is the result of using the latest electronic components. We will continue with research and development to create innovative body electric system capabilities that outperform those of our competitors in the mini-car sector.

Finally, we sincerely thank OMRON Co., Ltd. and all others concerned for their assistance in the development process.

References

(1) Naoki Kawashima et al.: Multiplex Communication System for Column Switch and Instrument Panel Switches, Mitsubishi Motors Technical Review, No. 10, 1998

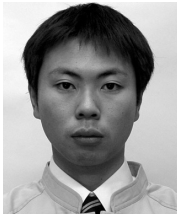
(2) Hiroki Fukatsu et al.: Development of a Next Generation Electronics Platform, Mitsubishi Motors Technical Review, No. 18, 2006



Naoki KAWASHIMA



Toshihide TANAKA



Masashi OGINO



Shuuhei ISHIKAWA

Development of MITSUBISHI POWER SOUND SYSTEM

Atsushi GOMI* Masayuki MIYATA* Yasuhiro SAKAMOTO*

Abstract

Mitsubishi Motors Corporation (MMC) developed a premium sound system called the MITSUBISHI POWER SOUND SYSTEM for the short-body PAJERO and the special editions of Europe-specification L200 (Japan name: TRITON). In the design of this system, MMC placed top priority on sound quality at mid-range and high frequencies. To avoid sacrificing space utility, MMC did not include a subwoofer in the system. However, it realized high-quality sound by means of vehicle-body revisions and detailed tuning. With the speakers, MMC took full advantage of its technological strengths and know-how to adopt speaker technologies that are the first of their kind to be used in automobiles.

Key words: Sound, Acoustics, Audio System

1. Introduction

In recent years, MMC's premium sound systems have been highly praised in the market for their superb quality. In line with this, there has been a growing need to install the systems on the PAJERO SHORT and the L200 ("TRITON" in Japan), where these options have not been available. However, their body shapes have geometrical restrictions without sufficient space for the subwoofer box, making it difficult to attain the target high sound quality. To solve this problem, MMC has developed an original audio system for these models that produces high-quality sound even without a subwoofer: the MITSUBISHI POWER SOUND SYSTEM (Fig. 1). This paper describes the components, product concepts and technologies of the system.

2. System components

Fig. 2 shows the layout of system components on the PAJERO SHORT and the L200. Both systems are based on an "8 speakers at 6 positions" configuration. These speakers consist of the following.

- Bottom of the A pillars: Aluminum hard dome tweeter with ridge line (high frequency range reproduction)
- At the front doors: Metallized hybrid polypropylene (PP) diaphragm midbass speaker (midbass frequency range reproduction)
- On the sides of the rear seats: Metallized hybrid polypropylene diaphragm 2-way coaxial speaker (full frequency range reproduction)

The system uses a power amplifier with a total output of 420 W (Max) that sends clear, powerful signals with little distortion to the speakers (while a 140 W



Fig. 1 MITSUBISHI POWER SOUND SYSTEM components

amplifier is built into the head unit in the standard audio system). To ensure high-quality sound reproduction, the digital signal processor (DSP) built into the power amplifier optimizes the output signals to suit the acoustic characteristics of the speakers and cabin.

3. Concepts and targets of MITSUBISHI POWER SOUND SYSTEM development project

As noted in the Introduction, some vehicles have geometrical restrictions due to their body shape which makes it difficult to install a large subwoofer box. On the other hand, a small subwoofer box that fits into the available space compromises the performance of the subwoofer. The MITSUBISHI POWER SOUND SYSTEM was therefore developed based on the concept of delivering high-quality sound without a subwoofer. Concretely, high priority is given to the quality of the mid frequency range and high frequency range sounds, but without abandoning the reproduction of high-quality deep bass.

* Electronics Engineering Dept., Development Engineering Office

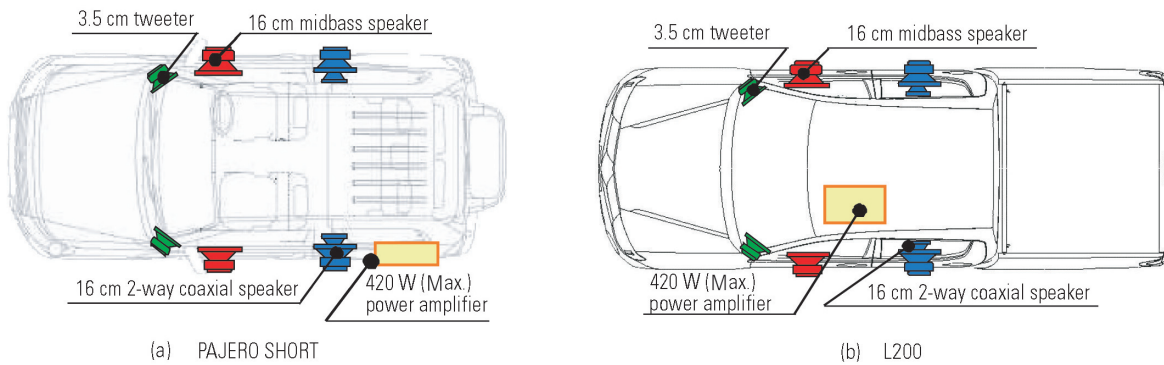


Fig. 2 MITSUBISHI POWER SOUND SYSTEM layout

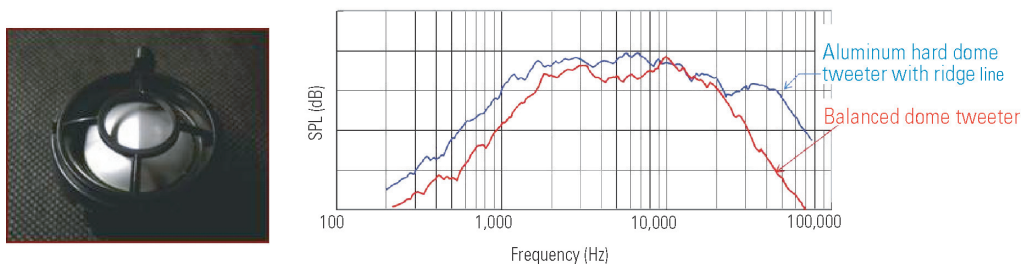


Fig. 3 Aluminum hard dome tweeter with ridge line, and comparison of its frequency characteristics with those of balanced dome tweeter

To achieve the best quality in the mid frequency range and high frequency range, the following areas were explored:

- Performance improvement of each speaker
- DSP sound tuning to make the system best match the vehicle

As a result, a high-quality sound system that satisfies the target standard was developed.

4. Technical features

4.1 The world's first aluminum hard dome tweeter with ridge line for vehicles

To improve the sound quality, the first task is to improve the performance of the speakers, so we first carefully reviewed the high frequency range speaker as described below.

To achieve high-quality sound reproduction in the high frequency range, a hard dome tweeter with higher high-end frequency limit has been adopted. **Fig. 3** compares the frequency characteristics of the aluminum hard dome tweeter with ridge line of the MITSUBISHI POWER SOUND SYSTEM with those of the balanced dome tweeter of the standard audio system. As clearly indicated by the graphs (details omitted for confidential reasons), the hard dome tweeter has a much higher high-end frequency limit than the balanced dome tweeter. This makes it possible to achieve highly realistic reproduction of the original sound in the high frequen-

cy range. The hard dome tweeter also has a lower low-end frequency limit than the balanced dome tweeter. As a result, the vocal image can be positioned at a higher location, which is a benefit for the sound system configuration. The hard dome tweeter has a straight ridge running across the center of the diaphragm; this ridge is designed to stabilize secondary vibration caused by the diaphragm, as well as to uniformly spread the vibration of the diaphragm across itself. With this method, vibration peaks can be dampened, preventing outstanding peaks and dips from emerging in the frequency characteristics and achieving clear high-frequency sound with very little distortion.

To ensure the hard dome tweeter achieves optimum performance, thin perforated metal with a high aperture ratio is used for the tweeter garnish (**Fig. 4**). The aperture ratio of the speaker garnish substantially affects the quality of sound of the speaker; with low-aperture-ratio garnish, even a sophisticated speaker can produce only mediocre performance. This was fully taken into consideration when designing the tweeter garnish of this system.

Through these techniques, our target for high-quality clear reproduction of the original sound has been achieved.

4.2 Metallized hybrid polypropylene diaphragm speaker

This section describes the development of high-quality reproduction of the mid frequency range.

High-quality reproduction of the mid frequency



Fig. 4 Tweeter garnish (L200)

range requires a stiff cone diaphragm, so we chose a highly-stiff concave center cap made of polypropylene containing reinforced mica. This increased the rigidity of the cone diaphragm to improve the speed of transmission of sound across the diaphragm for reproducing the midbass range with presence. To further improve the sound transmission speed, a titanium coating is sputtered onto the diaphragm surface, which makes sound travel faster onto the surface, improving the transient property and offering more realistic reproduction of the midbass range.

As previously described, this MITSUBISHI POWER SOUND SYSTEM does not include a subwoofer, so we also needed to develop a 16 cm speaker which can reproduce the deep bass range. To achieve this, mica-containing polypropylene, which is the same material as used for the center cap, was chosen for the diaphragm. Polypropylene is very light and offers excellent bass response while the inclusion of mica increases its stiffness, leading to bass reproduction with little distortion. The diaphragm edge is made of high-linearity butyl rubber to produce a deep and rich bass. A large ferrite magnet is used for the magnetic circuit. To reproduce sharp rich bass and deep bass, the voice coil must be located in a strong magnetic field, and this speaker embodies all these features (Fig. 5).

With these techniques, the MITSUBISHI POWER SOUND SYSTEM achieves high-quality reproduction of the mid range together with a sharp, tight bass.

4.3 DSP sound tuning to match the vehicle body

Even a high-performance speaker, when installed in the unique environment of a vehicle, may generate outputs with unintended frequency peaks and dips due to the body shape, body rigidity, aperture ratio of garnish and other elements. Such sounds cannot be considered "high-quality sound".

To lessen the external impact and achieve the intended sound quality, DSP sound tuning was fully used in developing the MITSUBISHI POWER SOUND SYSTEM. This method is built on the know-how and expertise of Mitsubishi Motors developed over the years. Attention has been paid to every detail to ensure that the speakers achieve their best performance. This is the way we "craft" our sound systems.

As previously described, in developing the MI-

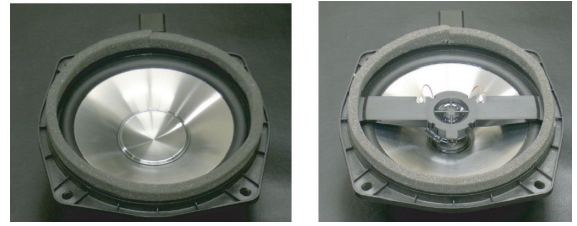


Fig. 5 Metallized hybrid polypropylene diaphragm speaker

TSUBISHI POWER SOUND SYSTEM, we put top priority and effort on reproducing high and mid frequency ranges.

As part of the sound tuning trial, speakers installed on a PAJERO SHORT and the acoustic characteristics of the cabin were measured without DSP control (flat output), and extreme peaks were identified at around 200 Hz caused by the characteristics of the trims and body (Fig. 6). The resulting sound was dark and dull across the entire range. After removing these peaks with DSP tuning, the sound became well unified and balanced (Fig. 7).

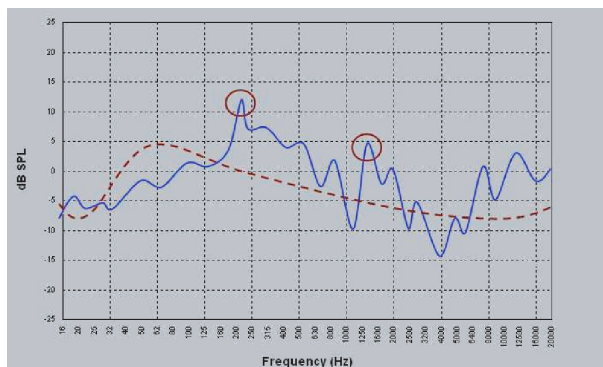
As this system does not have subwoofers, reproduction of deep bass should be taken into consideration. Deep bass is produced by using the interference between output signals from the left and right speakers. By programming the signal delays for the speakers, the timing for signal interference at the listener's location was measured to amplify deep bass.

With the DSP tuning method, which is intended to turn a cabin into an ideal acoustic space, the MITSUBISHI POWER SOUND SYSTEM delivers high-quality sound reproduction.

5. Conclusion

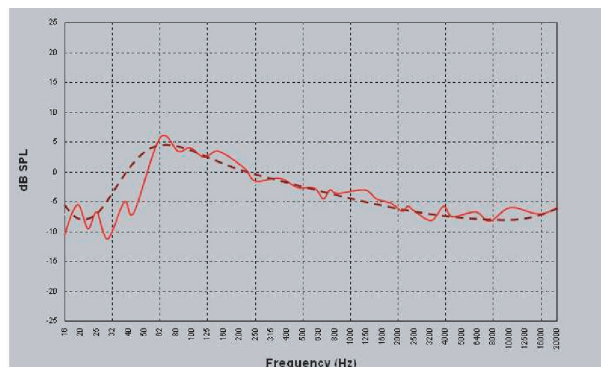
By developing high-performance speakers and optimizing the output characteristics of the amplifier to fit the speaker characteristics and cabin acoustics, we have created a high-quality audio system for vehicles in which a subwoofer cannot be mounted.

With the expertise gained during this project, the authors will try to expand these high-performance speakers to other vehicle models to add more value to the on-board audio system.



Blue solid line: Cabin acoustic characteristics before tuning
Brown dotted line: Ideal cabin acoustic characteristics

Fig. 6 Cabin acoustic characteristics before tuning

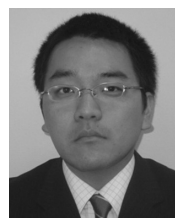


Red solid line: Cabin acoustic characteristics after tuning
Brown dotted line: Ideal cabin acoustic characteristics

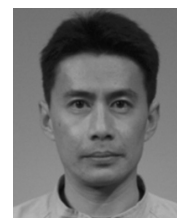
Fig. 7 Cabin acoustic characteristics after tuning



Atsushi GOMI



Masayuki MIYATA



Yasuhiro SAKAMOTO

Usability Evaluation in Product Development

Satoshi HORIE* Arihiro ISOMURA* Yoshihiro MURASE*
Tomiji OHWADA* Yudai YATABE* Kenji KISHIUE*
Singo IRIKATA*

Abstract

Usability evaluation is not only a means of evaluating a product's ease of use; it also serves as a means of determining whether the product is appealing, as a means of determining whether the product meets users' needs, and as a means of finding potential user needs. One method for evaluating product usability is a usability test, whereby users evaluate the product to determine whether it satisfies the development goals and, if it does not, the points that need to be improved⁽¹⁾. Using a usability test as an example, this paper describes some of Mitsubishi Motors Corporation (MMC)'s development processes and evaluation indices.

Key words: Usability, Testing, Human-Machine-Interface, Driver Behavior

1. Introduction

The term "usability", which is the theme of this paper, refers to "fitness for use" or "quality in use", although it is generally used to mean "ease of use" (Fig. 1).

In the Japanese automotive industry up to the 1980s, the word "quality" most often implied reliability or durability. From the 1990s, the principal meaning of this word has shifted to more sales-oriented concepts such as customer satisfaction and attractiveness. In other words, higher quality has become synonymous with greater customer satisfaction, and fitness for use or quality in use is now the most important factor when considering quality in product development. This transition in meaning of the word "quality" implies that the factors of customer satisfaction vary with time and place. This is why firms must constantly evaluate usability to identify what customers need before they can improve the level of quality.

2. Usability definition

ISO 9241-11 defines usability as "Extent to which a product can be used by specified users to achieve specified goals with effectiveness, efficiency and satisfaction in a specified context of use"⁽³⁾.

- ① Effectiveness: Accuracy and completeness with which users achieve goals.
- ② Efficiency: Resources expended in relation to the accuracy and completeness with which users achieve goals.
- ③ Satisfaction: Being free from discomfort, and positive attitudes towards use of the product.

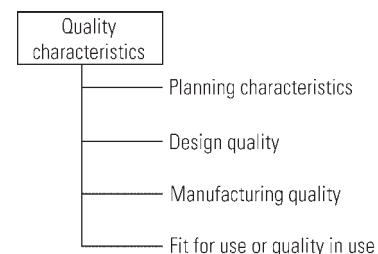


Fig. 1 Quality characteristics⁽²⁾

3. Usability evaluation

3.1 What is the usability evaluation?

To achieve user satisfaction, it is crucial to guarantee the quality in use of a product in addition to the quality of the functional and performance characteristics of the product. "User-centered design" is the key to guaranteeing the quality in use of the product. The quality of a product incorporating user-centered design is evaluated by the "usability evaluation" (Fig. 2)⁽⁴⁾.

3.2 Usability evaluation techniques

Broadly classified, there are two types of usability evaluation technique: the expert evaluation and the user evaluation.

In the expert evaluation conducted in MMC, the usability evaluation experts use ergonomics-based evaluation indices. In the user evaluation, selected users are asked to actually use the product under pre-established conditions and their actions are observed to evaluate the usability of the product. This type of usability evaluation in which users participate is called the "user test" and is useful because it can provide feedback that precisely reflects changes taking place in the marketplace (Fig. 3).

* Testing Control Dept., Development Engineering Office

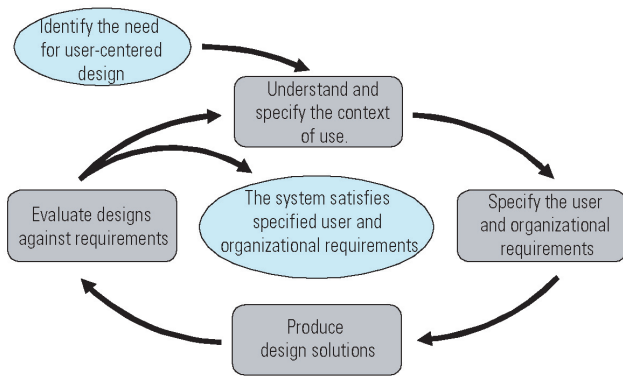


Fig. 2 User-centered design process

3.3 Evaluation subjects

When evaluating the usability of a vehicle, there are two major categories of items to be evaluated. One is the vehicle's individual components and the other is the vehicle as a whole.

4. Usability test⁽⁵⁾⁽⁶⁾

This section discusses the typical flow of the usability test and the tasks of the staff in charge.

4.1 Obtaining relevant information from development personnel

The first step is to gather the relevant information from the staff in charge of developing a specific product. This information should include the following: what is the product to be evaluated; what is the target of the product development; what are the major applications of the product; what are the intended types of user; and what are the details to be identified by the usability evaluation.

4.2 Preparations for test

The next step is to select users to participate in the test, decide the contents (tasks) of the test, set up the necessary test equipment and environment, and draw up a test schedule based on the information obtained from the development personnel. Deciding the tasks is particularly important; to obtain worthwhile results, the tasks must reflect the situations in which users use the product in daily life.

4.3 Execution of the test

The usability test staff then introduce each participant user to the test and ask him/her to perform the pre-determined tasks. They observe what the user does together with the development personnel to evaluate the usability of the product. To identify the reasons for each user's action, the test staff give guidance to the user on how to think aloud method (which means verbalizing everything that comes to mind while performing a task) before the user starts the first task. The persons observing the user's actions can then understand why the user does a particular action. The test staff

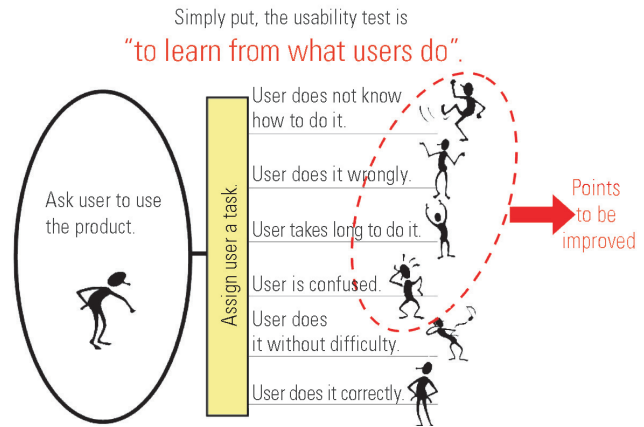


Fig. 3 Image of usability test

should then consider the test environment to make the user feel at ease.

4.4 Analysis and evaluation

The usability evaluation examines the effectiveness, efficiency and satisfaction aspects as defined for usability. The test results are analyzed to judge whether each user could achieve a task, whether the user took a long time to complete the task, and whether the user was irritated in performing the task.

MMC uses the scheme shown in Fig. 4 for the usability evaluation, in which an evaluation score is assigned for the effectiveness, efficiency and satisfaction and each of them is weighted with a coefficient specific to the characteristic to obtain a final evaluation rating.

The evaluation results are fed back to the development department, which then makes necessary improvements to the product, and then the improved product is re-evaluated. This cycle is repeated to raise the level of completeness of the product in a process of iterative development.

5. Example of usability test

The following is an example of the usability test conducted on the Multi-around Monitor system, which is incorporated in the DELICA D:5 that MMC released in January 2007 (Fig. 5)⁽⁷⁾.

5.1 Component features and development target

The Multi-around Monitor system was developed with the following three targets⁽⁵⁾.

- Displaying images covering virtually all main blind spots at the front, at the rear, and on the side opposite the driver.
- Merging two different images for display on the same screen to avoid switching between screens.
- Providing an auto-display mode that automatically selects the camera whose image is to be displayed according to conditions, without having to press the camera switch.

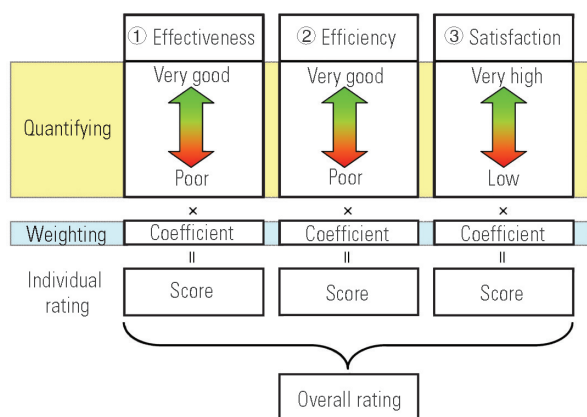


Fig. 4 Method of calculating evaluation score



Fig. 5 Usability test in progress

5.2 Test purpose

The usability evaluation was necessary to determine the product's specifications at the design stage. Situations for the actual use of the product were prepared, under which the test participant users are asked to use the product. The test results were evaluated, and the resultant usability rating was used to establish specifications that would raise the rating.

5.3 Evaluation method

A total of 26 male and female users were selected as test subjects. They were in their twenties to fifties because a wide age range was desirable for evaluating the product. About one-third of the test subjects were selected from users who usually used a rearward view camera or other driver view assist systems.

Subjective evaluations and action measurements were conducted for two prototype products and the final specification product, including items such as the display screen configuration, image display restrictions, method of setting the auto-display mode, and location of the switches for selecting the images from individual cameras and screens (hereafter, "camera switches").

The tests were conducted on a proving ground where ordinary road environments were simulated

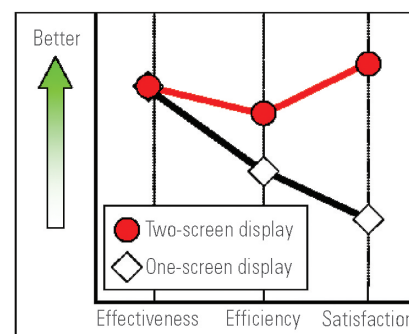


Fig. 6 Evaluation result for two-screen display

under different conditions, i.e., weather conditions of fair, cloudy, and rainy, during the daytime, twilight, and nighttime.

The following four tasks were assigned considering the situations in which general drivers most often wanted to view blind spots:

- (1) Reversing the vehicle into and out of the garage
- (2) Forwarding the vehicle into and out of the garage
- (3) Turning in the opposite direction to (or the same direction as) the driver at an intersection with poor visibility
- (4) Pulling over to the side opposite to the driver

5.4 Evaluation results

As an example of the usability evaluation results of the test, Fig. 6 shows the evaluation of the screen configuration. The two-screen configuration is more highly rated than the one-screen display, for both efficiency and satisfaction.

As to the effectiveness, there is almost no difference in rating between the two types of screen configuration, because only the extent of task completion was evaluated and the users could achieve the task successfully with both types of display.

With regard to efficiency, the two-screen display was rated higher, because the users could achieve the task more quickly without having to change the screens. In contrast, with the one-screen display, the users had to select the screen and then perform the task while checking the screen.

With regard to satisfaction, the two-screen display was rated much higher than the one-screen display. Reasons included: "no need to change the screen" and "two-screen display conveniently shows two different images".

Fig. 7 shows another example of the evaluation results. As is clear, the camera switch layout of Prototype 1 was rated low in terms of effectiveness, efficiency and satisfaction. The camera switch location was then reviewed and improved; this increased the evaluation rating in both effectiveness and efficiency, and eventually resulted in a higher satisfaction rating.

As these examples show, the usability level of each component factor (item) of a product is rated by observing and measuring actions, as well as by subjective rating. The problem areas identified by the usability eval-

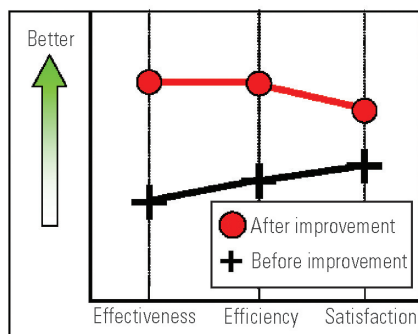


Fig. 7 Evaluation result for camera switch location

uation are then improved in the development process to make the product better suit the users' needs.

The Multi-around Monitor system described above was developed through the processes of "Prototype 1 → Prototype 2 → Final specification product", in a repeated cycle of evaluation and improvement. The result is a product with high usability (Fig. 8).

6. Conclusion

The power slide door was a very attractive feature five years ago, but is now commonplace. Market trends are changing rapidly. Just as young people are becoming less interested in passenger cars, customers' views on vehicles and their roles are changing today. Auto manufacturers need to be able to promptly and precisely detect such changes in the marketplace.

The usability test, which evaluates a product by users actually using it, is useful not only for identifying market needs but also eliciting potential needs in the marketplace. When applied to a new type of product, the test can assess how well the product matches market needs, and suggest improvements.

MMC will continue to use this test approach to develop attractive products that meet the needs of the future market.

References

- (1) Jakob Nielsen: Tokyo Denki University Press, Usability Engineering, 2006
- (2) Masaaki Kurosu: "Usability Testing", Kyoritsu Shuppan, 2004
- (3) ISO 9241-11: 1998 Ergonomic requirements for office work with VDTs – Part 11: Guidance on usability
- (4) ISO 13407: 1999 Human-centred design processes for interactive systems

Items evaluated	Prototype 1	Prototype 2	Final specification product
Display screen configuration	☹☹☹	☹☹☹☹	☹☹☹☹☹
Image display restrictions	☹☹	☹☹☹	☹☹☹☹
Camera switch location	☹☹	☹☹☹☹☹	☹☹☹☹☹☹
Assist lines	☹☹	☹☹☹	☹☹☹☹☹
Image quality	☹☹	☹☹☹☹	☹☹☹☹☹
Auto-display mode	☹	☹☹	☹☹☹☹

Fig. 8 Improved results for individual items

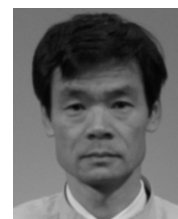
- (5) Research Institute of Human Engineering for Quality Life: "Workshop: Human Engineering for Quality Life", Vol. 3, Maruzen, 2005
- (6) Tetsuya Tarumoto: "Usability Engineering", Ohmsha, 2005
- (7) Keiji Ueminami, Kenji Hayase, Eiji Sato: "Multi-around Monitor system", Mitsubishi Motors Technical Review, No. 19, 2007



Satoshi HORIE



Arihiro ISOMURA



Yoshihiro MURASE



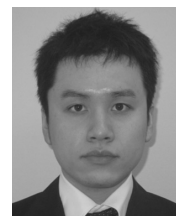
Tomiji OHWADA



Yudai YATABE



Kenji KISHIUE



Singo IRIKATA

Influence of Work Hardening during Metal Forming on Crashworthiness Simulation

Katsuhiko TAKASHINA* Kazuhiro UEDA** Takeo OHTSUKA**

Abstract

To improve the accuracy of crashworthiness simulation, it is important to consider the effects of metal forming. However, this approach was difficult in practice since analyzing the stamping simulation in detail requires much work. This paper describes the influence of residual strain, work hardening and material thickness changes resulting from the stamping process on the crashworthiness simulation. In almost all impact load cases, the results show that deformation is reduced by the work hardening effects. These results are verified by actual experimental data.

Key words: *Crashworthiness, CAE, Forming*

1. Introduction

To improve the accuracy of crashworthiness simulation, various approaches have been performed. These approaches have included modeling of detailed part shape, application of modeling to more parts, and re-determination of the properties of materials. This paper studied the influence of residual strain and change in metal thickness during the stamping process on the crashworthiness simulation, in order to improve the accuracy.

2. A method to apply a stamping result to crashworthiness simulation model

One effective method to include the influence of residual strain and metal thickness changes during metal forming into crashworthiness simulation is to conduct stamping simulations using actual dies (called "detailed stamping simulation") and to apply the results to the crashworthiness simulation model (Fig. 1). However, this type of simulation is difficult to apply in practice, particularly that it requires almost the same amount of calculation time as needed for crashworthiness simulation at every part. Furthermore, the process of providing the stamping results to the crashworthiness simulation model is very complicated. To solve these difficulties, an inverse method⁽¹⁾⁽²⁾ can be applied to an implicit finite element model ("FE") to estimate the developed shape of the blank from an FE that represents the shape of the finished product, and to estimate the residual strain and metal thickness distributions (called the "simplified stamping simulation") (Fig. 2). By this method, the stamping results on hundreds of parts are provided to the crashworthiness simulation model without modification in about one hour. However, it is necessary grasping the simulation accuracy by comparing the results of the detailed stamping

simulation, because the method is a simplified one.

3. Accuracy of the simplified stamping simulation

To grasp the accuracy of the simplified stamping simulation, its results are compared with those of the detailed stamping simulation in terms of the residual strain and metal thickness distribution of a cowl top panel, which is a drawn panel part (Fig. 3 and Fig. 4).

Although the residual strain obtained from the simplified stamping simulation is smaller than that from the detailed stamping simulation, the distributions are similar. The detailed stamping simulation shows relatively large strain in the peripheral areas of the panel, but these areas are cut off after stamping, so these strains are not included in the crashworthiness simulation model. Also, the two results show almost the same metal thickness distributions. The main reason why the simplified simulation estimated smaller residual strain than the detailed simulation is considered to be the following: On an actual draw die, the blank is held constrained at its peripheral areas, which causes a tensile force to be generated there during metal forming (Fig. 5), but this constraint condition is not considered in the simplified simulation.

4. Crashworthiness simulation providing residual strain estimated by stamping simulation

4.1 Impact load cases and parts subjected to stamping simulation

The simplified stamping simulation is carried out for the multiple impact load cases. The parts chosen for the simulation are those most likely to have an influence on vehicle crashworthiness. Table 1 shows the number of parts subjected to the stamping simulation and the

* Digital Engineering Dept., Development Engineering Office

** Stamping & Plastic Engineering Dept.,
Production Engineering Office

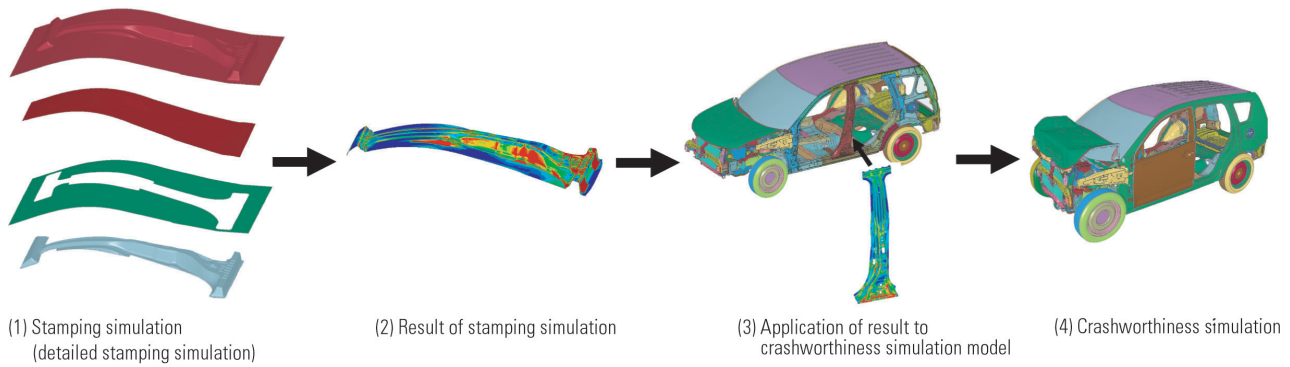


Fig. 1 Conventional process

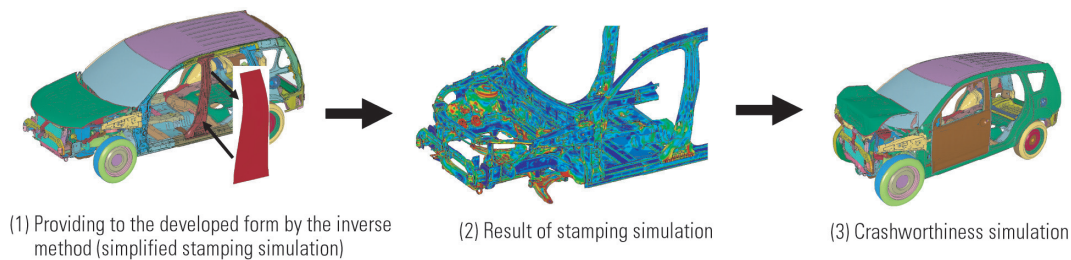


Fig. 2 Newly adopted process

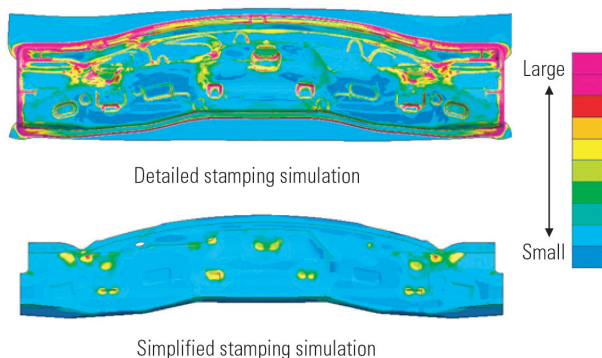


Fig. 3 Residual strain distribution

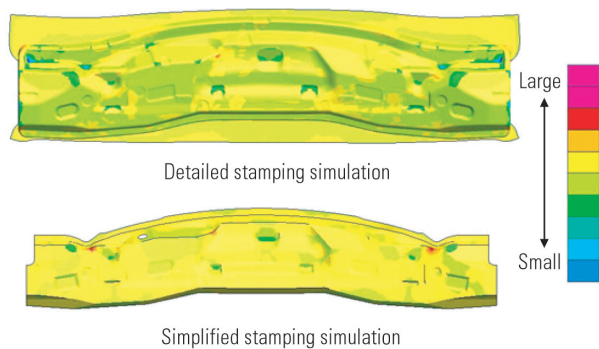


Fig. 4 Sheet thickness distribution

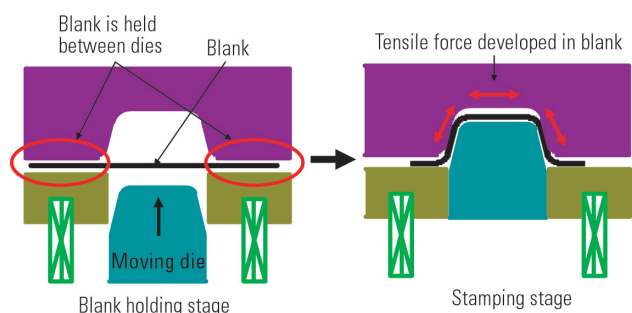


Fig. 5 Structure of draw die

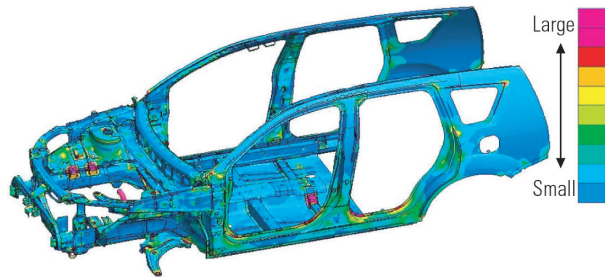
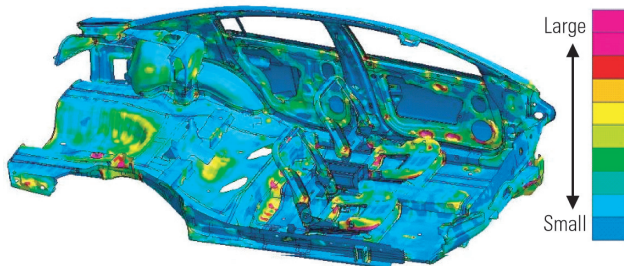
time (in hours) taken for the simulation. Incidentally, the detailed stamping simulation takes roughly 10 hours per a part. Examples of the residual strain distribution derived from the simplified stamping simulation are shown in Fig. 6 and Fig. 7. These results are provided to the crashworthiness simulation model.

4.2 Results of crashworthiness simulation

In the impact load cases where deformation extends to a large number of parts (cases ①, ② and ③ in Table 2), the application of the stamping results allows the hardening to be included in the estimation for the areas subjected to plastic deformation. The deformation of a vehicle body is reduced to a similar level to actual experimental results. On the other hand, in those impact load cases where deformation occurs only locally (cases ④ and ⑤ in Table 2), the work hardening effect does not reach the areas subjected to plastic deforma-

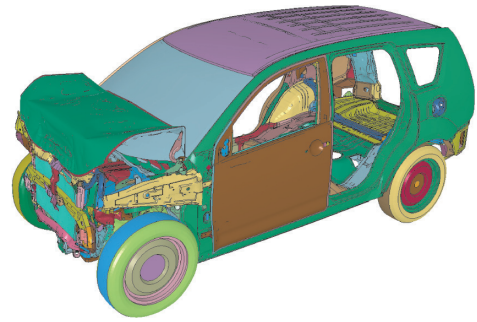
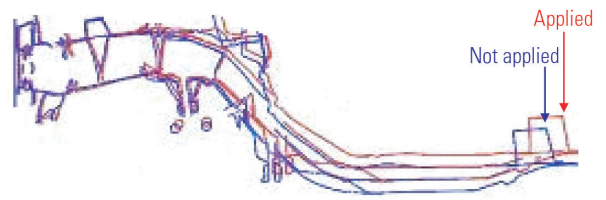
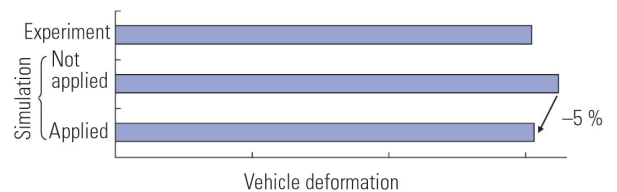
Table 1 Load cases

	Impact load case	Number of analyzed parts	Calculation time by simplified stamping simulation
①	35 mph frontal impact	Approx. 250	Approx. 1.0 Hr
②	18 mph side pole impact	Approx. 250	Approx. 1.0 Hr
③	50 mph rear offset impact	Approx. 350	Approx. 2.0 Hr
④	Pedestrian head impact	Approx. 130	Approx. 0.5 Hr
⑤	5 mph bumper impact	Approx. 50	Approx. 0.2 Hr

**Fig. 6 Residual strain distribution (example for parts in frontal impact simulation)****Fig. 7 Residual strain distribution (example for parts in side impact simulation)****Table 2 Influence on crashworthiness simulation**

	Impact load case	Extent of deformation	Accuracy
①	35 mph frontal impact	Reduced	Improved
②	18 mph side pole impact	↑	↑
③	50 mph rear offset impact	↑	↑
④	Pedestrian head impact	No change	No influence
⑤	5 mph bumper impact	↑	↑

tion, and thus there is little difference (approximately 2 %) in body deformation between the simulation and experimental results. Comparison of the results between the simulation and the experimental are shown for the load cases of frontal impact (Fig. 8 to Fig. 11), side impact (Fig. 12 to Fig. 14) and pedestrian head impact (Fig. 15 and Fig. 16).

**Fig. 8 Vehicle deformation (① frontal impact)****Fig. 9 Side member deformation (① frontal impact)****Fig. 10 Comparison of extent of vehicle deformation (① frontal impact)****Fig. 11 Comparison of extent of rearward movement of dash panel (① frontal impact)**

5. Conclusion

By applying the residual strain and metal thickness distribution change derived from the simplified stamping simulation to the crashworthiness simulation, the deformation is reduced to a similar level to actual experimental results in almost all impact load cases. This reduction in deformation is considered to be due mainly to the work hardening during the stamping process (Fig. 17), and its influence overcomes the influence of the reduction in metal thickness. This approach takes only a few hours even when applied to hundreds of

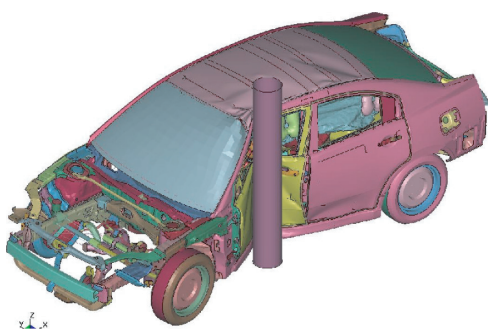


Fig. 12 Vehicle deformation (② side impact)

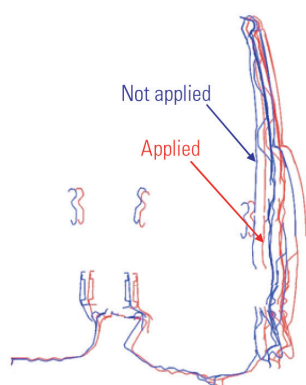


Fig. 13 Center pillar deformation (② side impact)

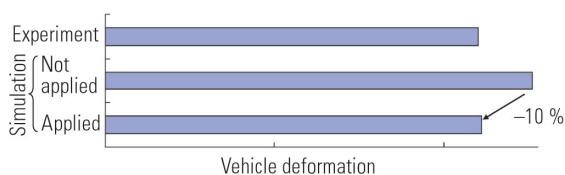


Fig. 14 Comparison of extent of vehicle deformation (② side impact)

parts, and requires no detailed data for metal forming. Therefore, this approach enables the metal formability to be included in the crashworthiness simulation, thus improving the accuracy of the results. However, the simplified simulation method tends to estimate less residual strain than the detailed stamping simulation. It must be improved in the future.

Finally, we sincerely thank JRI Solutions Limited and all concerned for their assistance throughout the study.

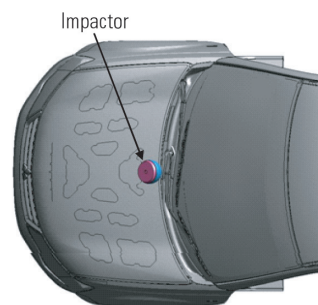


Fig. 15 Impact location (④ pedestrian head impact)

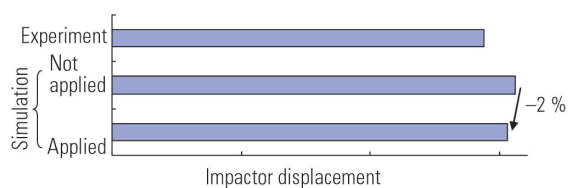


Fig. 16 Impactor displacement (④ pedestrian head impact)

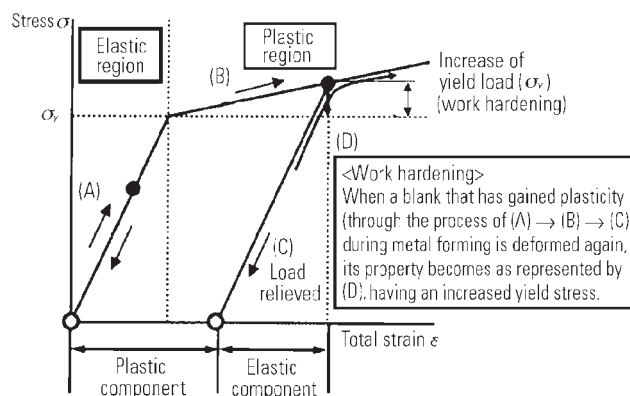


Fig. 17 Concept of work hardening process during metal forming

References

- (1) JRI Solutions, Ltd.: HYCRASH Ver1.1 (rev061214) USER'S Manual, 2006
- (2) Yasuyoshi. Umezu, Yuko. Watanabe, Ninshu. Ma: Development of JSTAMP-Works/NV and HYSTAMP for Multipurpose Multistage Sheet Metal Forming Simulation, 2005



Katsuhiko TAKASHINA



Kazuhiro UEDA



Takeo OHTSUKA

Design Concept for GALANT FORTIS

Hiroaki MATSUNOBU* Kenichi NODA**
Kei HAMADA** Chigusa YASUI**



Abstract

Mitsubishi Motors Corporation (MMC) developed the GALANT FORTIS to be its flagship sedan in the domestic market and a strategic model for rebuilding the Mitsubishi brand in the highly competitive C-segment in overseas markets. Recognizing a need to accommodate global demands with the GALANT FORTIS, MMC studied market attributes and customer preferences around the world and took them into account in its pursuit of an instantly recognizable design identity, a combination of comfort and functionality, and an overall freshness in the sedan experience. MMC developed the LANCER EVOLUTION X in parallel with the GALANT FORTIS, so it was able to implement efficient development processes involving common use of components, differentiation of the two models' designs from each other, and tests. This paper gives an overview of the design concept for the GALANT FORTIS.

Key words: *Development, Concept, Styling*

1. Introduction

In the development of the GALANT FORTIS, the simultaneous development of the LANCER EVOLUTION X, which is based on the GALANT FORTIS, is an important factor for describing the design concept. This is because the LANCER EVOLUTION is symbolic of the Mitsubishi sports DNA, and the inclusion of the GALANT FORTIS in this lineage was indispensable for creating a brand strategy for the GALANT FORTIS as a strategic world vehicle. Also, based on the validation of successful cases of Mitsubishi Motors' sedans up to now, it is considered that the progressive adoption of the inverted slant nose is an important point which was taken up seriously from the viewpoint of effective utilization of traditional design.

On the other hand, regarding the platform which constitutes the base of the vehicle, pedestrian protection measures were incorporated. Comfort, ease of access, and maneuverability (due to the high eye point) were also enhanced. As a result, the vehicle's height was high for a sedan, and difficulties were experienced

in expressing sporty styling. Despite this, the vehicle had both adequate comfort and unique styling as a strategic world vehicle, which are product value points that enable this vehicle to be promoted on the market.

2. Design concept

The establishment of a high quality sporty sedan design that holds its own in the world – this is the design concept pursued during the development of the GALANT FORTIS. Development of this vehicle was aimed at the realization of Mitsubishi-like body styling which is descended from the LANCER EVOLUTION, and is also a high quality design that charms customers throughout the world while being based on a wide body which has been adapted for the global market.

3. Exterior design

There are three themes concerning the exterior design. The first is the simultaneous realization of comfort & safety and sporty design that enables this vehicle

* Design Dept., Design Office

** Design Promotion Dept., Design Office

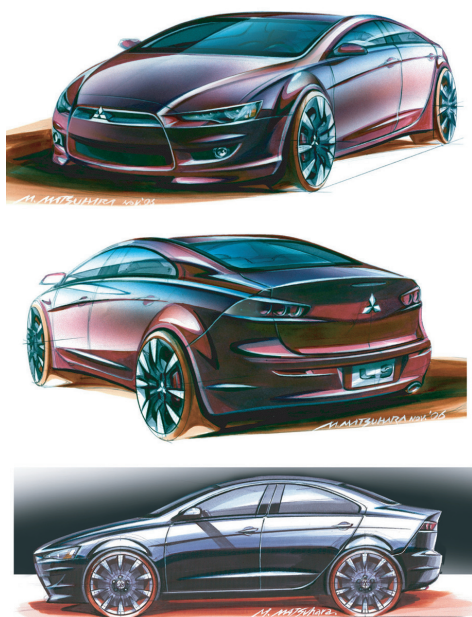


Fig. 1 Exterior image sketches

to sell on the world markets. The second is the establishment of a new generation front face design which is the starting point of the construction of the Mitsubishi sedan brand. The third is the pursuit of the creation of high quality and fastidious design beauty worthy of a sedan.

Design development was carried out aiming at the realization of these themes which are demanded in a new generation worldwide sedan (Fig. 1).

3.1 Simultaneous realization of comfort & safety and sporty design

It was considered that a "sedan" is the best model, of all the current vehicles, in terms of transporting its occupants with the greatest degree of comfort. Accordingly, a sporty styling that was nurtured through successive Mitsubishi sedans was pursued while a roomy interior with an overall height of 1,490 mm was utilized to the full.

The adoption of 18-inch diameter radial wheels with large diameter tires, which are the largest for this class of vehicle and emphasize excellent driving performance and the massive fender form which envelops each wheel, contribute to the optimization of the belt-line position, resulting in the simultaneous realization of a lower body which imparts a sense of ease and provides adequate interior space and an airy, slim cabin.

The unfettered long nose shape which has an appropriate degree of roundness, and also the smooth roof line and the sharp short rear deck style make for a vibrant and clean-cut sedan form and also contribute to high aerodynamic performance (Fig. 2). This exterior design also serves to promote the good lineage of the GALANT FORTIS as the base vehicle of the LANCER EVOLUTION X.

The front and rear of the sides of the vehicle were narrowed down, and the overhang of the fenders was



Fig. 2 Side proportion



Fig. 3 Sporty stance

Fig. 4 COLT
GALANTFig. 5 GALANT
(1989)Fig. 6 GALANT
(1996)

emphasized, aiming at a three-dimensional shape that evokes a sense of ease (Fig. 3).

3.2 Establishment of new generation front face design

A new identity face for future Mitsubishi sedans was adopted for the front, and the trapezoidal grille which matches the three-diamond mark and imparts a sense of ease was combined with the inverted slant nose which has been traditionally used on Mitsubishi sedans (Fig. 5 and Fig. 6) since the first generation COLT GALANT (Fig. 4), resulting in a front design that has presence (Fig. 7). Regarding the trapezoidal grille graphic, the key design adopted was that of the CONCEPT X (Fig. 8) which was exhibited at the 2005 Tokyo Motor Show. The market response both inside and outside of Japan was monitored, and design tuning of the mass-production model was carried out accordingly. As a result, the image was unified with that of the LANCER EVOLUTION X (Fig. 9), and became the identity for popularizing the brand image by this synergy. This individualistic front section has both safety performance and pedestrian protection performance that conform to world standards.

3.3 Fastidious design beauty

The sense of high quality demanded of a sedan was intensively pursued, and great care was taken in the construction of the most detailed parts. The firm, sharp character lines and the body shape consisting of an accented, fascinating surface texture used shading to realize a sensual creation that shows various expressions. In the creation of this beautiful body design, digital tuning for reproducing the subtle nuances created



Fig. 7 New-identity face



Fig. 11 Head lamp, front grille and tail lamp



Fig. 8 Concept X



Fig. 9 LANCER EVOLUION X



Fig. 10 Premium image



Fig. 12 Interior image sketch



Fig. 13 Interior

by the modeler was carried out intensively when producing CAD surface data, and much time was spent ensuring that the customer would experience the joy and excitement of possessing a high quality sedan (Fig. 10). Thorough accuracy enhancement, measures were incorporated in each and every opening gap and body part matching edge, and the development team as a single entity took up the task of creating a high quality product.

The front grille, headlamps, rear combination lamps (Fig. 11), and all other component parts that are important elements for determining the character of a vehicle were made using the utmost care. This is the mission of a "Made in Japan" product, and is also the expression of a development philosophy aimed at the creation of industrial products that are of world class quality. The three-diamond mark, the plated trapezoidal grille that emphasizes a new identity, the component parts of the grille that create a three-dimensional appearance, the finely and elaborately constructed front and rear lamps that even took their illumination condition into consideration, the intricately and dynamically designed

large diameter aluminum wheels, and the plated parts that impart a premium image: all of these parts were aimed to have high design quality that can satisfy all customers.

4. Interior design

The two themes of the interior design were "the simultaneous realization of driving functions and a comfortable interior space" and "fastidious creation" (Fig. 12 and Fig. 13). Design development was based on the pursuit of the "enjoyment and comfort" of riding by eliminating superfluous stress on the driver through easy operation and also an interior space lined with the high quality surfaces. Each part was painstakingly made, while its function was adequately taken into account, so as to demonstrate the skill involved in its construction.

4.1 Simultaneous realization of driving functions and a comfortable interior space

Regarding the instrument panel, the center panel containing the operation system that is most frequently used was located as close as possible to the driver, and from there outward it draws an arc in order to provide

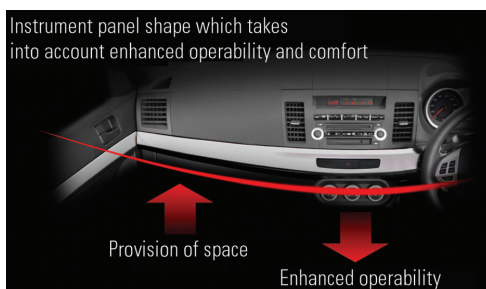


Fig. 14 Instrument panel shape characteristics

leg room. This shape realizes both enhanced functionality and interior comfort. Overall, the interior, which expresses comfort, is simple and has firm surfaces, creating a relaxing space that gently surrounds the occupants. The decoration of the instrument panel is thick at the center and becomes progressively thinner going toward the door trim. This use of perspective provides a roomy feeling to the interior (Fig. 14).

4.2 Fastidious creation

The various details, while being of functional design, express high quality that demonstrates the skill involved in their production. The steering wheel provides a natural grip, and the spoke part which is decoratively finished in silver contains the audio switches and so on, providing a high quality feeling (Fig. 15). The SUPER EXCEED uses high contrast meters. The font and dedicated meter graphic which emphasize legibility express high quality while enhancing readability (Fig. 16). The combination of the shift panel and instrument panel decoration, which are provided with a wood grain finish, and the brightly-finished trim further enhance its high quality appearance (Fig. 17 and Fig. 18).

The front sports seats employ a three-dimensional design which simultaneously realizes sportiness which takes into account sufficient support for driving comfort and also thick cushion shapes that gently fit the occupants (Fig. 19). The rear seat has a wide backrest with large side cushions and a seat cushion which firmly support the occupants – its shape follows the shape of the occupant's hips – and ensures luxurious relaxation even during long-distance driving (Fig. 20).



Fig. 15 Steering wheel



Fig. 16 High-contrast meters (SUPER EXCEED)



Fig. 17 Shifter panel (SUPER EXCEED)



Fig. 18 Instrument panel decorative panel (SUPER EXCEED)



Fig. 19 Front seats



Fig. 20 Rear seat

5. Color design

5.1 Features of the exterior color design

The GALANT FORTIS comes in eight body colors which further accentuate its clean-cut, symmetrical beauty (Fig. 21).

The metallic colors are intended to accentuate the firm, luxurious surfaces and sharp lines, and impart the impression of a firm body. Mica and pearl colors exhibit beautiful color variations and brilliance shown by the changes in light and shade, resulting in an impressive appearance that has presence (Fig. 21).

5.2 Features of the interior color design

The number of colors used throughout the interior is minimal, and different materials are effectively combined, resulting in a simple yet functional and sporty appearance. The various parts are surface-treated to further accentuate the different materials used. This produces a fastidious creation, high quality atmosphere that will captivate the occupants.

The interior of the SPORT is black monotone to provide a modern impression. The matching suede-like



Fig. 21 Body colors

knitted seat material has an embossed pattern which has a pleasant feel (Fig. 22).

The interior of the SUPER EXCEED is a unique bitter brown color which is intended to fill the owner with the joy of possession. The seat material consists of combinations of high quality leather (genuine leather or artificial leather) and Glanlux (suede-like artificial leather consisting of ultra-fine fibers) (Fig. 23).

The interiors of the SPORT and SUPER EXCEED clearly express the identities of the respective models. In addition, different combinations of specially selected materials can be used to meet a wide range of user need.

6. Conclusion

In this GALANT FORTIS project, the authors have dedicated their heart and soul into their work, and steadfastly carried out many enhancements, in order to establish a high quality sporty sedan design that holds its own in the world, and also to ensure that all customers feel the joy and excitement of owning a sedan.

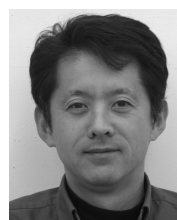


Fig. 22 SPORT



Fig. 23 SUPER EXCEED (black and beige)

As a result, Mitsubishi Motors is confident that the bold design of the GALANT FORTIS expresses comfort, environmental friendliness, and safety. The authors would like to take this opportunity to express their appreciation to the persons who provided valuable assistance during the often difficult development process.



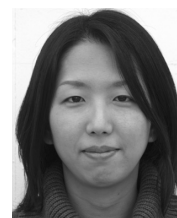
Hiroaki MATSUNOBU



Kenichi NODA



Kei HAMADA



Chigusa YASUI



EPA Climate Protection Award for High-Efficiency Mobile Air Conditioning System



Development of Power-saving Mobile Air Conditioning System

Tetsuji UKITA* Shigeharu NAKANE**

Mitsubishi Motors Corporation and Mitsubishi Heavy Industries won a 2007 Climate Protection Award from the US Environmental Protection Agency (EPA) for a power-saving mobile air conditioning (MAC) system that they jointly developed. The EPA gives such awards to corporations, groups, and individuals who help to protect the environment by contributing to reductions in greenhouse gas emissions.

1. Basic concept and configuration

For improved air-conditioning efficiency, we adopted a new type of scroll compressor with a three-dimensional scroll shape that makes higher compression efficiency. Also, we optimized the compressor's operating temperature, realizing the minimum compressor operation by setting the temperature of the air after passing through the evaporator when much cooling performance is not required (**Fig. 1**). The system's major components are compared with those of a previously used system in **Table 1**. We targeted an efficiency improvement of 30 % in line with the goals of the Improved Mobile Air Conditioning research program, which was launched by the Society of Automotive Engineers and the EPA.

2. Performance and benefits

To evaluate annual power consumption, we tested the system with various levels of outside temperature, humidity, and vehicle speed and took into account the frequency with which each variable occurs in the real world. The results showed a 39 % reduction in annual power consumption (**Fig. 2**). We also confirmed a 7 % improvement in maximum cooling performance with the new system equipping the newly developed compressor. To verify the new system's effect on the fuel consumption of an actual vehicle, we took measurements on a chassis dynamometer: With an outside temperature of 25 °C and no solar radiation, we simulated various driving patterns and compared the fuel consumption with and without air conditioning. Levels of fuel consumption recorded under various driving conditions (with the fuel consumption recorded with the original system on congested roads taken as 100 %) are shown in **Fig. 3**. As shown, the fuel consumption of the vehicle with new energy-saving MAC system was extremely low, meaning that air-conditioner operation had only a minimal impact on fuel efficiency.

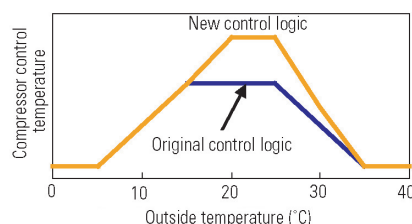


Fig. 1 Compressor control temperatures
(vs. outside temperatures)

Table 1 Comparison of system specifications

	Original system (2005 AIRTREK)	New system (improved OUTLANDER)
Compressor	MSC90CA Fixed scroll Pulley ratio: 1.58	New type Fixed 3D scroll Pulley ratio: 1.52
Condenser	Multi-flow 16 mm width	Multi-flow 16 mm width
Evaporator	Laminated Plate type, 58 mm width	Laminated Plate type, 38 mm width

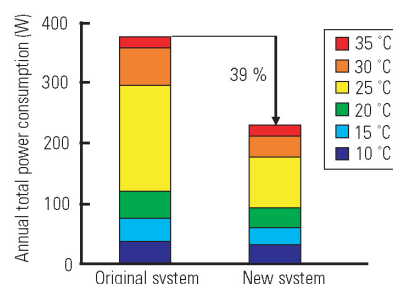


Fig. 2 Comparison of annual total power consumption

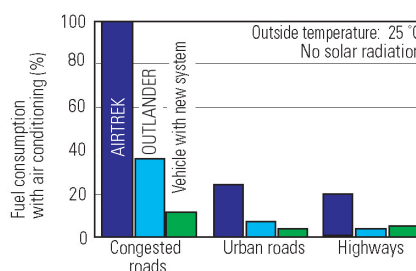


Fig. 3 Comparison of fuel consumption

* Testing Control Dept., Development Engineering Office

** Interior Design Dept., Development Engineering Office



SPORT



SUPER EXCEED

Mitsubishi Motors Corporation (MMC) launched the GALANT FORTIS, the first new Mitsubishi sedan in seven years, on 23 August 2007. The GALANT FORTIS is a sporty sedan that inherits the great performance attributes of earlier LANCER, GALANT, and DIAMANTE models. (MMC additionally launched the SUPER EXCEED version of the GALANT FORTIS on 23 October 2007.)

1. Targets

The product concept for the GALANT FORTIS was to create a global-standard sporty sedan with a superior combination of performance attributes in terms of safety, environmental compatibility, and comfort. In line with this concept, the GALANT FORTIS was developed to be a global strategic model with the bold personality and look and feel of stability that are unique to sedans. More specifically, it was developed to have a distinctive design that conveys a sense of energy and presence and an unmistakable Mitsubishi sedan identity, to deliver a sporty-feeling ride and refined performance, and to have a high level of safety.

2. Features

2.1 Exterior design

The GALANT FORTIS's exterior design reflects pursuit of three themes: a combination of comfort, safety, and a sporty design; a new-generation front-face design; and carefully considered beauty of form.

A properly comfortable cabin is wrapped within a sporty form that exudes energy, and a reverse-slanted nose (a tradition carried forward from earlier GALANT generations) incorporates a big, trapezoidal grille that gives a sense of stability, resulting in an expression of sportiness and refinement.

Attention was paid to creation of contrasts between voluptuous contours and sharp character lines and to intricate craftsmanship in details such as the lamps and grille, resulting in the kind of refinement expected of a new-generation sedan.

2.2 Interior design

For functionality befitting a next-generation sedan, the GALANT FORTIS's interior design reflects pursuit of two themes: a combination of driving functionality and a relaxing interior environment; and outstanding craftsmanship.

An arch-shape instrument panel and simple, taut contours create a sense of relaxing openness, and the switches, meters, monitor, and other items have a simple layout that reflects consideration of the ease with which the driver can see and operate them.

Further, the shapes of details give a sense of refinement and craftsmanship that appeals even to people accustomed to more expensive vehicles.

2.3 Packaging

For a combination of sporty styling and interior spaciousness, the GALANT FORTIS has ample dimensions in terms of overall width and overall height but is not unduly long. The result is a world-standard body size that reflects consideration of the European and North American markets.

Layout innovations enable an effective interior length of 1,715 mm (comparable with the effective interior lengths of large sedans). The rear seat has a large cushion that contributes to a relaxing environment that gently wraps around passengers.

A modest tumble angle for the body sides complements the wide body to realize plenty of shoulder room and headroom. Also, an ample overall height allows high seating positions for good driver visibility and easy ingress and egress together with plenty of headroom.

In all grades, the rear seatback has a 60:40-split design and a trunk-through mechanism to allow long items of luggage to be placed in the car through the trunk. Further luggage-carrying efficiency is realized by link-type trunk-lid hinges, which do not protrude into the luggage space when the trunk lid is closed.

Notwithstanding the interior spaciousness, wide treads and optimal positioning and alignment of suspension parts allow a minimum turning radius of five meters (comparable with that of a compact car), so the GALANT FORTIS is easy to maneuver on urban roads



Interior (Super Exceed)



SRS airbags

and in small parking spaces.

2.4 Performance

To realize a sporty driving experience, the 4B11 engine, which has high performance, high fuel economy, and compact dimensions, was developed based on the newly developed 2.0-litre, DOHC, MIVEC, 16-valve 4B12 engine, which has earned an excellent reputation in the OUTLANDER and DELICA D:5.

The 4B11 engine has advanced technologies including a die-cast aluminum cylinder block, a plastic cylinder-head cover, and a rear-mounted exhaust system with a double-skin stainless-steel exhaust manifold. Variable valve timing (realized by a Mitsubishi Innovative Valve timing Electronic Control system) on the intake and exhaust sides realizes optimal valve operation under all operating conditions. Also, the bore, stroke, and compression ratio are optimized to suit the characteristics of the vehicle. As a result, the engine delivers powerful performance (its maximum output is 113 kW, and its maximum torque is 198 N·m) together with superior economy and daily drivability. Plus, all GALANT FORTIS grades have exhaust emissions at least 75 % lower than those allowed by Japan's 2005 Standard and fuel efficiency that satisfies Japan's 2010 Standard.

2.5 Handling stability and ride comfort

A new-generation suspension system and a high-rigidity body realize high handling stability and a supple ride.

At the front, a wide tread and MacPherson-strut suspension with relatively long strokes yield superior turning behavior, roadholding, and ride comfort. Also, the rear-mounted exhaust system allows the suspension crossmember to be flat, meaning that the mountings for the lower arms have superior lateral rigidity and that steering response is concomitantly superior.

The rear wheels have trailing-arm multilink suspension with a lattice type crossmember. This arrangement yields superior wheel-mounting rigidity and alignment precision. The points at which the trailing arms are attached to the body are relatively high, so suspension movements when the wheels pass over bumps are

smooth. Also, the points at which the toe control arms are attached to the hubs are relatively low for superior toe and camber rigidity.

2.6 Collision safety

The body incorporates MMC's proprietary Reinforced Impact Safety Evolution technologies for superior protection of occupants from frontal, side, and rear impacts.

At the front of the body, the side members each have a front-end crush-box structure that helps to minimize damage in the event of a low-speed impact. Also, straight, octagonal-section front side members and a three-leg support structure effectively disperse frontal impact energy, thereby limiting cabin deformation and protecting occupants.

The sides and rear of the body incorporate ultra-high-tensile steel, which is stronger than the high-tensile steel used in earlier vehicles. Also, the body's side openings are surrounded by reinforcements that further protect the cabin by heightening the body's rigidity and limiting cabin deformation in the event of a side impact.

Also for passive safety, each grade has dual-stage driver and front passenger airbags, which sense the intensity of any impact and match their deployment intensity to it, and a driver's knee airbag. Plus, the bumpers, bonnet, fenders, and cowl have impact-absorbing structures for a high level of pedestrian protection.

2.7 Amenities

2.7.1 Adaptive Front lighting system (AFS)

An AFS is combined with high-intensity discharge headlights. The AFS enhances cornering visibility for the driver by means of fixed auxiliary lamps that illuminate in coordination with the steering wheel; the auxiliary lamps widen the driver's field of vision by illuminating the inside edge of each corner or bend. The AFS is particularly beneficial on twisty roads such as those encountered in mountainous areas.

2.7.2 Auto light control and rain-sensing auto wipers

Whereas the auto light control system used in earlier models had only an ambient illuminance sensor, the system in the GALANT FORTIS also senses illuminance

ahead of the vehicle. The new system can thus recognize when the vehicle is passing under a bridge or through a short tunnel, so it does not turn the headlights on and off unnecessarily.

Rain-sensing wipers detect raindrops on the windshield and automatically adjust their wipe speed in accordance with the amount of water. The system also allows the driver to adjust its raindrop detection sensitivity to suit personal preferences and the driving environment.

2.7.3 Rockford fosgate premium sound system

A premium sound system jointly developed by MMC and Rockford Corporation is available with the GALANT FORTIS. Based on an eight-channel amplifier with total power of 650 W, it has nine speakers in seven positions whose layout was precisely determined during the vehicle's design; speaker-box structures in the doors; and a digital signal processor. The resulting high-quality sound is characterized by clarity, presence, and powerful bass reproduction that surpass conventional expectations of factory-fitted audio equipment.



Rockford Fosgate premium sound system

3. Major specifications

Major specifications of the GALANT FORTIS are shown in the following table.

Specifications			Model	Mitsubishi DBA-CY4A						
				2WD			4WD			
				INVECS-III 6-speed CVT with sports mode			5 M/T	INVECS-III 6-speed CVT with sports mode		
				STMH	STHH STHH1	STXH STXH1	SNXH SNXH1	STMHZ	STHHZ STHHZ1	STXHZ STXHZ1
				EXCEED	SUPER EXCEED SUPER EXCEED NAVI		SPORT SPORT NAVI		EXCEED	SUPER EXCEED SUPER EXCEED NAVI
Dimensions	Overall length		(mm)	4,570						
	Overall width		(mm)	1,760						
	Overall height		(mm)	1,490						
	Wheelbase		(mm)	2,635						
	Tread	Front	(mm)	1,530						
		Rear	(mm)	1,530						
	Minimum ground clearance		(mm)	150						
Seating capacity		(persons)	5							
Performance	Minimum turning radius		(m)	5.0						
	Fuel economy (10-15 mode)		(km/L)	13.6			13.2			
Engine	Model			4B11 MIVEC						
	Valve mechanism and number of cylinders			DOHC; 16 valves; four cylinders						
	Displacement		(cc)	1,998						
	Maximum output (net)		(kW (ps)/min ⁻¹)	113 (154)/6,000						
	Maximum torque (net)		{N·m (kg·m)/min ⁻¹ }	198 (20.2)/4,250						
	Fuel supply			ECI-MULTI (electronically controlled fuel injection)						
	Fuel			Unleaded regular gasoline						
	Fuel-tank capacity		(L)	59			55			
Chassis	Steering			Rack and pinion (with power assistance)						
	Suspension	Front		MacPherson-strut						
		Rear		Multilink						
	Brakes	Front		15-inch ventilated discs		16-inch ventilated discs		15-inch ventilated discs		16-inch ventilated discs
		Rear		14-inch discs		16-inch discs		14-inch discs		16-inch discs
Tires			205/60R16		215/45R18		205/60R16		215/45R18	

(C-seg Product Development Project, Development Engineering Office: Kagawa, Mae, Ozaki, Mizuno)



Fig. 1 Exterior (GSR Premium Package)

Mitsubishi Motors Corporation (MMC) launched the LANCER EVOLUTION in 1992 in hopes of achieving victory in the World Rally Championship. The LANCER EVOLUTION has since evolved through feedback from motor-sport participation, most recently appearing in fourth-generation form as the LANCER EVOLUTION X – a new vehicle offering a new dimension of driving pleasure.

1. Targets

In developing the LANCER EVOLUTION X, MMC sought to further evolve the existing model's high level of dynamic performance and combine it with great driving pleasure. MMC also aimed to position the LANCER EVOLUTION X as a high-value-added product with wider customer appeal by means of higher levels of interior and exterior refinement.

In line with the above goals, MMC sought to deliver enjoyment and pleasure of ownership not only to existing LANCER EVOLUTION users but also to a wider range of motorists by completely updating the engine, transmission, body, and suspension system in pursuit of performance and refinement in both vehicle behavior and ease of control (**Fig. 1**).

2. Features

2.1 Exterior and interior designs reflecting pursuit of functionality

The exterior design incorporates extensive refinements reflecting pursuit of high levels of aerodynamic and cooling performance; the aerodynamically efficient body is an example of true functional elegance. Further, a taut-looking form with short overhangs embodies MMC's focus on performance.

In the cabin, pursuit of ease of control in diverse driving situations is reflected in a functional cockpit that heightens the driver's ability to concentrate on driving. Also, superior levels of functionality-based refinement



Fig. 2 Interior (GSR)

are reflected in equipment that includes high-contrast meters with carefully considered colors and typefaces, a small-diameter steering wheel on which even the stitching reflects attention to excellence, and Recaro seats that are outstanding in terms of materials, support, and user feel (**Fig. 2**).

2.2 Newly evolved driving experience yielded by enhanced basic performance

To ensure maximal functionality in all four tires, a better body balance is realized by means of improved basic specifications including wider treads, a lower center of gravity, and enhanced weight distribution.

Also, superior rigidity and an optimized layout for the new body and chassis combine with exceptionally good roadholding to enable users to experience the excitement of a high-performance sports car not only during sporty driving but also during urban use.

A new platform yields superior cornering performance and realizes a ride feel befitting a new-generation vehicle.



Fig. 3 Bare chassis

2.3 High performance delivered exactly in accordance with the driver's wishes

The engine in the LANCER EVOLUTION X is the lightweight, newly developed 4B11, which replaced the long-serving 4G63. With an aluminum cylinder block and other weight-saving features, it places a lighter burden on the front wheels. Rear-mounted exhaust system featuring this engine allows it to be mounted at a low position for lower center of gravity. This, together with lightness at the front, contributes to superior dynamic performance of the vehicle (Fig. 3).

The new engine has the same maximum output (280PS) as the 4G63, but it delivers significantly higher torque over a wide rev range. The torque difference is particularly marked at low and mid-range speeds. The higher torque combines with superior response to realize high performance that's easy for the driver to exploit. Notwithstanding the engine's high performance, the LANCER EVOLUTION X reflects consideration of the environment; its exhaust emissions are 50 % lower than those permitted by Japan's 2005 regulations.

The brakes use discs of larger size than those of the previous-generation LANCER EVOLUTION. In addition to delivering superior stopping power and fade resistance, they yield a better pedal feel, resulting in braking performance that inspires driver confidence.

The Super All Wheel Control (S-AWC) arrangement in the Lancer Evolution X represents the culmination of MMC's all-wheel-control development concepts. It newly adds the active stability control to the Active Center Differential (ACD), Active Yaw Control (AYC), and Anti-lock Braking System (ABS) in earlier LANCER EVOLUTION generations. By precisely controlling the four wheels' respective driving and braking forces in an inte-



Fig. 4 High Performance Package (factory-fitted option)

grated manner, the S-AWC arrangement heightens the vehicle's traction, cornering performance, and stability in situations ranging from normal driving to emergency hazard evasion, thereby enabling the driver to control the vehicle exactly in accordance with his/her wishes and keeping the vehicle outstandingly stable. The overall effect of the S-AWC arrangement is to realize driving pleasure and confidence in line with MMC's corporate philosophy and in harmony with dynamic performance that befits LANCER EVOLUTION of any generation.

The Twin Clutch Sport Shift Transmission (SST) in the LANCER EVOLUTION X behaves like two three-speed manual transmissions, with odd (1st, 3rd, and 5th) and even (2nd, 4th, and 6th) gears on separate input shafts, each connected to an individual hydraulic clutch. With the clutches alternately engaging, the Twin Clutch SST enables gearshifts with no interruption in power delivery and acceleration with a feeling of directness like that of a conventional manual transmission. Plus, it combines its unprecedented performance with fuel economy greatly superior to that of a conventional automatic transmission.

For customers who attach importance to motorsport and prefer a manual transmission, a newly developed five-speed manual transmission is also available. The manual transmission has ample durability and reliability to handle the output of the high-performance engine; its five-speed configuration limits weight; and it has multi-cone synchronizers for all gears to promote durability for motorsport. As a result, drivers can enjoy the shift-lever and pedal work that characterizes manual-transmission operation.

3. Grade and package availability

Like earlier LANCER EVOLUTION generations, the LANCER EVOLUTION X is available in two grades: the competition-oriented RS (with the five-speed manual transmission only) and the GSR (with a choice of the Twin Clutch SST or five-speed manual transmission). The GSR grade is offered with a range of package options to meet customer needs.

For customers who want even greater performance, Bilstein shock absorbers, Eibach springs, and two-piece front brake discs are offered as a High Performance Package (Fig. 4).



Fig. 5 Front grille (Stylish Exterior package)

People who desire even greater refinement in the exterior styling can choose a Stylish Exterior Package consisting of a chrome-plated and silver-painted front grille and body-color hood and fender air outlets (Fig. 5).

For even greater interior environment, there's a Leather Combination Interior package in which the seats have leather and suede-effect upholstery, the door trim and console-box lid have silver stitching, and the front door openings have aluminum scuff plates. This package also includes extra sound insulation for the cabin (Fig. 6).

Also available is a Premium Package, which combines the three above-mentioned packages and adds BBS forged-aluminum wheels for the ultimate combination of LANCER EVOLUTION X performance and refinement.



Fig. 6 Leather Combination Interior package

4. Major specifications

















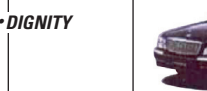
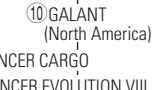


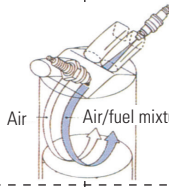
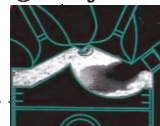
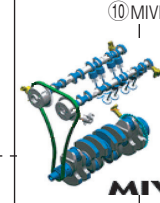
Major specifications of the LANCER EVOLUTION X are shown in the following table (This article pertains to the LANCER EVOLUTION X for Japanese market. The performance and equipment specifications of the model for another market may differ from those shown here).

Specifications			Model		
			LANCER EVOLUTION X		
			Mitsubishi CBA-CZ4A		
			Full-time 4WD		
			GSR [TC-SST]	GSR [5 M/T]	RS [5 M/T]
Seating capacity			(persons)		
			5		
Dimensions	Overall length	(mm)	4,495		
	Overall width	(mm)	1,810		
	Overall height	(mm)	1,480		
	Wheelbase	(mm)	2,650		
	Tread	Front (mm)	1,545		
		Rear (mm)	1,545		
	Minimum ground clearance	(mm)	135		140
Engine	Model		4B11 with MIVEC and turbocharger		
	Valve mechanism and number of cylinders		DOHC; 16 valves; four in-line cylinders		
	Displacement (cc)		1,998		
	Maximum output (net) {kW (PS)/min ⁻¹ }		206 (280)/6,500		
	Maximum torque (net) {N·m (kg·m)/min ⁻¹ }		422 (43.0)/3,500		
	Fuel supply		ECI-MULTI (electronically controlled fuel injection)		
Chassis	Steering		Rack and pinion (with power assistance)		
	Suspension	Front	MacPherson-strut		
		Rear	Multilink		
	Brakes	Front	Ventilated discs (18-inch, 4-pot)		Ventilated discs (15-inch, 2-pot)
		Rear	Ventilated discs (17-inch, 2-pot)		Ventilated discs (15-inch, 1-pot)
	Tires		245/40R18		205/60R16

(C-seg Product Development Project, Development Engineering Office: Iwata, Fujii, Ichiraku)

A 20-Year History of New Models and Major Technologies at Mitsubishi Motors Corporation

Circled figure indicates the year of the month. Each bold and italic item has a related photo.

	1988	1989	1990	1991	1992	1993	1994	1995	1996	1997	1998	1999	2000	2001	2002	2003	2004	2005	2006	2007
New Models	 ⑩ ETERNA  ⑥ LANCER  ① MINICA  ② MINICA TOPPO	 ⑤ DIAMANTE ⑪ SIGMA ⑩ GTO  ② ECLIPSE  ⑤ CHARIOT ② RVR ① MINICAB / BRAVO		 ① PAJERO ⑤ STRADA  ⑤ CHARIOT ② RVR ① MINICAB / BRAVO	 ⑩ DEBONAIR ③ DIAMANTE WAGON ⑤ GALANT / ETERNA ⑩ EMERAUDE ⑩ MIRAGE / LANCER ⑤ LIBERO ⑩ LANCER EVOLUTION 	 ⑤ GALANT / ETERNA ⑩ EMERAUDE ⑤ MIRAGE ASTI ⑩ LANCER EVOLUTION II ① LANCER EVOLUTION III ② LANCER EVOLUTION IV ⑤ DELICA SPACE GEAR ⑨ MINICA / MINICA TOPPO	 ⑩ FTO ⑥ ECLIPSE (U.S.A.) ⑩ MIRAGE / LANCER ② LANCER EVOLUTION III ② LANCER EVOLUTION IV ⑤ DELICA SPACE GEAR ⑨ MINICA / MINICA TOPPO ① PAJERO JR. ② PAJERO MINI	 ① DIAMANTE ⑩ MIRAGE / LANCER ② LANCER EVOLUTION III ② LANCER EVOLUTION IV ⑤ DELICA SPACE GEAR ⑨ MINICA / MINICA TOPPO ① PAJERO JR. ② PAJERO MINI	 ⑧ GALANT / LEGNUM ⑩ CARISMA ⑨ FREECA (Taiwan) ① LANCER EVOLUTION V ① LANCER EVOLUTION VI ① MIRAGE DINGO ① TOPPO BJ WIDE ⑥ TOWNBOX WIDE ⑨ PAJERO ⑥ STRADA ⑨ PAJERO EVOLUTION ⑩ CHARIOT GRANDIS ⑪ RVR ⑥ PAJERO IO ⑩ MINICA/TOPPO ④ TOWNBOX ⑩ PAJERO MINI ① MINICAB VAN/TRUCK	 ⑧ ASPIRE ⑥ SPACE STAR (Europe) ① DION ⑤ LANCER CEDIA ⑪ LANCER CEDIA WAGON ② LANCER EVOLUTION VII ② LANCER EVOLUTION VII GT-A ⑪ COLT ⑥ AIRTREK ⑩ eK WAGON ⑨ eK SPORT ⑤ eK CLASSY	 ② PROUDIA • DIGNITY ⑧ ECLIPSE (U.S.A.) ① LANCER CEDIA ⑪ LANCER CEDIA WAGON ② LANCER EVOLUTION VII ② LANCER EVOLUTION VII GT-A ⑪ COLT ⑥ AIRTREK ⑩ eK WAGON ⑨ eK SPORT ⑤ eK CLASSY	 ⑩ GALANT (North America) ① LANCER CARGO ① LANCER EVOLUTION VIII ② LANCER EVOLUTION VIII MR ⑩ COLT PLUS ⑤ GRANDIS ③ ENDEAVOR (U.S.A.) ⑤ eK ACTIVE	 ⑩ 380 (Australia) ⑤ ECLIPSE (U.S.A.) ⑨ LANCER EVOLUTION WAGON ③ LANCER EVOLUTION IX ⑧ LANCER EVOLUTION IX MR ⑧ LANCER EVOLUTION WAGON MR ⑨ RAIDER (U.S.A.) ⑧ TRITON (Thailand) ⑩ PAJERO ⑫ ZINGER (Taiwan) ⑩ OUTLANDER ① i ⑨ eK WAGON, eK SPORT	 ⑧ GALANT FORTIS ⑩ LANCER EVOLUTION X ⑧ LANCER EVOLUTION IX MR ⑧ LANCER EVOLUTION WAGON MR ⑨ RAIDER (U.S.A.) ⑧ TRITON (Thailand) ⑩ PAJERO ⑫ ZINGER (Taiwan) ⑩ OUTLANDER ① i ⑨ eK WAGON, eK SPORT						
New Technologies			 ⑩ Three-valve MVV Engine ⑩ Four-valve MVV Engine ⑩ MIVEC Engine ⑩ MIVEC-MD Engine			 ⑧ GDI Engine											 ⑩ MIVEC Turbocharged Engine ① MIVEC Turbocharged Engine for Minicars ⑩ MIVEC Engine (Intake and Exhaust Continuously Variable Valve Timing)			
Engines																				
Transmissions					④ INVECS															
Vehicle Dynamic Control System (Traction and braking force control system, brake system)																				
Active Safety																				
Passive Safety																				
Others																				
New Facilities																				

MMCS: Mitsubishi Multi Communication System
INVECS: Intelligent & Innovative Vehicle Electronic Control System
MIVEC: Mitsubishi Innovative Valve timing (and lift) Electronic Control system
MIVEC-MD: Mitsubishi Innovative Valve timing (and lift) Electronic Control system -Modulated Displacement
MVV: Mitsubishi Vertical Vortex

GDI: Gasoline Direct Injection
AYC: Active Yaw Control System
ASC: Active Stability Control System
RISE: Reinforced Impact Safety Evolution

ACD: Active Center Differential
EBD: Electronic Brake-force Distribution

S-AWC: Super All Wheel Control
SST: Sport Shift Transmission
ACL: Active Cornering Light
AFS: Adaptive Front-Lighting System

MITSUBISHI MOTORS

TECHNICAL REVIEW 2008 NO. 20

Published: July 2008

MITSUBISHI MOTORS CORPORATION

5-33-8 Shiba, Minato-ku, Tokyo 108-8410, Japan
Tel: +81-3-3456-1111
E-mail: technicalreview.et@mitsubishi-motors.com
<http://www.mitsubishi-motors.com>

